NON INVASIVE PARAMETER IDENTIFICATION OF POWER PLANT CHARACTERISTICS BASED ON RECORDED NETWORK TRANSIENT DATA

Graeme Iain Hutchison

A thesis submitted for the degree of

Engineering Doctorate

School of Electrical, Electronic and Computer Engineering

Abstract

Synchronous generators are the most widely used machines in power generation. Identifying their parameters in a non invasive way is very challenging due to the inherent nonlinearity of power plant performance. This thesis proposes a parameter identification method using particle swarm optimisation (PSO) for the identification of synchronous machine, excitation system and turbine parameters.

The PSO allows a generator model output to be used as the objective function to give a new, more efficient method of parameter identification. This thesis highlights the effectiveness of the proposed method for the identification of power plant parameters, using both simulation and real recorded transient data. The thesis also considers the effectiveness of the method as the number of parameters to be identified is increased, and the effect of using differing forms of disturbances on parameter identification.

Contents

List of Figures

List of Tables

Acknowledgments

I would like to start by expressing my gratitude to the backers of this research; The Engineering and Physical Sciences Research Council, Parsons Brinckerhoff and The Engineering Doctorate scheme at Newcastle University

Thanks are given to my academic supervisors. Firstly to Bashar Zahawi, who has been very supportive of the work over the years and offered advice when necessary to help me go in the right direction. He has also patiently read and commented on this thesis. I would also like to thank Damian Giaouris for his help and suggestions over the years. I also thank all the members of the department who have contributed advice and encouragement over the years of this Engdoc.

I would also like to thank my industrial supervisors Keith Harmer and Bruce Stedall who have been so supportive of the work over the years and have helped me structure my ideas into something coherent, it has been massively appreciated. Likewise I would also like to thank all the members of the Power Systems Group, past and present for their support of the work and patience.

Thank you to all the members of the UG lab, past and present, who gave a friendly and welcoming atmosphere whenever I came back into the department.

Finally, a special thank you to my wife Claire, whose unwavering support over the years has reminded me as to why we do this to ourselves. She has also proof read this thesis and must have the patience of a saint to put up with me. I'll finish building the decking now!

List of Symbols

Below is a list of symbols commonly used throughout the thesis. An example list of subscripts is also included as a point of reference.

t Time
C_b Boltzmann's constant
V Voltage
E EMF
I Current
L Inductance
X Reactance
R Resistance
N_p Pole number
H Constant of inertia
Θ_r Rotor angle
Ψ Flux linkage as a function of ω
λ Flux linkage
J Inertia
T Torque
X_A Armature reaction reactance
X_s Synchronous reactance
$X_{s\,(sat)}$ Saturated synchronous reactance
T_{mech} Mechanical torque
T_{elec} Electrical torque,
T_{acc} Accelerating torque
J_m Mechanical inertia
ω_m Rotor speed
v_d, v_q, i_d and i_q Direct and quadrature voltages and currents.
E_{fd} and i_{fd} Direct axis field EMF and current
R_a Armature resistance
R_{fd} Direct axis Field Resistance
ψ_d, ψ_q and ψ_0 Direct, quadrature and zero sequence components of flux linkage
V_0 and i_0 Zero sequence components of voltage and current
V_{ra} Rated terminal voltage
I_{min} Minimal magnetizing current
I_{max} Maximum magnetizing current
i_{sd0} Saturated direct axis current
θ_r Rotor angle.
v_{kd}, v_{kq}, i_{kd}, i_{kq}, r_{kd}, r_{kq} Direct and quadrature damper winding voltage, current and resistance
v_g , i_g and r_g Quadrature axis field voltage, current and resistance
L_d and L_q Direct and quadrature inductance
L_{md} and L_{mq} Direct and quadrature mutual inductance
L_{ls} Armature winding leakage inductance
L_{kdkd} and L_{kqkq} Direct and quadrature mutual damper winding inductance.
X''_d, X'_d and X_d Sub transient, transient and steady state direct axis reactance
X''_q, X'_q and X_q Sub transient, transient and steady state quadrature axis reactance

1. Introduction

Power system transient analysis depends largely on the ability to accurately model transient and dynamic behaviour of electrical networks. As part of this, the characterisation of power plants[1] connected to the network is critical. Power plants, as well as injecting power into the network that they supply, also have a significant impact on the behaviour of the network when responding to transient events that occur. In order to characterise power stations accurately, models that describe their behaviour under a wide range of operating conditions are required. The variables inside these models change from power plant to power plant, thus it is of fundamental importance that these values are appropriate for the power plant in question. In order to accurately characterise power plants correctly, invasive testing is done during manufacturing and commissioning in order to ascertain these variable values. In many power plants this information can be inaccurate due to differing standards of commissioning, or it can be simply lost. In order to regain this data, a full set of invasive tests are required. This would mean that the power plant would need to be shut down and disconnected from the network. The expense of this is significant at best and at worst, could cause blackouts through load shedding, loss of synchronism throughout the grid or require planned outages.

This thesis describes work done in order to non invasively identify the parameters of power plants. The research is performed using data recorded from transients that occur on the network and the generating stations' responses. The work is done in conjunction with Parsons Brinckerhoff, a power engineering consultancy that have encountered difficulties in trying to perform power system transient stability studies without sufficient modelling data to do so in the past. The most significant challenge is that, without a full dataset[2], modelling is not accurate. Because of this, models developed may not produce results consistent with the real network being modelled.

Conventional techniques for the determination of model parameters can have disadvantages in their application. The techniques involved can be based on significant assumptions with regard to operating conditions, when these are not correct then the assumptions invalidate

[1] In this work power plants will be used to describe the prime mover, synchronous generator and excitation system used in electrical power generation.
[2] Dataset describes the information required to perform a comprehensive transient stability study. The information included in this are generally details on the synchronous machines performance during transient and in steady state, an excitation model and basic details on the governor-turbine response.

the estimation. Furthermore, the techniques employed and the required equipment to facilitate these estimations may be expensive, time consuming and invasive to its operation.

This work considers the identification of differing types of power generating technologies available to power providers, more specifically gas turbine and steam turbine plants. From this, a model that accurately describes prime mover function is developed. This model drives an exciter fed synchronous generator model. Together they form the basis of a turbine-generator model that generically characterises a large cross section of differing power plants to a degree of accuracy that can be considered an accurate representation of their behaviour under transient and dynamic events.

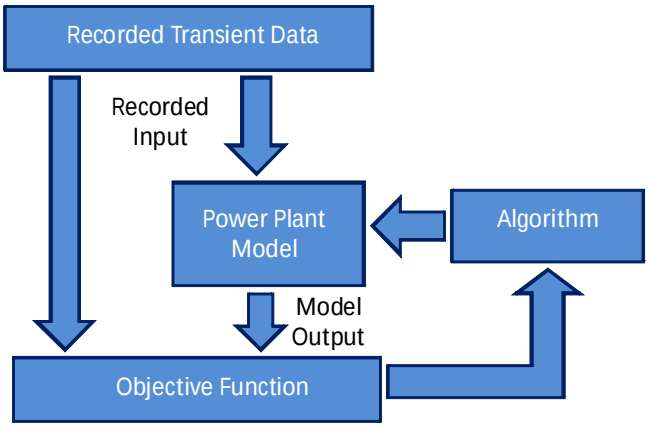

Figure 1 Parameter identification process

The model developed is used to perform the parameter identification of power plant characteristics as seen in Figure 1. Recorded transient data is used as an input to the power plant model. The model develops an output that can be compared against other recorded data. The comparison of the model output and recorded data provides an objective function that can be optimised by an algorithm. From this objective function value, the algorithm modifies power plant model values until they develop a matching output to the recorded transient data. At this point, the values inside the model hopefully match the real system parameters. This work seeks to prove that this methodology is possible and in doing so provides a significant addition to learning. This is because the work identifies exciter, synchronous machine and turbine governor parameters at the same time. Much work has been done individually identifying their characteristics but never together. This would be a significant step forward in this area of research.

Parameter identification is initially performed in conjunction with a set of artificially generated phase voltages and currents. These phase voltages and currents are generated using a

synthetic test network in DigSilent, a powerful, industrially accepted power systems analysis package. In order to perform parameter identification, an optimisation algorithm must be developed. This algorithm allows an objective function to be optimised. In this case, the objective function is formed from the recorded phase current output of either DigSilent or a real network and the output of the identification model already mentioned. As the output of the model and the recorded phase currents are compared the algorithm iteratively changes particular parameter values of the identification model until the phase current outputs match within a defined level. At this point the parameter values in the identification model match the parameters of the recorded network dataset.

After confirming the model and identification method is valid, real terminal data from a gas fired combined cycle power plant is used to demonstrate that non invasive parameter identification of power plant characteristics is possible. Having shown that the method is feasible, non invasive parameter identification could be used to ascertain parameters from differing power plants around the world.

1.1 Thesis Outline

1.1.1 Aims

The aim of this work is to develop a complete non linear model that describes the electrical function of a gas or steam turbine power plant. Most power stations have several generators connected together to a common busbar or busbars. This work considers the characterisation and parameter identification of one of these generators. Once a model is developed, the parameter identification and optimisation of model variables in a non invasive fashion is performed. The main aims sought from this project are:

- The development of a single robust power plant model that can characterise a wide range of differing station types effectively.
- Develop an appropriate algorithm that allows for the optimisation and parameter identification of a multi parameter search.
- To understand which parameters are identifiable using these new techniques.
- The non invasive identification of generator characteristics.
- The non invasive identification of excitation system characteristics.
- The non invasive identification of governor-turbine characteristics for varying energy sources.

- Identification of parameters that are not commonly derivable using classical non invasive testing.
- The identification of parameters using naturally occurring small perturbations, which would be expected to occur on a network throughout its day to day operation.

1.2 Structure

In order to understand the implications of modelling differing forms of prime mover, chapter 2 gives a brief overview of steam generation prime mover systems. In this, the differing forms of prime mover modelling and control are considered. Once a base of understanding has been established a review of existing literature on the modelling of steam turbines is performed. This allows for a better understanding of existing modelling techniques that are industrially accepted to be good representations of steam turbines and their associated control.

Having established the behaviour of a steam turbine driven prime mover, chapter 3 considers the behaviour of gas turbine driven systems. The gas turbine chapter establishes the differing forms of gas turbine as well as highlighting the differing ways in which they are operated. This includes a review of the use of combined cycle gas turbine systems and open cycle gas turbine systems. It also looks at the differing forms of design that are available and the implications this has to modelling. Once the differing forms have been introduced there is a review of literature on the modelling of gas turbines and the relative implications there are identifying their operating characteristics.

The synchronous machine is considered in chapter 4. Consideration is given to how a synchronous generator functions before considering the techniques that have been adopted in modelling of synchronous machines in the literature. Techniques and previous work on the identification of parameters using invasive and non invasive testing is also considered in order to understand the most appropriate technique to adopt in modelling what is the most critical aspect of the power plant from an electrical point of view.

Chapter 5 considers the varying forms of excitation that synchronous machines use and the industrially accepted models that go with them. In this chapter there is a brief introduction into the differing topologies. This leads to the identification of specific models that would be most appropriate to this work.

Optimisation algorithms are critical to the parameter identification process. In order to identify the parameters of the generator model, a search algorithm is used to minimise an objective function. The objective function is used to define the difference in behaviour

between the output of the model used to estimate the parameter values and the real or synthetic terminal data. Differing forms of search techniques are considered in chapter 6. The differing techniques are evaluated with respect to the current work in order to ascertain which form of algorithm would be most appropriate to achieve efficient and accurate parameter identification.

Having established the necessary base theory, chapter 7 illustrates the implementation of the test system and its initial validation. In this chapter, a base methodology is established as to how the parameter identification is to proceed. The models that characterise the power plant are established and then validated. The validation is performed by comparing the output of the identification model against that of an equivalent DigSilent model under differing forms of perturbation.

Having developed the methodology of the work, the implementation of the search algorithm is documented in chapter 8. This involves the initial search algorithm and further discussion regarding optimising the algorithm to make it more efficient for this specific work.

Having established a technique for parameter identification in chapter 7, chapter 8 highlights which power plant parameters are identifiable by considering the relative influence they have on the objective function used. This allows for the most efficient use of computational resources and allows an understanding as to which parameters are more likely to be identified and which have characteristics that make parameter identification more difficult for this method.

Chapter 9 considers the relative success of the parameter identification method using synthetic datasets and addresses any specific aspects of the optimisation algorithm that need further consideration in order to establish the most efficient algorithm form.

Having established which parameters are identifiable and the most efficient form of algorithm to be used using synthetically created datasets developed in DigSilent in chapter 10, chapter 11 tests the methodology against real terminal data collected from transient data at a combined cycle power plant connected to the UK national grid. The chapter details the aspects that were successful in using the method and the challenges that were faced in proceeding with the parameter identification.

Chapter 12 draws general conclusions on this research and suggests possibilities for the direction and nature of further work.

1.3 Contributions to published literature

- *Parameter Estimation of Synchronous Machines using Particle Swarm Optimisation.* G. Hutchison, B. Zahawi, D. Giaouris, K. Harmer, B. Stedall. Singapore : IEEE, 2010. IEEE International Conference on Probablistic Methods Applied to Power Systems.
- *Sychronous Machine Parameter Identification using Particle Swarm Optimization.* G. Hutchison, B. Zahawi, D. Giaouris, K. Harmer, B. Stedall. Brighton : IEEE, 2010. IET International Conference on Power Electronics, Machines and Drives.

2. Steam Generation

Steam generation involves the creation of pressurised steam which is used to rotate a turbine that is coupled to the rotor of a synchronous generator to generate electricity. Steam boilers convert the thermal energy from the combustion of fuels into steam. This is used for electric power generation and industrial process heating. Figure 2 below characterises the steam turbine power plant in a simplistic format.

A steam turbine power plant has many aspects that define its behaviour. The focus of the project is predominantly power systems based. Modelling an entire power station plant and then performing parameter identification on primarily mechanical systems is unnecessary. For this reason the focus of this section is the steam turbine speed governor control. There is however, a basic description of how the turbine is driven also included.

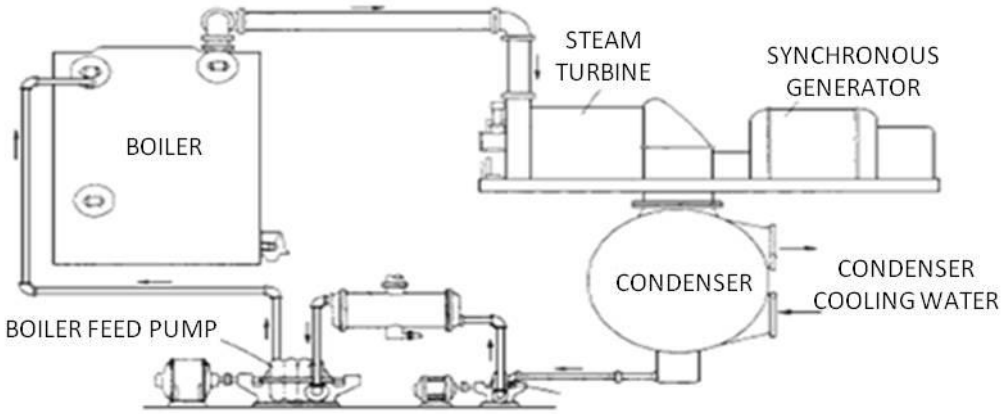

Figure 2 A Simple Power Plant Structure (1)

Figure 2 shows a boiler feeding a steam turbine. The steam generated by the boiler turns the turbine blades and thus the rotor of the synchronous generator, which generates electricity. The boiler itself is fed by a furnace. The furnace is an enclosure for the combustion of fuel. The enclosure confines the products of combustion and is capable of withstanding the high temperatures and pressures developed. Its dimension and geometry are adapted to the rate of heat release, the type of fuel, and the method of firing so as to promote complete burning of combustible materials and provides suitable disposal of the ash. Water-cooled furnaces are used with most boiler units, for all types of fuel and varying methods of firing. Water cooling of the furnace walls reduces the transfer of heat to the structural members; the temperature of which must be limited to maintain strength. Water-cooled tube construction facilitates large furnace dimensions and the usage division walls allow for an increased surface area of

heat-absorption in the combustion zone. The use of water-cooled furnaces also reduces the external heat losses.

The furnace heats water to create steam. Steam flow rates and operating conditions vary dramatically from one boiler to another: from 0.1 kg/s to more than 1260 kg/s and between 0.10 MPa to 31.0 MPa (2).

Once the steam is initially created, the addition of heat to steam after evaporation increases the temperature and the enthalpy of the fluid. Heat is added to the steam in boiler components called superheaters and reheaters. The advantages of superheaters and reheaters in power generation result from thermodynamic gain in the Rankine cycle and from the reduction of heat losses due to moisture in the low-pressure stages of the turbine. With increasing steam pressures and temperatures, more 'useful' energy is available. However, advancing to higher steam temperature is often restricted by the strength and the oxidation resistance of the steel and the metallic alloys available.

The term superheating is applied to the higher-pressure steam. The term reheating is given to the lower-pressure steam which has given up energy during expansion in the high-pressure turbine. With high initial steam pressure, one or more stages of reheating may be employed to improve the thermal efficiency.

The steam leaving the superheaters goes through the emergency stop valves and associated governing valves before entering the high pressure turbine. The emergency stop valves and governing valves are housed in steam chests. These steam chests are manufactured from closed die alloy forgings welded together, or from alloy castings. The steam chests are normally mounted alongside the turbine. There are conventionally four steam mains, together with four emergency stop valves and four governing valves which are normally arranged so that two are found on each side of the turbine. The governor valves control the steam flow entering the turbine. Since the generator converts mechanical energy to electrical energy, the governor valves control the generator power when the machine is synchronized to the grid. Modern power plants use the governor valves to throttle the steam flow during turbine run-up to speed.

2.1 Steam Turbines

Steam turbines are the most common prime movers in large scale power generation and can be manufactured in many different forms and arrangements. Steam turbines' upper range in output capacity is over 1,500 MW, termed 'Ultra super critical turbine systems'. The largest

ones are used to drive generators in central power stations in high efficiency systems. The differing steam turbine types can be significant in the way that they are dynamically modelled and are classified descriptively in various ways.

- By steam supply and exhaust conditions, e.g., condensing, non-condensing, automatic extraction, mixed pressure (in which steam is supplied from more than one source at more than one pressure), regenerative extractions, reheat.
- By casing or shaft arrangement, e.g., single casing, tandem compound (two or more casings with the shaft coupled together in line), cross-compound (two or more shafts not in line, often at different speeds).
- By number of exhaust stages in parallel as regards steam flow, e.g., two-flow, four-flow, six-flow.
- By details of stage design, e.g., impulse or reaction.
- By direction of steam flow in the turbine, e.g., axial flow, radial flow, tangential flow. In this country, radial-flow steam turbines have not been used; there are quite a few such machines abroad. Axial-flow units dominate; some small turbines in this country operate on the tangential- flow principle.
- Whether single-stage or multistage. Small turbines, or those designed for small energy drop, may have only one stage; larger units are always multistage.
- By type of driven apparatus, e.g., generator, mechanical, or ship drive.
- By nature of steam supply, e.g., fossil-fuel-fired boiler, or 'light water' nuclear reactor.

Any particular turbine unit may be described under one or more of these classifications, e.g., a single-casing, condensing, regenerative extraction fossil unit, or a tandem-compound, three-casing, four-flow steam-reheat nuclear unit.

In steam turbines, high enthalpy (high pressure and temperature) steam is expanded in nozzles (stationary blades) where the kinetic energy is increased at the expense of pressure energy (increase in velocity due to decrease in pressure). The kinetic energy (high velocity) is converted into mechanical energy (rotation of a shaft thus increasing of torque or speed) by impulse and reaction principles. The impulse principle consists of changing the momentum of the flow, which is directed to the moving blades by the stationary blades. The jet's impulse

force pushes the moving blades forward. The reaction principle consists of a reaction force on the moving blades due to acceleration of the flow as a result of decreasing cross-sectional area.

2.1.1 Turbine Control Systems

There are considered four main functions of a turbine governing system (2):

- To limit the speed rise to an acceptable limit upon a load rejection (when the unit is suddenly disconnected from the load).
- To control the power that is generated by controlling the position of the steam governing valve (or fuel valve in gas turbines).
- To control the speed of the turbo generator[3] during initial run-up and synchronization.
- To match the power that is generated to the power that is required by the load by responding to frequency changes (only when the generator is operating in islanding mode (i.e., alone), independently from the grid).

The limiting of speed rise during load rejection is critical to the safety and function of the generation system. If the circuit breaker connecting the generator to the grid opens during normal operation, the shaft speed will increase significantly due to the elimination of the opposing torque produced by the generator, causing serious damage if not protected against using schemes like over speed relay protection. The steam flow must be reduced immediately to limit the speed rise. Most machines have a separate over speed trip. This ensures the safety of the plant if the governing system has a critical failure. When a load rejection occurs, acceleration sensors trip the steam valves on high acceleration. The characteristics of the turbine system under load rejection are considered applicable more so when identifying the electrical machine characteristics as discussed in Appendix 1.

All steam turbines have at least two independent governors that control the flow of steam. The first shuts off the steam supply if the turbine speed exceeds a predetermined maximum. It is often called an emergency trip. The second, or main, governor throttles the flow of steam to maintain constant speed (in units not synchronized to a grid) or to vary the load (in units synchronized to a grid). The governors of extraction, mixed-pressure, and back pressure

[3] In the context of this work, turbo generator is a term describing either two or four pole synchronous machines that are conventionally found in larger gas and steam turbines.

turbines control the steam flow while the speed and pressures vary. These governors are usually extremely complex.

2.1.2 Speed Governors

The speed governor reference is the most important input used in turbine control. Speed control can be done by the operator or automatically. Generally, prior to synchronising the synchronous generator with the grid, the typical range of the speed reference is from 3 percent (minimum controllable speed) to 104 percent (highest speed at which the turbine generator is capable of synchronising). Once the synchronous machine is synchronized with the grid, the overall range of the speed reference is limited to typically between 94 and 106 percent. Before synchronising however, the rate of increase of the speed reference can be determined by the operator. The rate of decrease in the speed reference is normally constant. When the turbine generator approaches synchronous speed, the rate of increase of the speed reference will change. The new rate of increase of the speed reference is compatible with the auto synchronising unit. This is usually selected to provide fast efficient synchronising with the grid. Once synchronised with the grid, the rate of increase of the speed reference is typically set to travel the range from 0 to 6 percent in 1 minute. The governor speed reference is then used to load the machine.

2.2 Steam Turbine Modelling

Power plants and steam turbine models have become more prevalent, increasing the need for dynamic analysis of power systems in order to calculate operational characteristics or efficiency of function. Monitoring conditions in this form of heavy industrial environment can be considered hostile, with an increase in noise generated on signals. Turbine models are generally considered to fall into one of two categories; those being either used for plant studies and controller designs, or those used to analyse performance of turbines. Ray (3) develops a non linear model for a steam turbine controller and mathematically models the performance rather than modelling empirically to define parameters. The model produced is more complicated than other simpler models (4), but because of this, allows a further understanding of the turbine performance including the possibility of fast valving, which may not occur in the other models.

Models considering turbine performance analysis and turbine cycle efficiency like that by de Mello (5), who derive dynamic responses for boiler pressures are highly complex. This level of detail is required when deriving a thermo dynamic model of the turbine. Due to the nature of power system stability studies, in which only a preliminary level of detail (i.e. constant of

inertia, governor characteristics) is required, this would drastically over complicate the model to be derived with no real benefit. This is likewise the case seen in Lo *et al's* (6) work. The results presented based on the model adopted produce accurate characteristics that are favourable when compared to the empirical data presented. The level of data required to achieve this however is also not realistic.

Chaibakhsh and Ghaffari (7) present a nonlinear model of a steam turbine using a genetic algorithm for optimisation of the model. Parameters are also confirmed empirically. Due to the nature of the heat extraction system, heat transfer forms empirical equations, thus in this format the utilised system is not transferable from one turbine to the next. In this format, although the turbine model could be tailored to application specific turbines, it could not be considered suitable for the considered application as, operation data may not be freely available in this regard.

The IEEE committee of power engineering (8) present models for fossil fuel steam turbine and speed governors applicable to the design of the models. It is seen that the governor models do not utilise a dead band (Figure 3). This aspect is an area of interest as given the use in some dynamic studies, it is necessary to characterise this to accurately represent the system. In normal larger power system studies, these dead bands are not normally represented. To include a dead band in the model is an area of debate with regard to this work. This is because, although it is not necessary to model the dead band for large scale studies, it may be necessary to model the turbine accurately (i.e. dead band of governor included) when considering a single machine in dynamic studies. This is predominantly because if the dead band of the governor was not considered, the characteristics of the turbine would be shifted to compensate for this as well as the characteristics. Ultimately the use of a dead band in this work is not seen to produce sufficient benefit in regard to the turbine response to justify its inclusion.

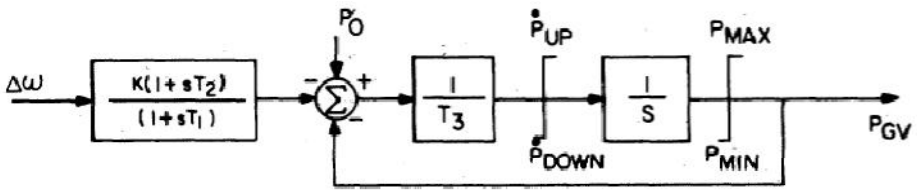

Figure 3 General model for a steam turbine speed-governing systems (8)

The committee report continues to present a flexible model for the steam turbine itself as seen below in Figure 4. For the purposes of this project, this level of detail could be

considered quite suitable. However WeissGeber (8) comments that, in practicality the dynamic mechanical changes in the model could be too rapid in comparison to the reality due to 'the isolated time constraints utilised'. This is because the real turbine is interdependent from one boiler stage to the next, thus the single feedback loop can produce "deceptively favourable results".

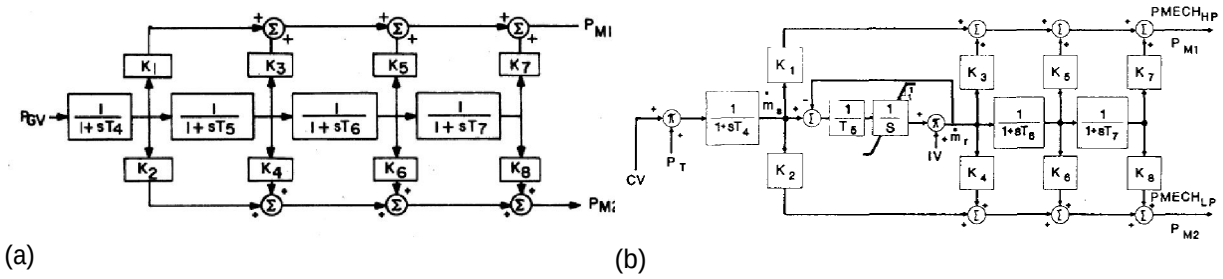

(a) (b)

Figure 4(a) General (8) and (b) revised models (9) for turbine systems

In addition to the committee report (8), the working group on prime movers and energy supply models for system dynamic performance studies (9) have taken the existing turbine model as shown in Figure 4(a) and enhanced it. It was noted by the working group that the existing model did not account for the controlling of intercept valves in reheat turbines. Figure 4(b) characterises the addition of this to the turbine to a reasonable level given its relative simplicity. However, one concern is that the use of the intercept valves throughout the power industry is not consistent. Model (a) is a versatile model that allows for many differing varieties of turbines to be characterised without need for alteration of the model itself, merely the constants. Whether the addition of the intercept valves to the model, and the control that it requires will offer the same versatility and accurate characterisation is irrelevant in that, if a generic model is required, the addition of this additional aspect would introduce modelling issues to the turbines that do not utilize intercept valves.

One aspect that the working group introduces is the use of 'fast valving' in the turbine models. Fast valving is the opening and closing of steam valves at high speeds to facilitate quicker changes in output power and turbine performance (10). Fast valving also maintains system stability after a severe fault by reducing mechanical input power to the turbine. Because of the change in the turbine characteristics a differing governor model must also be applied as the two adopt a symbiotic relationship where the turbine model cannot function adequately without the governor controlling its modified performance. Because of the coupled nature of the governor and the turbine, and because fast valving is not adopted throughout the power industry, the adoption of the newer model is also undermined. The capability of the conventional model to characterise systems with fast valving is unknown.

2.3 Summary

Significant work has been done in the characterisation and modelling of steam turbines. There does however appear to be a separation between what would be useful for thermodynamic modelling and that of the work that is considered here, where limited data is available and an intricate model is not practical for power system transient stability studies.

Ultimately it can be seen that the model that is developed for this work needs to be of an appropriate level of detail that allows it to be used in power system studies. This allows for a more robust interpretation of the turbines function than can be found in some of the more refined thermodynamic models seen in this section.

3. Gas Turbines

Through differing advancements in the technology, open cycle gas turbines have reached an efficiency of around 43 - 44 percent, with a firing temperature (inside the combustors) of up to 1371°C (12). The efficiency of the turbine is limited by the metallurgy of the first stage of moving blades in the turbine. In gas turbine generation, natural gas is ignited in air. The energy released from this burning is used to drive the turbine blades and the synchronous machine's rotor. The best heat rate in gas turbine systems have been realised by combining the gas turbine cycle with a steam turbine cycle. Heat recovery steam generation (HRSG) is used to generate the steam for steam turbine. HRSG is usually developed in the form of a heat exchanger which transfers the excess heat from the waste gases of the gas turbine and heats water to produce steam for a steam turbine. This arrangement is called combined cycle. Combined cycle plants (CCGT) are specifically mentioned on the basis that the recorded terminal data used as part of the final testing of this work is from a combined cycle gas fired power plant.

There are considerable advantages in a combined cycle system, the improved efficiency over convention single gas turbines being of major significance. This improved efficiency comes from the higher utilisation of the total enthalpy of the plant through the combination of the gas turbine Brayton cycle and the steam turbine Rankine cycle (thus originating the term combined-cycle). A typical simple-cycle conventional fossil fuel plant (e.g. simple cycle gas turbine (GT) or coal burning steam turbine (ST) plant) has an efficiency of 30-35%, while a combined cycle power plant can have efficiencies exceeding 55%. Combined cycle plants have become more prevalent since the 1990's. Previous to this, open cycle plants were most common as petroleum and natural gas reserves or the relative price at the time were not considered an issue that impacted on their use. The basic topology of a CCGT plant is seen in Figure 5.

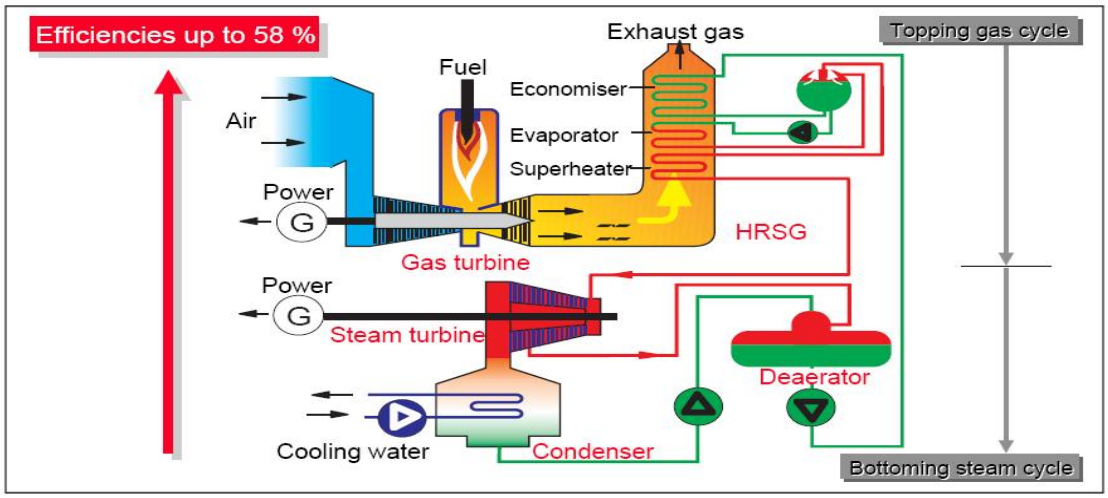

Figure 5 Basic topology of a combined cycle gas turbine (11)

Combined-cycle power plants can be configured in a number of arrangements. These can be categorized into two main categories, single-shaft units and multi-shaft units. The most common form of arrangement in combined cycle plants is using either two or three single shaft gas turbines powering a steam turbine of equal size on the exhaust heat that they produce.

Figure 6 below illustrates a simple-cycle, single shaft gas turbine. The power turbine operates on the same shaft as the high-pressure turbine and compressor. This is different to the two shaft gas turbine which has a variable speed range. Needless to say, when considering power generation the variation in frequency range is not particularly necessary as it would be expected to be running at 50 or 60 Hz. For this reason most heavy duty power generation gas turbines are single shaft designs.

The portion of the gas turbine which consists of the compressors, the combustors, and the high-pressure turbine is called the 'gas generator'. The power developed by the high pressure turbine is used to drive the compressors. The starting requirements for a multi shaft gas turbine can be considered less than the ones for a single-shaft gas turbine. This is because there is a reduced inertia from the spool, which carries the compressor and high pressure turbine. In a single shaft turbine the compressor turbine and the power turbine are coupled as one, meaning the inertia of the single shaft is far higher than that of the dual shaft. Because of this, its transient stability characteristics are different.

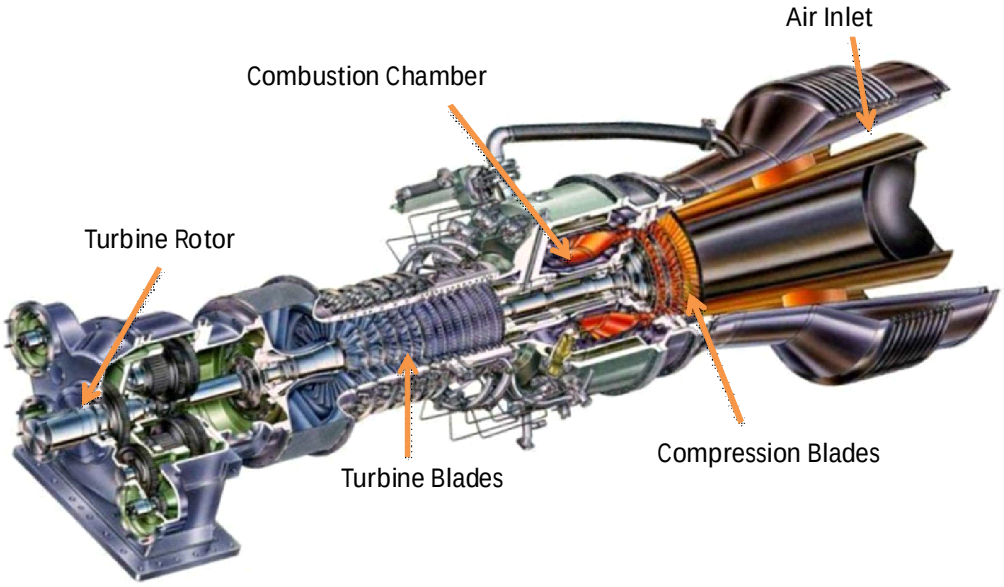

Figure 6 Diagram of a single shaft heavy duty gas turbine (12)

Gas turbines use axial and centrifugal compressors. Small gas turbines use centrifugal compressors while all the larger ones use axial compressors. Given the focus of this work is on large scale power generation attention is given to axial flow compression. Axial flow compressors increase the pressure of the fluid in the turbine by accelerating it in the rotating blades and then diffusing the fluid in the stationary blades. Each compressor stage consists of one row of stationary blades and one row of moving blades. There is also an additional row of fixed blades (inlet guide vanes). These are fitted at the inlet to the compressor so to direct air at the necessary angle to the first stage of rotating blades. An additional diffuser is used at the compressor discharge which diffuses the fluid further before it enters the combustors. The overall pressure increase across a compressor of a newer design of gas turbine is typically between 20:1 and 40:1. Axial flow compressors are considered more efficient than centrifugal compressors (11). They are also usually much smaller and run at higher speeds. Once the fuel has moved through the axial flow compressor it reaches the combustor.

Heat is added to the air flowing through the gas turbine in the combustors. In the combustor, the gas temperature increases while the pressure drops slightly. Combustors can be considered to be direct fired air heaters. The fuel is burned stoichiometrically[4] with around 25-35 percent of the air entering the combustors. The combustion products mix with the remaining air, which arrives at a suitable temperature for the turbine to function efficiently.

[4] Stoichiometrically in this case describes a burning process producing a balanced chemical reaction on both sides.

The three major types of combustors are tubular, tub annular, and annular. All combustors, despite their design differences, have 'Recirculation', 'Burning', and 'Dilution zones'.

In the recirculation zone, fuel is evaporated and partially burned. The rest of the fuel is burned completely in the burning zone. Air is mixed with the hot gas that is in the dilution zone. If the combustion of the gases is not complete by the end of the burning zone, dilution air can chill the hot gas. This reduces the possibility of complete combustion of the fuel. There is however, evidence that combustion can occur in the dilution zone. This occurs if the burning zone is run in an over-rich condition. During transient conditions, the fuel to air ratio varies. In the acceleration phase, the ratio is high, during the deceleration phase the ratio is low. Because of this, the combustor is able to function with differing fuel to air mixes. Combustor performance can be measured by the relative efficiency of the combustion and thus the pressure drop across the combustor. Distribution of outlet temperature is also a factor defining performance. Combustor efficiency is seen to be a measure of combustion completeness. The efficiency is the ratio of the increase in gas enthalpy and the heat input of the fuel.

In dual shaft turbines there is a second stage of compression in order to increase the overall gas turbine efficiency. Conventionally in single shaft gas turbines operating in open cycle, once the fuel has gone through the combustors section and turned the turbine blades, excess energy is evacuated with the exhaust gases. In combined cycle plants this excess energy is used to power the steam turbine, boosting plant efficiency.

3.1 Industrial Heavy Duty Gas Turbines

Industrial heavy-duty gas turbines first became commercially available in the 1950's. Because, unlike one of its other applications (i.e. aerospace engines) there were no design limitations with regard to size and weight, the design generally included heavy-wall casings, sleeve bearings, large-diameter combustors, thick airfoil sections for moving and stationary blades, and large frontal areas. The pressure ratios of fuel pressure to external atmospheric pressure the units are capable of achieving have increased from 5:1 for earlier units to 15 to 25:1 (2) for modern units. The inlet temperature for a modern turbine is typically 1093 to 1371°C (12), however with new technologies being developed it is envisaged that this will approach a temperature of 1649°C (12), significantly increasing machine efficiency. The industrial heavy-duty gas turbines normally use axial-flow compressors and turbines. In most North American designs, the combustors are can-annular. European designs use single-stage side combustors. The combustors of these units normally have heavy walls and are very durable. The liners are

designed to produce low smoke and low NO_X emissions. These designs are also flexible as to which fuel is used. The velocity of the inlet air drops in the frontal area of the turbine, resulting in a reduction of air noise. Auxiliary equipment required for the turbine operation includes heavy-duty pumps and motors. Heavy-duty governors are also used in the control system.

3.1.1 Gas Turbine Control

The control system of a gas turbine performs the following functions:

- Controls speed and temperature in the machine during operation.
- Controls the gas turbine during normal operation.
- Provides protection to the gas turbine.
- Performs start-up and shutdown sequence of events.

3.1.2 Speed Control

In many ways the speed control of a gas turbine is very similar to that of a steam turbine, the only difference being more choices available to control the speed of the gas turbine are larger in variation. The speed of the shaft is measured using magnetic transducers on the shaft with a toothed wheel. The transducers provide an AC voltage output with a frequency proportional to the rotational speed of the shaft. A frequency to voltage converter is the used to give a voltage proportional to shaft speed. This measured value of the speed is compared to the required value of the speed. If there is an error several differing methods can be used to control the speed. The fuel valve can be controlled in order to remove the error, as could the mix of air to fuel. Another possible method would be to modify the exhaust settings of the gas turbine. A proportional integral derivative (PID) control system is implemented to eliminate the error within minimal time and without instabilities (oscillations in the speed).

3.2 Gas Turbine Modelling

Gas turbines, and particularly combined cycle plants have become more common since the 1990's. This is generally because, with the deregulation of the power industry, there is an increased demand for high plant efficiency, manoeuvrability and lower emissions in order to make larger margins of profit (11). Because of this, it becomes essential to develop models for gas turbines and also combined cycle plants utilising heat recovery steam generation in order to accurately characterise their performance.

There are varying levels of detail when considering the modelling of gas turbines. The level of detail required is dependent on the application to which the model is to be applied. Fawke *et*

al (13) and Bassily (14) have discussed from first principles the modelling of energy, momentum balances and gas flow dynamics of gas turbines and aero derivative turbines. Fawke *et al* characterises the components of the turbine in order to simulate performance under transient conditions. The presented results show a discrepancy between real turbine performance and modelled performance in the initial and final steady state operating regions. It is inferred that this is due to not characterising the performance of the combustion engine over the entire output range. It is also stated that there was little information available to accurately characterise the turbine behaviour. Using this method, to model gas turbines behaviour under transient would require a full design specification to thermodynamically model the turbine, combustors and compressors. This is clearly unrealistic for the current area of research. Given the purpose of this project, and the assumed limited amount of freely available information to evaluate system parameters, the development of a complex model for a gas turbine or indeed a combined cycle gas turbine cannot rely on the manufacturers design constants. It is likely that the only information readily available will be power output, mechanical load and rotor speed.

Hung (15) models a twin shaft combustion turbine with the conventional approach of producing a linear model based on multivariable functions. The dynamic response of the turbine is based on the idea that the transient thermodynamic and flow processes are quasi static. This principle allows relationships to be derived between the input and output variables whilst moving along the performance curve. The presented results are seen to be encouraging given the function of the method. The validation of the model proves unfortunately, that to confirm the model to be an accurate representation of the real turbine, a significant quantity of design information is required. It can thus be said that although the model is extremely accurate, it is not practical for this work, much like Fawke *et al's* method. Hannett *et al* (16) carries the twin shaft turbine model further. Although not considering the electrical power generation aspect of the turbine, merely the mechanical operators, a robust mechanical turbine model is developed. The model is considered relatively simplistic in comparison to work done in this regard by Hung, however the results are consistent with that which would be anticipated for this form of turbine. A particular aspect presented by Hannett *et al* is the modelling of shaft dynamics under transient perturbations. Under transient perturbations it is possible for the high pressure shaft and low pressure shaft to lose synchronism with each other. Hannett *et al* stipulates that although possible, the likelihood of it actually occurring is very small, thus can be neglected. This is also advantageous as the non linear model of this is highly complex and well beyond the scope of this research, a particular

simple control system can also be utilised to limit the possibility of this occurring. The system simply compares the two shaft speeds, developing an error function which is used with a proportion integral derivative controller to reduce the difference between the two. This is seen in Figure 7.

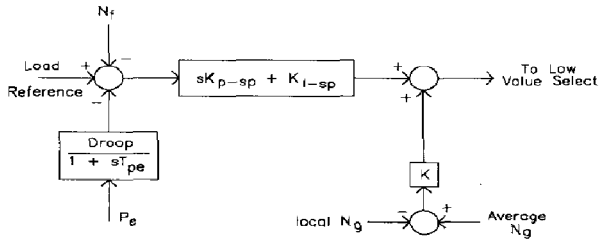

Figure 7 Model of control used to prevent loss of synchronism between shafts (17)

Hannett and Khan (17) note that in typically presented models, like that shown in Figure 8, there is an overreaction in the models operational curves under transient perturbations in comparison to the real systems behaviour. One area of operation and thus modelling that is necessary to consider is that of system frequency (18). The maximum steady state power output of a CCGT system is dependent on ambient temperature and system frequency. In gas turbine systems, if the exhaust temperature is too high then the fuel input is reduced as airflow reduces with shaft speed. Kunitomi *et al* (18) develops a long term dynamic model for transient frequency conditions.

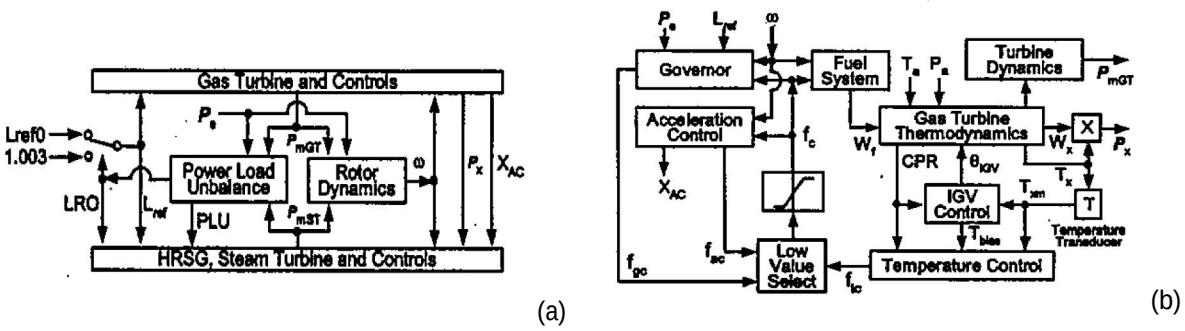

Figure 8 Plant model structure (a) and model structure of a gas turbine and controls (b) (17)

Validation of the Kunitomi *et al* model is done with load rejection tests and a low frequency perturbation on the model. Unfortunately no real experimental validation is provided, thus the conclusions have to be weighed against this point. This is unlike Pearmine *et al* (19), who developed a gas turbine model to characterise frequency response for transmission grid transient modelling. The model is validated against a recorded incident on a gas turbine and its impact on the gas turbine model's output. The authors point out that gas turbines are complex to model accurately, with large deviations in settings and control from one

manufacturer to the next. Due to the 'generic' turbine required for this work, it can be inferred that the model presented is not without merit, however far too complex to be utilised unless many constants for the turbine are assumed within a given tolerance. This takes Pourbeik's (20) work on this area further, showing that consideration has to be given in regard to the relative complexity of how gas turbines output power has a non linear proportionality to ambient temperature, which is a significant factor in defining the frequency of the turbine at large.

Nagpal *et al* (21) used a similar method of modelling to that of Pearmine *et al* who used major disturbances in the North American grid in 1996 to characterise a dynamic model for the gas turbine performance. This also suggests that the relative response of the gas turbine under transient perturbation and can help when considering the characterisation of the synchronous generator under transient. In particular, it may be possible from this to derive the inertia of the rotor and turbine under this particular transient during a rejection of system load.

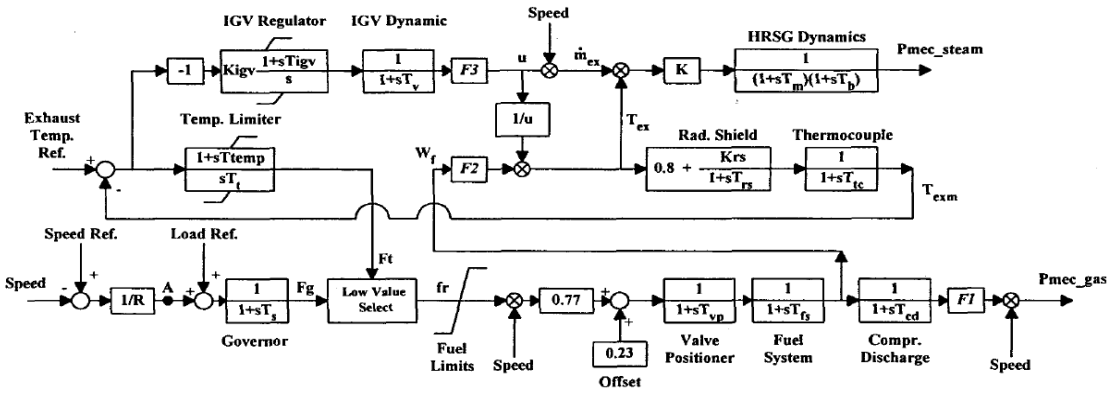

Figure 9 Combined cycle plant dynamic model (22)

Overall as seen additionally in Figure 9, there are many different offerings in the area of modelling combined cycle gas turbine systems ((11), (22) and (12)). Based on the literature presented several points become prominent in terms of defining how accurate the CCGT model actually is. Firstly, the accuracy of modelling of the control loops in regard to dynamic response with particular attention given to power output, frequency response and, ambient temperature is critical. When characterising the use of a heat recovery steam generator model, consideration has to be given to whether a single gas turbine, and thus, a small HRSG system is used. The alternative is, if there are multiple gas turbines, one larger steam turbine system could be used. The characteristics of the system are obviously different to each other when considered to a high level of detail.

3.3 Summary

Ultimately the question becomes what level of detail is required in order to perform an accurate power system stability study? It has been seen that the gas turbine is dependent on fuel, temperature, pressure and varying other aspects which are all critical in dynamically modelling the gas turbine accurately. From a power system analysis point of view it is questionable whether any of this data is available or actually necessary, thus a degree of pragmatism needs to be adopted with regard to the level of detail that the model is required to include.

Ultimately a pragmatic gas turbine prime mover model must be developed for this work. It has been seen that the overly complicated models utilised for thermodynamic modelling of turbines are not appropriate for power system studies. A middle ground in complexity has to be reached which considers the base function of the turbine but does not reach a point that highlights difference in design philosophies from one manufacturer to the next.

4. Synchronous Generators

Synchronous generators are the most widely used machines in power generation. Identifying the parameters of these machines has been a topic of academic interest for several decades in the hope of accurately characterizing their performance. Parameters are conventionally identified through invasive testing. This chapter will give a brief introduction into synchronous machine theory, discussing the conventional processes that allow for parameter characterisation, and then move into modelling and previous work in the area of parameter identification for synchronous machines.

4.1 Introduction

The three phase synchronous machine is a significant contributor to power generation worldwide, with 99% of all bulk electricity generation (2). The machines' high efficiency and ability to supply power (reactive or real) independently of one another makes them a large asset in AC networks around the world. Synchronous generators used for three phase supply usually have a three phase armature winding, conventionally found on the stator and a direct current field winding found on the rotor. There are two general types of synchronous machines, salient and non-salient (round rotor) machines. Salient pole machine construction can be used for machines of all ranges of output and for lower speed ranges. Medium to large size generators[5] that are designed for high speed prime mover inputs like gas combustion or steam turbine input would conventionally adopt a round rotor or 'non salient' design. The rotating field system allows for stationary armatures on which the windings are more easily mounted for a higher voltage whilst avoiding slip rings that carry high currents at high potential differences. DC excitation of the field winding is required, thus slip rings or other brushless excitation systems can be used. When used as a generator, a dc current is supplied to the field winding in the rotor. The resulting magnetic flux cuts the stator windings and the construction is such that three phase sinusoidal currents circulate in the stator windings. These currents give rise to a magnetic field whose angular speed is equal to that of the rotors speed of revolution. An electromagnetic torque is developed that opposes the mechanical prime mover torque.

The stator core is made of insulated steel laminations. The thickness of the laminations and the type of steel are chosen to minimize eddy current and hysteresis losses, while maintaining

[5] In this work medium to large generators are assumed to be two or four pole machines operating above 1500 revolutions per minute and over 40MW in power

required effective core length and minimizing costs. The core is mounted directly onto the frame or (in large two-pole machines) through spring bars. The core is slotted (normally open slots), and the coils making the windings are placed in the slots. There are several types of armature windings, concentric windings, split windings and lap windings. These differing winding methods are used to achieve differing levels of overall machine performance but are not considered in this work.

4.1.1 Rotor Windings

In generators, the main field winding is made from a number of coils in a single circuit which are energized with DC input. This can be fed via the shaft from the slip rings riding on the shaft. It is positioned outside the main generator bearings. In self-excited generators, shaft-mounted exciter and rectifier (diodes) generate the required field current. The shaft-mounted exciter is itself excited from a stationary winding. That the rotor field is fed from a relatively low power, low voltage circuit is a significant factor why these machines have the field mounted on the rotating member and not the other way around. Moving high currents and high power through slip rings and brushes (with a rotating armature) would represent a serious technical challenge, making the machine that much more complex and expensive. This in reality is the reason why a synchronous machines topology is the in this form. An example of a wound rotor is seen in Figure 10.

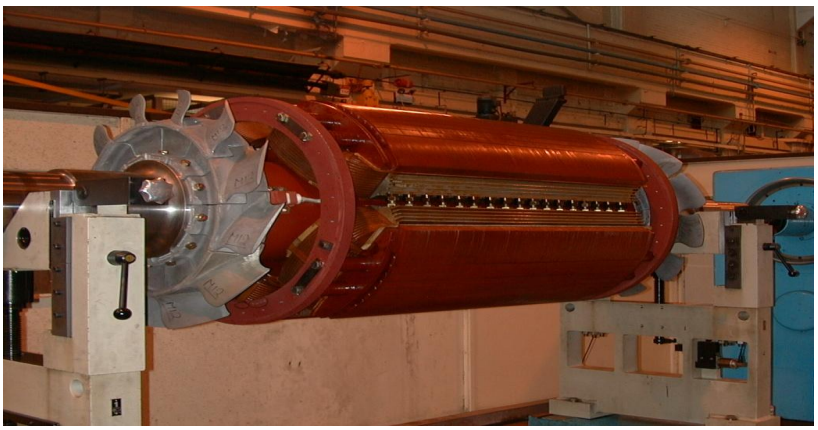

Figure 10 The rotor for a four pole turbo generator

4.1.2 Stator Windings

The magnitude of the voltage induced in the stator winding is a function of the magnetic field intensity, the speed of the rotor, and the number of turns in the stator winding. Coils are distributed in the stator in a number of forms. The aim is to obtain three balanced and sinusoidal voltages having very little harmonic content. To achieve a desired voltage and MVA

rating, the design may vary in the number of slots, and the manner in which individual coils are connected, producing different winding patterns. An example of a stator is seen in Figure 11.

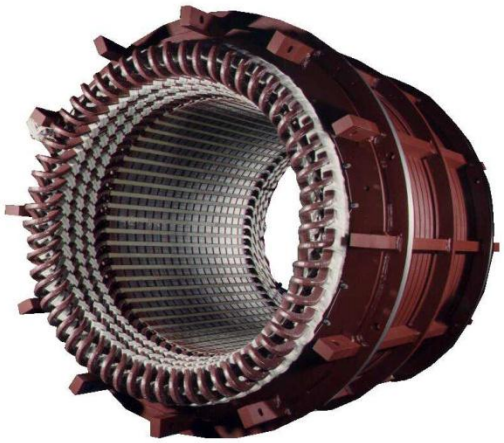

Figure 11 The stator of a synchronous generator

4.1.3 Mechanical and Electrical Behaviour

The mechanical equations defining the function of a rotating machine are very well established and are based on the swing equation of rotating inertia. The swing equation relates the machines rotor torque angle to its acceleration torque. The acceleration torque is the difference between the shaft torque and electromagnetic torque. Constant shaft speed for a given machine is maintained when there is an equal balance between the mechanical shaft and limiting electrical torques. Imbalance in the torques will cause the machine to accelerate or decelerate given the laws of motion of a rotating body, as seen in equations 1 and 2.

$$T_{acc} = J_m \frac{\partial^2 \theta_m}{\partial t^2} = T_{mech} - T_{elec} \tag{1}$$

where T_{mech} is mechanical torque, T_{elec} is electrical torque, T_{acc} is accelerating torque and J_m is mechanical inertia. It also assumes $\omega_m = \frac{\partial \theta_m}{\partial t}$

$$\therefore J_m \frac{\partial \omega_m}{\partial t} = T_{mech} - T_{elec} \tag{2}$$

Assuming balanced sinusoidal conditions and ignoring the effects of magnetic saturation, the steady-state operation of a synchronous machine can be derived using the simple equivalent circuit shown in Figure 12. This level of model is not suitable for the level of power system modelling that this work considers, but gives a basis of understanding.

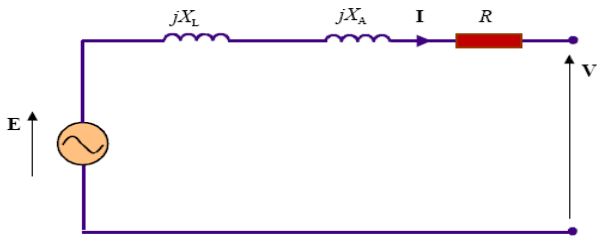

Figure 12 Base equivalence of a synchronous machine

Where the synchronous reactance of the generator X_s is given by $X_s = X_L + X_A$ where X_L is leakage reactance and X_A is armature reaction reactance. E is electromotive force, V is voltage and R is ohmic loss.

Based on the equivalence in figure 11:

$$V = E - jI_A X_A - jI_A X_L - I_A R \tag{3}$$

$$\therefore V = E - jI_A X_S - I_A R \tag{4}$$

The basic techniques for understanding the electrical characteristics of synchronous generators originated from the key concept of transforming stator variables into quantities rotating in synchronism with the rotor. This was developed by Blondel (23), Park (24) and (25), and remains the basis for synchronous machine analysis to this day. The armature currents and voltages are transformed into two sets of orthogonal variables, one set aligned with the magnetic axis of the field winding, known as the direct axis (d-axis), and a second set aligned along the rotor at a position 90 electrical degrees from the field-winding magnetic axis. This second axis is known as the quadrature axis (q-axis). This form of model is known as a d-q model.

Much of the simplification associated with such an approach stems from two key features of this analysis:

1) Under steady-state operating conditions, all of the currents and fluxes, including both those of rotor windings and the transformed armature windings, have constant (dc) values.

2) By choosing the two axes 90 electrical degrees apart, fluxes produced by currents in the windings on one axis do not produce flux linkages in the windings on the other axis. Thus, these sets of windings are orthogonal. This greatly simplifies the flux-current relationship of the model and gives rise to a model structure consisting of two independent networks, one for the direct axis and one for the quadrature axis.

The voltage equations for a synchronous machine with a three phase armature winding and a cylindrical rotor without damper windings[6] can be considered to be:

$$v_d = -i_d R_a + \left(\frac{N_p}{2}\right)\omega_m \psi_d + \frac{\partial \psi_q}{\partial t} \tag{5}$$

$$v_q = -i_q R_a + \left(\frac{N_p}{2}\right)\omega_m \psi_q + \frac{\partial \psi_d}{\partial t} \tag{6}$$

$$E_{fd} = i_{fd} R_{fd} + \frac{\partial \psi_{fd}}{\partial t} \tag{7}$$

$$v_0 = -i_0 R_{fd} + \frac{\partial \psi_0}{\partial t} \tag{8}$$

where v_d, v_q, i_d and i_q are direct and quadrature voltages and currents. R_a and R_{fd} are armature or stator resistance and direct axis field resistance. E_{fd} and i_{fd} are direct axis field EMF and current. ω_m is rotor speed. ψ_d, ψ_q and ψ_0 are direct, quadrature and zero sequence components of flux linkage. v_0 and i_0 are zero sequence components of voltage and current.

The direct axis of a synchronous machine can be considered to have two terminals. These are the direct-axis equivalent armature winding and the field winding, and it assumes that there are no other current paths in the direct axis other than the direct-axis armature winding and the field winding. However, damper-winding currents (in the case of salient-pole machines) or rotor-body currents (in the case of solid-rotor machines) are significant in determining the characteristics of the direct axis. These can be represented by additional windings on the rotor and can be used to characterise the damping effects of the solid iron portions of the rotor poles. This is advantageous given the machine that will be predominantly considered is a large 2 pole generators (26). If the rotor is not laminated the damper winding currents flow in the rotor body as well as the slot wedges, thus giving a very high number of current paths. To model this would be extremely difficult and not provide sufficient benefit in terms of characterisation to justify its conclusion. For this reason the d and q classical winding structure provides a robust characterisation of the rotor. An example d-axis equivalent circuit is seen in Figure 13.

[6] The use of damper windings is discussed later.

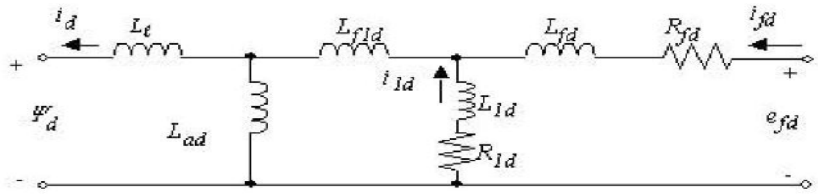

Figure 13 d-axis equivalent circuit (27)

Because there is no rotor winding with terminals on the quadrature axis, the quadrature axis need be represented only as a single-port network as seen in Figure 14. In addition to the quadrature-axis armature winding, varying numbers of damper windings can be included in the quadrature-axis model.

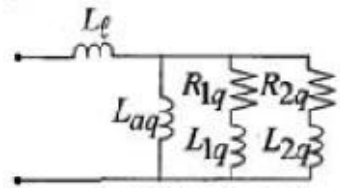

Figure 14 q-axis equivalent circuit (27)

The flux-current relations for the quadrature-axis models are directly analogous to those seen previously for the direct-axis. This is seen for the model which includes two damper windings in the quadrature axis shown above.

4.1.4 Magnetic Saturation

For magnetic materials, saturation is a state when a material struggles to allow the further absorption of a stronger magnetic field past a certain level[7], so although the current can be significantly increased, the magnetic flux density of the material does not go up proportionally.

The equation $B = \mu H$ defines the relationship between magnetic field H, magnetic flux density B and magnetic permeability μ. This is characterised in the hysteresis curve of the material used in the machine, much like what is seen in the typical curve seen below (Figure 15).

[7] Sometimes classified as the knee point

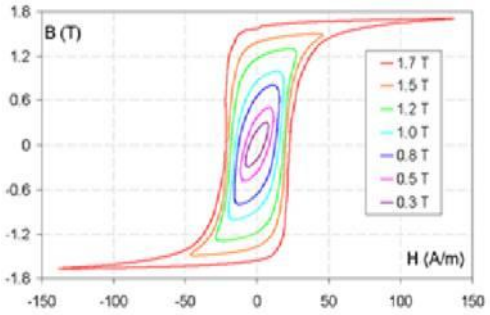

Figure 15 B-H curve of iron

As can be seen from the graph, the BH curve is a non linear relationship, thus the behaviour of a synchronous machine cannot be considered linear when operated into the saturation region.

Saturation occurs generally in the rotor and stator teeth and the rotor and stator core back. The most highly saturated areas in a synchronous generator are the stator teeth and the rotor pole on the trailing edge (for generation). Classically, to measure saturation characteristics an open circuit test is performed, with the armature open circuited and the field supplied with current. Thus, as $V = E_f = \omega L_{ad} i_f = X_{ad} i_f$ (27) the inductance in the windings can be therefore characterised.

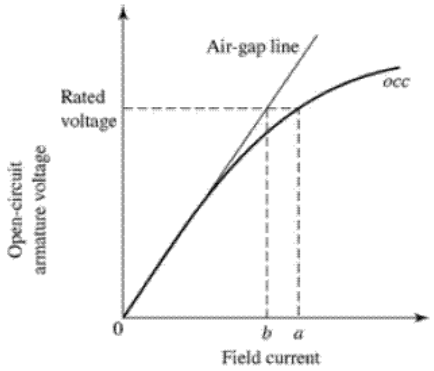

Figure 16 Open circuit characteristics of the synchronous machine (28)

The relative effect of saturation in the synchronous machine is seen in the nonlinearity of the open circuit characteristic curve in Figure 16.

4.2 Typical Invasive Synchronous Machine Testing

Parameter identification in synchronous machine design/operation can be considered invaluable when considering a system where test data and equipment specifications are not forthcoming. It is critical in power systems studies that certain information is either available or derivable so that a valid model can be created.

In understanding parameter estimation, there are many areas of invasive testing that are adopted. The open and short circuit characteristics of a synchronous machine are highlighted because they are essential tests performed but further detail on the varying methods of invasive parameter identification is seen in Appendix 1.

4.2.1 Open Circuit Characteristics

The typical open circuit characteristics are shown below giving the relationship between armature voltage and excitation current on the field winding. For the determination of the open circuit characteristics for a machine, the rotor is driven at synchronous speed with its armature windings open circuited. The line voltage readings of the armature terminals are taken with a cross section of field currents. The range of field current, I_f goes from 0 to the maximum rated current of the winding. Figure 17 shows a linear range of I_f to characterise this. In practice, the line to line voltage of the armature is measured to give the phase to neutral voltage.

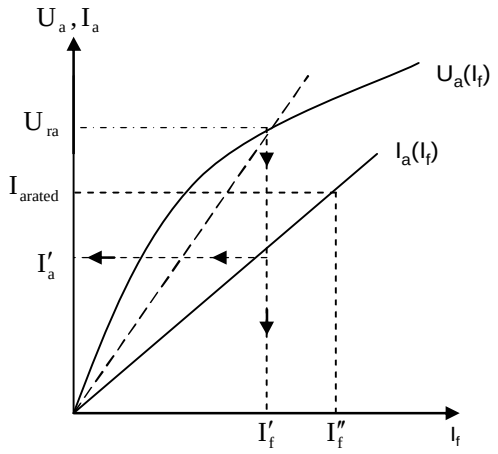

Figure 17 Open and short circuit characteristics of a synchronous machine (28)

4.2.2 Short Circuit Tests

The typical short circuit characteristics of a synchronous machine are displayed below with the relationship of armature current to field current. This is obtained by shorting the armature terminals of the machine whilst driving the rotor at synchronous speed. The armature current varies with the magnitude of field current, usually around or above the rated current. The characteristics seen below also assume a smooth air gap machine to give ideal results.

The short circuit envelope that the short circuit test is very useful in parameter identification as it allows the characterisation of many of the direct axis reactance and time parameters. This is seen in Figure 18 below.

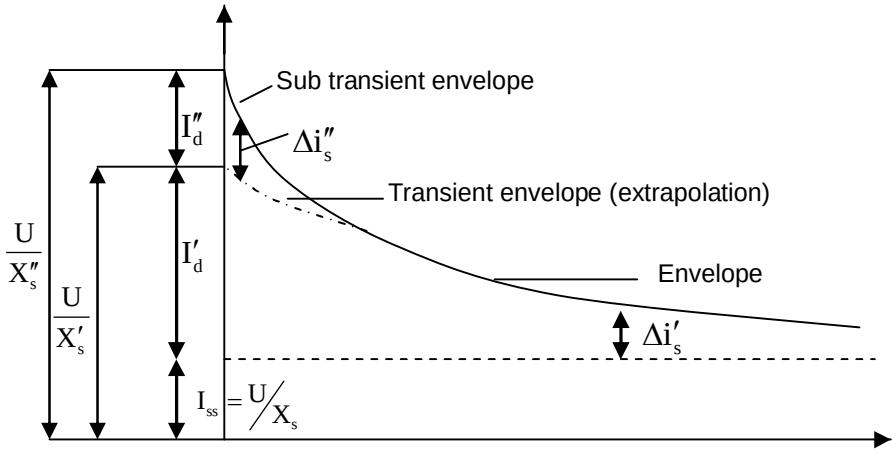

Figure 18 The phase current envelope of a synchronous machine during a short circuit

As can be seen, the envelope allows for the separation of the steady state, transient and sub transient time periods which is very valuable in characterising the performance of a synchronous machine. In using this envelope, it is possible to derive sub transient, transient and steady state reactance empirically. This is seen from the measurements on the Y axis of the diagram.

4.2.3 Saturated Synchronous Reactance

Assuming a synchronous machine with a smooth air gap, the saturation value of synchronous reactance $X_{s\,(sat)}$ is developed using the open circuit and short circuit characteristics of the system (31). The machine is replaced with an equivalent machine possessing open circuit characteristics (magnetization curve) with a straight line at rated terminal voltage. The rough $X_{s\,(sat)}$ is thus seen to be

$$X_{s\,(sat)} \approx \frac{U_{ra}}{I'_a} \qquad (9)$$

It is seen that I_f corresponds to the rated terminal voltage U_{ra} and is found from I'_f and I'_a, which are equal to $I_a(I'_f)$. This is found from the short circuit characteristics of the machine. The saturated value of synchronous reactance is equal to the quotient of the rated terminal voltage and the armature current.

4.2.4 The Slip Test

X_d and X_q of a salient pole machine are obtained by the application of a no load test. This is also known as the slip test. In the test, the armature windings of the machine are excited by a reduced voltage at the rated frequency of the machine. The rotor is driven mechanically slightly above, or below synchronous speed with the field winding not excited and open

circuited. The phase sequence of armature voltage must be that the armature MMF and the rotor rotate in the same direction.

Because of the applied stator voltages, a rotating field is produced in the air gap at synchronous speed (n_1). As stated the rotor is driven at either slightly above or below synchronous speed, thus the d and q axes of the rotor will slip round the armature field alternately. During rotation, the rotating stator magnetic poles are aligned with the rotor iron pole structure, thus with a small air gap there is a small reluctance to the stator MMF. This gives minimal magnetizing currents I_{min}. Later in the time domain, the d axis of the rotor will be in 'space quadrature' to the axis of the stator poles. Because of this, the air gap becomes larger, so the reluctance is small. A larger magnetizing current I_{max} creates the same air gap flux level needed for the applied voltage. With rotation, an increase in armature currents is monitored showing the fluctuation between I_{min} and I_{max}. The fluctuation is related to the frequency and the slip frequency. Ideally this would be low enough so maximum and minimum values of armature currents can be seen, however not low enough to allow the rotor to regain synchronism with the stator rotating field.

Considering armature currents and voltages, X_d can be considered to be the ratio of applied armature voltages per phase to armature current per phase for a d axis position. Likewise X_q is considered in the q axis position. The ratio of the maximum to minimum armature currents is equal to the ratio of X_d/X_q. From this it becomes obvious that if X_d is found from open circuit and short circuit tests for a smooth air gap machine then X_q can be derived from the slip test ratio.

When armature current is at minimum, the voltage induced in the field winding is zero as the flux linking the winding is effectively at its highest and the rate of change of flux linkage is zero. It is also seen however, that when the armature current is largest (I_{max}), the field winding is in the space quadrature to the axis of the rotating armature field and the voltage induced in the field winding is minimal. This is achieved by either monitoring the circuits with oscilloscopes or ammeters. The X_d is thus obtained when the rotor pole axis and the stator magnetic poles are aligned, which is when I_{min} is reached (31). It is seen thus that:

$$X_d = U_{max} / (\sqrt{3} I_{min}) \quad (10)$$

$$X_q = U_{min} / (\sqrt{3} I_{max}) \quad (11)$$

Where the maximum to minimum armature current is proportional to X_d / X_q. This test can only be considered applicable with values of slip less than 0.01 per unit, otherwise the derived reactance's would not correspond to actual synchronous reactance.

4.2.5 Determination of X'd through the opening of a 3 phase short circuit on the armature winding

The unsaturated d axis sub transient and transient reactance's X''_d and X'_d are deduced when the field winding of the machine is excited by field current I_{f0} (giving the no load armature voltage U_{a0})and is driven at synchronous speed with the windings shorted in a star formation. In steady state, the short circuit current can be considered I_{ashort}. As seen below, the switches S are opened and the voltage across the armature terminals is measured. The instantaneous variation of voltage U_a is used to obtain X'_d and X_d thus, less data is needed than other possible methods.

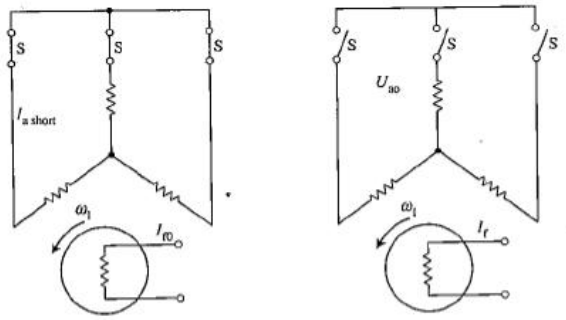

Figure 19 Test to obtain X"$_d$ and X'$_d$ (29)

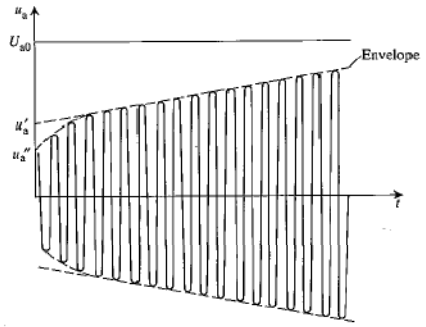

Figure 20 Variation of armature terminal voltage (29)

The armature voltage increases exponentially until it reaches $U_{a0,}$ which is the no load armature voltage. The envelope of this voltage is found from the peak of the armature

voltage and the initial value at instant of switch opening. U''_a is obtained as seen above. From this the sub transient d axis reactance can be considered to be:

$$X''_d = \frac{U''_a}{I_{ashort}} \tag{12}$$

The transient d axis reactance is considered to be:

$$X'_d = \frac{U'_a}{I_{ashort}} \tag{13}$$

4.2.6 D and Q Axis Load Rejection Tests

The d and q axis load rejection tests are considered a simpler test, measuring the voltages and load angles. It is also more advantageous than the slip test because it doesn't risk damage to the machine, which can occur during the slip test. The comparison between the load rejection test and the frequency response test is favourable. This is beneficial as the frequency response test works well in labs, but is more complex and less reliable when predicting saturation characteristics.

In the case of the d axis load rejection test, a synchronous generator will be initially assumed to be connected to a network, having no active power, but absorbing or generating reactive power, thus there is only direct axis flux. The machine is assumed to be under excited, thus not operating in saturation. The machine is then suddenly disconnected from its supply with the armature current at this instant considered i_{sd0}. The armature voltage and field current are measured allowing the calculation of the d axis synchronous reactance's X_d, X'_d and X''_d and the d axis no load transient and sub transient time constants T'_{d0} and T''_{d0}. To obtain parameters under saturated conditions, the same test is carried out but with the machine overexcited as an initial condition.

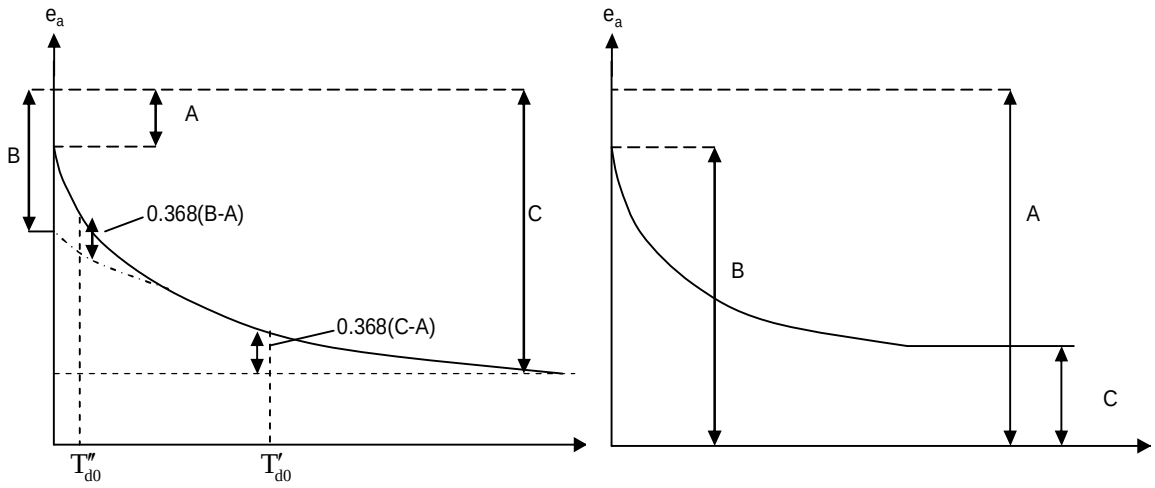

Figure 21 Decaying terminal voltage of a synchronous machine after load rejection (a) and variation of terminal voltage after load rejection (b)

$$X_d = C / i_{sd0} \quad (14)$$

$$X'_d = B / i_{sd0} \quad (15)$$

$$X''_d = A / i_{sd0} \quad (16)$$

where the i_{sd0} is saturated direct axis current. It is also seen from (a) that T''_{d0} and T'_{d0} can be derived from the graph above if field current is measured also. This is seen in Figure 21.

The determination of quadrature axis parameters is performed with a quadrature axis load rejection test. This is only done however, if the armature current only has a quadrature component. The sudden switch off is performed when the armature current has only a quadrature component and the reactive power is adjusted to allow the power factor to be equal to the load angle.

4.2.6 Arbitrary Load Rejection Test

Due to it being difficult to adjust a load to be ideal for a quadrature axis load rejection test, an arbitrary axis load rejection test is utilised. The synchronous generator is suddenly switched off while armature current has both a direct and quadrature component. The load angle is measured as well as terminal voltage. The armature current is measured but split into its direct and quadrature components. ($e_a\cos\delta$, $e_a\sin\delta$, i_{sd0} and i_{sq0}) as seen in Figure 22.

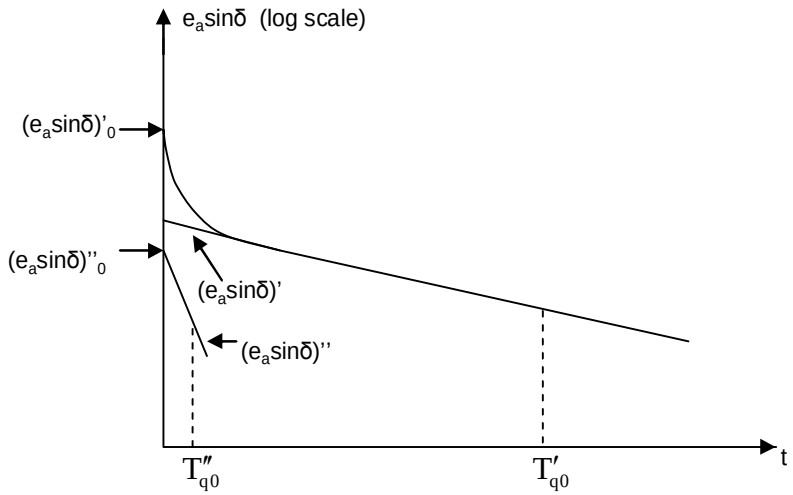

Figure 22 Variation of voltage $e_a \sin\delta$

Based on this, the equations for transient, sub transient and steady state can be obtained:

$$X_q = e_a \sin\partial \big/ i_{sq0} \tag{17}$$

$$X'_q = X_q - (e_a \sin\partial)'_0 \big/ i_{sq0} \tag{18}$$

$$X''_q = X'_q - (e_a \sin\partial)''_0 \big/ i_{sq0} \tag{19}$$

4.2.7 The Zero Power Factor Test

The zero power factor test allows for the identification of the armature leakage reactance. The synchronous generator is loaded with a purely inductive load connected to the armature. Because of the effective resistive voltage drop, a power factor of less than 0.2 is acceptable, thus this load is generally an unloaded synchronous motor of the same rating for simplicity. The generator is driven at synchronous speed, with armature phase voltage and field current measured. Field current is incrementally increased from minimum to maximum levels with these readings taken.

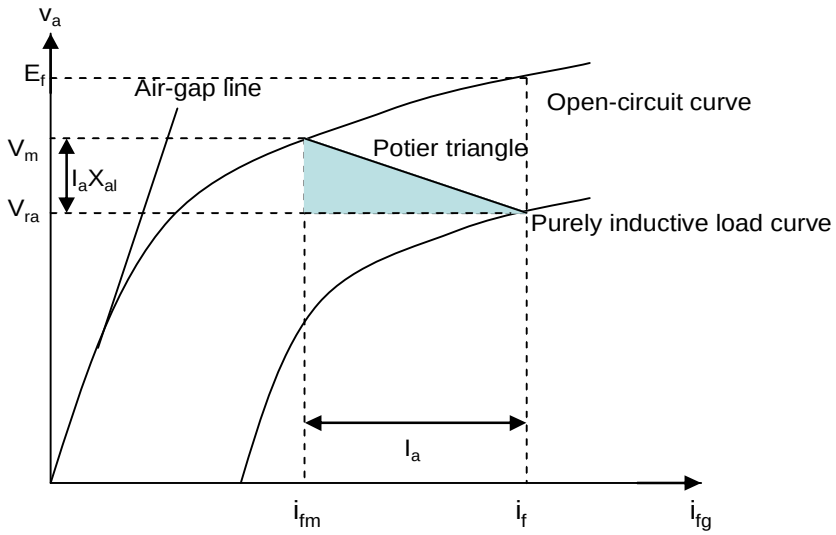

Figure 23 Open circuit and purely inductive load (zero power factor) characteristics

Figure 23 shows the zero power factor characteristics of the synchronous generator with the open circuit characteristics. The zero power factor curve is considered purely inductive with it going between the point where the stator windings are short circuited and the point of rated armature voltage (V_{ra}). The zero power factor curve and the open circuit curve are seen to run in a similar shape although displaced to one another. Neglecting ohmic loss, this can be considered to be due to armature reactance (X_{al}). Because the load is purely inductive, the armature voltage and the magnetising voltage are considered in phase. The MMF and the resultant MMF are in phase and the modulus of the field MMF is equal to the resultant MMF and armature reaction MMF moduli.

The Potier triangle method for parameter calculation is used to determine the I_aX_{al} term of the machine. The other sides are used for other characteristics like field current. The method, when used to identify armature reaction, X_{al}, is dependent on the open circuit characteristics of the machine (unless the open circuit and the zero power factor curves are the same in shape and there is a constant leakage). This is limiting as the curves are conventionally not the same. At high values of field current, the field leakage flux linkage is considered to add to the magnetising flux linkage. This is less significant in smooth air gap machines, however in salient pole machines, this can be more relevant. This is because of the possibility of large leakage flux in long slim poles.

It is also noted that this method cannot be considered applicable for smaller machines due to armature leakage reactance differences that would undermine the validity of the results calculated.

4.2.8 DC Decay Tests in the Armature Winding (Rotor Standstill)

DC decay tests are used for various parameter estimation methods, however must be considered unconfirmed by most sources due to the nature of the results (31). In a direct axis test, the rotor is aligned with the d axis of the stator. A DC voltage is applied between two terminals of the armature windings, with the rotor at standstill and the field winding short circuited. The initial value of the decaying DC armature current is considered around 0.05 to 0.1 per unit. The direct axis decay test data gives a step response in the axis. The measured stator current is considered the sum of exponentially varying current components.

The data provided can bare a resemblance to the direct and quadrature axis time constants of the machine. However, there can be significant variations in the reliability of results generated, hence it not classed as a conventional and reliable technique of parameter estimation.

4.2.9 DC Decay Tests in the Field Winding (Rotor Standstill)

A DC decay test can also be used for the determination of direct axis parameters through performing the DC decay test in the field winding.

The machine is at standstill and a DC voltage is applied to the terminals of the field winding. There are two tests carried out. In the first test, the armature is open circuited with the armature voltage and the decaying field current recorded after the field winding is shorted. The second test involves recording the decaying field current and armature current after the armature is short circuited.

These tests develop values for direct axis time constants and direct axis magnetising inductance. The results from the field winding decay test are more reliable that the armature decay test however questions still remain to the validity of the results when compared to other recognised methods.

4.2.10 Standstill Frequency Response Test

The standstill frequency response test involves the testing of the synchronous machine over a frequency range of 0.001 to 100 hertz. The armature or field winding is supplied with a single phase variable frequency supply. From the test data collected of voltages and currents, the variation of modulus and phase angle of the direct axis operational impedance and the variation of the quadrature axis operational impedance at the particular frequency is

developed. Based on this, a transfer function between direct axis flux and field voltage is produced.

$$G(p) = [\frac{\Psi_{sd}(p)}{V_f(p)}]_{i_{sd}=0} \quad (20)$$

It is seen that the magnitude of the transfer function varies with frequency; these variations are used to define certain parameters in the synchronous machine. These derived parameters are limited however, in that, the standstill frequency response tests are not representative of the parameters of the machine under saturation conditions as the machine cannot reach these levels at standstill due to the large field current required for this to be achieved. Thus to identify parameters more accurately in saturation conditions a non standstill form of frequency response test is needed to be utilized.

4.2.11 Non-Standstill Frequency Response Test

The non-standstill frequency response test allows the determination of direct and quadrature axis operational inductances in synchronous generators at low speed by the application of a modified frequency response test. In the test, the synchronous generator runs at reduced speeds with a phase to phase short circuit between two armature windings with a constant excitation. The instantaneous values of short circuit armature current, the operational armature winding current and the rotor angle are recorded whilst running at steady state velocity. These values are then used to derive the direct and quadrature operator inductances and needed time constants through a process of 'curve fitting' methods.

Other forms of invasive testing for parameter identification are documented in Appendix 1.

4.3 Synchronous Generator Modelling

Having observed the basic theory surrounding the synchronous machine, it is necessary to move onto how they are mathematically modelled. This will allow a basic understanding as to how the synchronous machine model will be developed in this thesis.

When considering the modelling of a synchronous machine, it is critical to recognise the context in which the machine model is being used (29). It is seen that for a large disturbance rotor stability analysis, saturation effects should be adequately characterised particularly if the machine can and does operate in an overexcited form or in the saturation region in order to maximise the relative output whilst minimising costs of raw materials such as steel. The relative effect of saturation and the implications with regard to modelling are discussed by El-

Serafi *et al* (30), who although modelling a small salient pole machine, come to the conclusion that in saturation, the changing of the power/load angle curves are largely defined by mutual coupling between the d and q axes, or a cross magnetising effect. This would have ramifications with consideration to this work if cross-magnetising was included. It would also have an impact in regard to the open circuit curve operating region which the differing generator manufacturers design their synchronous machines to operate around. In this work, it may be difficult to adequately characterise the saturation region because machines operate in different positions on the open circuit curve and unless testing is available in this regard it is unknown where the machine would operate. Marti and Louie (31) and Tamura and Takeda (26) also discuss the modelling of saturation with differing methodologies. In conventional power system transient stability simulations, the saturation of the main flux in synchronous machines is expressed in terms of variable magnetising inductances. Tamara and Takeda choose to represent the saturation region using auxiliary currents which, they infer, will reduce the iterations and thus overall simulation time. Essentially, most of the method is the same as conventionally presented (29) until the saturation region is considered. It is stipulated that although the method attempts to reduce simulation time, significant amounts of data are required and the repeated calculations for coefficients in the machine equations at every time step undermines the methods practicality. In fact the authors present a figure of 35557 iterations to reach an accurate result, which would appear very high.

Marti and Louie (32) introduce a phase domain model for transient system analysis in order for more accurate representation of machine function, including saturation effects. Marti and Louie stipulate that Blondels two reaction theory (23) does not characterise the reluctance in the air gap accurately as it treats it as entirely uniform in the machine which in practicality may not be the case. This is a possibility, and because of its non uniformity, would not translate to a dq model. For the basis of this research it would appear prudent to not consider this aspect due to the relative insignificant difference it will cause to the actual results under transient. Further to this, Dandeno discusses that the model has significant limitations in that, if self and mutual inductance values for the machine windings are not present, the model cannot be utilised. Given the scope of this project, the per-phase model presented is not practical.

Ultimately the overriding conclusion regarding the modelling of saturation is that the accurate characterisation of it requires significant quantities of data to be done correctly, data that is not available for this work. For this reason the ability to characterise the saturation region of the machine is undermined. Thus, it would appear prudent to operate under a linear

characteristic to limit the computational effort required to achieve a functional result that would be appropriate to perform a power systems stability study.

Jackson and Winchester (32) present a model for the direct and quadrature axis equivalent circuits of a solid rotor turbo generator. As seen below with the direct axis representation, the equivalent is significantly complex. Although the Jackson-Winchester model provides insight into the important current carrying paths found in the rotor, the complexity is such that, even with a full set of invasive tests, parameter estimation to this extent would be extremely difficult. Thus the idea of using this model to characterise a machine online, on load, non invasively, using a perturbation to provide parameter stimulation is wholly unrealistic.

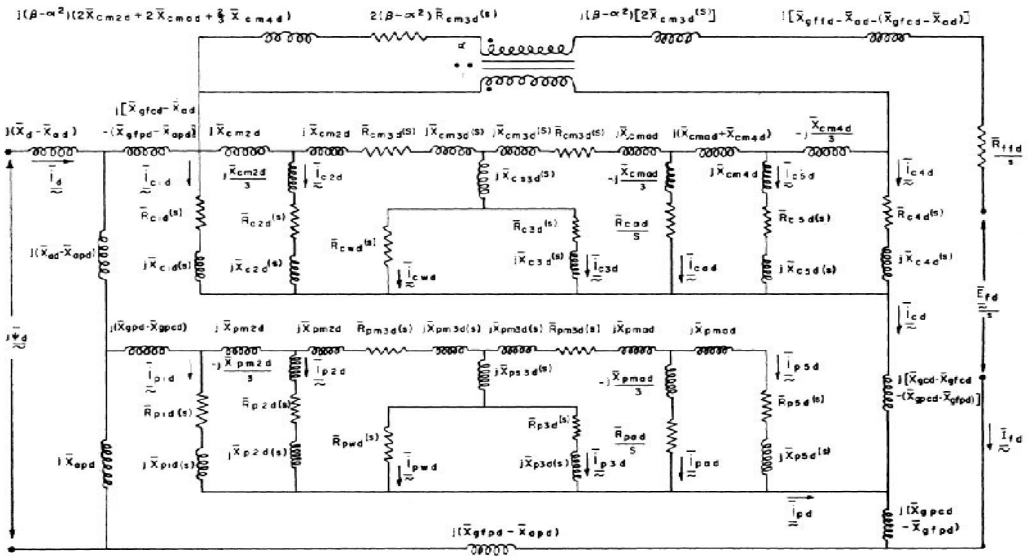

Figure 24 The Jackson-Winchester direct axis equivalence [8]

One aspect of consideration is that of the rotor model. For simplicity, or in the case where it is impossible to make measurements at the field winding terminals, the convention adopted is that of using lumped parameters in order to characterise the effective model. When considering merely the d axis of the machine this would be the d axis operational inductance L_{ad}. This basis of modelling seems to contradict the principle that rotors in steam turbo generators and gas turbines at large are not laminated (26). It thus becomes difficult to model the rotor because, in effect the damper coil currents flow in the rotor body as well as the slot wedges, thus an infinite amount of current paths exist. This undermines to a certain degree the use of a lumped parameter model as seen in (29) or the third order model presented by Kirtley (33). The issue is further emphasised by Dandeno *et al* (34) who illustrate the use of using a single model to define the performance of 3 turbo generators, all with differing rotor designs. It is shown that the damper winding characteristics play a significant role in defining

the rotor characteristics and are also very sensitive to ambient network operating conditions. Canay (35) further supports the position of the difficulty of creating a single model with lumped parameters to encompass machine performance. This evidently becomes problematic when considering the design of a generic synchronous machine model, however the level of detail that Canay and Dandeno *et al* describe the differences is very high, and it may be that from a higher level, these differences are slight.

As noted by Umans *et al* (36), modelling the d axis is considered more complex than that of modelling the q axis. From standard manufacturer data it is not possible to characterise the individual aspects of the model. Due to this, parameter estimation techniques (as discussed in later sections) were developed to derive these parameters. When considering the use of frequency response data as also used by Jack and Bedford (37), Umans *et al* maintain that although frequency response would provide an accurate model, the measurement of current induced in the field winding by the stator winding currents provides sufficient information to model the machine under transient perturbations to an appropriate level.

Another area of consideration to not only that of machine modelling but to parameter estimation in synchronous machines is that of torsional vibration on the rotor and also turbine shafts (38). Excitation systems that are used to damp power angles have been seen to cause a build up of torsional oscillations in the rotor (39). In order to reduce problems like this in the machine, damper windings are introduced to the rotor. There are however, many choices of how to represent the damper windings in a dq model (29). Damper windings are important to the behaviour of the machine in the sub transient region. Examples of d and q axis models of a synchronous machine are seen in Figure 25 Direct (a) and quadrature (b) axis representation of a synchronous machine Figure 25.

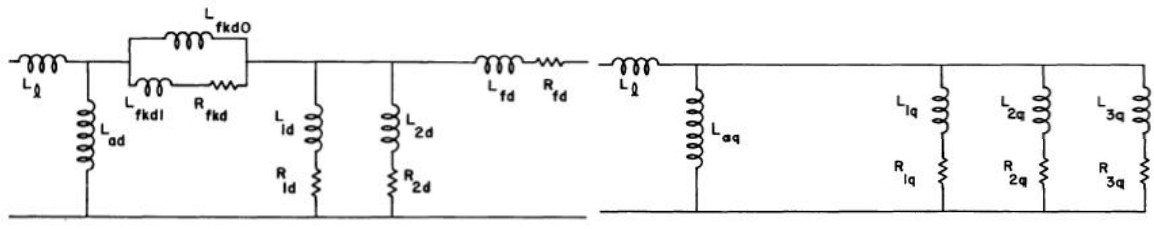

(a) (b)

Figure 25 Direct (a) and quadrature (b) axis representation of a synchronous machine (29)

Based on the work by Jackson and Winchester, and based on observations from many solid iron rotor generators, Schultz *et al* (40) discuss their experience on working with the solid iron rotor model and present the model as seen above. The model above is specified to enable the

determination of machine coefficients to the level of accuracy as required from a power system transient stability study. Unfortunately there is limited validation to the model and its adherence to real test data. Dandeno *et al* (41) (working with Schultz) compares the relative benefits of this model and advocates the use of a model not dissimilar to model 2.2 (29). This model seems to characterise the required parameters for this research in an appropriate fashion, but the relative number of damper windings is a concern as it is yet to be determined whether with the type of perturbations concerned in this work, the damper windings will exert sufficient influence on the final result to allow them to be identified.

Varying forms of models have been observed to be good representations of synchronous machines. The work presented does however raise questions as to the level of detail that is appropriate to the project. It seems that in reality the computational effort required to characterise saturation is significant and wouldn't add a significant extra value results produced.

Additionally, although the Schultz and Dandeno work advocates more detailed damper winding structures, particularly on the q axis, the reality is that the testing for this was done under lab conditions with specific tests. The likelihood of achieving the same level of detail from less severe disturbances is not high. It should also be stipulated that although an accurate model is required, ultimately the 'bulk' properties of the model are required for power system stability studies. Because of this, the level of detail when considering the damper windings should be no higher than one on the quadrature and direct axis respectively.

4.4 Parameter Estimation of Synchronous Machines

Much research has been done on the parameter estimation of synchronous machines. In some respects the current work is similar to the previous attempts, in that, a model has been built that has been used with an optimisation algorithm to allow parameters to be identified. The main areas that are fundamentally different to previous work are that previous work has been done using a controlled perturbation or done invasively under lab conditions. This work will be passive, allowing normal operation of the machine. Previous work has also never included a turbine or excitation model for identification. Although different in many regards, the literature below allows important conclusions to be made as to the best way to proceed.

Vermeulen *et al* (42) propose a technique for online parameter estimation using a "pseudo random binary sequence" to create perturbations in the field excitation applied. Using a parameter estimation algorithm, values for parameters such as d and q mutual inductances, leakage inductances, field and damper resistance are developed. The method appears to

generate favourable results for mutual inductances and field resistance, however the results estimated for field and damper leakage reactance deviated by 30% from the expected value from previously discussed test methods. The manufacturers values for these characteristics are further considered by Canay (35), inferring the necessity to do significant testing of machine characteristics rather than assuming them to be accurate in all cases.

In regard to the method utilised by Vermeulen *et al,* it can be said that the method itself has merits with regard to the relatively small perturbations required to generate parameter values. The only aspect which is not applicable to this research is that there will not be any possibility of invasively disturbing the field excitation of the system. The determination of results is dependent on recorded naturally occurring perturbations on the network itself (through line switching, faults etc), thus although the method produces positive results, it cannot be considered a valid methodology for this current work.

Karayaka *et al* (43) present a parameter estimation technique using real time data and a recursive maximum likelihood method to devise the linear behaviour of the synchronous generator. This is supplemented using neural networks to devise performance characteristics in saturation. The results presented have to be considered quite favourable. One particularly unfavourable aspect of this method with respect to the current work is that the results presented required significant disturbance to the rotor excitation in order to identify parameters. This is completely unfeasible in regard to the current research. This suggests that although the parameters can theoretically be identified, another form of perturbation would be necessary. Further to this, the very nature of the neural network based system would be impractical for this application as the parameter identification will be required to function over a broad range of generator sizes and for differing manufacturers who utilise differing design philosophies. This is different to the many journal papers that have considered parameter estimation for a single machine (44), (45), (46), (47), and (48). Because of this, the neural network based system of identifying large quantities of data in order to predict behaviour of a system has no credibility when there is not sufficient data to 'train' the neural networks into set behavioural patterns.

Karayaka *et al* (49) also present the results of the identification of a 460MVA large steam generator, with no consideration given to the turbine or excitation control. The linear parameters are derived using an output error technique in conjunction with a recursive estimation which seemed to produce reasonable results. The saturation region results are

again seen to be derived from a neural network based method, which, as previously stated cannot be considered practical given the application being considered.

Wamkeue *et al* (50) introduce a modified least square technique which re-weights each iteration to more accurately estimate the machine parameters. The method was tested on a hydro generator under large disturbance, producing reasonable results however given the requirements of this project this method must be considered unsuitable unless it was proven that the method functioned satisfactorily under small signal perturbations that were not deliberately introduced.

Tsai *et al* (51) use the maximum likelihood algorithm (52) in order to identify the linear operating conditions of the electrical machine. Again, this appears to be reasonably successful in the identification of parameters. The results presented for the machine in saturation however are less successful, with the authors stating the results showed "A monotonic dependency on machine MMF" which supports the decision to neglect it in the identification process. Shultz, Gutman and Bhat also question the choice of model (53), inferring that the choice of the Potier saturation model[8] was ill suited to machines with a salient pole configuration. Tsai *et al's* response to this was that other Potier reactances were considered but no other values improved the model significantly. This suggests that if the Potier model has limitations in its ability to accurately characterise the saturation region, and no other methods are significantly better, the decision to neglect saturation was appropriate when considering parameter identification.

Zhao *et al* (54) utilise the least square estimation technique to develop synchronous machine parameters. Using this method the estimated values were within 5% of the real value which would be considered sufficiently accurate given the application. The characteristics of the machine were not considered in saturation under the presumption that given the size and expense of large synchronous generators, the machines would not be forced far into saturation under operation. This presumption could be considered very useful given the application that Zhao *et al* discusses is similar to that is considered in this project.

Zhao *et al* also raises a significant point, in that, manufacturer's declared parameters can have large deviations between the stated value and the values developed from physically testing the machine in the open circuit and the short circuit. This raises the question of manufacturer

[8] A description of Potier saturation is found in Appendix 1.

data validity without full compliance testing. It may also need to be considered when modelling and evaluating the results of parameter estimates towards the end of this project.

4.5 Summary

When considering the published material on parameter identification in regard to synchronous machines, the most resonant point noted in many of the articles is the relative simplicity of the models that are used for parameter identification. Specifically second and third order models[9] of the machines have been adopted in the past. This is generally simply down to the computational cost that trying to solve a more significant model would create. The other reason for a simplistic model to be utilised is that, in many of the methods an algorithm is used in order to optimize the output. Because of this it becomes necessary to develop an objective function that can be optimized. This has been done using state space models to optimize the objective function (55) and by using representations of the machine phase current envelope to develop an equation that can be used to define d axis reactances under short circuit conditions (56).

[9] Second and third order models adopt two and three differential equations in their structure respectively.

5. Excitation of Synchronous Generators

As part of a power plant, an excitation system is employed to provide direct current to the field winding of the synchronous machine. The excitation system also provides control and protection to the field voltage and thus the field current. This control allows the control of voltage, reactive power and gives a method of modifying the excitation voltage to give increased stability in the system.

From a modelling point of view, much work has gone into accurately describing varying forms of excitation system behaviour (57). For this reason, developing a model for this project seems unnecessary. It becomes more important to focus on which form of model would be the most suitable to characterise a broad range of excitation systems and which would be most suitable for parameter identification. For this reason in this section, the varying types of excitation will be discussed as well as their respective models before considering literature on parameter identification for excitation systems.

The excitation system used is significantly influenced by the synchronous machine and the application in which it is used (58) (59) (11). Essentially, the excitation system supplies a field current to the field winding of the synchronous machine. As one of its functions the excitation system maintains a stable, constant stator voltage at the terminals of the machine. The excitation system responds to transient conditions that occur on the network the machine is connected to, be it a short circuit fault, line switch, load change or many other possible events. These events all have implications for the synchronous machine and the excitation system that drives its field voltage.

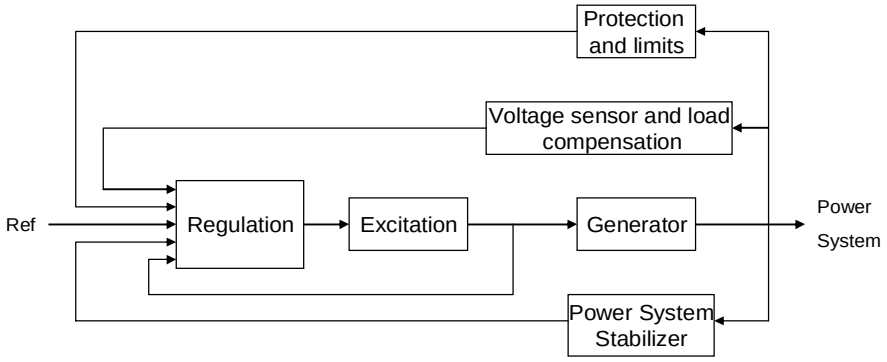

Figure 26 Functional block diagram of an excitation control system (10)

Figure 26 above can be considered to characterise the main aspects of excitation. The excitation system itself gives dc power to the rotor field winding allowing ac voltage to be induced in the stator windings. The regulator uses input data to control the excitation system. A terminal voltage sensor and load compensation detects generator terminal voltage and

compares it with a desired reference voltage. The terminal voltage sensor and load compensation also maintains required network voltage levels. The power system stabilizer would conventionally damp power systems oscillations using inputs like rotor speed and frequency deviation.

The conventional method of excitation was to use a bus fed from the armature of the main synchronous generator. This would feed all field windings for all synchronous generators at the site of generation. This is no longer common however, with a greater emphasis on each generator using its own individual excitation system. The use of individual excitation systems has advantages in that it has a greater reliability, i.e, if a severe transient occurs causing the magnitude of generation to be reduced, the generator feeding the excitation system bus could be tripped off, meaning there would be no method of feeding the excitation of other generators dependent on that bus. This would signify the collapse in voltage for those generators concerned. The generation site also becomes far more complex in layout with the additional bus bar and the related switchgear required for safe operation. The use of a single bus system also precludes the use of automatic voltage regulators (AVR's) to control reactive power of an individual machine to its maximum capability (11).

Excitation systems can be seen to take one of three forms:-

- DC Excitation systems
- AC Excitation systems
- Static excitation systems

The three main types are discussed further in this chapter to give a more detailed understanding of their function. DC excitation systems are the oldest form of excitation system still in service. They use DC machines as sources of excitation, with current fed to the rotor of the synchronous machine using slip rings. AC excitation systems use AC rotating machines as a source of excitation power with rectifiers used to produce a DC voltage source. Ordinarily AC excitation systems are found on the shaft of the turbine. Static excitation systems use stationary rectifiers, controlled or uncontrolled to supply field current for large AC generators. The power for supplying the rectifiers is fed directly from the generator.

5.1 DC Excitation

DC excitation systems use DC machines as sources of excitation, with current fed to the rotor of the synchronous machine using slip rings. This form of excitation uses either a motor or the turbine shaft to drive the excitation system. The excitation system may be separately excited. If separately excited the exciter field is derived from the pilot excitation system using a

permanent magnet machine. These forms of system are not as common as they were in the past, losing popularity in the 1960's to AC excitation systems (11). An example of a DC system is seen below in Figure 27 utilising an amplidyne voltage regulator.

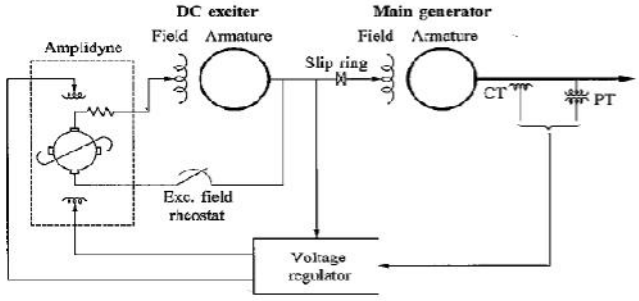

Figure 27 A DC excitation system utilising an amplidyne voltage regulator (10)

The DC1A excitation model (57) as seen in Figure 28 can be used to represent the function of the real excitation system seen above. It can be used to represent most field controlled dc commutator exciters with continuously acting voltage regulation. The model is also seen to be used commonly throughout the energy industry to characterise other forms of excitation systems when limited data on the excitation exists.

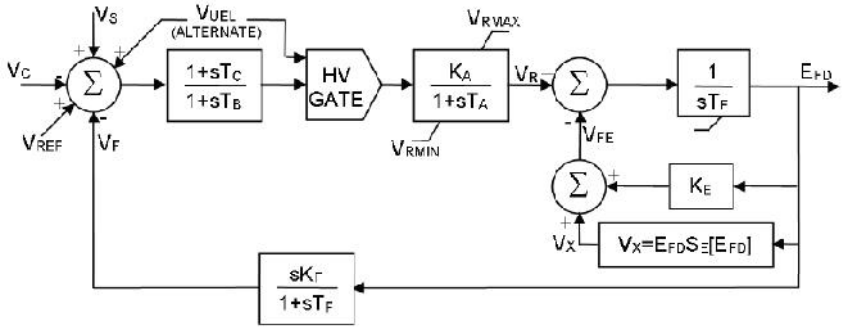

Figure 28 Type DC1A—DC commutator excitation system (57)

In the DC1A model, terminal voltage transducer output is subtracted from V_{Ref} as is stabilising feedback V_f. The power system stabilising signal V_s is added. This gives an error voltage. In steady state V_s and V_f are zero, giving only terminal voltage error. This is then amplified in the regulator with T_A and K_A defining the amplifier power supply limitations. T_C and T_B are used when further, more accurate characteristic modelling is required. Equivalent time constants of the voltage regulator are generally assumed to be very small or zero without and information to the contrary. V_R is used for excitation system control. The value of K_E is defined by the use of a 'Rheostat'. When using a self excited shunt field K_E is equal to 1 in a separately excited exciter. The '$V_X=E_{FD}S_E[E_{FD}]$' block considers the excitation system loading and saturation effects. In some respects the saturation of the excitation machine is impossible

to characterise without manufacturers data. Due to this, it is difficult to give an accurate representation of saturation in the machine. In comparison to characterising the synchronous machines saturation behaviour, this is less critical, as to use the IEEE models available, typical values could be assumed in order make the model function correctly and perform a power system transient stability study (58).

5.2 AC Excitation

An AC excitation system identifies the use of AC machines as a source of excitation power. Ordinarily the excitation system is found on the shaft of the turbine. The AC output of the exciter is rectified to produce direct current to the field winding. The rectification can be embedded on the rotor shaft or be stationary. AC exciters can take varying forms (61) (62) (63), the most significant characterised as either stationary rectifier systems or rotating rectifier systems.

5.2.1 Stationary Rectification Excitation Systems

In stationary rectification, the direct current output is fed through slip rings to the field winding. To use non controlled rectifiers allows the control of the AC exciter field, thus the voltage. This system can be equated roughly to those seen in Figure 29.

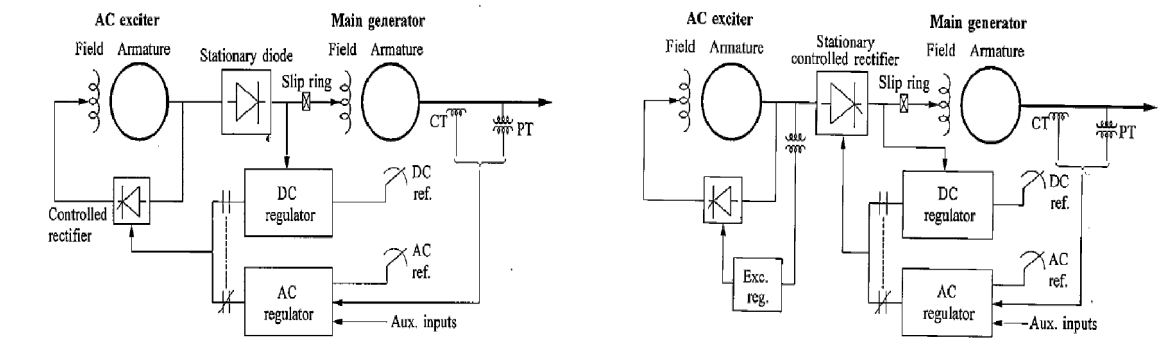

Figure 29 Field controlled alternator rectifier system (a) and alternator supplied controlled rectifier system (b) (58)

The field controlled alternator rectifier system representation is seen to be driven from the generator rotor. The exciter is self excited with its field voltage delivered through the rectifier. The use of a pilot excitation system as the source of excitation system power is equally possible in this case. When controlled rectifiers are used the DC output voltage of the excitation system is directly controlled by the regulator. The regulator controls the thyristor firing sequence. Given the thyristor firing controls, the output of the excitation system, the response time is considered small. From a modelling point of view the difference between the

two topologies is negligible. This is advantageous as it allows both to be characterised using just one model.

5.2.2 Rotating Rectifier Systems

The use of rotating rectifiers removes the need to use slip rings and brushes in the transfer of direct current to the field winding of the synchronous machine. The armature of the AC excitation system and the rectifiers rotate with the main generator. Using a pilot exciter, the rectified output of the pilot excitation system energises the stationary field of the AC main exciter as seen in Figure 30. The automatic voltage regulator controls the AC exciter field which then controls the synchronous machine field winding voltage. This is a brushless excitation system. Fast response in such systems is achieved through high voltage forcing of the exciter stationary winding.

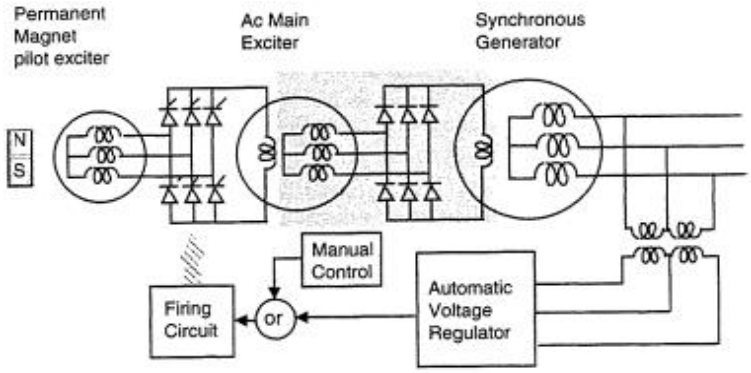

Figure 30 Topology of a permanent magnet pilot exciter (64)

One potential area of conjecture regarding the use of this system is that the brushless excitation system doesn't allow the measurement of the field winding voltage or current of the synchronous machine directly. Voltage control of the generator is achieved through the use of an adjustable DC input setting on thyristor firing circuit as seen above. The inability to monitor field voltage and currently directly is problematic because it would be useful in allowing the use of several more forms of excitation system model. This is because several of the IEEE standard models require field current as an input variable in the model. In reality this is a moot point as it is invariably not measured in a most power plants.

There are varying forms of IEEE standard models that characterise AC excitation systems for synchronous generators and the use of either rotating or stationary rectification to give the DC field requirements. The AC1A model is primarily used for stationary rectifier systems, where a 'non controlled alternator rectifier excitation system' is used (57). The excitation system does not employ self excitation and voltage regulator power is taken from a separate safe source.

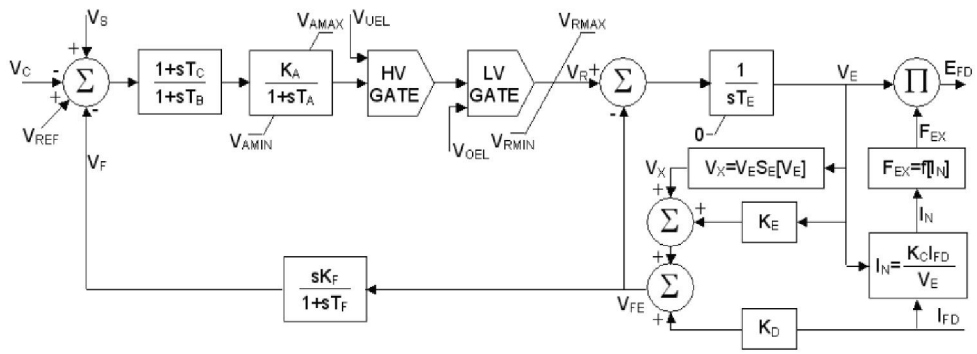

Figure 31 Type AC1A—Alternator-rectifier excitation system with non-controlled rectifiers and feedback from exciter field current (57)

The AC2A model characterises a field controlled system. This is used to model a stationary or a rotating rectifier system. The AC2A is similar to the AC1A aside the presence of an excitation system time constant and an excitation system field current limiting element, the time constant consists of a direct negative feedback which increases small signal response and thus relative speed (57). The structure of the model type requires input of field current in order to function. This is not advantageous given the lack of data that may be available in this regard.

Further models are presented by the IEEE standard 421.5. One particular brushless model of interest is that of the simplified model AC5A as seen below. The system uses a permanent magnet generator in a pilot excitation system and has limited effect on system disturbance. This model is also used commonly to characterise other AC type excitation systems and has the distinct advantage of not requiring field current feedback, much like the DC1A model.

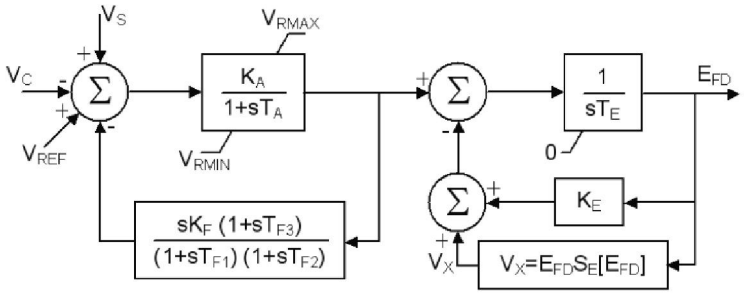

Figure 32 Type AC5A—Simplified rotating rectifier excitation system representation (57)

5.3 Static Excitation Systems

Static excitation systems use stationary rectifiers, controlled or uncontrolled to supply field current for large AC generators. The power for supplying the rectifiers is fed directly from the generator. There are 3 main forms of static excitation that have been utilised in this area:

5.3.1 Potential Source controlled rectifier systems

In this system, the excitation systems power is supplied via a transformer, the primary of which is connected to the generator terminals or a station auxiliary. This form of system is transformer or bus fed static excitation. Because of the structure of the excitation, there is a small time constant. As previously mentioned, the maximum field input is defined by the terminal output, thus, under transient, there is a possibility of voltage collapse[10], though this is offset with field forcing. Field forcing is the application of a higher than steady state excitation voltage under a transient or dynamic event in order to maintain stator voltage at the required level.

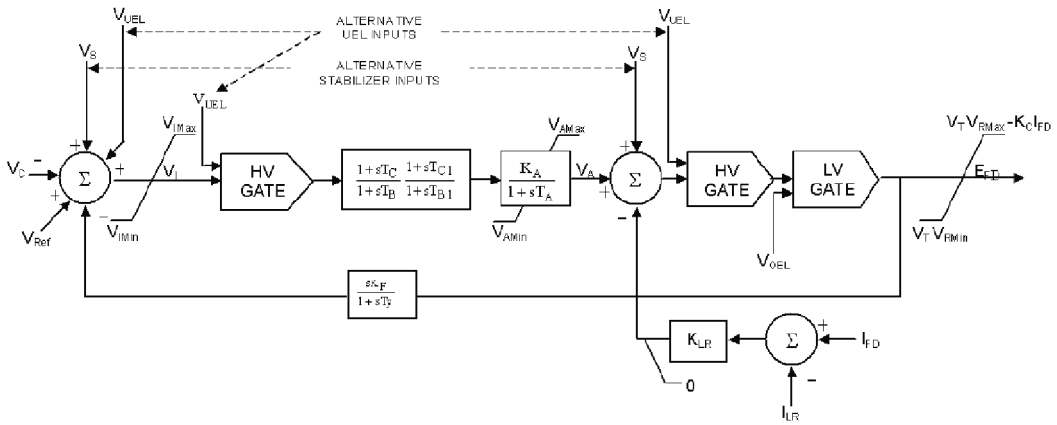

Figure 33 Type ST1A—Potential-source, controlled-rectifier exciter (57)

There are many predefined models set forth by the IEEE. In many of these models, the excitation system ceiling voltage is very high; for such systems additional field current limiter circuits may be used to protect the excitation system and the generator rotor. When considering the modelling of the potential source controlled rectifier excitation system, the ST1A IEEE model can be considered a reasonable representation with the excitation power coming from the generator terminals via a transformer and regulated with a controlled rectifier. Another presented model is that of ST5B, which is similar to ST1A but has an alternative over excitation and under excitation inputs and differing limits.

5.3.2 Compound Source Rectifier Systems

The compound source rectifier system is much like potential source controlled rectifier systems. One difference is that, instead of using terminal voltage, terminal power is used with a power potential transformer and a saturable current transformer where the excitation

[10] In this work voltage collapse highlights the possibility of the generator stator voltage feeding the excitation being severely depressed through a transient event thereby depressing the voltage fed to the excitation system. This low field voltage could further depress the stator voltage.

system power is controlled using a saturation of the current transformer. When the main synchronous generator is not supplying load, armature current is zero, thus potential source supplies the excitation power. Likewise under transient, the current is used for field forcing. The compound source rectifier system is represented by ST2A as seen in Figure 34.

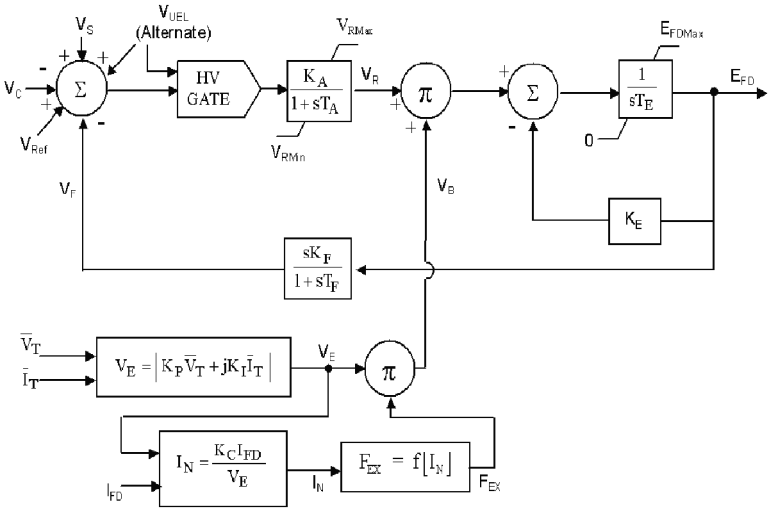

Figure 34 Type ST2A—Compound-source rectifier excitation system (57)

5.3.3Compound Controlled Rectifier Excitation Systems

The compound controlled rectifier excitation system uses controlled rectification in the excitation system output circuits and the compounding of voltage and current derived sources for excitation power which comes directly from the stator of the main generator. This gives the system a fast response.

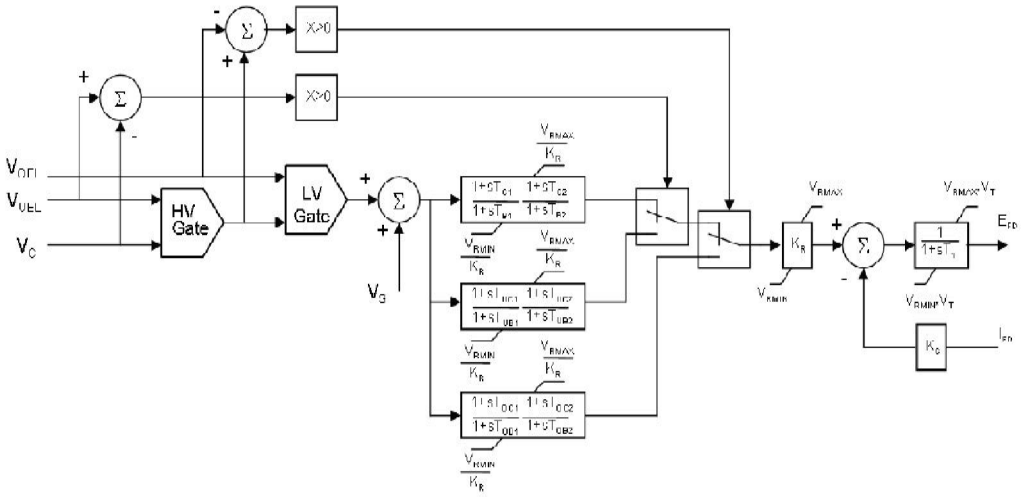

Figure 35 Type ST5B—Static potential-source excitation system (57)

Compound controlled rectification systems in the past have been represented by the ST3A model which, being versatile, allows the modelling of compound source and potential source

excitation systems. The ST5B was then introduced which replaced the lead / lag regulator system with a proportional integral regulator block. The use of the 5B also facilitates the further utilisation of power systems' stabiliser models which may be required in other applications. This is seen in Figure 35.

The static excitation systems main advantage in an operational sense is the relative speed that it can adjust to perturbations on the system. This is largely due to the control topology and lack of electrical machine in the excitation path. This lack of machine is advantageous from a modelling point of view in that it is simpler, but from a point of view of trying to develop a single model that can characterise all forms of excitation system, the lack of machine is unfortunate as it undermines the model's ability to be used for the DC and AC excitation system types.

5.4 Parameter Estimation in Excitation Systems

Parameter identification in excitation systems has diverging ideas on how to characterise system behaviour. One of the methods used to accurately describe the system is by its component parts in order to model the system response. The other method is to take a generic IEEE standard model and alter constants in order to characterise the system.

Demello and Concordia (64) characterise the effects on electrical machines stability by controlling its excitation. The models presented and later work in this area forms the basis of IEEE standard 421.5 (58).

As mentioned previously, there have been attempts to accurately characterise an excitation system from its component parts using a method of testing and evaluation similar to that used in electrical machine manufacture. Aliprantis *et al* (65) provide an effective example of this. The significant drawback to this method is that it is unlikely that manufacturers will provide much detail as to the design of the system, making it hard to model, which makes this method unlikely to be commonly used in excitation system characterisation.

The conventional method of characterisation would be the use of a predefined control model (i.e. as set out by standard 421.5). This would be used to consider the outputs of the system and define the constants of the model in order to match the model to the real machine behaviour. This can be done invasively (59) with field tests to quantify the excitation system characteristics, or non invasively using a transient incident like Wang *et al* (66). Bhaskar *et al* (67) considers this further in order to characterise non linearities in systems more accurately by using pseudo random binary signals to identify the model under controlled conditions. This

was done to avoid reaching, and exceeding limiters in the system that may mask some of the dynamics that can be used to identify non-linear characteristics. Using perturbations to stimulate a system response is needless to say invasive to the system in which it operates. This undermines its usefulness in comparison to methods that use pre recorded data for the characterisation like Wang *et al.* The only disadvantage is that only the excitation system was considered in this work and is thus less applicable.

The work using perturbations is quite useful as it would suggest that a perturbed input to the excitation system model can facilitate reasonable parameter identification. Admittedly it is not performed with both the synchronous machine and the turbine, thus for this work, the mutual interaction of the differing power plant parts may provide differing results. The combining of the excitation system model and the synchronous machine should provide interesting insight in this regard.

5.5 Summary

Excitation systems are employed to provide direct current to the field winding of a synchronous generator. There are three main topologies available to achieve this, all offering differing characteristics. Direct current excitation system models offer a bus fed system that is an older technology and has been prone to voltage collapse. That said, the DC1A exciter model is highly versatile and capable of characterising differing exciter technology types. The AC5A pilot exciter model is equally versatile and has the added advantage that rotating rectifier systems are still widely used in newer power plants.

Static excitation systems and models, although arguably the best technologically, in that its speed of reaction can be significantly faster than the other technology types, does not offer the same level of versatility in characterising other model types that the other models provide.

6. Parameter Identification Search Algorithms

In developing a parameter identification method, it becomes critical to select the appropriate method of stochastic optimisation in order to achieve an accurate, but also efficient result. Stochastic optimisation[11] is most suitable for this work due to the nature of the data available. Due to the necessity to identify many differing machines without 'training' data, neural networks are not practical thus are not considered in this evaluation. This section considers many stochastic methods that are outlined and evaluated as to which would be most appropriate to the current work.

Stochastic optimisation is used to optimise an objective function. This classically takes the form of a nonlinear function that defines the behaviour of a model or system. More commonly in elaborate optimisations; a state space model is developed that enables several equations to be simultaneously optimised provided that the state variable is consistent for all the equations. In this work, because the identification of turbine, excitation and synchronous machine parameters are being identified, the state variable would differ depending on which part of the power plant was being identified. For this reason the classical objective function cannot be adopted. This is also the reason why classical optimisation, such as the Newton Raphson method cannot be adopted in this work. Algorithms of this variety can be very powerful when optimising low variable functions that are defined in simplistic objective functions. Unfortunately the function will not be of a classical form and the number of variables to be identified is much larger. This invariably makes the classical methods difficult to adopt and impractical computationally.

An objective function is developed as briefly discussed in the introduction. The output phase currents and voltages of an identification model are compared against recorded phase currents and voltages from a real or synthetic network in order to develop an objective function. Because of this format the objective function cannot be optimised in the conventional way. This is because conventionally an objective function is a nonlinear function that can be solved by finding either a minimum value or a maximum value. This cannot be the case give the data available. For this reason the algorithms have to be considered according to their computational cost, because every time a new objective function value is developed, a

[11] Stochastic optimisation is the optimisation of a objective function without the use of probabilistic or deterministic methods.

simulation has to be run. This has a high computational cost, thus the relative success and the computational efficiency of the differing algorithms are evaluated according to this criteria.

6.1 Generational Evolutionary Algorithms (GEA)

Generational evolutionary algorithms are based on Darwinian principles of evolution. A selection is applied, crossover and mutation then occurs to that selection as seen in Figure 36. The resulting population is then better suited to the environment that the evolution is based in. Goldberg (68) made the method popular, although it was predominantly developed by Holland (69).

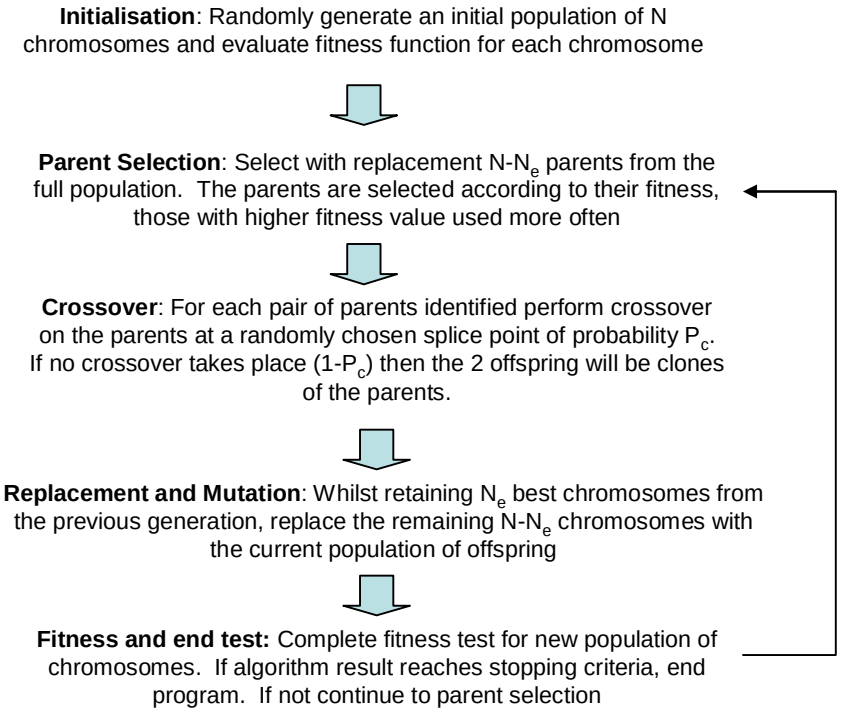

Figure 36 Characterisation of a generational evolutionary algorithm (68)

GEA begins with a population of randomly created individuals. These individuals are vectors. The GEA then creates new individuals from the parent population. Initially, tournament selection is used to choose the parental individuals in the population. Tournament selection dictates that a few individuals compete to be parents of the next generation of individuals, i.e. survival of the fittest. If tied, a winner is randomly chosen. The tournament occurs twice to develop two parents to allow cross population, i.e. crossover of genetic material. The two new offspring of the union of the individuals are new individuals. Mutation occurs (where perturbations of vector components are randomly generated). These mutated individuals are submitted into the population for selection of the next generation. The iterative cycle continues until the population reaches a specified size.

Genetic algorithms have many advantages. They converge well and are seen to consider the search space appropriately. The main disadvantage that genetic algorithms possess is that, to explore the search space, each member of the search population has to be compared against every other member of the population. Conventionally this would not be particularly problematic as the format of the classic objective function that is used facilitates this efficiently. In the case of this work, the objective function that is optimised cannot take the classical form that would be adopted in optimisation. Because of this, in order to compare each member of the population against each other it would be necessary to use the parameter values for each and every population member, run the model simulation using the recorded terminal data and develop a new value for the objective function. This process would need to be carried out during every iteration and result in very high computational cost.

6.2 Steady State Evolutionary Algorithm (SSEA)

Steady state evolutionary algorithms have many similarities to generational evolutionary algorithms. One difference is that SSEA do not possess a single population of solutions. The SSEA does create two offspring at every evolutionary step but unlike the GEA, the SSEA replaces the least useful population with offspring generated.

Steady state evolutionary algorithms possess many of the advantages of standard genetic algorithms. They also are subtly different in the way that they improve from one iteration to the next. Unfortunately, they also possess the same major disadvantage that was seen previously with GEA. This high computational cost does undermine its ability to optimise the objective function that this work requires in an efficient manner.

6.3 Differential Evolution (DE)

Differential evolution is a population based algorithm with the purpose of optimisation of functions on totally ordered search spaces (70). Differential evolution algorithms can adopt differing strategies classified as DE/X/Y/Z where 'X' denotes the method of selection of the individual, S_i. This can be at random (Rand), or best so far (Best). 'Y' denotes the number of difference vectors utilised. 'Z' defines the crossover. An example of the format could be 'DE/Rand/1/bin'.

The differential evolutionary algorithm is unlike GEA or SSEA in that the candidate individual is the sum of three randomly weighted populations other than the parental individuals. The parents then participate in the creation of the candidate. The candidate is cross pollinated by the parental individual. The candidate is evaluated, and if better than the parent, it replaces the parent in the populations. This is because, in effect, it is a more evolved member of the

population in comparison to its parents. This process repeats for all parent individuals in the population. When all done, the parent order is randomly changed. The procedure is then repeated.

Again much like the algorithms that have been previously mentioned, in order to evaluate the search space, each candidate needs to be individually evaluated in order to be optimised. This process is effective but computationally very high.

6.4 Particle Swarm Optimisation (PSO)

PSO is a cooperative population-based stochastic search optimization algorithm. Since its introduction, it has been used to solve a large cross section of optimization tasks. Using "Socio cognition human agents" (56) and evolutionary operations to mimic the behaviour of groups of animals in social activities where multi lateral group communication is needed. In PSO the individual animals are characterized as particles, all with certain velocities and positions in the search space (71). The group of particles is classed as a swarm. The swarm generally begins with a randomly initialized population, each particle 'flying' through the search space and remembering its optimal position thus far. The particles communicate and based on the best positions found, dynamically adjust the search position and relative velocity of the swarm. Because of this, the swarm will 'fly' towards better possible results (56).

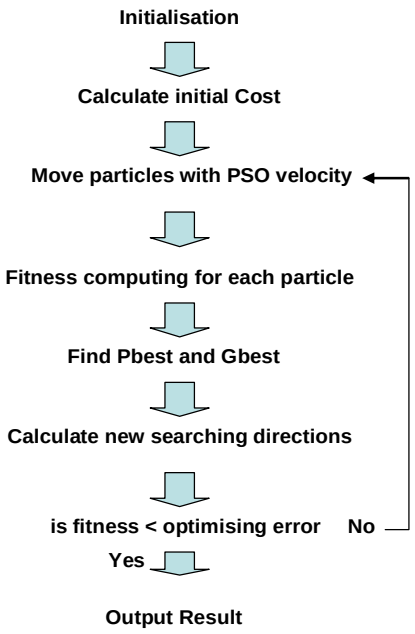

Figure 37 A particle swarm optimisation algorithm (74)

As seen in Figure 37, the PSO algorithm initializes with a set of randomly generated variable velocities and location values. In terms of this application, as the PSO operates, a resultant

value for the objective function is developed at the output of the model. The value of the objective function is used to define how far away from an accurate result the current particles are. Informants are randomly assigned with the best overall result defining which informant influences the search area for the next iterative cycle. Based on this new search information, new values for the location and the velocities are developed. These new values are then used to again develop a new objective function error which is propagated as stated (73).

In PSO the general consideration is that there may be many local minima, but only a single global minima. The global minima is seen to be the best solution to the equation. The searching process is characterised by the equation below.

$$V_i^{K+1} = \omega_i V_i^K + C_1 r_{and} * (P_{besti} - X_i^K) + C_2 r_{and} * (G_{besti} - X_i^K) \quad (21)$$

$$X_i^{K+1} = X_i^K + V_i^{K+1} \quad (22)$$

where C_1 and C_2 are positive constants classed as acceleration coefficients, ω is the inertia weighting factor and r_{and} is a function that generates the inherent randomness in the PSO. X_i represents the position of the i[th] particle, P_{besti} is the best previous position of X_i and G_{besti} is the best previous position among the members of the population chosen at random as informants. V_i is the velocity of particle X_i. This combination of equations calculates a new velocity that drives the particles towards P_{besti} and G_{besti}.

Unlike the previously discussed algorithm types, PSO has the distinct advantage that the computational cost in using it is significantly less than the other evolutionary methods mentioned previously for this application. This is because PSO uses informants as a representation of the iteration for its optimisation rather than requiring every particle to be evaluated. This means that where a GA may need to run 20 simulations per iteration, a PSO algorithm could perform only four.

6.5 Ant Colony Optimisation (ACO)

Ant colony optimisation is another evolutionary algorithm. It is based on the search behaviour of ants when looking for food. Much like PSO, the search is optimised through communication of the ants to reach common goals. A pheromone is secreted by each ant; it is used by the ants as a marker to identify the shortest route to a target. Ants set off searching different routes for food. Some take a short route, others takes longer routes. The explorer ants come to the realisation of the shortest route. The probability of picking the shortest route is defined

by the relative difference of route length. This form of optimisation is applicable to problems with more than two solutions.

A colony of ants is generated and is situated inside the search space. The individual ants have a fitness defined by the distance from the optimal point, i.e. food. The ants then move to a node (each node being a possible solution). Which node the ant moves to is defined by the pheromone deposition on the routes and thus, the probability of finding a more efficient route. It is noted that the quantity of the pheromone between the nodes is a reflection of the quality of the solution found.

There are variations in this algorithm such as the trace functions which can give a better convergence (74), likewise, the max/min ant system, where the ant with the best path, i.e. local best is the only ant to deliver the pheromone trail.

When considering the suitability of this form of algorithm to the task at hand, questions arise. The relatively large quantity of variables required for optimisation and the format of the search call into question the relative efficiency of the method in regard to optimisation. The concept of the relative reinforcement of the path being slowly built doesn't suggest the speed at which the method converges on a solution would be fast, particularly for a model which has many linear and nonlinear components in a discrete format. Like many optimisation methods it is difficult to estimate the relative speed of convergence is defined by the problem it faces (75). It has been seen however that the larger the ant colony the faster a convergence can occur. This large colony would have a detrimental effect on the computational cost required in this work without any guarantee that the convergence would be any faster than other algorithms with a similar metaheuristic[12] topology.

6.6 Bacterial Chemotaxis Optimisation (BCO)

Bacterial Chemotaxis (76) with regard to particle swarm optimisation and ant colony optimisation can be considered a solution to certain more problematic aspects of those algorithms. Essentially in PSO and ACO (77), when particles or ants are searching for the optimal, the only consideration is finding an optimal solution by being attracted towards the best solution. This could thus be classified as being defined by attractants. There are however other considerations in BCO, there are repellents, obstacles that force the particle to traverse around them before reaching the optimal solution. The principle behind BCO is that bacteria colonies are attracted to food/nutrients (attractants) and repelled by substances that would

[12] Metaheuristics are computational methods that optimise problems iteratively by trying to improve a candidate solution with regard to a given measure of quality.

kill them (repellents). In this scenario the optimum solution for the bacteria to reach the attractant/optimum solution is also defined by the repellents location

The original PSO equation is modified to consider repellents. In this case P_{worst} is now the worst position the particle has been and G_{worst} is the worst position any particle has been.

$$V_i^{K+1} = \omega_i V_i^K + C_1 r_{and} * (P_{worsti} - X_i^K) + C_2 r_{and} * (G_{worsti} - X_i^K) \quad (23)$$

Simply considering the equation, it is obvious there are limitations. The method doesn't allow for the distinction between repellent and attractive stimuli in the process. It becomes obvious that because it is not proceeding directly to the optimal solution, the computational effort becomes higher to reach an optimal solution. On the other hand, for problems in which the algorithm is better suited, this may have advantages. Another problematic aspect to this form of algorithm is that the algorithm uses repellents in order to navigate the search space. This would not necessarily be a problem if the repellents or in this work, local minima[13] had predefined locations, but this is not the case. Because of this, it becomes difficult to see how this method has added value over the PSO algorithm in this regard.

6.7 Simulated Annealing (SAN)

The concept of annealing comes from the cooling of liquid or solids. At high temperatures, molecules have a high kinetic energy, thus move a lot. As temperature reduces, the kinetic energy reduces and molecules 'may' tend to align themselves into a polycrystalline structure. The temperature is not the only defining factor to this alignment, or whether the alignment is the minimum energy state. In thermodynamics, if the rate of cooling is great, then the likelihood that the material will reach its minimum energy state is reduced. Likewise, the slower the cooling, the higher the probability of reaching a minimum energy state. Needless to say this is analogous with search optimisation algorithms.

Simulated annealing is a probability based algorithm. It possesses similarities to steady state evolutionary algorithms, in that the previous solution is replaced by the new solution as can be seen in Figure 38. In this case the proposed solution is created to replace the previous best solution. From this a probability function is developed to give the likelihood that the newly created solution will replace the old. The algorithm is defined by temperature (as defined in the algorithm) and controlled by the user.

[13] Given the unknown formation of the search space it is impossible to quantify any other forms of repellents.

The annealing is designed to enhance the likelihood of avoiding local minima en route to a global minimum. Injected randomness is used to limit the possibility of premature convergence to a local minima point rather than global by inflicting an inherent perturbation in its solving algorithm. One fundamental aspect of SAN which differs from other optimisation algorithms that came before it, was its 'willingness' to give up a relative quick gain of a fast decrease in objective function in order to ultimately reach a better objective function (77).

Simulated annealing is a very popular algorithm for optimisation, with a fairly high likelihood of a successful search given the appropriate problem. For the current work, the question becomes, is it the most appropriate algorithm? The method operates on single result self improvement. Now in many cases that would be very computationally effective, but in this case the probability of many local minima is unknown. Likewise, depending on the number of parameters, the search space could be dimensionally very high resulting in a large area to be analysed, in which case more than one 'searcher'[14] per iteration has to be considered more likely to reach a solution quickly when considering a large multi dimensional search area.

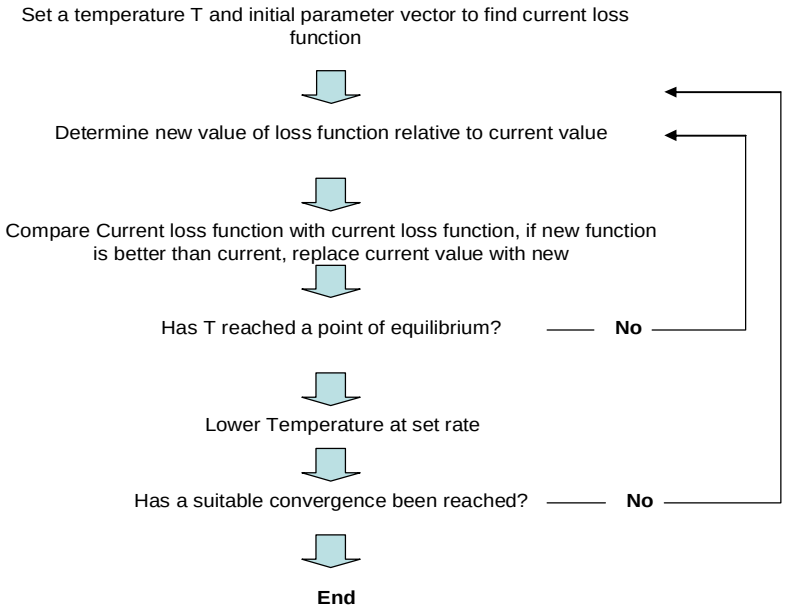

Figure 38 Simulated annealing algorithm

6.8 Electromagnetism-like Algorithm

The electromagnetism-like algorithm (EM) was proposed by Birbil and Fang (78). EM heuristic optimisation is similar to particle swarm optimisation in many regards. The difference is EM's method in calculating moves in the search space. In each iteration the EM algorithm moves to

[14] Searcher in this work defines the use of a single input variable that defines the course of the search. This would differ to that of PSO in that each particle could be considered an input to the search.

a new position. Unlike PSO though, the particle best and global best solutions do not exclusively influence the search behaviour of the algorithm.

In multi dimensional search space where each point represents a possible solution, a charge is associated with the individual points and calculated upon the objective function value of the solution. The population of solutions created are able to repel or attract each other and the magnitude of this is defined by the relative distance between them (Coulomb's law), or, if considering celestial bodies, Newtonian physics. The movement of a point, defined by the general populous is expressed as a force vector, thus worse solutions are repelled, better ones attracted, therefore moving towards better solutions. In many respects this is similar to Bacterial Chemotaxis and because of that similarity, has similar application difficulties to this work that are focussed around the unknown search space and the location of local minima.

6.9 Gradient Descent

Gradient descent's ability to optimise a function is highly dependent on the initial value of estimate that it is given. Several methods exist like the Newtonian method or 'steepest descent' (79). The concept of this algorithm is that the objective function optimises fastest when the gradient is at its highest (79). When the gradient reaches zero, the optimal solution has been reached. Gradient descent is a very fast algorithm and converges on a solution very efficiently. It has however been seen to fail to converge when considering a search space with local minima (81) and become trapped in the minima, unable to escape. This inability to escape from local minima must be considered a major area of concern. Given that the work seeks to identify non linear variables in a multi dimensional search space, it would be prudent to assume that there are local minima. For this reason the suitability of this form of algorithm has to be called into question. Other methods like gradient descent i.e. quazi Newtonian algorithms (82) exist, however considering the likelihood that gradient descent is impractical for the optimisation challenge, then quazi-Newtonian algorithms are unfeasible.

6.10 Summary

When considering the use of optimising algorithms there is always a trade off of some description. Sometimes this is the algorithm's relative efficiency at the detirment of accuracy, or its ability to recognise optimal paths but not necessarily the most sensible one to avoid local minima. Wolpert and Macready (83) called this manifestation the 'No Free Lunch' (NFL) theorem. The theorem says, in essence, that if an algorithm is efficient in one problem, it's guaranteed to not be efficient in another differing problem. Blind searching is inherently flawed and it is seen that a search without boundaries is less useful than blind luck. The

algorithm is only as good as the boundaries that are set. If tighter, there is a higher chance that a more accurate search can be performed as the search area is limited. In setting tighter limits for optimisation however, there is the need for a greater level of knowledge regarding the behaviour of the problem and the parameters being optimised. Setting limits without understanding the practical dimensions and locations that the parameters may occupy could result in making an accurate optimisation impossible. For this reason understanding of the parameters is critical in optimisation.

Considering the algorithms mentioned, there are algorithms which theoretically can efficiently derive the objective function. The more critical aspect from an implementation point of view is the relative number of simulations that would be required per iteration of the algorithm. This has a significant impact on the computational cost of the differing algorithms.

The overriding factors in the selection of an appropriate algorithm are the computational cost involved in performing the search and the likelihood of finding a suitable result. The computational cost of the genetic evolutionary algorithms is seen to be high due to the number of simulations required per iteration to evaluate the populations within the algorithms. Other forms of algorithms with a lower computational cost are available however it is seen that several use a single 'searcher' to consider the search space incrementally. This may not be the most efficient method of considering the search space. Bacterial Chemotaxis and electromagnetism theory based algorithms have many advantages but due to the inherent lack of characterisation of the search space, their ability to use repellents in searching is undermined.

Ultimately of the algorithms presented and the others considered, particle swarm optimisation appears to be the most appropriate to the current work. The computational efficiency is high (71) due to the particle swarm traversing the search space and the search will be efficient on an iteration to iteration basis given the number of simulations per iteration is minimised. PSO is also seen to have a high probability of convergence.

7. Parameter Identification Methodology

7.1 Introduction

In deciding on a method of applying parameter identification to generation models, it is imperative to develop a vehicle that can be used in conjunction with the algorithm in order to find the correct values in the model. For this reason a pragmatic approach of modelling is chosen. It has also been seen in the previous chapters that there are logical directions in modelling that provide the most appropriate basis for building the power plant model for the identification.

In considering gas and steam turbines, several main conclusions can be made. It can be seen that the prime mover model that is developed for this work needs to be of an appropriate level of detail that allows it to be used in power system studies. This allows for a more robust interpretation of the turbines function than can be found in some of the more refined thermodynamic models seen in the previous chapters.

For this reason the models presented by the committee for prime movers (9) present the most appropriate type of model for the project. The general versatility that these models can exhibit in characterizing differing forms of prime mover, make them useful when considering different forms of generation. This relative versatility is advantageous in some regards as, if looking at the gas turbine in a more basic form, the similarities between it and that of the steam turbine become apparent. Both prime movers are essentially the same in behavioural terms, granted they have differing inertia's but that is easily negated in modelling. It could be stated therefore that, from the point of view of performing a power systems transient stability study, the basic model for the gas turbine could be very similar to that of the steam turbine, given that the main consideration of this work is not the thermodynamic properties of the prime mover, more its base behaviour in a electrical power systems context.

In considering the modelling of synchronous machines for power system studies, there is a wealth of validated and industrially accepted models that could be adopted. The level of effort required for the development of one of these models is a thesis in itself, and even then it would not be industrially accepted without significant validation. For this reason a model that is based on a classical structure is the most appropriate for this work to reach an appropriate solution.

In considering excitation systems, there are three main varieties available, all offering differing characteristics. Direct current excitation system models offer a bus fed system that is an older technology. The DC1A exciter model is highly versatile and capable of characterising differing exciter technology types. Considering the AC excitation systems, the AC5A pilot exciter model is also very versatile and has the added advantage that rotating rectifier systems are still widely used in newer power plants. Static excitation systems and models do not offer the same level of versatility in characterising other model types that the other models provide.

The excitation models most able to characterise differing forms of excitation systems and to be used in parameter identification are the DC1A and the AC5A exciter models. These models are developed and compared in this chapter.

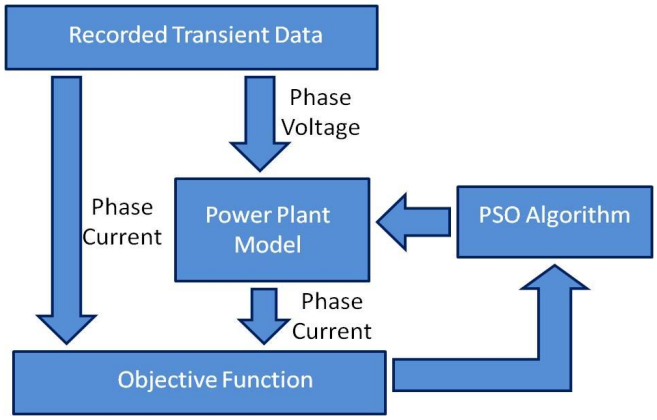

Figure 39 Base structure of the parameter identification process

As seen in Figure 39, because recorded terminal data is required for the parameter identification process, it is input phase voltages and currents that are primarily relied upon. For this reason phase voltages and phase currents are recorded with their respective time stamps. Phase voltages are fed into the 'Power Plant model' which then turns the phase voltages into dq quantities that are used in the dq representation of the synchronous machine. Excitation control and a turbine prime mover are also implemented in this model with the output of the model being phase currents. These output phase currents are compared against the recorded phase current terminal data. This comparison allows for the definition of an error which is the objective function that is used in the optimisation algorithm to develop a new set of values to be applied to the estimator model. This process continues until the error between the estimator model phase currents and the terminal data phase currents are within a defined tolerance, at which point, the set of values identified by the process are expected to be very similar to the real identified values.

In this chapter, the implementation of the model and the challenges in the implementation will be identified and discussed as well as identifying any particular aspects of the research that require further analysis

7.2 Synchronous Machine Modelling

The base structure of the synchronous machine model is seen in Figure 40. In this it is seen that the recorded phase voltages are fed into the model. These phase voltages are converted into direct and quadrature voltages. The direct and quadrature voltages are fed into the d axis and q axis models. Combined with input from the excitation system and the rotor block, direct and quadrature axis currents are developed. These are then converted back into phase currents.

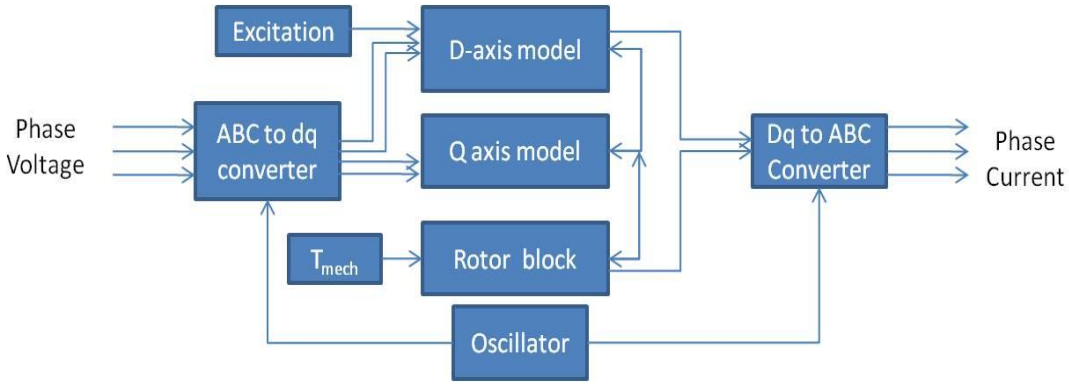

Figure 40 Overview of the synchronous machine model

As apparent in the introduction of this chapter, the synchronous machine model forms the backbone of the estimator model structure. A classical model as seen in previous chapters allows the formation of the machine model without looking too deeply into their structure or validation. Given that these models are already accepted and offer little in terms of novelty for this work, the full derivation of the model implementation is found in Appendix 2 and only the significant mathematics and project specific implementation are included. Based on the information previously seen, it was decided that one damper winding would be implemented on the direct axis and one on the quadrature axis. This allows the model to take into account the relative effects that the damper windings have on synchronous machine performance, while not overcomplicating the model to the extent that adding further windings would.

It was decided that although modelling saturation has obvious benefits in terms of characterisation of the machine, much of the previous work in this area has considered a single machine analysed in greater detail than is necessary for power system studies (49). Additionally the likelihood of having sufficient data available to do this is not very high. For

this reason saturation of the machine was neglected and a linear behavioural characteristic was adopted.

The fundamental equations that define the synchronous machine are (63):

$$v_q = r_s i_q + \frac{d\lambda_q}{dt} + \lambda_d \frac{d\theta_r}{dt} \tag{24}$$

$$v_d = r_s i_d + \frac{d\lambda_d}{dt} - \lambda_q \frac{d\theta_r}{dt} \tag{25}$$

$$v_0 = r_s i_0 + \frac{d\lambda_0}{dt} \tag{26}$$

$$v'_f = r'_f i'_f + \frac{d\lambda'_f}{dt} \tag{27}$$

$$v'_{kd} = r'_{kd} i'_{kd} + \frac{d\lambda'_{kd}}{dt} \tag{28}$$

$$v'_g = r'_g i'_g + \frac{d\lambda'_g}{dt} \tag{29}$$

$$v'_{kq} = r'_{kq} i'_{kq} + \frac{d\lambda'_{kq}}{dt} \tag{30}$$

where v_d, v_q, i_d and i_q are direct and quadrature voltages and currents. r_s and r_f are armature or stator resistance and direct axis field resistance. v_f and i_f are direct axis field voltage and current. Rotor quantities are referred to the stator using the appropriate turns ratio. This denotes the equivalent rotor currents referred to the stator by a prime superscript. θ_r is rotor angle. λ_d, λ_q and λ_0 are direct, quadrature and zero sequence components of flux linkage. v_0 and i_0 are zero sequence components of voltage and current. $v_{kd}, v_{kq}, i_{kd}, i_{kq}, r_{kd}, r_{kq}$ are direct and quadrature damper winding voltage, current and resistance. v_g , i_g and r_g are quadrature axis field voltage, current and resistance.

Flux linkages are defined as:

$$\lambda_q = L_q i_q + L_{mq} i'_g + L_{mq} i'_{kq} \tag{31}$$

$$\lambda_d = L_d i_d + L_{md} i'_f + L_{md} i'_{kd} \tag{32}$$

$$\lambda_0 = L_{ls} i_0 \tag{33}$$

$$\lambda'_f = L_{md} i_d + L_{md} i'_{kd} + L'_{ff} i'_f \tag{34}$$

$$\lambda'_{kd} = L_{md} i_d + L_{md} i'_f + L'_{kdkd} i'_{kd} \tag{35}$$

$$\lambda'_g = L_{mq} i_q + L_{mq} i'_g + L'_{mq} i'_{kq} \tag{36}$$

$$\lambda'_{kq} = L_{mq} i_q + L_{mq} i'_g + L'_{kqkq} i'_{kq} \quad (37)$$

where L_d, L_q, are direct and quadrature inductance and $\lambda_d$and λ_q are direct and quadrature flux linkage. λ_0 is zero sequence flux linkage. λ_f and λ_g are direct and quadrature field winding flux linkage. λ_{kd} and λ_{kq} direct and quadrature damper winding flux linkage. L_{md} and L_{mq} are direct and quadrature mutual inductance. L_{ls} is armature or stator winding leakage inductance. L_{kdkd} and L_{kqkq} are direct and quadrature mutual damper winding inductance.

Graphically these equations are represented by the circuits seen below:

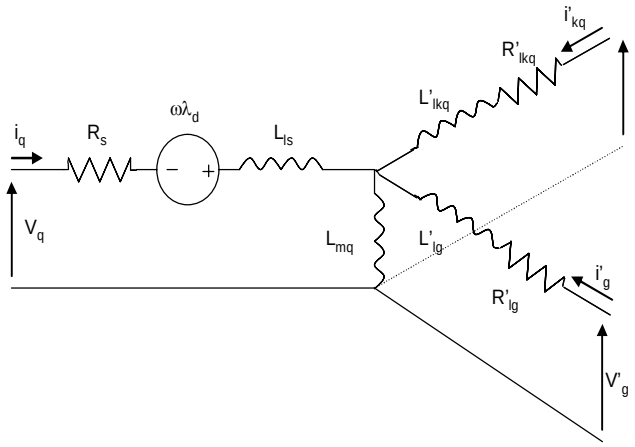

Figure 41 q-axis model

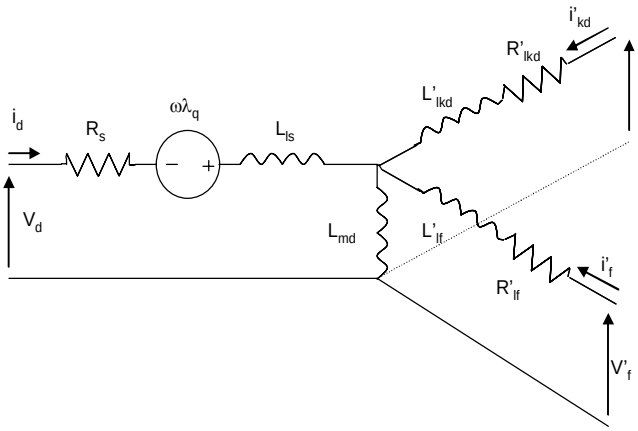

Figure 42 d-axis model

torque is developed by the machine across the air gap:

$$T_e = \frac{P_e}{\omega_r} = \frac{3}{2}(\lambda_d i_q - \lambda_d i_q) \quad (38)$$

where T_e and P_e are electromagnetic torque and power and ω_r is rotor speed.

Equations 12 to 18 describe the machine behaviour in the form of voltages. In order to develop the output currents required for the model to function the voltage equations are manipulated to allow the state variable to be flux linkage Flux linkage changes in symbol assignation from λ to ψ to signify its dependence on base synchronous speed ω_b. This is seen in the equations below:

$$\psi_q = \omega_b \int \left[v_q - \frac{\omega_r}{\omega_b} \ \psi_d + \frac{r_s}{X_{ls}} (\psi_{mq} - \psi_q) \right] dt \tag{39}$$

$$\psi_d = \omega_b \int \left[v_d - \frac{\omega_r}{\omega_b} \ \psi_q + \frac{r_s}{X_{ls}} (\psi_{md} - \psi_d) \right] dt \tag{40}$$

$$\psi_0 = \omega_b \int \left[v_0 - \frac{r_s}{X_{ls}} \psi_0 \right] dt \tag{41}$$

$$\psi'_{kq} = \frac{\omega_b r'_{kq}}{X'_{lkq}} \int [(\psi_{mq} - \psi'_{kq})] dt \tag{42}$$

$$\psi'_{kd} = \frac{\omega_b r'_{kd}}{X'_{lkd}} \int [(\psi_{md} - \psi'_{kd})] dt \tag{43}$$

$$\psi'_f = \frac{\omega_b r'_f}{X_{md}} \int \left[E_f + \frac{X_{md}}{X'_{lf}} \left(\psi_{md} - \psi'_f \right) \right] dt \tag{44}$$

where the following define the internal flux linkages of the machine:

$$\psi_{mq} = \omega_b L_{mq} (i_q + i'_{kq}) \tag{45}$$

$$\psi_{md} = \omega_b L_{md} \left(i_d + i'_{kd} + i'_f \right) \tag{46}$$

$$E_f = X_{md} \frac{v'_f}{r'_f} \tag{47}$$

$$\psi_q = X_{ls} i_q + \psi_{mq} \tag{48}$$

$$\psi_d = X_{ls} i_d + \psi_{md} \tag{49}$$

$$\psi_0 = X_{ls} i_0 \tag{50}$$

$$\psi'_f = X'_{lf} i_f + \psi_{md} \tag{51}$$

$$\psi'_{kd} = X'_{lkd} i'_{kd} + \psi_{md} \quad (52)$$

$$\psi'_{kq} = X'_{lkq} i'_{kq} + \psi_{mq} \quad (53)$$

here ω_b is base synchronous speed, ψ_{md} ,ψ_{mq}, X_{md} and X_{mq} are direct and quadrature mutual flux linkage and mutual reactance respectively, X_{ls} is armature or stator winding leakage reactance. X_{lkd} and X_{lkq} are direct and quadrature damper winding leakage reactance. r_{kd} and r_{kq} are direct and quadrature damper resistance.

From this, dq currents are developed and then turned into phase currents as the output of the synchronous machine. The derivations of these are found in Appendix 2.

7.2.1 Rotor Assembly

The generator mechanical equation of motion is given by:

$$\omega_r(t) - \omega_e(t) = \frac{2J}{P} \int_0^t (T_{elec} - T_{mech} - T_{damp}) dt \quad (54)$$

where T_{elec}, T_{mech} and T_{damp} are electrical, mechanical and damping torques. This allows the characterisation of the rotor behaviour of the machine.

The synchronous machine model allows a real machine to be characterized accurately including stator transients which would be ignored on lower order models[15]. The direct and quadrature current waveforms seen in Figure 43 are consistent with what would be expected (10). The waveforms are generated by the application of a three phase short circuit to the machine. The direct and quadrature axis currents demonstrate the behaviour of the synchronous machine model. The direct and quadrature axis trend lines demonstrate the direct and quadrature axis currents if stator transients were neglected in the model. This shows the advantage of their inclusion for the purposes of parameter identification.

[15] The addition of stator transients provides greater understanding of the transient behaviour of synchronous machines which is why they are included. They are however sometimes neglected in power system studies in order to simplify the study.

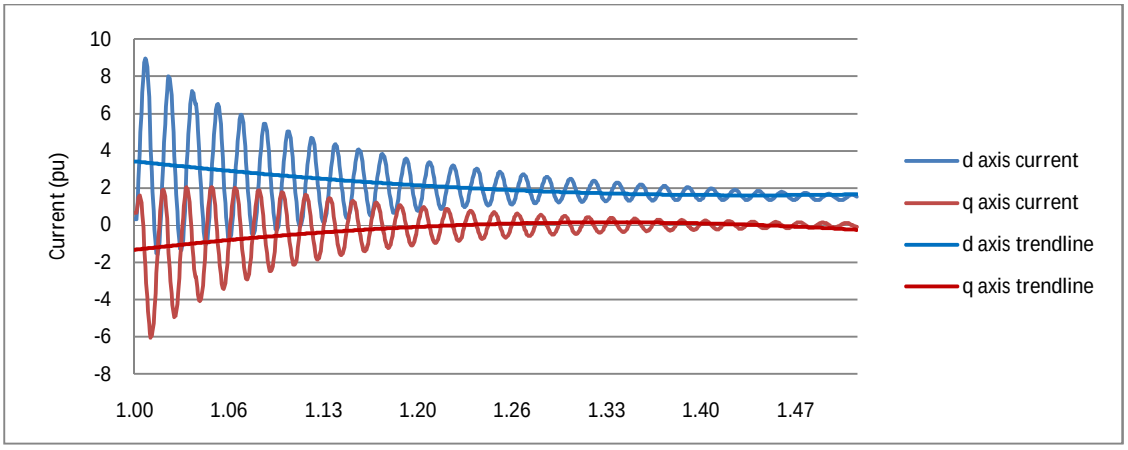

Figure 43 Representation of direct and quadrature stator transients

7.2.2 Validation of Turbogenerator Model

In this section, the generator model developed earlier in this chapter is validated against results obtained from a commercial software package (DigSilent) and also against a set of real short-circuits currents obtained from an 828 MW machine. Conventionally, a power system modelling package like DigSilent runs a load flow and other underlying processes to allow a dynamic or transient simulation to be suitably initialized to obtain a steady state response. This is not possible with our model, so instead a set of generic equations are used to develop initial values for the state variable flux linkages (see Appendix 2) giving an initial transient (Figure 44) which must be allowed for when comparing the two sets of results.

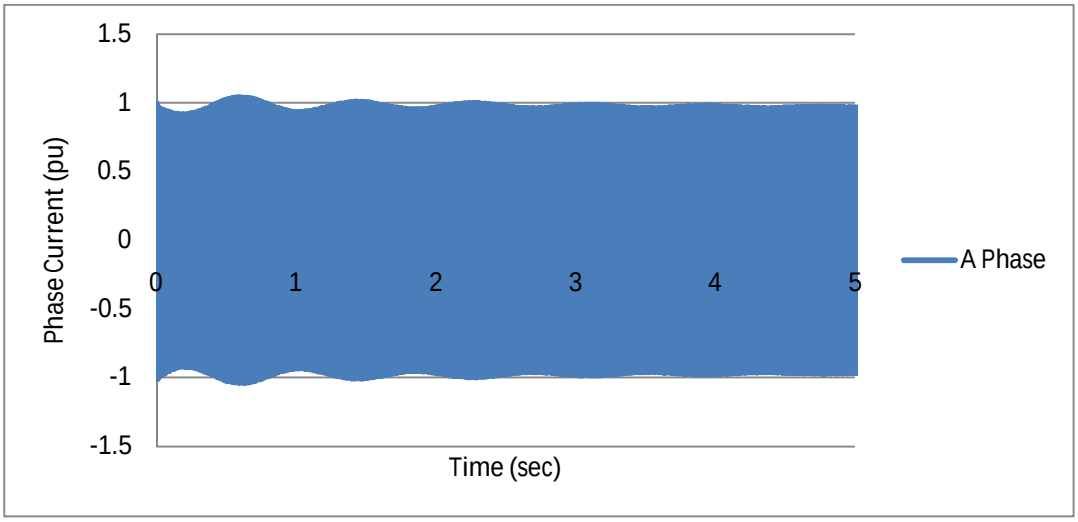

Figure 44 Model initialisation

Probably the most onerous and most useful test that is carried out on a synchronous machine is a three phase short circuit to ground. In this case, the synchronous machine is driven at rated synchronous speed and the stator terminals are simultaneously shorted. Figure 45 shows the short-circuit currents produced by the generator model using parameters from a

828MW, 18kV, 4-pole synchronous generator. This form of event is useful in many respects in that, not only does it allow the comparison of the machine model output waveform and the waveform of the real machine, but it also allows for the empirical derivation of certain machine parameters using the envelope of phase current. The currents and reactances from the short circuit envelope define the ac component of current as defined in equation (43) below. Further parameters can also be derived as shown in Figure 46.

$$I_{ac} = E\left[\frac{1}{X_d} + \left(\frac{1}{X'_d} - \frac{1}{X_d}\right)e^{-\frac{t}{T'_d}} + \left(\frac{1}{X''_d} - \frac{1}{X'_d}\right)e^{-\frac{t}{T''_d}}\right] \qquad (55)$$

where E is the open circuit voltage of an unsaturated machine (27). X''_d, X'_d and X_d are sub transient, transient and steady state direct axis reactance. T''_d and T'_d are the sub transient and transient direct axis time constants.

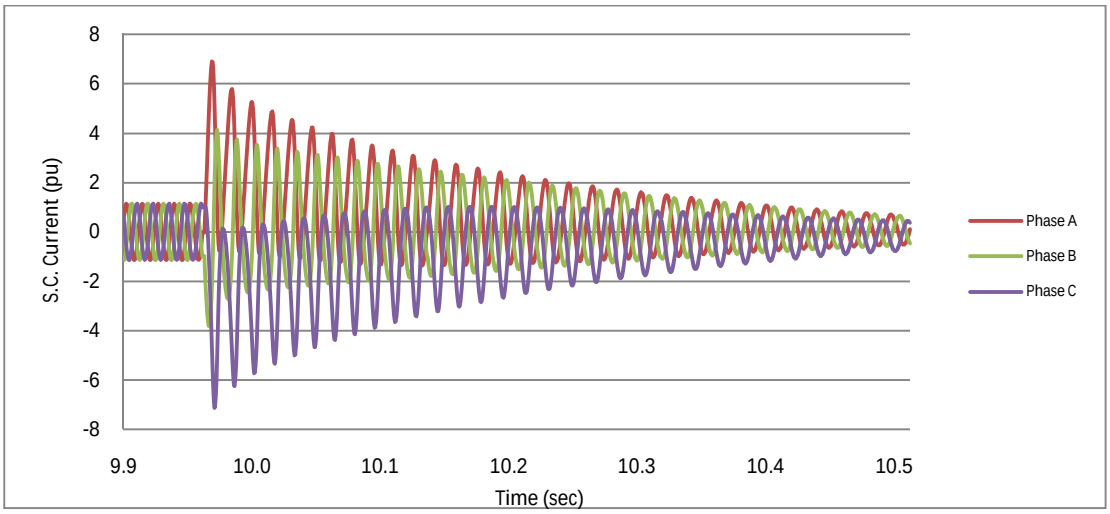

Figure 45 Simulation of short circuit; generator model

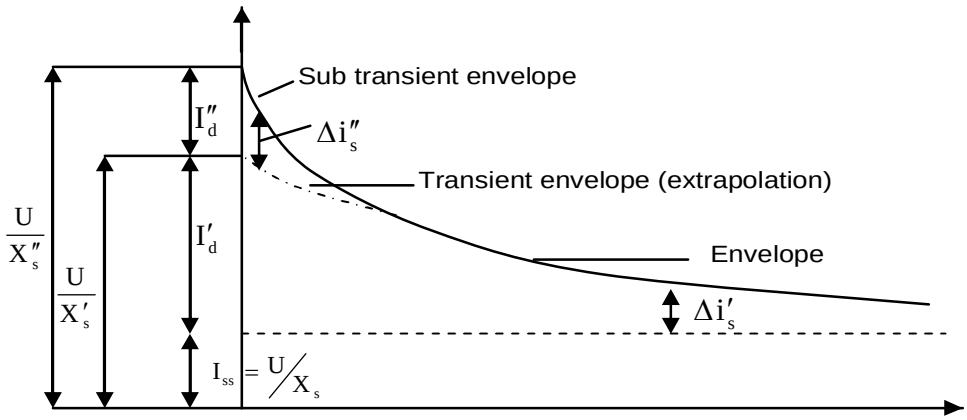

Figure 46 Empirical derivation of synchronous machine parameters

As seen in (82) and (83) the machine model has been successfully used to identify parameters of differing machines. Given that the results derived by the identification had a good

resemblance to the manufacturer data it would be reasonable to conclude that the machine model is suitable under the tested conditions. The question does arise as to whether the model is valid for different levels of saliency. In this case, (82) was a salient pole machine and (83) was effectively a round rotor machine. An argument could be made that given the short circuit, empirical derivation only really allows d-axis parameters to be directly identified (with the exception of X''q). Additionally, as saturation is not an aspect of consideration in regard to short circuit tests, it could be said that the machine performs appropriately under such conditions. This work was performed as in intermediate step to establish the primary function of the method before moving further into less defined transients.

From a practical point of view, the machine model is now considered under a series of differing stimuli that would likely be seen by a network connected synchronous generator through the course of its lifetime. This will ascertain whether the machine model behaves correctly under a variety of perturbations. For this reason, a secondary data source is used in order to create appropriate synthetic waveforms for the simulation of transient events. Using a secondary data source for the creation of synthetic data also gives an independent level of validation. For this reason, DigSilent, a power system simulation package was utilized.

DigSilent is industrially accepted and is capable of simulating electromagnetic transient events and provides the ability to model larger power networks efficiently with a high degree of confidence that the result is valid under the required conditions. For this purpose a small power network is developed as seen below. As seen, there is an AC voltage source connected to a bus bar which becomes a 'slack bus'. This bus is attached via two transmission lines to a secondary bus with loads and a synchronous machine connected.

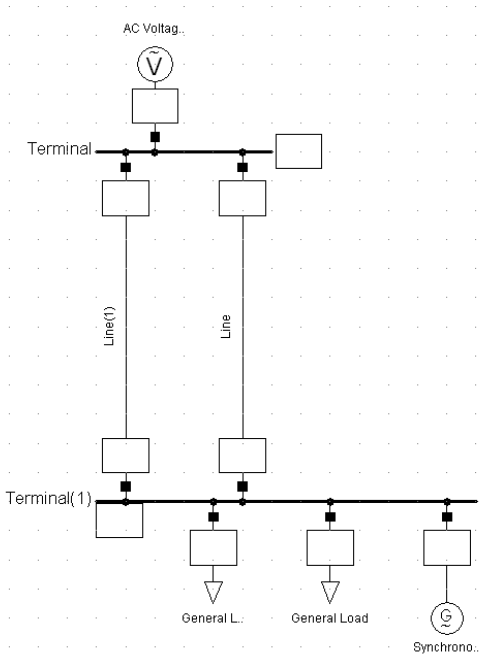

Figure 47 Synthetic power network

The synchronous machine, excitation system and governor are found in Appendix 3, as are the network specifications used in the test network. The test network seen is a simple representation using typical network parameter data that could be found in a real power network. The machine parameters in the DigSilent model and the machine parameters that are used during the synthetic testing and validation are the same. Because the machine model is used under differing situations for parameter identification, varying situations were considered for validation purposes. During each of these transient events phase voltage, phase current and the change in rotor speed were recorded at the stator terminals of the synchronous machine model in DigSilent. The events simulated were as seen below. Traces taken from DigSilent demonstrating the actual events are found in Appendix 3.

- A Line fault on the transmission line (half way down), then cleared after 100ms
- A Line fault on the transmission line (half way down), then the line is switched out after 100ms
- A Line fault on the transmission line (at voltage source end), then cleared after 100ms
- A Line switched into service
- A Line switched out of service
- A Load drop of 10%
- A Load increase of 10%

An example of one of the DigSilent traces is seen below in Figure 48.

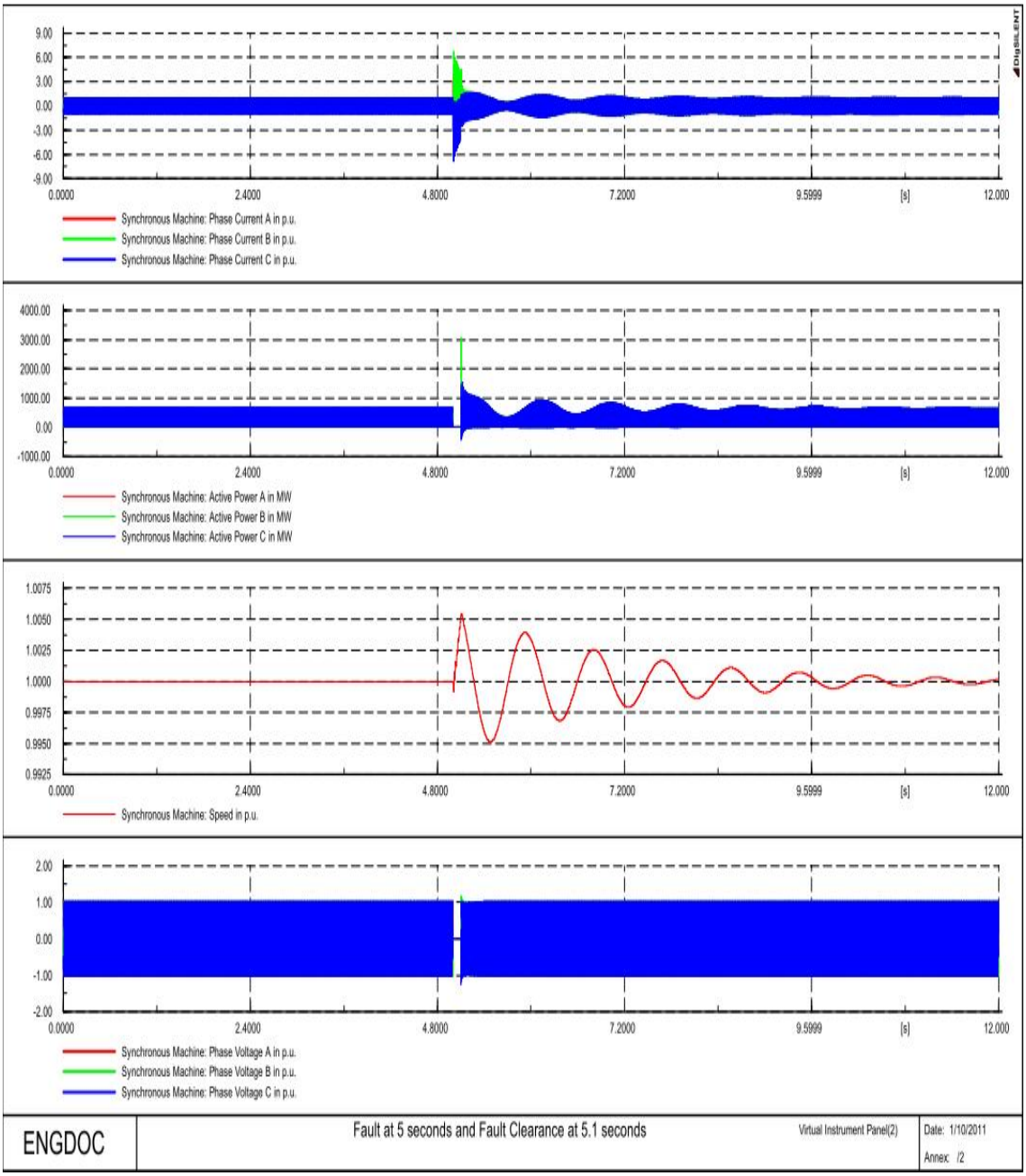

Figure 48 DigSilent trace

In order to confirm the consistency of the model phase current outputs to the synthetically created phase current data from DigSilent, a method of evaluation is necessary to numerically identify the difference between the two datasets. As described in the introduction to this chapter, phase currents are required to be compared against each other in order to develop an objective function for the PSO algorithm to use to derive a set of values for the parameters that are being identified. The error between the two phase current waveforms is seen to be:

$$fn(i) = \left\{\left[\int |i_a - \widehat{i_a}|dt\right] + \left[\int |i_b - \widehat{i_b}|dt\right] + \left[\int |i_c - \widehat{i_c}|dt\right]\right\} \quad (56)$$

where i_a, i_b and i_c are model output phase currents and $\widehat{i_a}$, $\widehat{i_b}$ and $\widehat{i_c}$ are recorded phase currents to be compared against.

This in effect produces a cumulative time varying error that defines the difference between the waveforms with respect to time. The gradient of this could be seen to be a reflection of the relative adherence of the model to the synthetically created data set, (i.e. the closer to a gradient of zero, the closer to an identical waveform).

As previously discussed the initialization alone provides an error between the two signal sets. Because of this initialisation settle time, the first 5 seconds of the simulation is neglected in order to reach a steady state function for the introduction of test perturbations. Using differing software for modelling and validation does provide a subtle discrepancy between the outputs. This is likely to be due to how the models are applied in the differing software, but is difficult to confirm without knowing exactly how the DigSilent machine model is implemented. The difference between the two signals is very subtle but still numerically recordable when looking at calculated error. Figure 49 shows the cumulative difference between the recorded outputs from the DigSilent recorded perturbations compared against the generated outputs of the power plant model used in this work. The base numerical error is evident in Figure 49 where the perturbations have an initial error of about 0.001. This could be considered the base line of cumulative error. Based on the relative gradients of the differing validation and test sets seen below, the error gradient is low, which infers a high level of adherence between the two datasets. Because of this it is prudent to suggest that the machine model, under the transient events shown, provides an accurate reflection of the DigSilent machine model, which in many respects self-validates its performance under these circumstances. It is seen that certain perturbations have non linear characteristics in Figure 49 below. This will be further analysed in the results and discussion chapters.

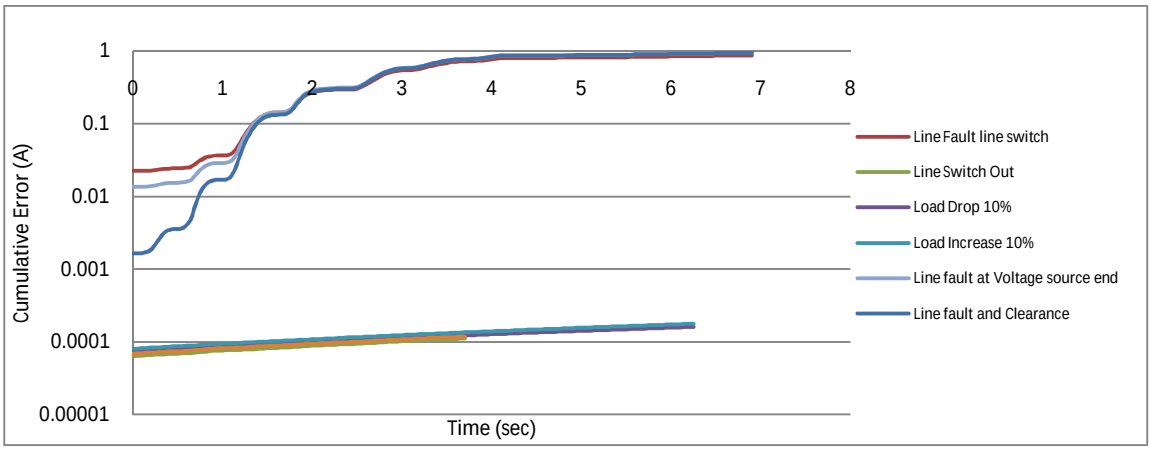

Figure 49 The cumulative error for differing transient events (base of 1A)

7.3 Excitation Implementation

Much like the synchronous machine model, mathematically there is a wealth of previously utilised models that provide a good adherence to real excitation system behaviour and are industrially accepted. The primary question that needs to be asked is not so much which model should be adopted but more so what exciter model gives a reasonable representation of different excitation system. This will allow the modelling of different excitation system types with a single model to a reasonable level of adherence to the real system.

As previously discussed, the main physical types of excitation are bus fed, pilot and static excitation. They all possess differing structures and control behaviours. A critical aspect to be considered is that of the three main IEEE control model types, the AC and the DC types both possess a feedback loop that characterises saturation in the excitation system. Static excitation systems don't have this specific aspect given the thyristor fired, slip ring fed system to provide the dc power to the rotor of the synchronous machine. Because of this the validity of using the static models are called into question as, although the static models are valid for their own excitation system topology, not being able to characterise saturation in the excitation system of a pilot excitation system is limiting.

There is the question however, as to whether it is necessary to model the excitation method to such a high degree as the excitation system saturation characteristics. This is because the perturbed voltage waveform may not provide sufficient influence to physically affect the phase current output to a degree that will facilitate parameter identification of the excitation system saturation. For this reason static excitation systems were not discounted as the fact that there is no representation of excitation saturation has less impact on the behaviour than might be thought.

An area that limits the varying options of the excitation model is the availability of excitation field current data during the simulation. This is because a significant proportion of excitation system models use field current as a form of feedback. The synchronous machine model is implemented in a way that makes it impossible to develop a value of this to be used as an input in this regard. For this reason models with field current feedback are impractical for this work. It is also unlikely that time dependent field current input data will be available from a power plant as conventional recording equates to a set of current and voltage transformers on the machine terminals with a recorded value every minute. It is very unlikely that field current is recorded in power plants.

There are some AC and DC excitation models available that do not use field current. In these cases a curve fitting process is used to characterize the saturation characteristics of the excitation system. This is used as the feedback to the excitation system instead of field current. The curve fitting process merely requires the output field voltage of the model which is freely obtained from the output of the excitation system model, so it isn't necessary to monitor it synthetically or in reality.

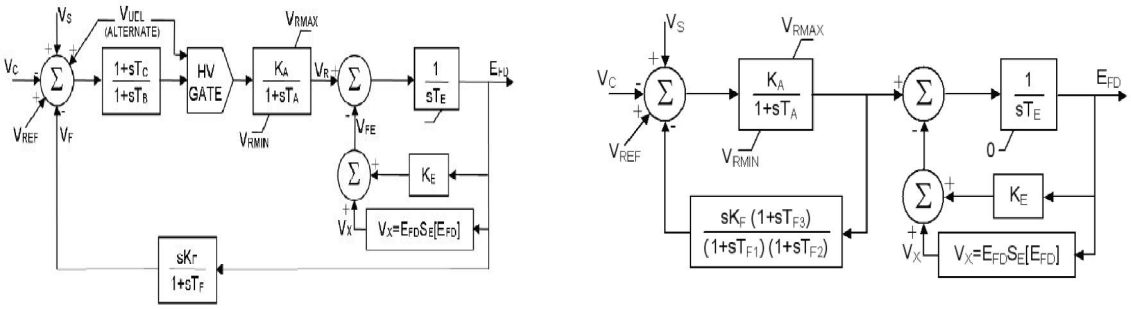

Figure 50 (a) The DC1A excitation system model (b) the AC5A excitation system model

Ultimately two options become apparent as viable options as a model to characterize differing excitation systems. These are seen in Figure 50. As mentioned in previous chapters, the DC1A excitation system model has previously been used to characterize other forms of excitation system with a reasonable level of success. Another option is that of the AC5A excitation system model, which is a representation of a pilot excitation system and has also been used to characterize other excitation system topologies previously. Rather than choose one of these in an arbitrary manner, both models were built and tested in order to identify which would be the more versatile of the two when considering the three main excitation system topologies under several transient types.

As can be seen from both the AC5A and the DC1A, the models saturation feedback is essentially the same although there are differences in the way that the curve fitting process calculates $S_E[E_{FD}]$ (57). A question that arises from this form of model and referenced datasets (84) is the ability of either of the models to be used for parameter identification given that, "The regulator is supplied from a source, such as a permanent magnet generator, which is not effected by system disturbances". It would be assumed that the implications of this are more so towards the AC5A pilot excitation system, but the similarities between the models is striking and it should not be assumed that given this similarity, the effects of this in modelling terms cannot be discounted. From this the general suitability of using such model types for parameter identification has to be considered further and tested because, if, as the standard

stipulates, there is limited effect of disturbance on the excitation system, then there may be little effect from the excitation system to influence the synchronous machine, which may inhibit the ability to perform parameter identification of the excitation system.

When considering testing and validation of the excitation model, two methodologies are possible. There is the direct testing method where the excitation system model is tested individually by applying step functions and other forms of stimuli directly to the V_c input and observing the E_{FD} output. This would seem somewhat redundant in many respects as, past making sure the model is working correctly, it would be just confirming that an industrially accepted model works in the way that the industry has already deemed appropriate. The other approach of connecting the machine model and observing the response to differing stimuli from the synchronous machine much like the way the machine model itself is validated. As previously stated there is a possibility that the response to transient events may not produce a significant response unless the transient was sufficiently onerous to cause an effect on the field current output.

The excitation system models were applied to the synchronous machine model. The transients to be included in the testing would be the same as included in the synchronous machine model testing in order to provide differing levels of severity of transient to the model. This also provides continuity in testing for the differing parts of the power plant model. A distinct advantage to synthetic datasets is that additional simulations can be run with or without excitation systems, so it is possible to appreciate the differences between the two. From this it is possible to identify the capabilities of such models and the levels of severity of transient required to make a change in field voltage and thus the stator current to be able to perform parameter identification.

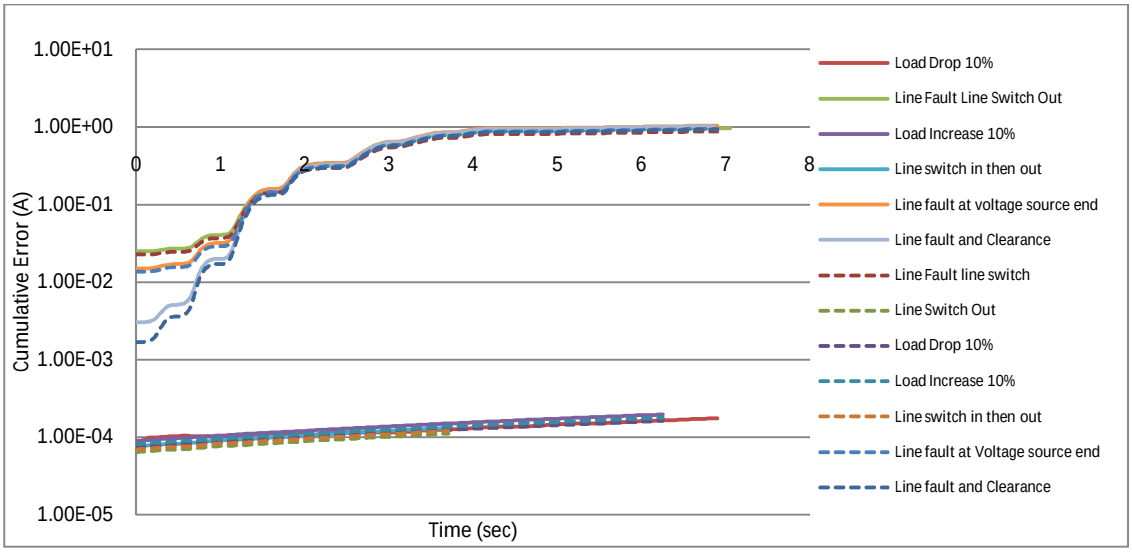

Figure 51 Cumulative error of AC5A excitation system (dashed lines) and the DC1A (whole lines) (base of 1A)

The purpose of this section is not identify whether parameter identification is possible or to what level, more so to identify the model type and highlight any particular aspects of interest. The two exciter models highlighted were modelled and tested. Both excitation models had synthetic datasets created for them for differing transient types. As seen in Figure 51, both compare well to the DigSilent synthetic data. An added advantage is that, fundamentally, both the DC1A and the AC5A excitation system models are very similar. Provided the correct parameter values are implemented (found in appendices), the outputs and responses of both are very similar. Because of this, both could be used as a reasonable representation of each other without significant detriment to phase current output error.

As can be seen from the results, although both perform favourably and are quite reasonable, the AC5A's response is slightly better, particularly with the line fault perturbations. This coupled to the fact that the DC excitation systems, although still used in some parts of the world, are not commercially available any longer, mainly due to the risk of voltage collapse, leaves the AC5A model being the more practical to move forward with.

7.4 Turbine Implementation

Modelling of turbines, gas and steam alike is a field that has been covered significantly as seen in previous chapters. Models exist for heavy duty gas turbines, aero derivative gas turbines, non reheat steam turbines, tandem compound single reheat steam turbines, etc. More critical to this project and to parameter identification in general is which model type is fit for purpose? Considering the limited amount of data that would be available from a real power plant it is pretty obvious that using large and complex models that accurately characterise each main category of turbine is not feasible. Data would not be available in order to be able

to perform the parameter identification in a thermo dynamic context and the crossover between one complex turbine model to the next does not allow the versatility required for this form of 'hybrid' identification of differing turbine types.

As previously seen, gas turbines essentially consist of an axial compressor, a combustion chamber and a turbine operating under a Brayton cycle. Air is drawn into the axial compressor and compressed through varying blade sets. This increases the static pressure of the air which is then mixed with fuel and burned in the combustion chamber. The combustion causes thermal expansion of the gas which turns the turbine blades and powers the turbine. From a mathematical model point of view, gas and steam turbines are quite similar. Effectively, the steam turbine achieves a similar end to the gas turbine in that the turbine blades are turned by thermal expansion of a high pressure gas, the difference being one is from burning a natural gas directly the other from using steam created from an external fuel source.

The effective resulting input seen by the synchronous machine is the same from both turbine types (i.e. a mechanical torque or power). This also translates similarly between heavy duty gas turbines and aero derivative gas turbines which, although different in layout (heavy duty gas turbines occupy a common shaft with the synchronous machine whereas aero derivative gas turbines can have multiple shafts), are essentially the same in many ways. The only significant difference with regard to the work at hand is that because the aero derivative gas turbine has more than one shaft, its relative inertia is far lower than its heavy duty counterpart. This in terms of a modelling perspective is ideal to perform parameter identification using a single model as it allows both to be characterised using the same model structure by adjusting parameter values. The analogy continues into the realm of steam turbines. If not trying to characterize the turbine from a thermodynamic point of view then a turbine, for both gas and steam, is essentially a governor that controls its speed, and a transfer function that defines how fast the turbine can reach the governors defined speed. Because of this the generic turbine can be used to model the turbine behaviour to a level of detail suitable for the method of parameter identification adopted. The generic turbine and governor are seen in Figure 52. Given the model is industrially accepted as being an adequate representation of a basic steam prime mover, validation becomes redundant other than proving that the model adequately characterizes a gas turbine response.

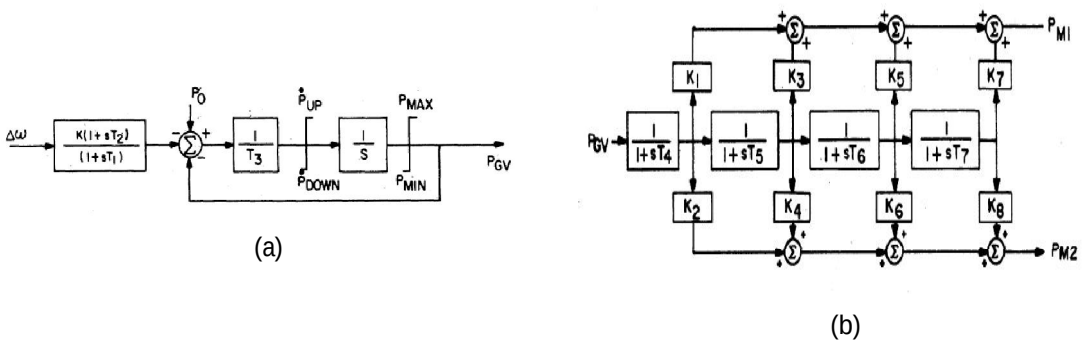

Figure 52 Models for governor (a) and turbine (b) (9)

There are limitations to the model adopted; the model doesn't allow for the characterisation of outside temperature and pressure. In gas turbines this is really quite important as it has a significant effect on the turbine to produce the manufacturer's specified output. Other influential facets of gas turbine performance are exhaust temperature and the fuel to air mix. This must be counter balanced by the fact that the overall error or objective function used in the parameter identification is from the phase current output and, although experimental simulations are yet to be seen and discussed; the influence of the turbine would probably not allow for a more elaborate turbine model. It could also be said though that creating a model to consider such aspects would not be as practical in power system analysis modelling.

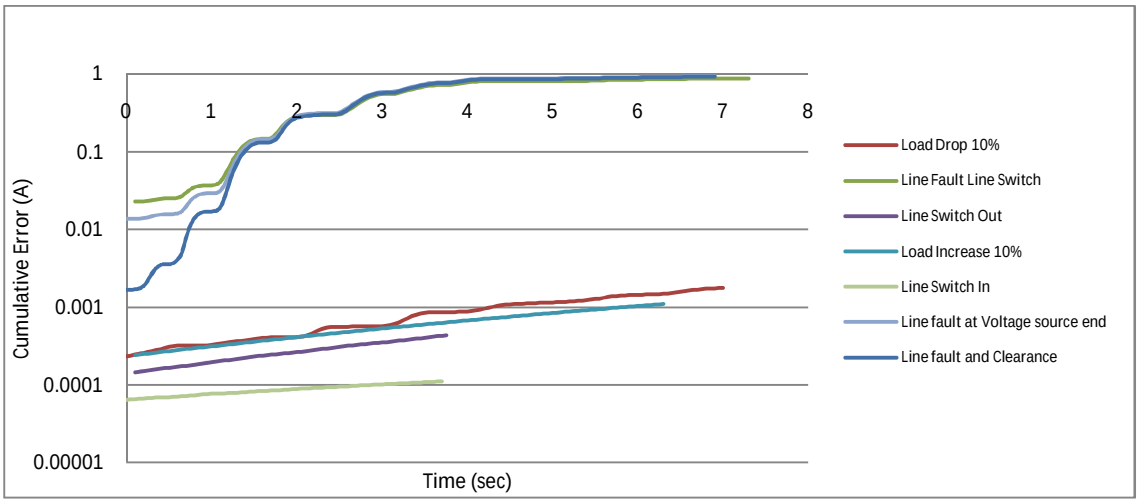

Figure 53 The cumulative error from the introduction of the turbine model (base of 1A)

The turbine model is applied to the synchronous machine model for testing as previously seen with the excitation system. The turbine and governor parameters can be found in Appendix 3. Figure 53 shows the results are consistent with the synthetically created datasets using DigSilent. It is noted that the relative errors seen correspond quite similarly to that of the synchronous machine model tests seen above in Figure 49. This would suggest that the relative impact and influence on the behaviour of the turbine is not as significant when

considering the transient time period. This would be logical given the turbine's base function and time constants associated with it would be more influential over a longer time. Because is likely the turbine would exert more influence on perturbations where electrical load is directly impacted. It will be interesting going forward to see the relative influence that the turbine and governor have on the overall phase current error and whether this enables them to be identified.

7.5 Combined Model

Finally as part of the validation of the model, the turbine, excitation system and synchronous machine model are tested together. As seen in Figure 54 the results of the testing shows a reasonable level of adherence between the synthetically created dataset in DigSilent and the outputted phase currents from the model. It is seen in the results that the error maintains a reasonable gradient throughout the simulation. The results which are slightly higher in gradient are that of the line fault and then line switch out, the line fault at the source end and clearance and the line fault and clearance perturbations. It would appear that this discrepancy is from the different way in which the synchronous machine model is applied in DigSilent to the way the model in this work is implemented as there is little else to create it. It is interesting to note that, of the transients tested, this discrepancy is only prominent in double perturbations (i.e. there is a line fault causing the initial perturbation, and then because of this the line is switched out, causing a secondary perturbation). This is investigated further in the results chapters. Even with this subtle discrepancy it would still be reasonable to infer that the power plant model behaves in a way consistent with that of an industrially accepted power systems package. This would support the principle that the model is a valid and reasonable representation of a generator in common usage.

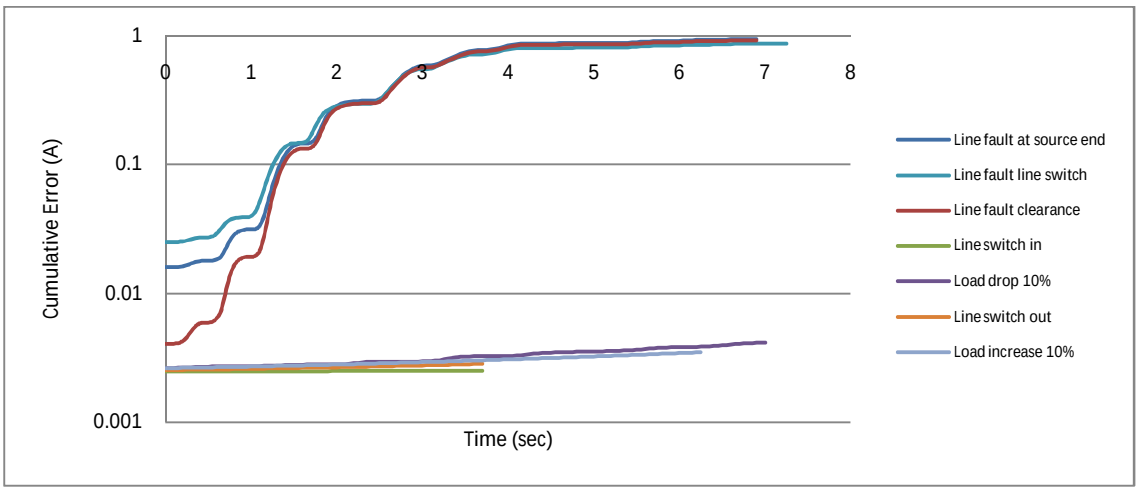

Figure 54 Cumulative error of complete system model (base of 1A)

7.6 Summary

A methodology and model for the identification process to utilise has been developed. The base structure of the synchronous machine, exciter and governor/turbine model allows recorded phase voltages to be fed into the model. These phase voltages are converted into direct and quadrature voltages. The direct and quadrature voltages are then fed into the d axis and q axis models. Combined with input from the excitation system and the rotor block, direct and quadrature axis currents are developed. These are then converted back into phase currents. The phase currents are then compared against recorded waveforms to create an error which forms the basis of the objective function. This objective function is used by the optimisation algorithm for the identification process.

After comparing the two possible excitation system models, it is seen that the most appropriate model to be used for this work is that of the AC5A pilot exciter model.

The model's response has been tested in comparison to synthetically created perturbations in DigSilent, an industrially accepted power systems package. This provides a high degree of confidence that the model's response is consistent with what would be expected from real equipment.

8. PSO Algorithm Implementation

Parameter identification of power plant characteristics are heavily influenced by the model adopted and the algorithm used to estimate the variables held inside it. In order to analyse the results of the parameter identification using an algorithm like particle swarm optimisation[16] it is necessary to understand how the algorithm is implemented and examine relevant aspects relating to it.

Before going into greater detail regarding particular aspects of the algorithm it is necessary to discuss the type of PSO algorithm adopted. In many ways, the two forms of algorithm are parametric or adaptive. Adaptive algorithms require the user to define the problem, or in this case, the parameters and the objective function itself. The algorithm then finds a solution on its own without further input. Parametric algorithms require the method of resolution to be defined; this may be with coefficient modification or more drastic measures. Admittedly, there are advantages and disadvantages to both philosophies; for repetitive problems which have numerical differences but no change in difficulty, then parametric functions allow the modification of coefficients to find a solution faster than an adaptive method. That said, if a minima is found swiftly due to the inherent randomness in the search then the coefficient 'tuning' becomes redundant as not only does it become pointless, but also there has not been sufficient time for patterns in the search to be developed and thus further tuning to reach the final minima becomes impossible. In this regard adaptive algorithms becomes more advantageous.

In choosing the methodology it is also necessary to remember the most basic of requirements of the parameter identification process. The algorithm must take an objective function value (a cumulative error per unit time in this case) and optimise the variables in order to minimise the objective function value. It could be argued that either methodology would achieve this, but in considering that the parametric form requires guidance for the optimisation to be effective, when this guidance isn't available, adaptive algorithms are the only solution.

From this, the base structure of the algorithm is found below. The flow chart is used to explain specific aspects of the algorithm that require further discussion.

[16] In the context of this work, the particles in PSO become multi dimensional vectors with each dimension holding a parameter value that changes through the search.

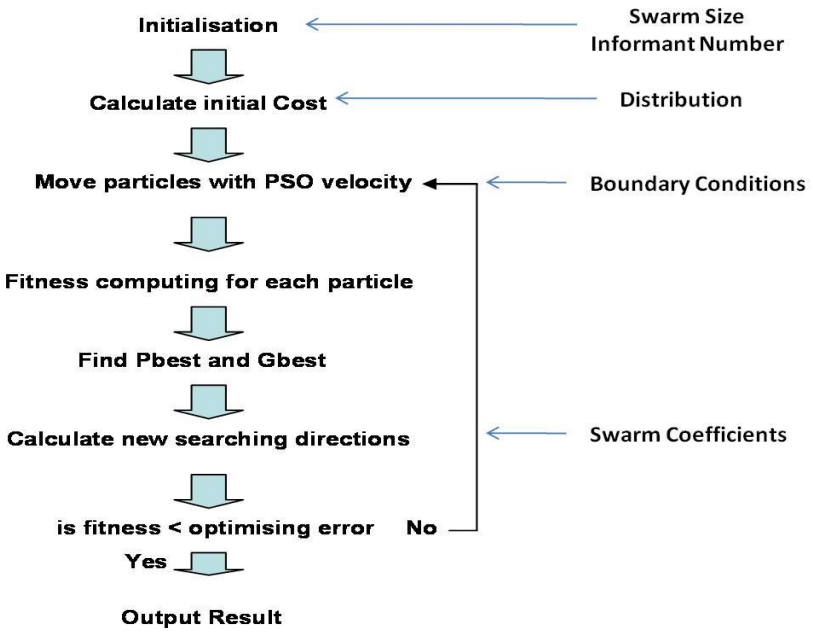

Figure 55 PSO flow chart

8.1 Initialization

8.1.1 Swarm Size

As part of initialization it is necessary to define the number of particles used in the search. This has been a subject of debate for several years. It would seem that the larger the particle number, the more likely a solution would be found in fewer iterations, but this is not actually the case. A larger particle number requires a high computational cost to evaluate the large number of particle locations which equates to a large number of parameter values. Likewise if a swarm of particles is small, logic would dictate that the computational cost would be low, thus a solution found faster. Again, this is not the case as the low particle number would result in a search that does not cover the search area appropriately and therefore, again take longer. From this it becomes obvious that a compromise is required. Empirically fifteen to twenty is considered sufficient to perform an adequate search (86).

8.1.2 Informants

As part of the PSO algorithm, information is passed to particles by a small group of chosen particles called informants during each iteration. The number of informants is dependent on two aspects; diversity and propagation. Diversity decreases as the informant to standard particle ratio increases. This is because each particle receives less information about what solutions other particles have achieved. This is counterproductive in many ways as common sense would dictate that the more information the particles have, the easier and swifter it is to find a good solution. In doing this however, there is an inherent risk that this causes a too

uniform a search, which means that the required randomness in PSO is marginalised, undermining the ability of the method to conduct a thorough search. On the other extreme of this, if there are too few informants, the information used by the particles for defining its next search choice will be limited and thus compromised. It is also less likely to find and transmit a good result around the particle swarm. Propagation of information becomes faster and better as the particle informant to standard particle ratio increases.

The requirements of diversity and propagation need to be balanced in order to reach a reasonable informant to standard particle ratio. This allows for an appropriate level of information to be disseminated around the swarm. Given the swarm size, four informants would be considered a reasonable number (86). Any larger amount creates a denser level of particle influence that propagates information at too fast a rate, meaning the swarm simply doesn't have sufficient time to look for other minima and so runs the risk of not finding a global solution, instead, focussing on a local one. Four informants in the swarm also balances the level of computational cost that is required for the evaluation algorithm. This is because the objective function is in effect, an error, to develop a solution for an informant; the parameters held by it need to be evaluated. Thus for every iteration, four simulations of the generator model has to be evaluated to develop the objective function value.

8.1.3 Particle Distribution

The distribution of the particles during initialisation is an area that is problem dependent in many respects and thus requires further evaluation. Varying forms of distribution are simulated and evaluated in the results and discussion chapter with the differing forms of distribution highlighted in this section.

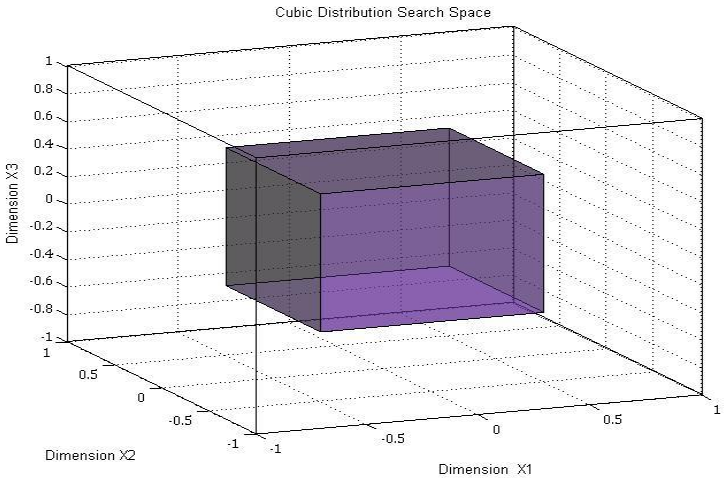

Figure 56 A cubic search distribution

A rectangular distribution as seen in Figure 56 is the obvious and most simplistic form of initial distribution. For simplicity of explanation, in a three dimensional search, the particles are distributed in a cubic format equidistantly placed throughout the cubes volume. The cube occupies the search area considered for the algorithm. But what if the boundaries that define this search area are not as 'hard' as would be presumed, and in actuality porous? Likewise what if many of the particles are distributed along the search boundaries or axes, which isn't unthinkable given the relative magnitude of some of the parameter values. An example of this would be armature resistance which has a very small per unit value. In this regard, the axes provide a natural boundary giving the value of the particle location in that dimension a value of zero. This would have an effect on the vector that would be calculated in the next iteration and implications for the search as it continues. One could argue that by definition if the particles are uniformly distributed, surely they have the best chance of finding a solution in the most efficient manner. This is something to be ascertained. Other distributions considered are ellipsoidal positive sectors. Again, thinking in three dimensions for simplicity, in ellipsoidal distributions the cubic distribution is replaced with a form seen below in Figure 57. Other distributions to be considered include an independent Gaussian distribution where instead of a uniform distribution, a normalised distribution is used. This will be considered further with the results of implementing the varying distribution types found in the results and discussion section.

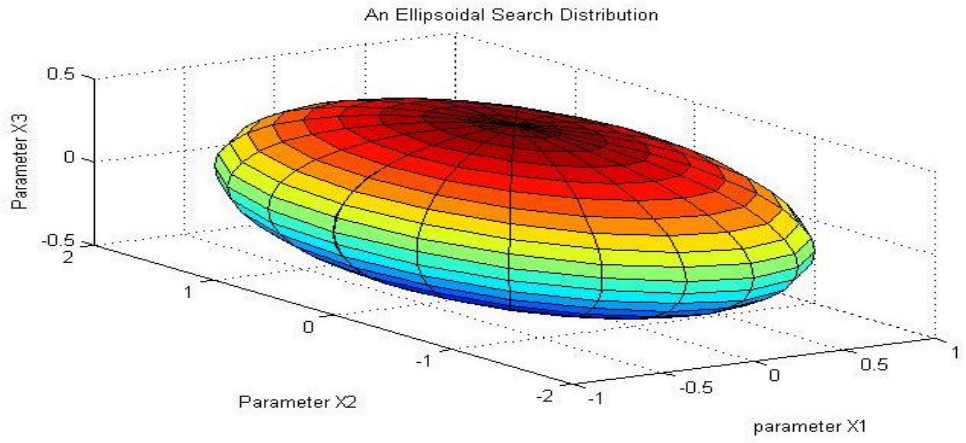

Figure 57 A spherical or ellipsoidal search distribution

8.2 Boundary Conditions

Unlike other methods of optimisation PSO has the ability to define the search space which the particles occupy. This confinement has differing forms which could have a significant effect on the optimisation and the identification of the parameters in the model. For this reason

differing methods of confinement are investigated and the relative implications of using them will also be considered.

In many ways, the method and the application of this algorithm is unorthodox. This non conventional application also applies to boundary conditions. Conventionally the objective function would be constrained by limits to define its behaviour. This is effectively irrelevant as the objective function that is to be optimised is the compared error between a model output and recorded terminal data. In this regard the 'classical' form of confinement that would be adopted for a nonlinear function such as Ackley (86) or Rosenbrock (87) cannot be followed.

The only aspect that can be constrained in an effective way is the parameters that are to be identified (these are the multidimensional vectors of the particles in the search). This in actual fact is advantageous as, although a lower error, or objective function is good, without the correct parameter values defining the error, the result becomes meaningless. Confining the parameter values limits the number of random combinations that could create an error that is without merit, although doesn't remove the possibility of local minima being allowed to manifest within the search space.

In understanding the need for confinement, it is necessary to investigate the varying forms of confinement that exists and how effective they are with respect to this form of problem. Imperative and indicative confinement creates a two tier boundary condition where the inner boundary is indicative of when the search reaches the edges of the search space, but merely uses this information to set the next iterations search vector. The imperative outer boundary is a 'hard' boundary where, if the search steps outside this boundary, the search will be reset to a vector within the search space. Because of the way that the method is applied, imperative and indicative confinement (86) is difficult to apply. In considering this form of confinement for the application, the use of 'hard' and 'soft' boundaries is redundant because the possible variation in variable values is known, but nothing more, thus the application of imperative boundaries would be achievable, but indicative would achieve very little.

The most obvious form of implementing boundary conditions would be that of interval confinement. This is defining the search space with upper and lower limits per dimension of the search. Without the introduction of indicative boundaries, imperative boundaries can be equated to interval confinement. In many ways this may be the most practical form of confinement as it allows the variables to sit within realistic operational limits, like for example saying that, for a two pole round rotor turbo generator, the direct axis reactance would be

within 0.95 and 1.45 per unit in value (27). This allows the user to be pragmatic as to the search area and realistic as to the values the parameters can occupy. Mathematically this is seen below

$$X_d \notin [X_{min}, X_{max}] \begin{pmatrix} V_d \leftarrow 0 \\ X_d < X_{min} \Longrightarrow X_d \leftarrow X_{min} \\ X_d > X_{max} \Longrightarrow X_d \leftarrow X_{max} \end{pmatrix} \quad (57)$$

Granularity confinement is another method where discrete variables are given acceptable values from a start point and incrementally the value is stepped through by ∂ to find the correct final result as seen.

$$X_d \leftarrow X_{min} + \partial E\left(\frac{X_d - X_{min}}{\partial} + \frac{1}{2}\right) \quad (58)$$

Both interval and granularity confinement create boundaries. If those boundaries are exceeded then the method will essentially pull the particles back into the defined search space. The new vectoral characteristic of the particle is an area of consideration that will be evaluated with the differing confinement methods. A method that is also investigated is that of confinement by dichotomy. Confinement by dichotomy posses a differing philosophy to the other discussed forms of confinement. In this form, when the particle steps outside of the search boundaries, instead of being 'reset' to within the boundaries, a median position between the old position (within bounds) and the newer position (outside of bounds) is used to reposition the particle. This could allow for a more thorough search of boundary areas which the other methods do not allow for.

The differing forms of confinement are evaluated in chapter 10 of the results and discussion.

8.3 Swarm Coefficients

There are varying forms of PSO algorithm, likewise differing forms of PSO equation. This work is not to so much to develop a new algorithm, more so evaluate if it the algorithm is physically able to perform the parameter identification required. The form of algorithm adopted is that of a constricted PSO. The functionality of such a PSO type has been proven (83). For this reason it is adopted in this format in the equations seen below:

$$V_i^{K+1} = K(\omega_i V_i^K + C_1 r_{and} * (P_{besti} - X_i^K) + C_2 r_{and} * (G_{besti} - X_i^K)) \quad (59)$$

$$X_i^{K+1} = X_i^K + V_i^{K+1} \quad (60)$$

where C_1 and C_2 are positive constants classed as acceleration coefficients, ω is the inertia weighting factor and r_{and} is a function that generates the inherent randomness in the PSO. X_i represents the position of the ith particle, P_{besti} is the best previous position of X_i and G_{besti} is the

best previous position among the members of the population chosen at random as informants. V_i is the velocity of particle X_i. This combination of equations calculates a new velocity that drives the particles towards P_{best} and G_{best}. K is the constriction factor of the search. Every particle's current position is then evolved, which produces a new position in the solution space.

As previously mentioned, the PSO type adopted is constricted PSO. This method is not common to other examples of PSO for parameter identification purposes and is mathematically defined as K (88). This factor limits the search space per iteration. The constriction factor is a constant and the value used is calculated from the chosen values of C_1 and C_2:

$$K = \frac{2}{\left|2 - \sigma - \sqrt{\sigma^2 - 4\sigma}\right|} \tag{61}$$

where $\sigma = C_1 + C_2$ and $\sigma > 4$.

As seen above r_{and} is in effect a command that allows for the injection of randomness into the search process. It could be argued that perhaps this command doesn't create a sufficiently random number generator to that which could be used, such as KISS[17] (86) but the relative improvement does not outweigh the relative computational cost of implementing it, thus is neglected.

Constriction itself has specific advantages over non-constricted PSO. During the initial stages of a search, the constriction coefficient forces the particles to converge rather than risk the possibility of population explosion (86). This allows for a more efficient convergence.

8.4 Summary

As part of the development of the most appropriate version of PSO, varying aspects of the algorithm have been considered. The base swarm structure has been identified as using fifteen to twenty particles and four informants per iteration. The form of PSO adopted for this work is constricted PSO. This is because is it allows the highest likelihood of a efficient convergence.

Other areas such as the initial distribution of the particles, boundary conditions and swarm coefficients have been highlighted. These aspects are reviewed and the results found in chapter 10.

[17] KISS is a methodology for random number generation. The acronym stands for 'Keep It Simple Stupid'.

9. Parameter Influence on Identification

In order to address the overriding questions that this work asks, the results and analysis is split into three main sections:-

- The influence of parameters and perturbations on the objective function (chapter 9)
- The results of parameter identification using PSO on synthetic datasets (chapter 10)
- The results of parameter identification using PSO on real recorded terminal data (chapter 11)

Firstly it is fundamental to understand how each parameter has an impact on the phase current output error, or the objective function of the model that is to be optimised. Without such analysis the results of parameter identification could be developed but have no real value as the parameter may have no, or little influence on the objective function and thus cannot be optimized. In this case the value derived would likely be defined by the limits of the search and little else. The influence of the type of perturbation is also considered as an area that has an influence on the ability of the parameter to affect the phase current output error. This is covered in chapter 9.

Chapter 9 also considers the relative merits of the influence that the parameters possess regarding parameter identification. This could include the relative gradients of the influence curves[18] or the relative width of the minima and the implication this has on parameter identification. This chapter does not use an algorithm in its data analysis. It simply considers the objective function as a standalone output.

Once the parameters which are capable of parameter identification have been identified, the effect of using differing perturbations is considered in order to observe whether this has an impact on the ability of the optimisation algorithm to identify the correct parameter value.

Moving to the use of the PSO algorithm with synthetic datasets[19], the implications of using differing forms of PSO algorithms and other settings as mentioned in the implementation is considered in chapter 10. This includes algorithm settings, such as the initial search distribution and how it affects the ability of the algorithm to optimize. Likewise it considers confinement strategies and the practical limits of the optimisation algorithms.

[18] An influence curve or characteristic is created by incrementally modifying a single parameter value and observing the effect that this has on the objective function during differing perturbations.
[19] The raw synthetic data results from DigSilent are found in Appendix 5.

Finally, in chapter 11, once the parameters that have the optimal influence, and thus the highest likelihood of being optimised have been identified, and the most appropriate settings regarding the PSO algorithms are decided on through the use of synthetic data, the optimal solution will be used with recorded terminal data. From this it is possible to understand the relative issues regarding real terminal data, such as the implications of relay protection on the phase current waveform with regard to parameter identification. Once these aspects have been considered, the results of the parameter identification are analysed.

9.1 Influence of Parameters and Perturbations

Looking at the influence of each individual parameter by analysing the phase current output error will allow a greater understanding of how, and if a parameter has any influence on the phase current output of the machine model. This coupled with the analysis of differing perturbation types allows an understanding of the influence the perturbation type has on the parameter identification. This means that not only will the parameters most suitable for identification be derived, but also under which conditions these parameters are best sought. A comprehensive list of the parameter values used is given in Appendix 3. These are typical parameter values for power plant equipment. The parameter values are used in DigSilent for the creation of the synthetic transient waveforms used to assess the parameters influence to the output phase current waveforms.

In Chapter 7, in order to validate the model, seven differing perturbations (created in DigSilent) were used. It was seen that several produced very similar results. For this reason, the number of perturbations used in further testing was reduced to four for simplicity. These four (the line fault and clearance, line fault line switch out, line switch out and a 10% load drop) are representative of the behavioural traits already investigated.

9.1.1 Steady State Direct Axis Reactance

The steady state direct axis reactance is a significant parameter in synchronous machine modelling and in many respects there are already tight boundaries that govern what values X_d can occupy in reality. The results observed come from a machine with a fairly high level of non saliency and a real X_d value of 1.79 per unit.

Figure 58 shows the change in error that is created by incrementally modifying the model value of X_d and running the simulation through differing perturbation types. This translates to several hundred simulations which is computationally intensive.

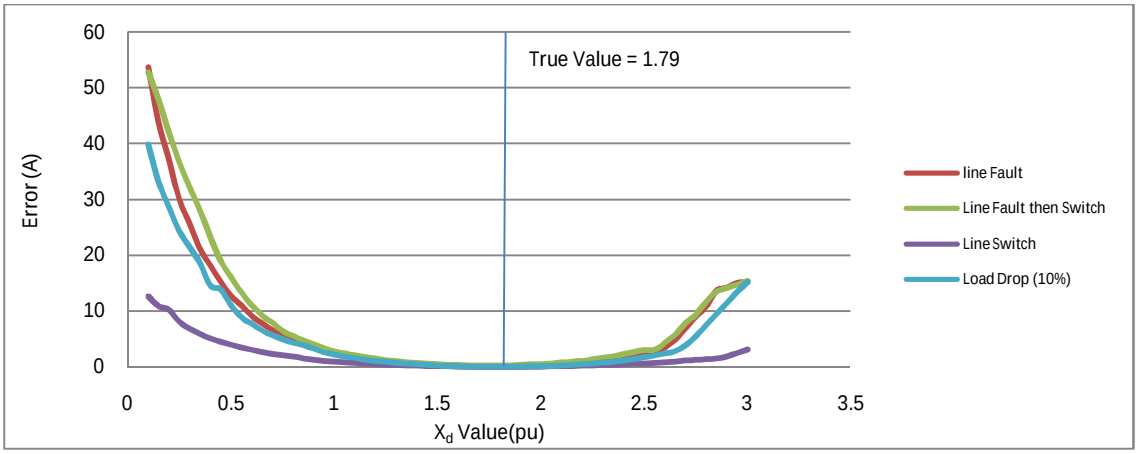

Figure 58 The influence of X_d from differing perturbation types on phase current output error; linear scale, (base of 1A for all influence curve graphs)

Primarily the most significant aspect to this result is that the error forms a 'bathtub' curve around the real parameter value. This, at its most basic level infers that steady state direct axis reactance has a significant effect on the model behaviour. This, although expected, also suggests that parameter identification would be possible using this parameter.

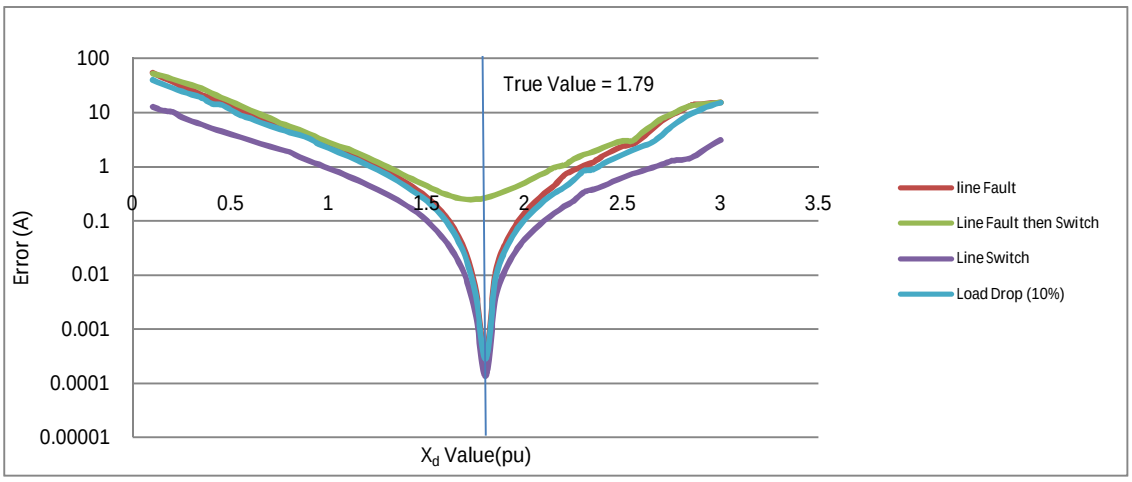

Figure 59 The influence of X_d from differing perturbation types on phase current output error; log scale

Looking further at Figure 58 it can be seen that depending on the perturbation type, the gradients of the 'low end' X_d values are different, particularly when looking at the line switch perturbation. The others possess a similar gradient approaching what appears a near zero value. This could infer that due to the line switch perturbation being lesser in magnitude than the other perturbations; it doesn't allow as much parameter influence on the phase current output error as the other more onerous perturbations. This is again seen when looking at the higher values of X_d.

Considering the data on a logarithmic scale shows the result in a differing light. Although in Figure 58 the line switch perturbation is seen to have a lesser effect on parameter influence, in Figure 59 it is seen that the minima it reaches is sharp at the correct value. This behaviour is evident in the line switch, the load drop and line fault perturbations. It is seen that although the line switch perturbation may not physically effect the error to the same order of magnitude, the convergence on the minima is good, which in terms of optimisation is more important in many respects.

Based on Figure 59 it is seen that the relative difference in minima value between the line switch perturbation, the load drop perturbation and the line fault clearance perturbation is relatively small (within half an order of magnitude). These all provide sufficiently accurate values of parameters to be able to perform parameter identification with a high level of confidence that the result is reasonable for the machine type. Another area that is encouraging for identifying X_d is the relative gradient of descent to the minima and range of values that the perturbations create. It is seen that between values of 1.5 and 2.25 per unit, the gradient of descent in error is very high; meaning from a parameter identification point of view, there is a high likelihood of continuous improvement until reaching the minima. Likewise if a local minimum was found in a multidimensional search and was not improved on, the value that X_d would occupy would still be reasonable for a machine of this type, although not exactly correct.

In Figure 58 and Figure 59 the relative influence that the line fault line switch perturbation has on phase current output error is different to that of the other perturbation types. On a linear scale the perturbation behaves similar to the others. When seen on the logarithmic scale however, it is observed that the perturbation appears to affect the ability of the parameter to influence the phase current output in the same way as the other perturbations. This is seen particularly at the minima or point of real parameter value, where unlike the other perturbations which have errors of magnitude around the 0.0001 to 0.001 range the error is of the order of around 0.25 which is significantly worse than would be expected for a successful conversion. Because of this, from an optimisation point of view, if iteratively searching to reach a specific error level the optimisation would continue searching until reaching a predefined iteration number rather than reaching a suitable convergence error. It is also seen that the gradient the perturbation produces is far shallower, making it harder for an optimisation algorithm to find an improvement in phase current output error.

The lesser gradient makes it more difficult to solve the optimisation but is not fatal. The minima point is in the correct location, likewise there is a gradient, even if it is a shallower one, and this means that even with the reduced influence there is sufficient embedded information in the curve to assume that parameter identification is possible.

Although the relative influence of the perturbation has been considered, the reason why has not been explored. The question that becomes prominent from this is why the line fault and clearance is so different to that of a line fault line switch out? When considering the difference between the line fault and clearance and the line fault and line switch, it is seen that the difference in parameter influence between the two is quite significant. If the line is faulted and cleared the relative error of the defined parameters is reasonable whereas if the line is faulted, but the line is switched out the parameter value against error is ill defined and fairly flat in relative output. This would appear illogical because the two in many respects are the same. There is one significant difference however; the line is switched out rather than a clearance.

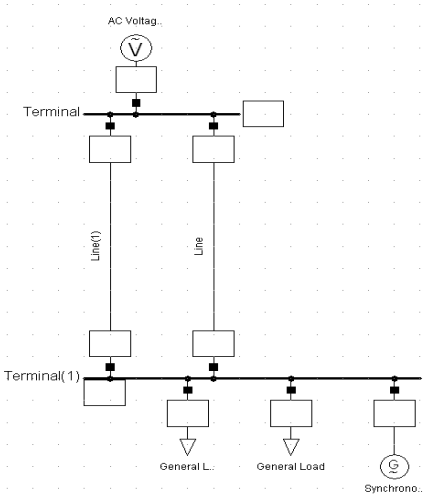

Figure 60 Basic test network for the creation of synthetic transients

The network model in Figure 60 shows two long transmission lines where the fault is instigated half way along one of them. If a fault is instigated, and the fault is cleared, then in effect the transmission line returns to a steady state position after a small secondary perturbation. In this respect, there is less to influence the machine behaviour. Because of this, there is a more defined 'dip' in error as it reaches its characteristic real value. If this is compared to the line fault then line switch out, up until the point of clearance both networks are exactly the same in every respect. When the line is switched out the transmission lines are no longer a double circuit and become a single circuit, causing the relative impedance between the slack bus and the machine bus to be doubled.

It would seem logical that the larger secondary transient the switching creates has a slightly different response in the DigSilent model to that of the estimator model. This difference creates a change in bus voltage input at the machine bus. This masks any relative change in parameter influence meaning that it becomes difficult to identify the influence of parameters under such circumstances. This is supported by the relative change that the direct axis reactance produces under these circumstances which can be seen under every other perturbation to have a significant influence.

Another question that arises from this is then, does the relative location at which the perturbation occurs have a significant effect on the ability of the parameter to influence the machine phase current. Considering the load drop of 10% performed on the machine bus, the single line switch and the line fault and clearance, the line fault and clearance is performed half way down the transmission line in comparison to the other two which effectively occur at the machine bus. The relative difference in the influence of the parameter though is seen to be minimal though which suggests that it may have a lesser effect than would be assumed.

What is interesting however, is noting that of the four perturbations tested, two have what can be considered a single transient event. In the load drop perturbation, the load of the bus is dropped by 10% and the effect is observed. Likewise the line switch, although a line is switched out, only one transient occurs for the machine to respond to. This means that if more than one perturbation event occurs in an overlapping time period, the different transients causes a change in the model's response to that of the DigSilent response which means the relative influence of the machine parameters to the error is masked.

Looking at Figures 51 and 52, it is clear that a strong secondary transient (like the line fault line switch case) has an effect on both the shape and magnitude of error function when comparing the model results with those generated from DigSilent. The likely explanation for this is the different ways in which the various model blocks are integrated to give the overall response creating a minor discrepancy between the two sets of results. The fact that the line fault and clearance influence characteristics are better than that of the line fault line switch perturbation is because the secondary perturbation is weak in comparison to the line switch secondary perturbation. X_d is a very influential parameter to the machine model characteristics, thus only a significant secondary perturbation will have sufficient effect to disrupt the influence characteristics of the parameter. It will be interesting moving forward to see if less influential parameters cope with similar effects as well.

Although the influence of the transient type is an area of research, the primary consideration is that of the influence of the parameter itself on the phase current output error. Given the relative influence it has on the error, it seems reasonable to say that X_d affects the phase current output error on all perturbation types tested to an extent that it is reasonable to infer that the parameter could be identified through optimisation. This is particularly visible on Figure 59.

9.1.2 Transient Direct Axis Reactance

Proceeding further into the direct axis reactances, the transient reactance X'_d presents some interesting performance traits which are somewhat different to steady state reactance X_d.

Looking at the error plotted on a linear scale[20] for X'_d in Figure 61, there are some distinct differences between X'_d and X_d. It becomes obvious that the line fault and clearance and the line fault line switch perturbations have a more significant effect on the error than that of line switch and load drop which are largely unmoved throughout the range of values. An interesting aspect of these two more influential perturbations is that although they exhibit minima, they occur at different locations.

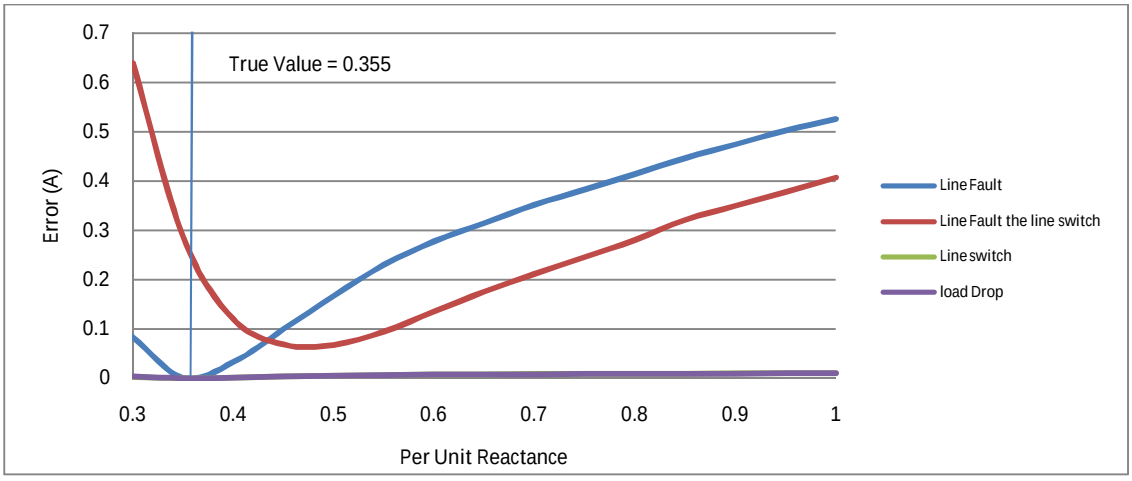

Figure 61 Influence of X'_d from differing perturbation types on phase current output error; linear scale

Considering the logarithmic performance more closely provides further insight. It becomes apparent that although the relative influence that the load drop and the line switch possess is not significant, they both possess a very good local minima, better in fact than that of more influential perturbations. It is also observed that the minima point and gradient for both of these and for the line fault and clearance perturbations are not only in the right place, but also exhibit characteristics that are suitable for parameter identification.

[20] The error plotted on a linear scale is referred to as linear performance for expediency. Likewise this is the case for the error plotted on a logarithmic scale, being referred to as the logarithmic performance.

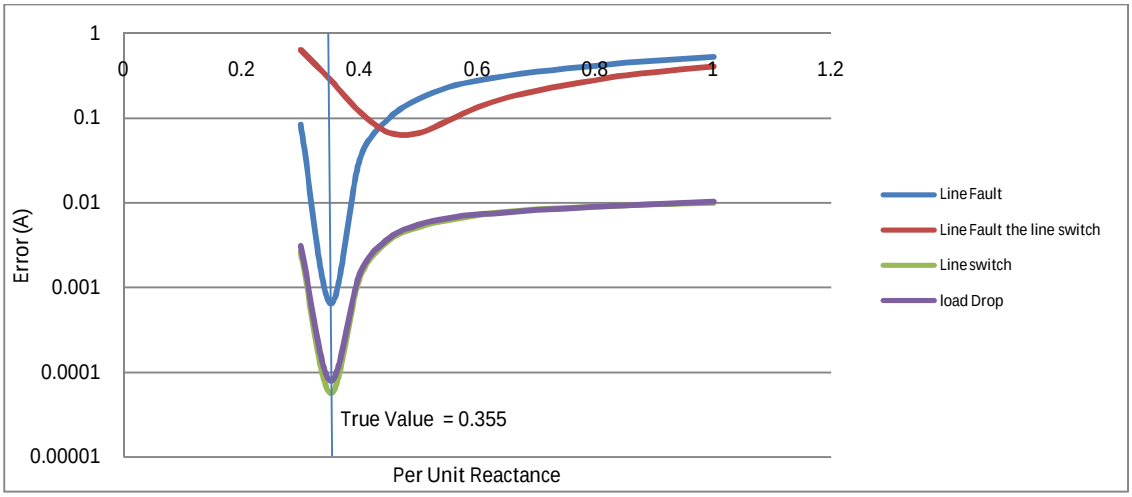

Figure 62 Influence of X'_d from differing perturbation types on phase current output error; log scale

As previously mentioned, looking at the line fault line switch out perturbation raises interesting aspects for consideration. The minima, which would be assumed to be at the point corresponding to the actual parameter value is not (in this case the real value is 0.35 per unit), and is found in a higher position. As previously discussed, this could be due to the secondary transient that causes a difference in machine output causing a larger phase current output error. The larger magnitude of the secondary perturbation means the overall influence of the parameter is adversely affected. In itself that raises some interesting questions as to the ability of parameter identification to function under more than one transient occurring at a time.

It is also observed that under the line fault line clearance perturbation, the relative influence the parameter has on the error is effectively an order of magnitude worse than that of other perturbations like the load drop and line switch out perturbations. In considering the fault clearance, the clearance of the fault causes a small perturbation to the system, which although not of the same magnitude as that of a line switch out, causes a sufficient discrepancy between the two machine model outputs to effect the phase current output error to the extent that is seen. This is supported by the phase current waveform seen in Figure 63 where, upon clearance there is a second, smaller perturbation seen on the phase current output of the synthetic dataset. This small secondary perturbation seems to produce a discontinuity between the synthetically generated dataset from DigSilent and that of the machine model adopted for this work. The relative difference appears minute which is why the difference between the waveforms of the line switch and load drop perturbations and the line fault clearance perturbation is only an order of magnitude different, (between 0.001 and 0.0001). This would suggest the DigSilent transient characteristics are slightly different under these

conditions. The difference in the two models for the line fault and clearance perturbation is seen in Figure 63 below. It is observed that the initial perturbation response is the same, but the secondary perturbation has a subtle discrepancy in magnitude of behaviour.

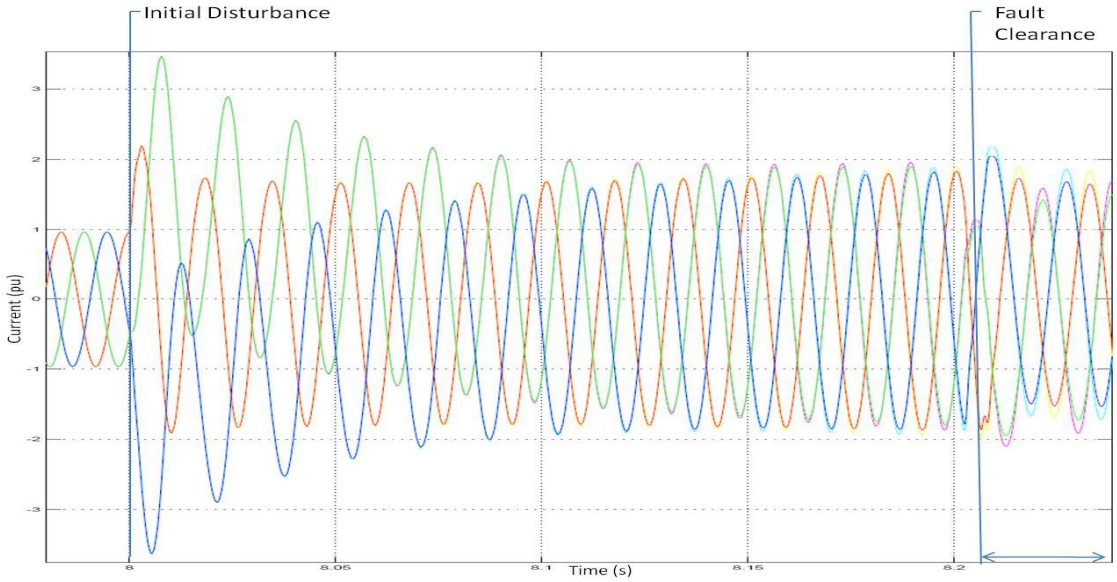

Figure 63 DigSilent and estimator model perturbation responses

Because of the discrepancy in error caused by the line fault and clearance perturbation, it is fair to say that the influence it allows the parameter to have is lesser than that of other perturbation types, which, when achieving the correct parameter value, recreates the current waveform to a higher level of adherence to the synthetic dataset. Much like X_d, although this aspect is interesting, it may not necessarily inhibit the ability of the parameter to influence the phase current output to such an extent that optimisation is compromised.

From this it seems reasonable to infer that the optimisation of X'_d is possible. Because of this parameter identification under most forms of perturbation is also likely. Its inability to solve to a satisfactory level with a line fault line switch event is an aspect that will be further considered through other parameters.

9.1.3 Sub transient Direct Axis Reactance

The final direct axis reactance considered is that of sub-transient reactance X''_d. Again, as seen in Figure 64, its effect on performance is very different to its predecessors in many ways:

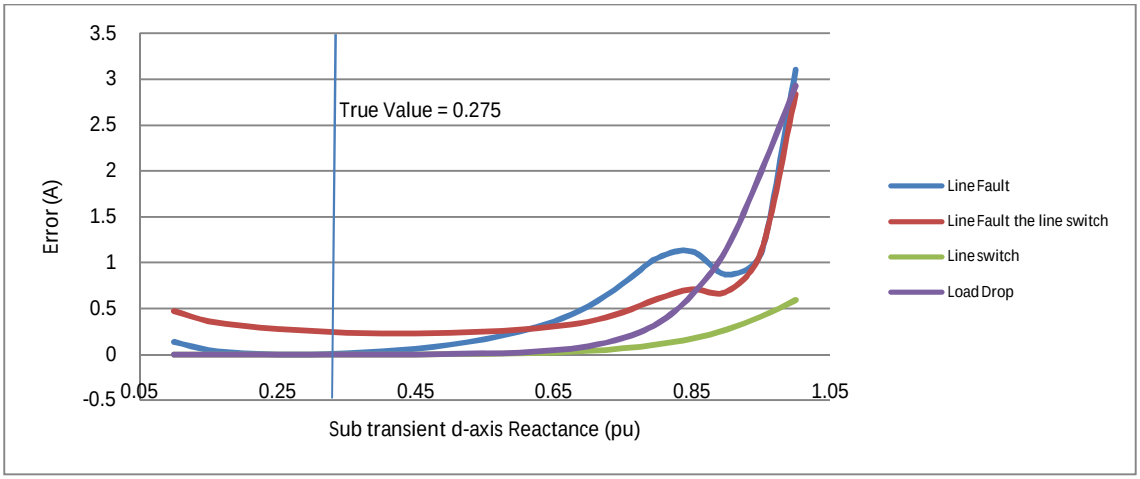

Figure 64 Influence of X''_d from differing perturbation types on phase current output error; linear scale

Looking at the X''_d against X'_d several similarities are prevalent. Firstly the line fault and clearance has a similar level of parameter influence with regard to phase current error. This corroborates what is seen in X'_d. What is different to that of X'_d for all of the perturbations is that when reaching the parameter minima or true value, the plateau of the minima is far larger than what has been seen previously. This wider range of values created by the larger minima plateau makes it harder for the optimisation algorithm to find the global minima, and for the minima to be the correct parameter value.

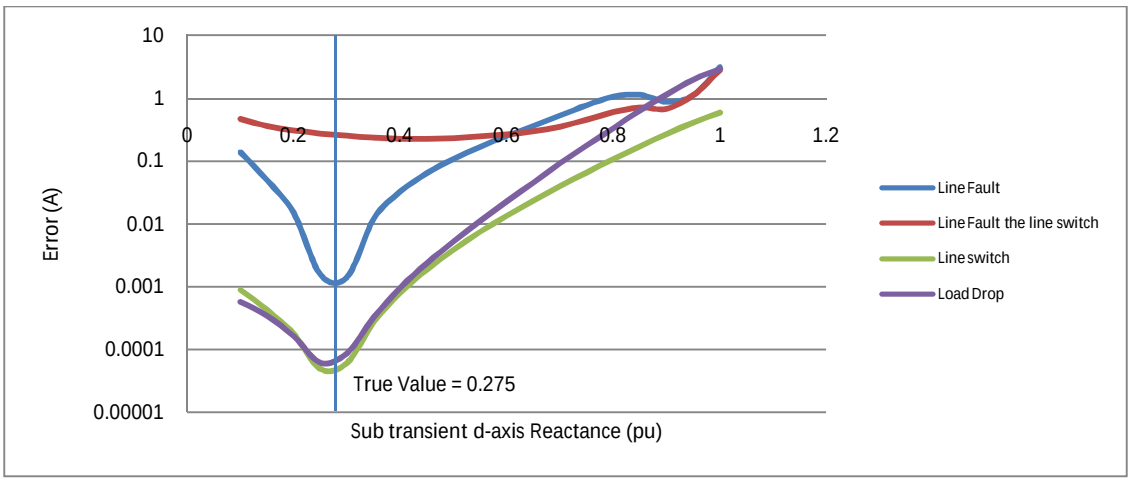

Figure 65 Influence of X'_d from differing perturbation types on phase current output error; log scale

Another aspect which is somewhat different to that of transient and steady state reactance is that of the gradient of descent to the minima. Ignoring line fault line switch which will be addressed later, the gradients are shallower and the relative value of the parameter has to increase significantly in order to achieve the same level of error improvement to that of previous parameters. In many ways this is immaterial to PSO in that, a registered improvement is treated with the same response no matter the size of improvement. This does

mean though that the influence on phase current is lesser than that of X'_d and X_d which is to be expected. The ultimate minima value achieved by the line switch and load change perturbation is very low, meaning a great level of similarity which is encouraging. This could mean that although X''_d has a lesser influence on phase current output than that of the other direct axis reactance values, the likelihood of finding an accurate value with good waveform adherence to the original is high.

When considering the influence that X''_d posses on phase current output for a line fault line switch perturbation, the influence the parameter is able to exert on the error is minimal. The gradient is very shallow and the minima widely distributed creating an unsuitable error distribution for optimisation. It seems that as the parameter becomes less influential to the phase current output error, the perturbation type plays a larger role in its overall influence. The most likely cause for this discrepancy is differences between the mathematical model implementation of the optimisation synchronous machine model and that of the synchronous machine model in DigSilent as already discussed.

It would appear that the results for X''_d supports the principle that as parameter influence is reduced, the gradient of descent to the minima is also reduced and may marginally reduce the ability of the algorithm to perform an identification. This is seen with all perturbation types. The decline in parameter influence is also seen to go hand in hand with the increased effect of the secondary perturbation. To support this looking at X_d, which can be considered a more influential parameter to the machine models function, it was seen that although the secondary perturbation was present in the line fault and clearance transient, the relative effect was limited. The change in parameter influence is observed from X_d to X'_d and from X'_d to X''_d. As the parameter becomes less influential, the less it is able to limit the effect the perturbation has on the overall influence characteristic.

9.1.5 Direct Axis Transient Open Circuit Time Constant

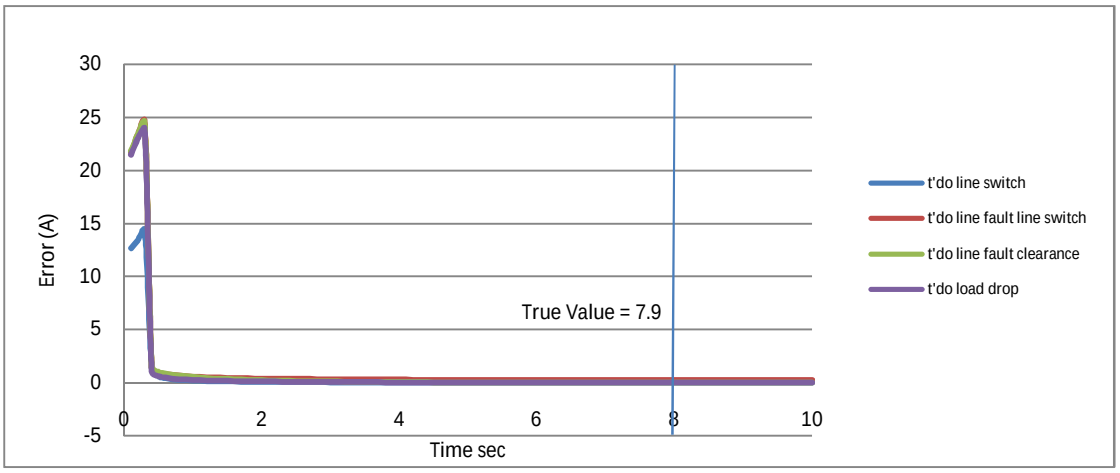

Figure 66 Influence of T'_{do} from differing perturbation types on phase current output error; linear scale

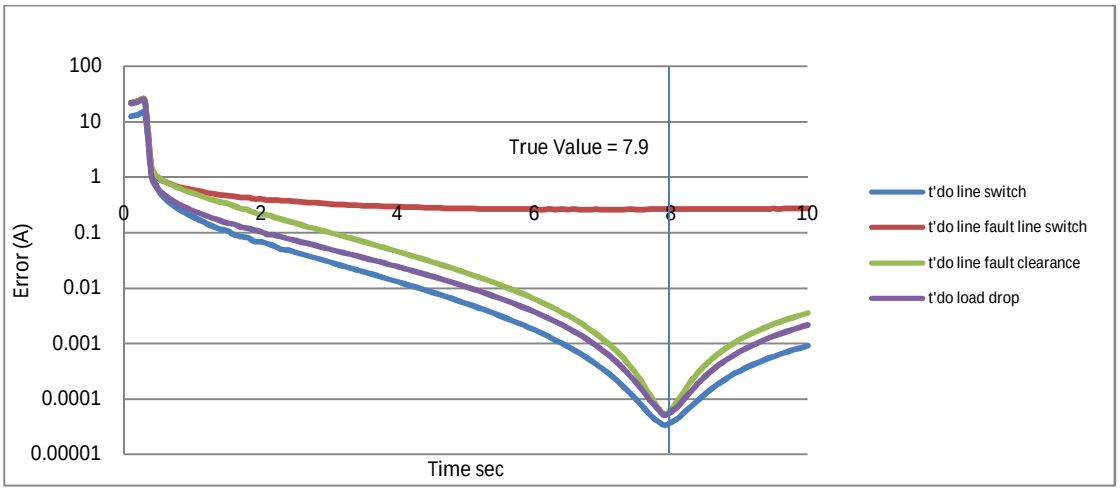

Figure 67 Influence of T'_{do} from differing perturbation types on phase current output error; log scale

The transient direct axis open circuit time constant behaves somewhat differently to that of X'_d. As can be seen in Figure 66, the error drops significantly to a near zero value after reaching a value of 0.2 seconds. From this point it becomes difficult to observe any particular trends regarding its performance. Observing the logarithmic performance in Figure 67 shows that there is an obvious minima around the true value as well as a defined gradient descent to the minima on both sides. The relative gradient of the descent is quite poor, opening a wide range of possible values with acceptable error which increases the possibility of locating local minima. The minima point is of a low value for all perturbations other than line fault line switch, this includes line fault and clearance which is interesting, in that it suggests that certain parameters are less affected by the differences in modelling of synchronous machines from one implementation to the next.

Overall because of the characteristics seen in Figure 66 it can be said that the influence the parameter has on the overall phase current error is quite low, however from an optimisation point of view, the parameter exhibits good characteristics to be optimized and thus identified. As previously stipulated, the gradient of descent to the minima is shallower than other parameters however its overall characteristics are considered acceptable.

9.1.6 Direct Axis Sub transient Open Circuit Time Constant

The sub transient open circuit time constant T''_{do} posses quite interesting characteristics. The two single perturbation types exhibit similar behaviour to that of the transient open circuit time constant. There is a shallow gradient and a good sharp minima which would be suitable to optimise. The performance of the line fault then clearance perturbation in Figure 69 is particularly interesting in that there is a sharp descent to the minima with a minima value close to that of the previously mentioned perturbations. The level of minima isn't surprising when considering the transient open circuit time constant which exhibits a similar pattern regarding the minima, more so the relative gradient exhibited. This would support the concept that the influence of the perturbation to the parameter is not constant, thus some parameters are more influenced by the perturbation than others.

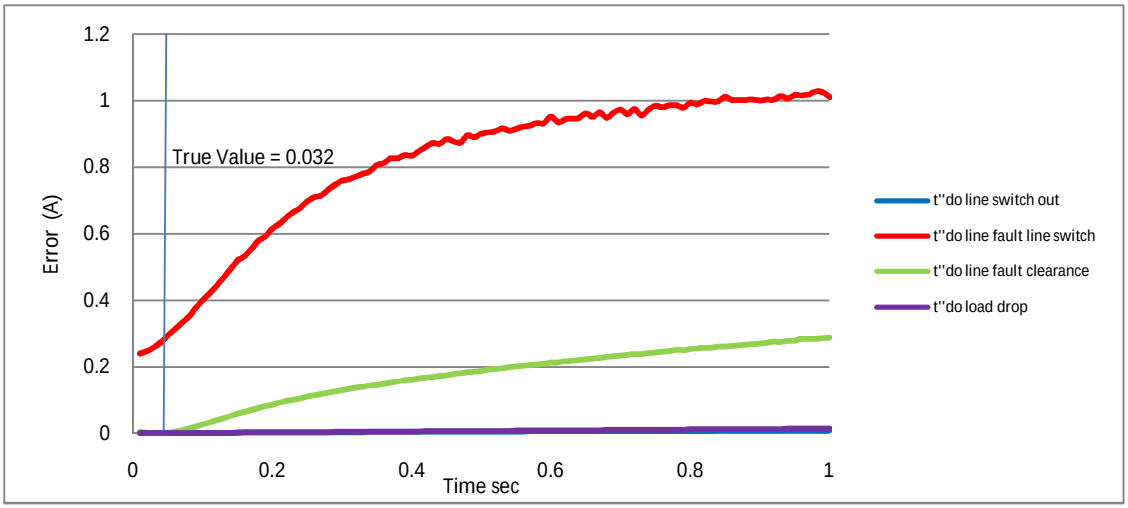

Figure 68 Influence of T''_{do} from differing perturbation types on phase current output error; linear scale

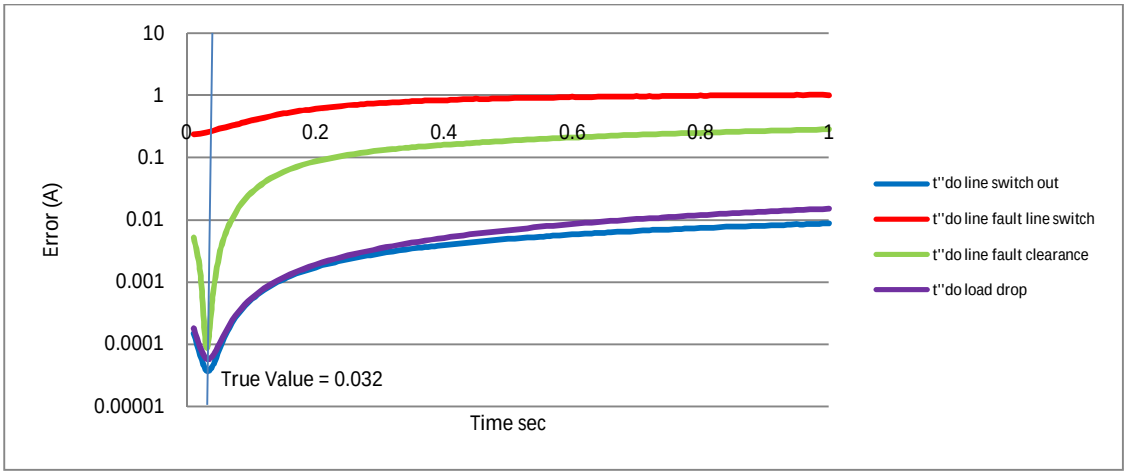

Figure 69 Influence of T''_{do} from differing perturbation types on phase current output error; log scale

It is significant that the line fault line clearance perturbation has a clear decline to the minima on the linear scale as seen in Figure 68. This is not typically the case as has been seen previously. The fact that this is seen on the linear scale reflects that for this perturbation type, the parameter has a significant effect on phase current output error which is not necessarily seen in other perturbations aside the line fault line switch whose ultimate minima is significantly higher than that of the line fault line clearance perturbation as already discussed.

Considering the suitability of the sub transient open circuit time constant, for optimisation and thus parameter identification the results would suggest that the parameter is acceptable though the relative speed of convergence may be defined by the form of perturbation.

9.1.7 Steady State Quadrature Axis Reactance

In understanding the influence of the quadrature axis and its components, it is first necessary to consider steady state q-axis reactance and its influence with regard to differing perturbations much like the direct axis.

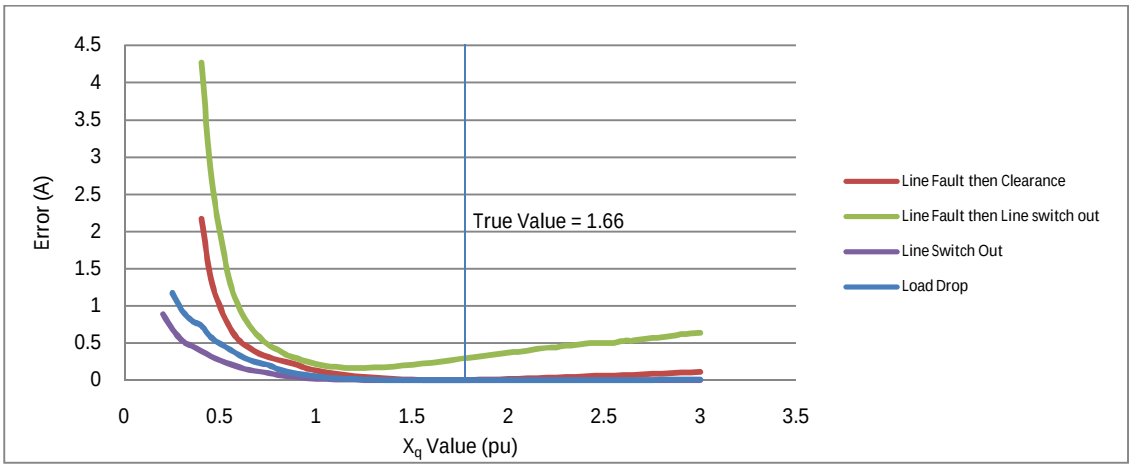

Figure 70 The influence of X_q from differing perturbation types on phase current output error; linear scale

Figure 70 shows in a more obvious form than Figure 71, the relatively fast drop in error on the lower side of the parameter value (in this case 1.66 pu). This suggests that in terms of search area, the most productive optimisation would be found on this side (i.e. more likely to register significant improvement). Figure 70 also shows on values higher than that of the real parameter value, the influence on the overall phase current waveform is far less in comparison to the lower side. Once a low error around the minima is reached, the relative change in phase current waveform remains largely unchanged.

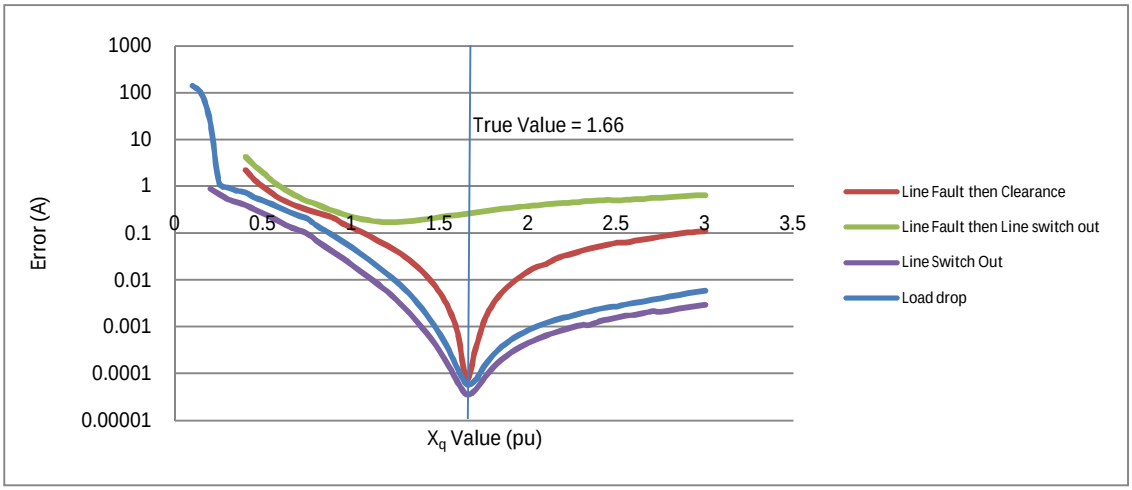

Figure 71 The influence of X_q from differing perturbation types on phase current output error; log scale

Considering X_q logarithmically in Figure 71 gives further insight to its performance. It is seen that much like the direct axis reactances, depending on the perturbation type, the minimum error attained by the parameter can vary significantly. Likewise the high side gradient is seen to vary in a similar pattern to that of the sub transient direct axis open circuit time constant in Figure 69 with a steeper gradient on the line fault and clearance perturbation and a shallower approach to the minima on the less onerous perturbations. This creates a larger search range with lesser improvement for the less onerous perturbations.

Following from the direct axis results, the influence of the line fault line switch perturbation is seen again to be poor in regard to the relative influence that is allows the parameter to exert on the phase current waveform. The likely reasoning as to why this is has already been discussed so it would be consistent to mention that the poor performance it delivers may inhibit a search if such perturbations were utilised.

Overall it can be seen that X_q has a sufficient influence on the phase current output error to be considered acceptable for parameter identification. Further to this, it is seen to be more

reliable under singular perturbations and small secondary perturbations; this is consistent with the results already discussed.

9.1.8 Transient Quadrature Axis Reactance

Looking at transient q axis reactance X'_q logarithmically in Figure 72, it becomes clear to see that transient reactance in this model type has no influence on phase current under any form of perturbation and cannot be considered suitable for parameter identification. This is not necessarily a surprise when looking at the relative performance of a synchronous machine under a transient.

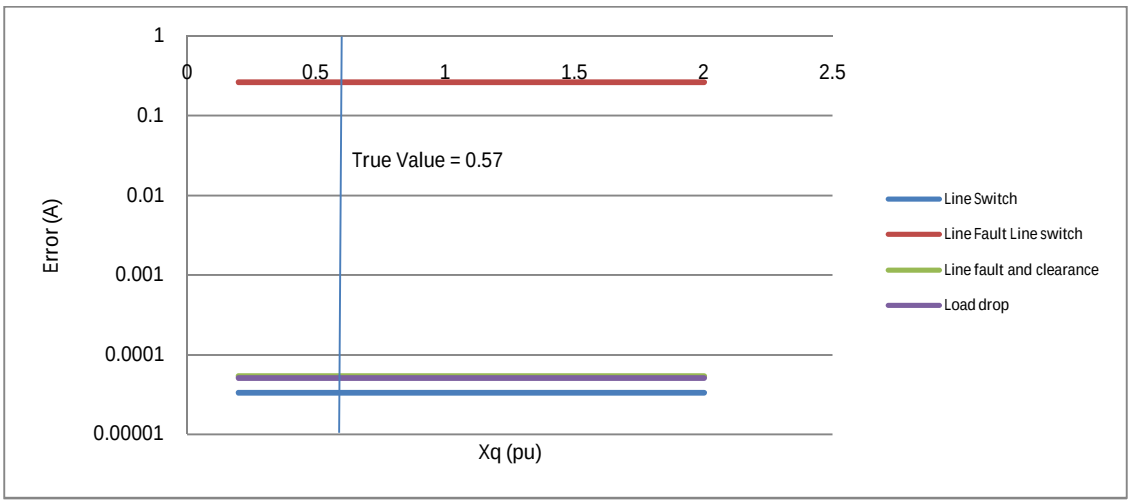

Figure 72 The influence of X'_q from differing perturbation types on phase current output error; log scale

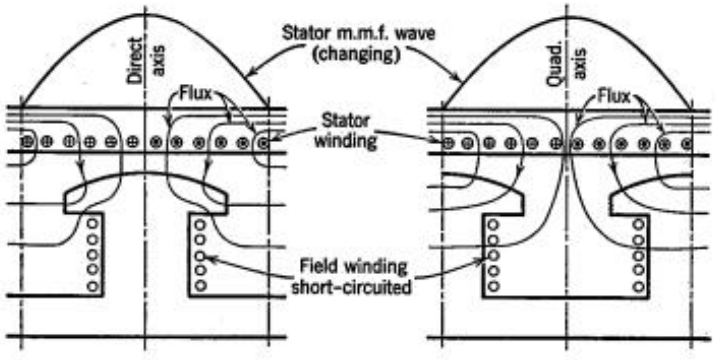

Figure 73 The distribution of flux in a synchronous machine in the direct axis (a) and the quadrature axis (b) in the transient time frame (27)

Figure 73(b) shows that the air gap corresponding to X'_q is large producing a small inductance value and consequently less influence on the machine characteristics. For this reason its influence is minimal. For this reason it seems logical to neglect X'_q as a parameter for identification.

In reality it is possible to identify X'_q as a parameter value using a modified slip test, but this form of testing is uncommon and very expensive. It is also very specific in the form of perturbation required in order to stimulate the reaction required for parameter identification. This form of perturbation would not be observed in the day to day running of the synchronous machine so it is of little surprise that the perturbations used in the influence testing proved unusable.

9.1.9 Sub transient Quadrature Axis Reactance

The influence of the quadrature axis sub transient reactance X''_q is consistent with what has previously been seen. The line fault line clearance perturbation creates a quite advantageous distribution, with a steep gradient leading to a fairly sharp minimum at the correct parameter value. Again as previously seen the final minima value that is reached for this perturbation type is about an order of magnitude higher than that of the single perturbation types.

The line switch and load drop perturbation types have poorer characteristics than what has previously seen for these perturbation types. They exhibit a very shallow gradient and fairly ambiguous minima (although roughly located around the expected minima). Based on the data presented, the likelihood of optimisation and thus parameter identification is less than that of other parameters. The fact that only the line fault and clearance perturbation produced good results in this regard undermines the parameter slightly as a parameter worthwhile for identification. This pessimism is tempered by the fact that although the singular perturbations results are poor, based on them, there is still a minima and a shallow gradient that would allow optimisation, albeit less efficiently than if all the perturbations exhibited the characteristics of the line fault and clearance perturbation.

The results are consistent with the concept that, as the relative effect the parameter has on the model behaviour under transient conditions is reduced, the influence it is able to exert under perturbation is also reduced. This leads to poor gradients of descent and an increased range of possible minima values.

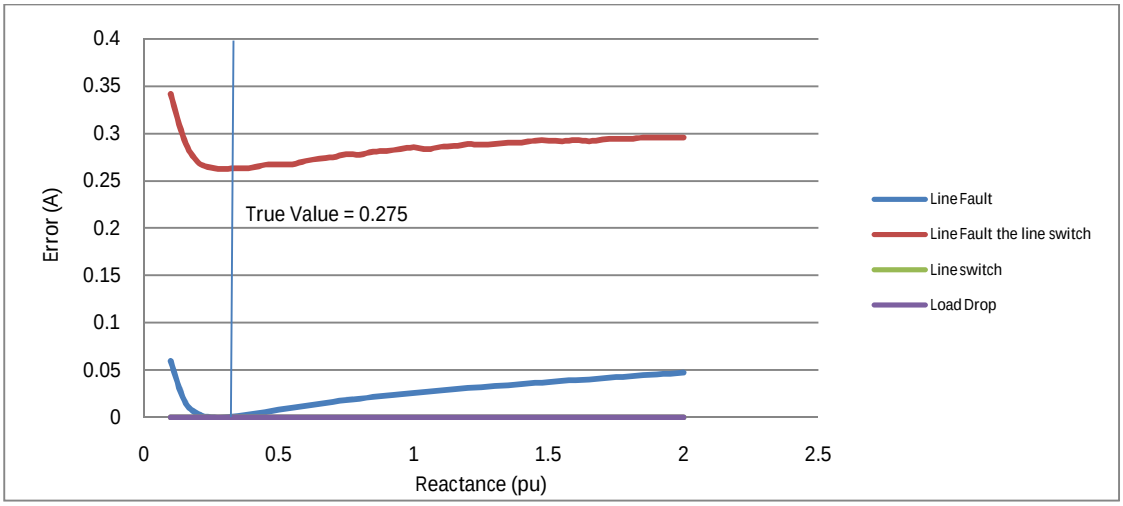

Figure 74 The influence of X''_q from differing perturbation types on phase current output error; linear scale

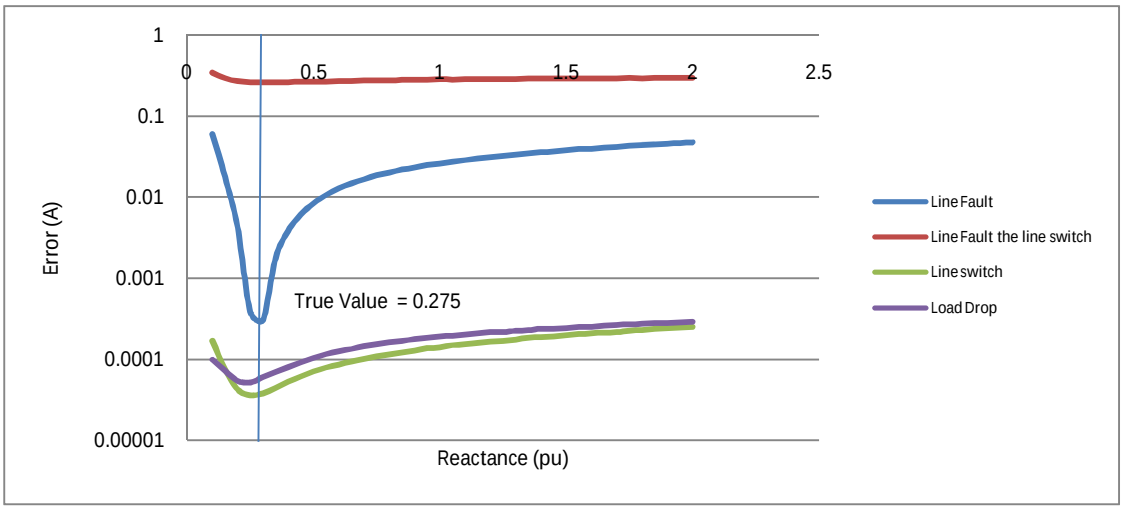

Figure 75 The influence of X''_q from differing perturbation types on phase current output error; log scale

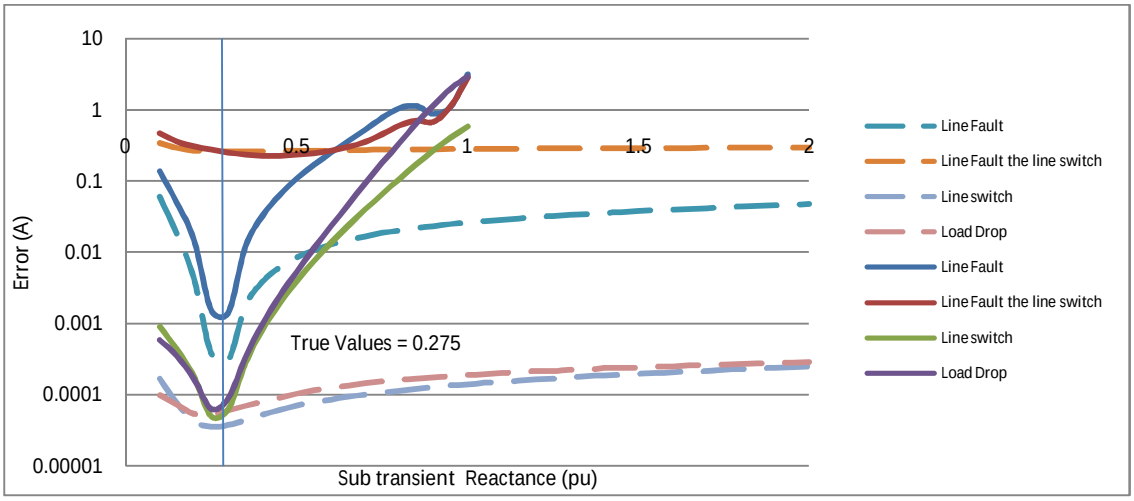

Figure 76 The influence of X''_q (dashed) and X''_d (solid line) from differing perturbation types on phase current output error; log scale

Overall, if direct and quadrature sub transient reactance distributions were compared as seen in Figure 76, it is clear that in virtually every case X''_d is more favourable for searching as it provides a higher gradient of descent to the minima indicating a swifter optimisation. The poorer results may translate directly to the differences in flux path at the air gap seen between the two. This could create a more significant change in phase current for the direct axis component during perturbations. This would be consistent with basic machine theory. In either case, if the choice had to be made as to which to identify, it could be said that the results presented for the direct axis sub transient reactance are far more likely to be optimised, thus X''_d would be the better choice for parameter identification.

9.1.10 Quadrature Axis Transient Open Circuit Time Constant

Moving to the quadrature axis open circuit time constants, the influence of the transient time constant is observed in Figure 77. It is seen that the influence it provides under all perturbations is negligible. This would be consistent with q axis transient reactance, thus supporting the principle that neither can be identified through this form of identification presented.

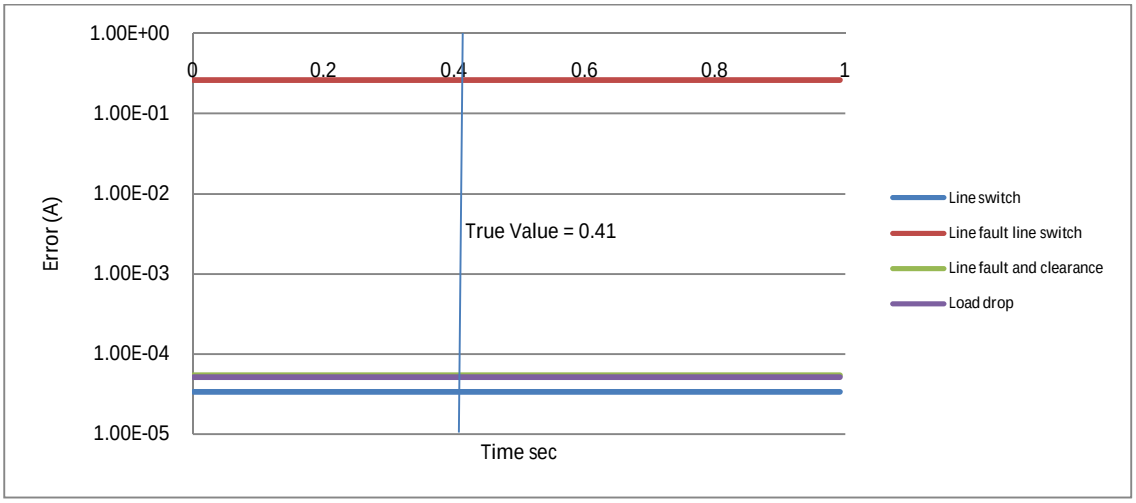

Figure 77 The influence of T'_{qo} from differing perturbation types on phase current output error; log scale

9.1.11 Quadrature Axis Sub transient Open Circuit Time Constant

When considering the relative performance of the sub transient time constant the level of influence observed is seen in Figure 78 and Figure 79. In Figure 78, the results shows a sharp decline to a near zero value. In this regard the behaviour exhibited for the line fault line switch and line fault and clearance provides insight as to the parameter influence. Although neither perturbation reaches a minima anywhere near the level of magnitude that the load drop and the line switch perturbations achieve. It does show however the relative influence the time constant has over a broader range when considering a more onerous set of

perturbations. The other perturbations provide results that are similar in many regards to that which have already been seen, the shallow gradient of descent and wider minima on the singular perturbations, and the higher gradient with sharper minima on the line fault and clearance.

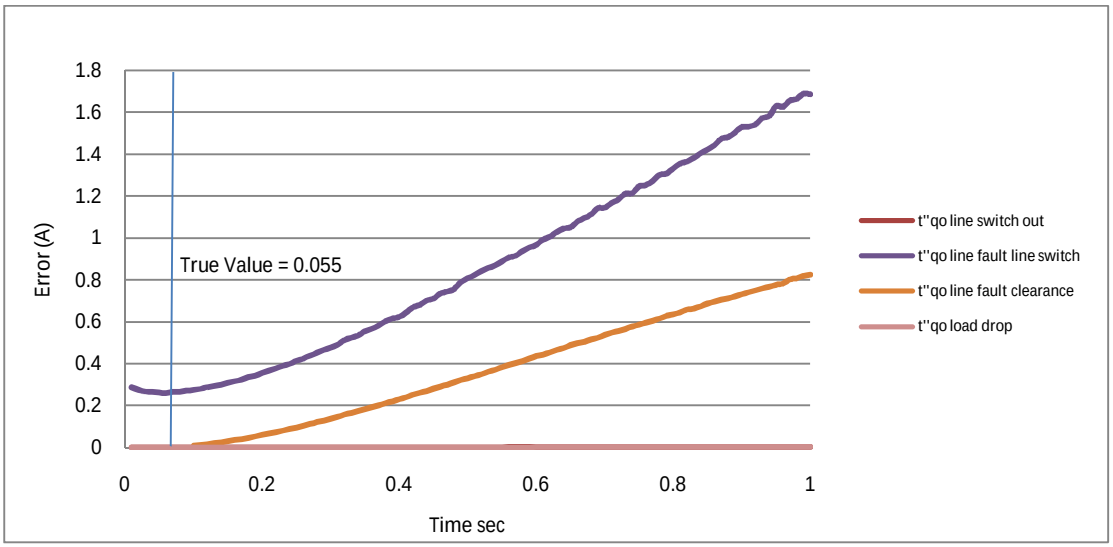

Figure 78 The influence of T''_{qo} from differing perturbation types on phase current output error; linear scale

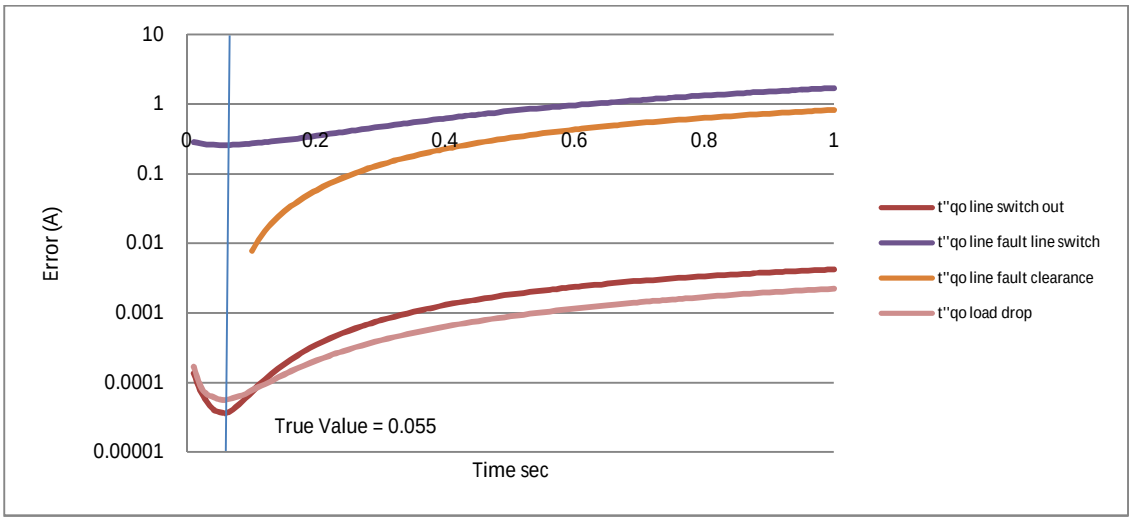

Figure 79 The influence of T''_{qo} from differing perturbation types on phase current output error; log scale

Overall the results presented for T''_{qo} seem very consistent with that of the sub transient reactance. This would infer that both parameters, although reasonable for optimisation, are dependent on the perturbation type to define the relative speed of optimisation.

9.1.12 Leakage Reactance

Leakage reactance as a parameter has been historically difficult to identify directly. It is the reactance resulting from the difference between total flux produced by armature current and

the flux in the air gap. This breaks down to slot leakage flux, end winding flux and differential leakage flux. For this reason it cannot be classically measured as a single component directly. This difficulty in measurement translates to an irregular distribution of influence as seen in Figure 80.

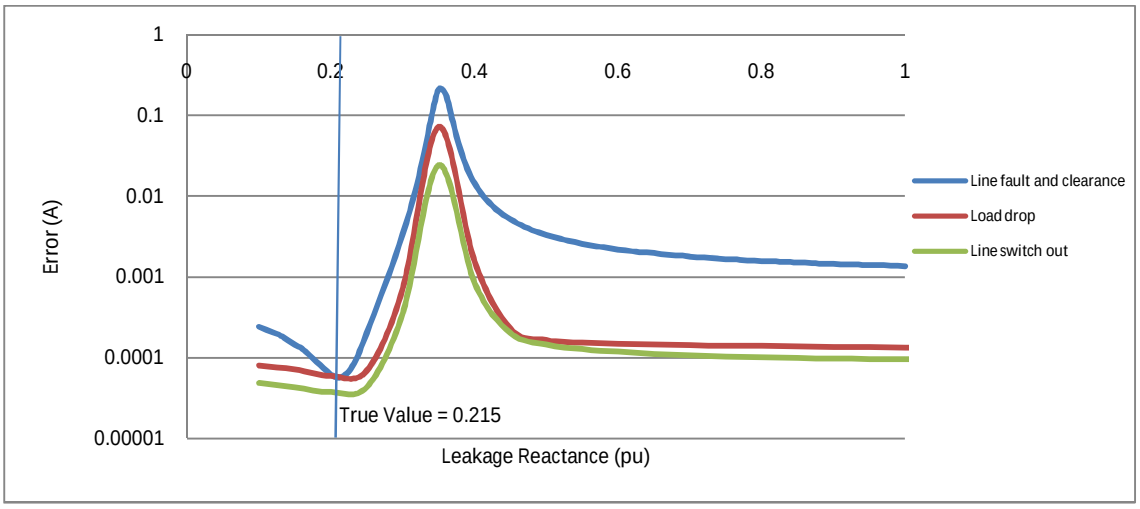

Figure 80 The influence of X_{ls} from differing perturbation types on phase current output error; log scale

Dividing the performance into a pre-ridge (left hand side) and post-ridge (right hand side), the pre ridge characteristics are seen to be consistent with what has been previously seen. There is a minima, albeit poorly defined, a shallow low end gradient and the gradient of the characteristic above the minima point has a high gradient until reaching the defined peak. This high side gradient would be suitable for identification, however the shallow low side gradient and poorly defined minima and varies with perturbation type would be less appropriate in this regard. The poorly defined minima is not uncommon to parameters, as has been seen previously but the movement of the minima is an interesting issue likely created by leakage being made up of several components which may differ depending on the perturbation. The load drop and the line switch perturbations are seen also to have a fairly linear gradient on the lower side of the minima, where as the line fault and clearance has a more classical characteristic. This higher gradient is likely to be from the more onerous perturbation as has been seen in previous parameters.

It is noted that the line fault line switch perturbation is not included in the results. This is because the result exhibited a larger error. This high error had characteristics of limited use and was therefore neglected. It can only be assumed that the reason for this is the strong secondary transient (similar to what was previously identified with other parameters, just more onerous). The relative difference in magnitude is significant however, which would suggest that the parameter itself had an impact on the result in this regard. This would infer

that this was due to a component of the leakage reactance parameter which is adversely effected by this perturbation type.

Looking at the second part of the influence curve, or post ridge (values of greater that 0.38) there is a unique characteristic in that the ridge actually drops to near zero This is unique as it would be more consistent to level off at a value as has been seen in other parameters. It must be assumed that this manifestation occurs because the model has a range in which the model can operate correctly and past this point, the parameter ceases to produce meaningful results.

Considering the influence characteristics in their entirety, this unique behaviour generates a dangerous search space with regard to optimisation, in that there is a clearly definable local minima over a large search range. This local minima, is also bordered by a ridged gradient which separates the global minima from the local which may make it hard for the search algorithm to search outside such boundaries. This issue with regard to local minima is mitigated by the use of PSO as opposed to a method like gradient descent, which would never find the correct result if caught in the local minima. The relative efficiency of search that form of distribution creates is not likely to be particularly good for obvious reasons. The efficiency can be increased somewhat by tightening the boundaries for leakage reactance, but this may not necessarily aid the search greatly as there is a likelihood the local minima will still be influential in the applicable search area. This specifically becomes quite pertinent when considering the tuning of the PSO algorithm described later in this chapter.

9.1.13 Armature Resistance

Returning to a more conformal characteristic distribution it is seen that armature resistance displays a more classical distribution in comparison to that of leakage reactance. Given the characteristics seen in Figure 81, the performance observed more closely in Figure 82 is somewhat surprising. Although the classical high gradient of descent and sharp minima are obvious in all of the perturbations observed, the minima not only has differing error levels, which is surprising for load drop and line switch, but is also slightly shifted in parameter value.

This difference could be accounted for in the implementation of the armature resistance itself, where there is inherently an ac and dc component observed. The dc component would vary with perturbation severity leading to a subtle change in value as observed in Figure 82. Again, the line fault line switch results are neglected with a similar magnitude of error to that of leakage reactance.

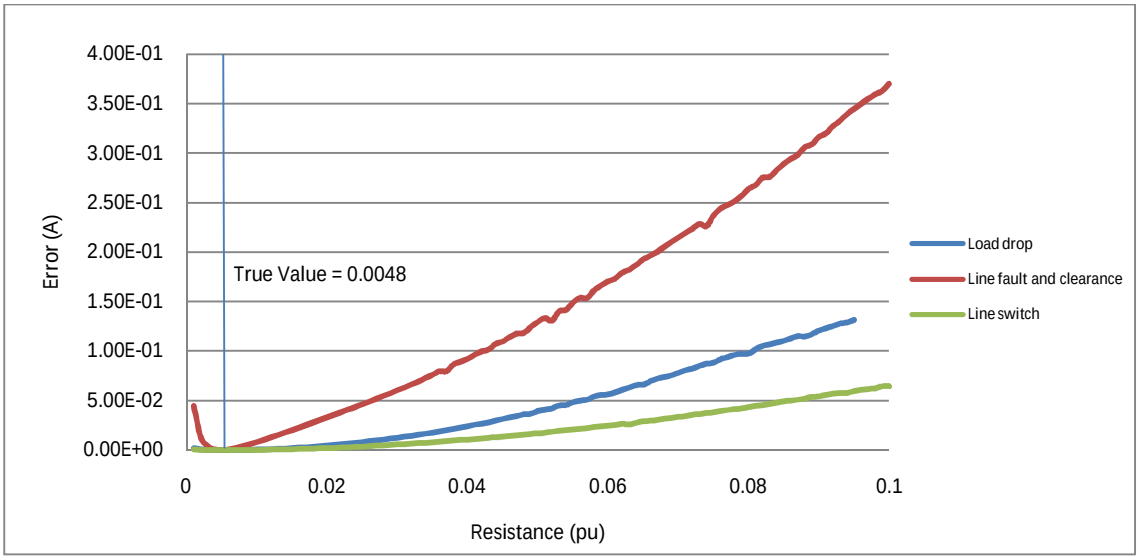

Figure 81 The influence of R_a from differing perturbation types on phase current output error; linear scale

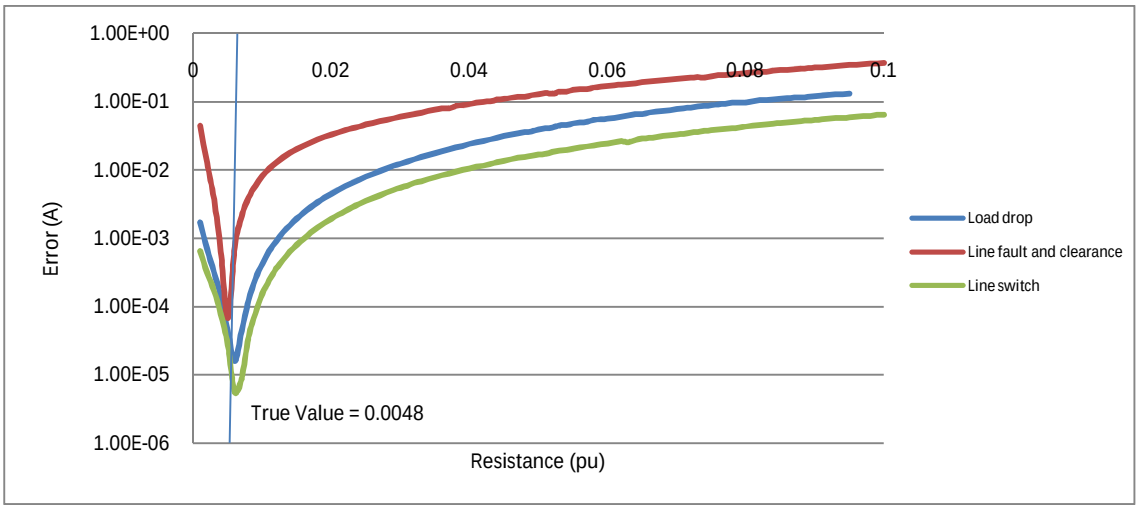

Figure 82 The influence of R_a from differing perturbation types on phase current output error; log scale

From an optimisation point of view this subtle change in value is actually irrelevant as the PSO will not have a true value to be compared against. It will merely try and find the minima and thus find the appropriate parameter value, which is dependent on the perturbation. For this reason armature resistance must be considered suitable for parameter identification.

9.1.14 The Constant of Inertia

The constant of inertia is a significant parameter effectively detailing the physical size and angular momentum of the synchronous machine rotor.

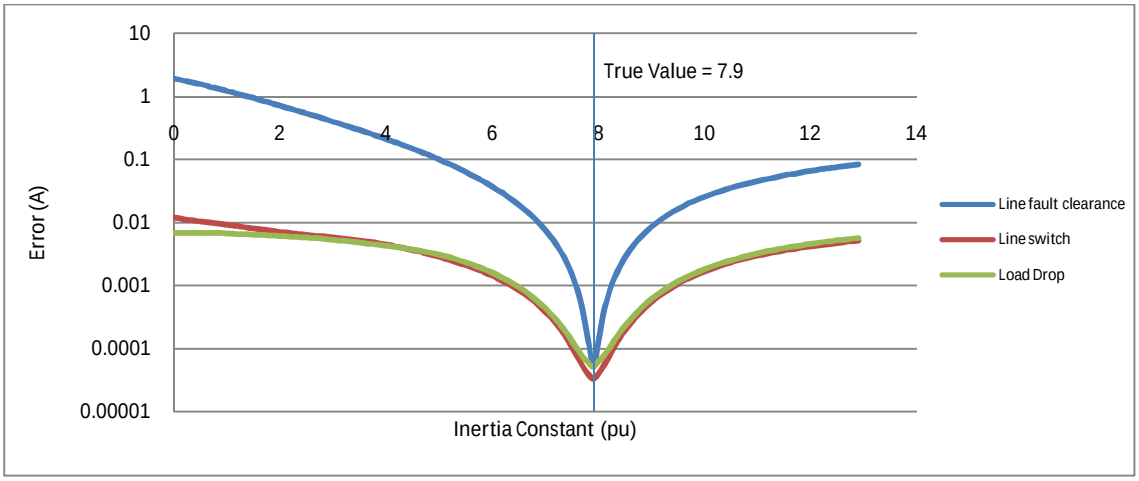

Figure 83 The influence of H from differing perturbation types on phase current output error; log scale

Considering the distributions presented in Figure 83, it is seen that the line fault and clearance produces a higher value of phase current error surrounding the minima. It is also seen to possess a favourable gradient approaching the minima. This is consistent with the previously seen results where the onerous nature of the transient gives the parameter a higher influence but the secondary perturbation causes a subtle change in the phase current output waveform which creates the higher error surrounding the minima. What is surprising in this regard is that the minima presented in all three perturbations are roughly of the same magnitude. This is advantageous in some respects as, unlike other parameters with variable levels of minima depending on the perturbation type, a constant would allow a convergence criterion to be set with a higher level of confidence that if this error is reached the minima has been found.

Due to the nature of the results it seems reasonable to conclude that the constant of inertia H has a significant influence on the phase current output error and that this would suggest that it would be a suitable variable for parameter identification.

9.2 Excitation System Parameters

Having considered the critical areas of the synchronous machine model, several aspects regarding parameter identification have become apparent regarding whether or not parameters can realistically be identified. Moving on to the excitation system it is necessary to refresh the memory as to the parameters inside the model and their relative significance.

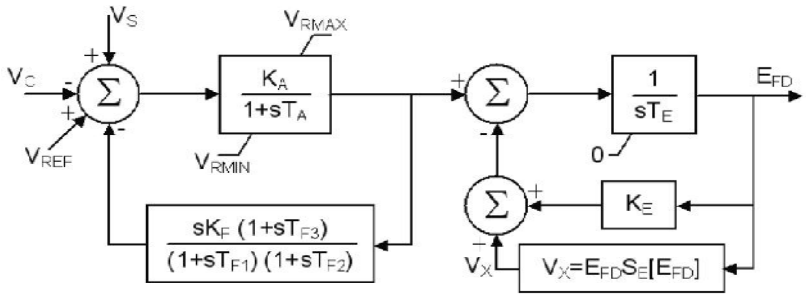

Figure 84 The AC5A excitation system used for optimisation and parameter identification

Figure 84 shows the AC5A excitation system model. Looking at the model from a practical point of view, the gain K_A and T_A are critical components to the excitation system behaviour, as are K_F and T_{F1} (T_{F2} and T_{F3} are neglected as their conventional value is zero (57) making both bracketed sections redundant). Continuing to the excitation system saturation loop, T_E and K_E are significant given the limited input that would be applicable for the $V_X=E_{FD}S_E[E_{FD}]$ term, which requires further data that would not be available.

Voltage regulator gain K_{A1} is fundamental to the performance of the model, yet with a limited V_{Rmax} and V_{Rmin} it is also critical that the regulator time constant T_{A1} is also correct in order to provide the correct excitation system response. The logarithmic response is seen in Figure 85 and Figure 86.

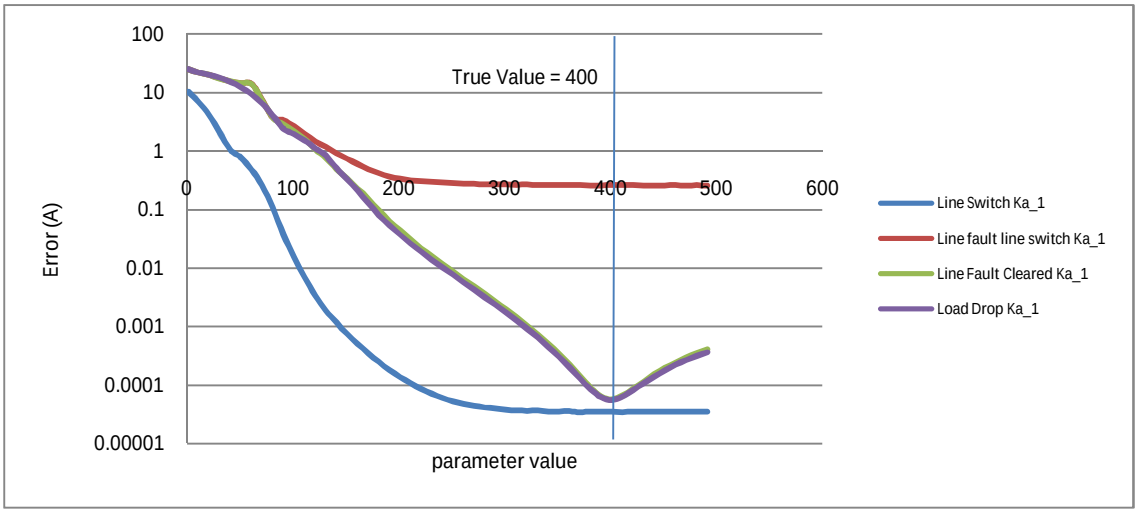

Figure 85 The influence of K_{A1} from differing perturbation types on phase current output error; log scale

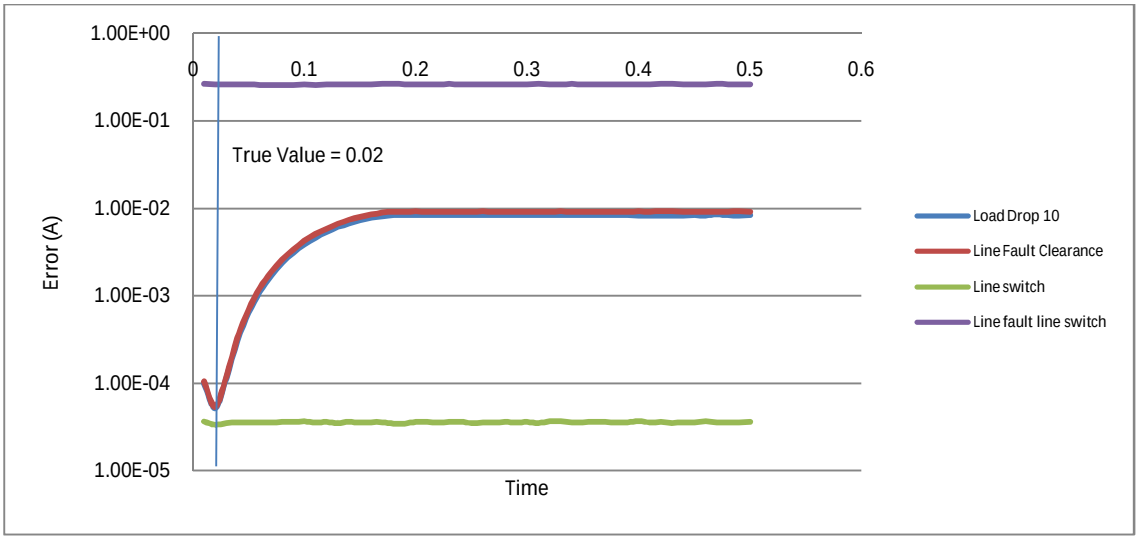

Figure 86 The influence of T_{A1} from differing perturbation types on phase current output error; log scale

Looking at the voltage regulator gain, several aspects become apparent. Firstly, the line fault line clearance and the load drop perturbations produce good, very similar (to each other) results which is somewhat surprising in that, although the line fault and clearance is usually formed in a similar manner to that of the load drop, its final minima is not usually in the same order of magnitude. The influence of regulator gain seems to be fairly wide however, meaning that the variation in gain is of the order of several hundred, which is considerable. From an optimisation point of view, for these two perturbations, there is a minima and a well defined gradient of descent surrounding the minima, suggesting that optimisation would be suitable in this respect. The line switch perturbation is perhaps the most interesting perturbation, with a slow curvature down to a stable minimum phase current output error which is over a large range. The fact that it is so different in format is interesting as, up till this point the line switch perturbation has produced good results that would allow for optimisation. In this case optimisation would certainly not be possible. The question then becomes, why? It would be logical to assume that with having V_{Rmax} to create a top value limit, the gain simply hits a saturation point, at which point it has limited influence, the reason this is not the case for the other perturbations is that they are still able to exert influence when not saturated.

The results obtained for K_{A1} are supported by the results of T_{A1}. It is seen that unlike K_{A1} the line switch perturbation is totally ineffectual, with a linear influence throughout the range of parameter values. Given its relatively poor performance for K_{A1} this comes as little surprise, but it does raise questions as to whether, unless the exact transient is known, both parameters can be identified given the changeable influence that seems apparent. On a positive point, the line switch and load drop perturbations were consistent with what was

seen with K_{A1}. The relative gradient and minima proved to be more suitable for parameter identification.

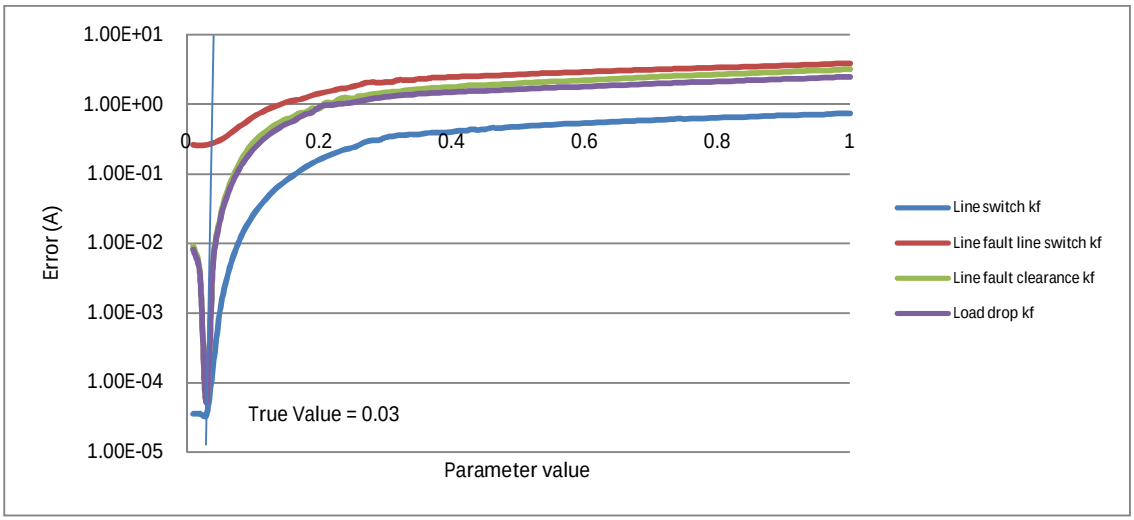

Figure 87 The influence of K_F from differing perturbation types on phase current output error; log scale

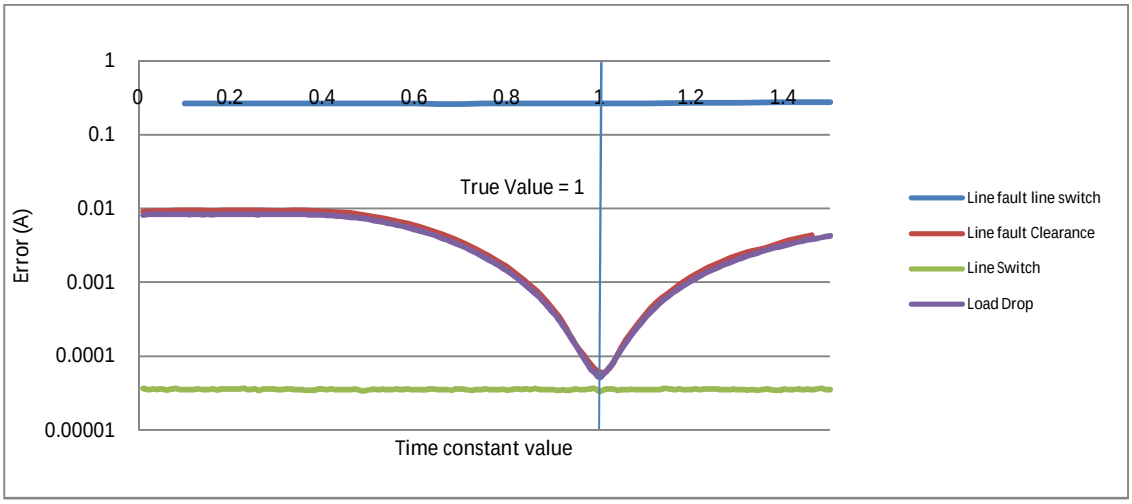

Figure 88 The influence of T_{f1} from differing perturbation types on phase current output error; log scale

Moving forward to the feedback loop transfer function resulting error seen in Figure 87, K_F is the closed loop stabilisation gain. Because of the relatively low real value of K_F, zero is effectively a hard boundary in terms of optimisation. The results provide a fairly high degree of confidence that the parameter would be suitable for optimisation and identification provided the right form of perturbation was utilized. This is supported by the results of the line fault, line switch perturbation which has been seen throughout to produce less convincing results. In this case however, the behavioural pattern shows that even this perturbation displays influence on the phase current output error. As such the parameter is able to deliver a reasonable optimisation though not to an appropriate final minima. This would suggest that

the influence the parameter is able to exert is sufficient enough to reduce the overall impact of the line fault line switch perturbation.

Looking at T_{F1} in Figure 88, there is again a similar behaviour exhibited for the line switch perturbation as was seen in T_{A1}. It could be suggested that due to the nature of the perturbation, there isn't sufficient impetus for the time constants to actually influence the phase current output error in a satisfactory way in regard to optimisation. This would support that an excitation system, other than providing a stable excitation source for the synchronous machine, is a method of voltage stabilisation. If the perturbation does not warrant stabilisation, it is unlikely that the excitation system will influence the synchronous machine, and thus the phase current output will be minimal. The lack of influence from the excitation system under these specific conditions could affect certain parameters more so than others. This will be considered further for the second closed loop defining the excitation system saturation characteristics.

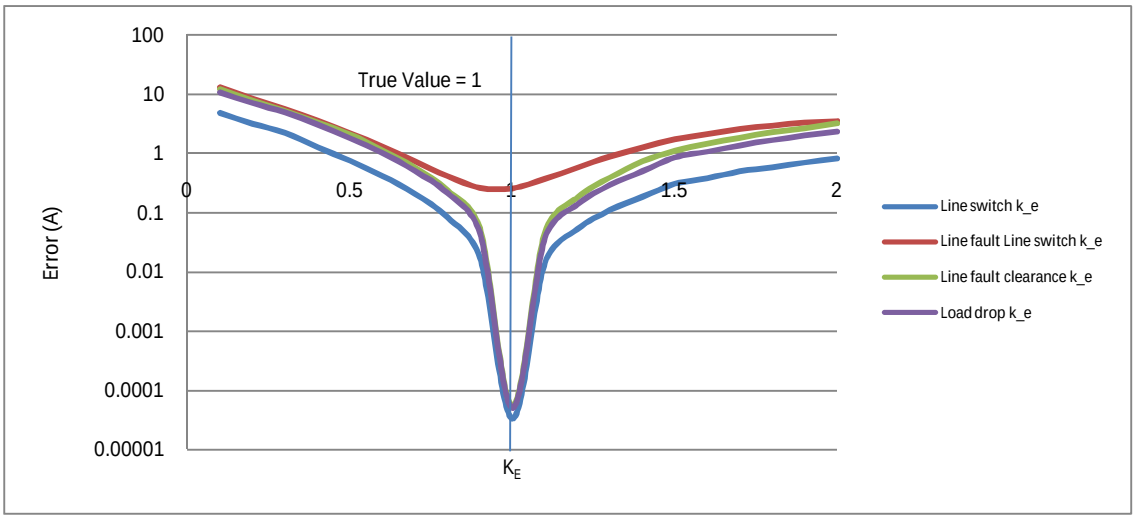

Figure 89 The influence of k_E from differing perturbation types on phase current output error; log scale

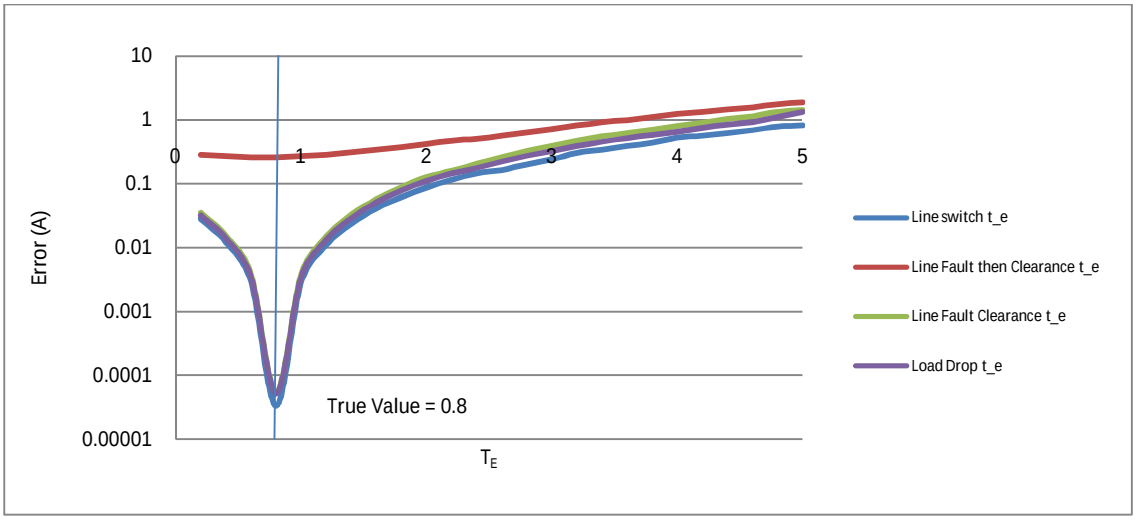

Figure 90 The influence of T_E from differing perturbation types on phase current output error; log scale

In the excitation system saturation loop, K_E is the constant related to the self excited field and has an associated time constant T_E. It is seen in Figure 89 and Figure 90 that both parameters possess a classical distribution with regard to optimisation. The high gradient and sharp minima provide a high likelihood of optimisation. It is observed also that the line fault line switch perturbation trends roughly with the other parameters, suggesting a limited parameter strength of influence. This is quite positive in that it infers that for the majority of single perturbations and for some two staged perturbations, the behaviour will support optimisation.

The relative implications of using a model with a transfer function for saturation for static excitation systems cannot be fully quantified without real data from such a system. That said, given the overall response of the excitation system model transfer function, it seems reasonable to suggest that the saturation transfer function would simply have derived values that marginalised its effect if parameter identification of such a system occurred. For this reason including the saturation loop would have limited effect on such excitation system methodologies.

9.3 Governor and Turbine Influence

Before considering the parameters, it is necessary to look at the governor and turbine models to understand which parameters are being discussed. As seen in Figure 91(a), governor time constants T_1, T_2 and T_3 form the main parameters that define governor performance. For the turbine representation seen in Figure 91(b) T_4 and turbine gain define its performance and are the most critical parameters.

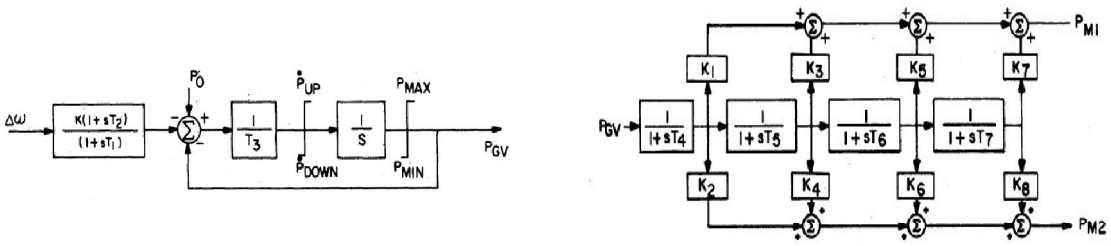

Figure 91 Models for Governor (a) and Turbine (b)

Considering the governor and the turbine as separate entities, it is seen in Figure 92 that governor time constants T_1, T_2 and T_3 produce poor results which are not conducive to parameter identification. This would imply that the Δω input, although providing the change in speed of the rotor, does not have a significant influence on the overall output phase current. This is due to the limit terms P_{up} and P_{max}. Ultimately it has to be recognised that the governor defines a butterfly valve angle that defines the prime mover energy input, but not the speed at which the turbine reacts. For this reason and the results seen in Figure 92, it is logical that the governor is not an entity that can be used in parameter identification given that the types of transients used in this work are of a length that are shorter than the governor time constants. For this reason they aren't able to exert significant influence

For Figure 92 seen below LFC is the line fault then clearance perturbation. LD10 is the load drop perturbation. LSO is the line switch out perturbation and LFLS is the line fault line switch perturbation seen previously.

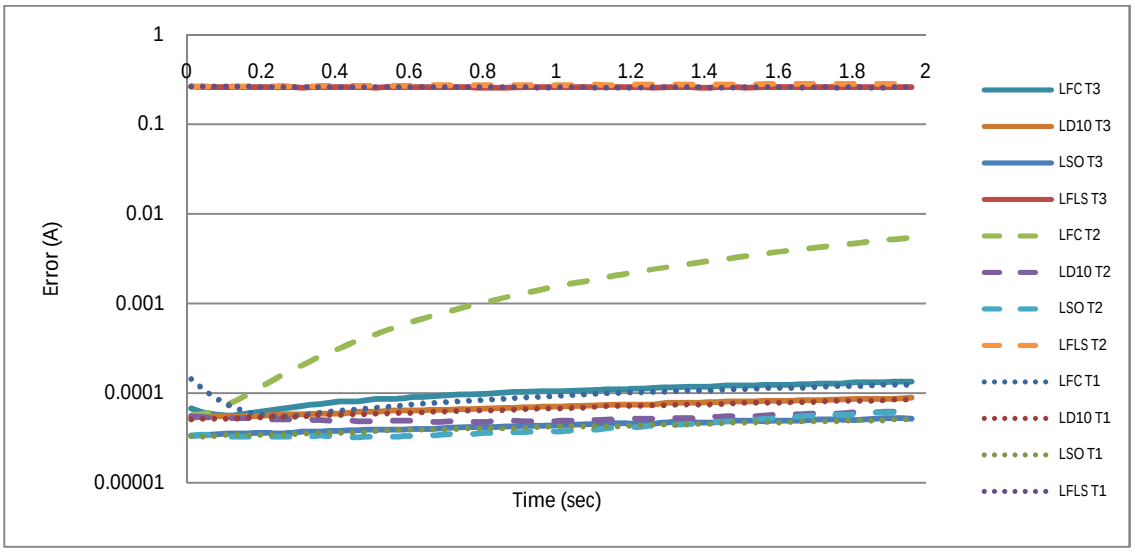

Figure 92 The influence of time constants T_1, T_2 and T_3 from differing perturbation types on phase current output error; log scale

Tempering the relatively poor results seen above for the governor model parameters, it is seen in Figure 93 that T_4, the turbine time constant has more influence on the phase current output error. T_4 has a low error during an elongated minima, then rises with a reasonable gradient. It is not surprising that the minima between 0 and 0.5 exists, with a real value of 0.35 and an inertia constant defining the momentum that the rotor and turbine exhibit. Its influence in the lower end of values is therefore going to be limited. The influence the parameter possesses after this point is seen to rise but because of the very large minima surrounding the parameter value, it could be said that parameter identification for this parameter would prove very difficult with a high risk of identifying minima with incorrect values.

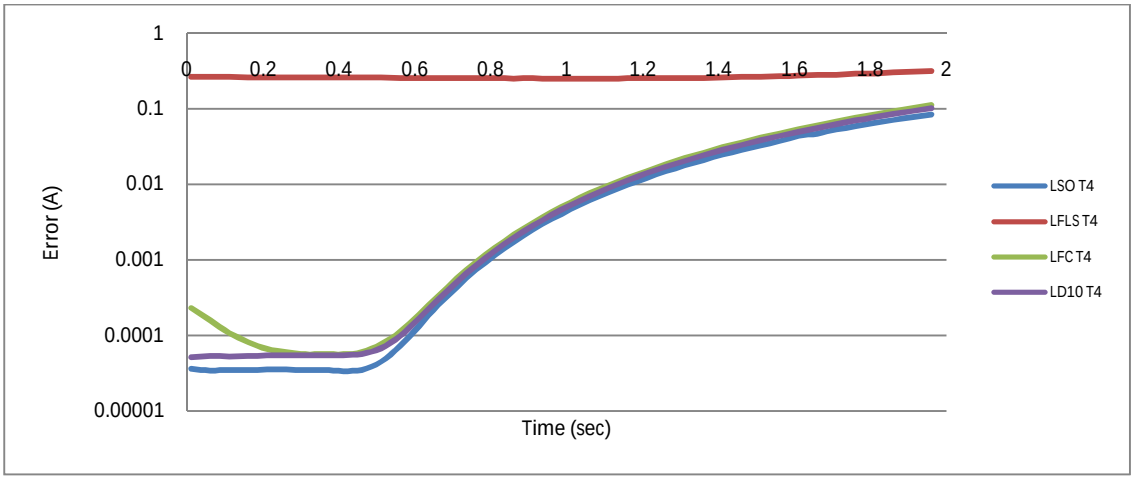

Figure 93 The influence of turbine time constant T_4 from differing perturbation types on phase current output error; log scale

It is worth noting that, specifically considering the elongated minima, if the inertia of the machine was low enough, the likelihood of finding a more sharply defined minima would be increased, in which case this shortened minima could be used to facilitate parameter identification.

Moving on to the turbine gain value, $K_{turbine}$ in Figure 94; It is seen that the turbine gain constant offers a reasonable probability of parameter identification. The classical response pattern would suggest that it would be appropriate even considering less well defined perturbations like line fault line switch which is quite significant. The strength of the relative response and the ultimate phase current output error achieved is such that the turbine model could be expanded to take into account a larger and more intricate turbine type, for instance a cross compound single reheat turbine. Because of the nature of this work, making the turbine type more niche would be counterproductive as it must be able to describe all turbine types to an appropriate standard, not describe one exactly. It stands to reason though, that if that was

an aim in further work, the evidence does suggest that expanding the turbine model for optimisation and parameter identification would be possible.

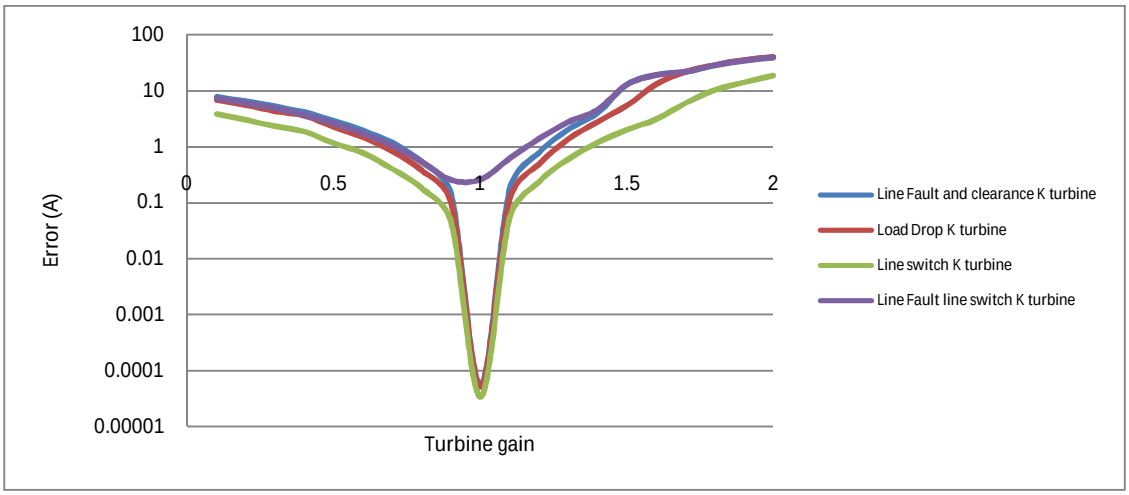

Figure 94 The influence of turbine gain $K_{turbine}$ from differing perturbation types on phase current output error; log scale

9.4 Summary

In considering the influence each parameter has on the output phase current of the model it is possible to understand which parameters are suitable for parameter identification and which produce poor results for optimisation. From this part of the work it is seen that the direct axis reactance parameters seem to be good candidates for parameter identification but some of the quadrature axis components are totally ineffectual. Transient quadrature axis components provide little influence on the output phase current, and the sub transient quadrature components, are better than the transient component, but provide influence characteristics that have limited parameter influence and may be prone to local minima. Both the related time constants for these reactances behave similarly in this regard.

In looking further at parameter influence of the synchronous machine, it is seen that armature resistance provides good stable results for parameter identification, as does the constant of inertia. Leakage reactance is a difficult parameter to quantify: its influence on phase current is seen to be very large, however the influence characteristics it has means there is a great possibility that local minima will be derived and not real parameter values. For this reason boundary conditions and their application in the PSO algorithm increase the chance of a successful identification.

Moving onto the excitation system model, certain parameters are seen to be surprisingly appropriate for parameter identification. Parameters like the K_F, K_{A1}, K_E and T_E produced

encouraging results in this regard; however this is guarded with evidence that excitation system parameter identification may be influenced by the perturbation type that is used.

The governor and turbine produced mixed results in some regards. It becomes obvious that parameter identification using this technique is impossible for a turbine governor as the relative influence it has on phase current output is insignificant. Looking at the turbine gain constant however suggests that it has a strong influence on the output error and that it is suitable for parameter identification.

The ramifications of using differing forms of perturbations for the parameter identification process, and the results have been very insightful. The results suggest that certain variables respond to specific transient characteristics in a different way to others. In some cases this makes them susceptible to parameter identification and in other cases makes them unsuitable. This as an area is quite interesting, in that, the type of transient in reality may not be known, thus unless the transient is of the 'correct' form, it will become more challenging for these parameters to be identified.

In looking at the model's behaviour to differing perturbations further, it is seen that some perturbations produce slightly different responses in the DigSilent model to the estimator power plant model. This discrepancy causes a subtle change in error that has an influence on the function of the parameter identification. Further analysis regarding whether the secondary perturbation has ramifications to the parameter identification process is considered in later sections, but it seems logical that the most favourable form of perturbation for the parameter identification would be that of a single perturbation with no secondary transient. A good example of this would be the load drop perturbation used in this chapter.

An area that is likely to become more prominent in later sections is the compound influence of several parameters. The parameters considered in this section all have individual behaviours, some quite similar, others unique. In identifying more than one parameter at a time, the characteristic influence of each these parameters will be added together. This communal behaviour is likely to create local minima in the search area.

The minima characteristics are also an aspect of interest. Depending on the shape of the minima and its characteristics, the global minima will be altered. For this reason the range of values at the minima may be increased as the parameter number to be identified is increased. This means that the range of identified parameter values gets bigger as the number of parameters to be identified is increased.

10. Parameter Identification Using PSO

The results from the previous chapter have shown that it is possible to identify which parameters can, cannot and may be identifiable. This chapter will focus on how successful parameter identification is using particle swarm optimisation with the DigSilent synthetic transients used in chapters 8 and 9. In this chapter several areas are considered:

- Establish whether the base PSO algorithm functions for parameter identification.
- Consider parameters which are particularly difficult to identify by classical means.
- Analyse and improve the PSO algorithm's function in respect to initial distribution and boundary conditions to move forward with real recorded data.

The function of the parameter identification method is evaluated. This establishes whether the parameter identification algorithm works with regard to the model, the objective function and the parameters to be identified. In this chapter further analysis is performed in regard to the behaviour of the PSO algorithm and highlights any specific points of interest regarding the optimisation algorithm.

Moving forward from the base function of the parameter identification, parameters that have been historically difficult to identify by classical means are highlighted and discussed as to whether the results delivered suggest that this method may be practical for their identification.

The final area of consideration in this chapter is the optimisation of the algorithm itself. Up to this point, the base functionality of the algorithm has been assumed to be optimum. Here, specific aspects of the algorithm are evaluated in the hope of identifying areas of the algorithm that can be improved to produce a more thorough and faster search. The initialisation distribution is an area of evaluation in this regard as it may provide an improvement in searching, likewise is the use of differing boundary condition philosophies.

10.1 Parameter Evaluation

The previous section of results and discussion showed that different parameters in the synchronous machine, excitation system and turbine-governor model have differing influence on the output phase current error. This influence has shown which parameters have the capacity to be optimised and thus which parameters can be identified. The table below separates the parameters into performance groups in order to establish which parameters are worthwhile pursuing and which are not.

High likelihood of identification (High influence)	Possible identification (Lower influence)	Dependent on perturbation (Variable influence)	Not identifiable (No influence)
X_d, X'_d, X''_d, T'_{do}, T''_{do}, X_q, R_s, H, K_F, K_R, T_E, $K_{Turbine}$	T''_{qo}, X_{LS}, T_4	X''_q, K_{A1}, T_{A1}, T_{F1}	X'_q, T'_{qo}, Gov (T_1, T_2, T_3)

Table 1 Evaluation of Identifiable parameters

As can be seen in chapter 9 and in table 1, five parameters can be totally discounted as being unidentifiable; others have been classified as dependent on perturbation type where there is a large difference in influence from one perturbation to the next. The other groups are split into identifiable and possibly identifiable. The possibly identifiable group are parameters that have influence on the phase current output error but have a characteristic distribution that is not as favourable for optimisation (i.e. the minima may be elongated or the gradient of descent to the minima may be very shallow).

Moving forward into the parameter identification results, the data is evaluated in the three main successful categories listed in Table 1: most influential parameters, parameters that could be identifiable and parameters that are perturbation dependent.

PSO as an optimisation algorithm has been proven to function well under many circumstances and it would not add significant value to prove the algorithm is generally capable of optimisation. Instead the work will move directly into the parameter identification process and its results.

Given that the direct axis parameters have a clear influence on the phase current output error, the parameter identification begins with these parameters, adding further variables as the parameter identification complexity is increased until nine parameters are considered in one search. This allows the evaluation of the computation cost of the optimisation and gives a better understanding of the limitations of the optimisation.

Figure 95 was developed by running the parameter identification process eight times, incrementally increasing the number of parameters to be identified. The transient used was a 10% load drop. The criterion for convergence was set to zero in order to observe how the parameter number affects convergence over an extended number of iterations. The maximum number of iterations per process was set to one thousand iterations. Acceleration coefficients c_1 and c_2 were both set to 2.05 giving a constriction factor of 0.729. The distribution was set at random and interval confinement was utilised.

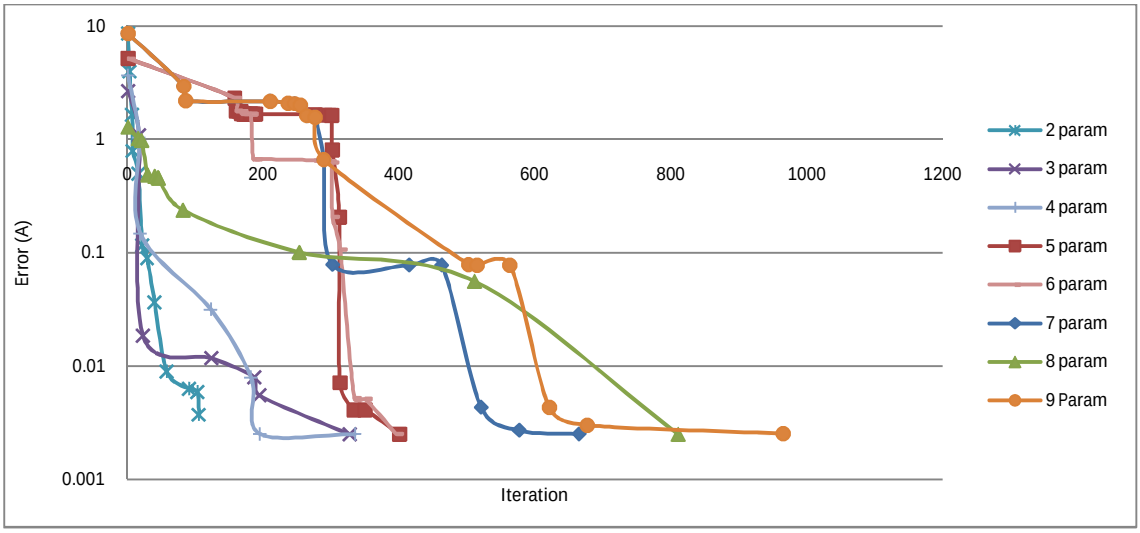

Figure 95 Performance of the PSO algorithm for a load drop perturbation; log scale

Figure 95 shows the effective improvement of phase current output error against the number of iterations it takes to reach this value for a load drop perturbation. This perturbation type is chosen specifically for its good influence characteristics as seen in the previous Chapter. In looking at this, several things become apparent: as the number of parameters to be indentified increases, so does the number of iterations required to reach the same level of error considered to be suitable for convergence. This is no surprise given that the search area is increased with every added parameter or dimension. Because of this the swarm has a larger area or volume to cover in its search. This increase in iterations evidently goes hand in hand with an increase in computational cost.

The results of the five parameter and nine parameter searches seen in Figure 95 demonstrates the presence of local minima. It is seen that both searches 'plateau' at certain points before moving on to improve. In reality this is likely to be where the influence characteristics have compounded together to form a local minima, which the search swarm finds, then takes several iterations to escape from.

Another interesting aspect that is observed in Figure 95 is that the best result achieved or the effective minima value is very similar. This suggests that although individual parameters are seen to reach minimas of the order of 0.0003A (X_d for load drop), the cumulative error created by identifying numerous parameters at the same time is not capable of reaching the same order of magnitude. As previously discussed the difference in phase current output from the synthetic dataset from DigSilent and that of the identification model contributes to this limit of improvement. This limit would logically form the basis for a successful convergence. The minima achieved in this case may not be consistent for every form or perturbation.

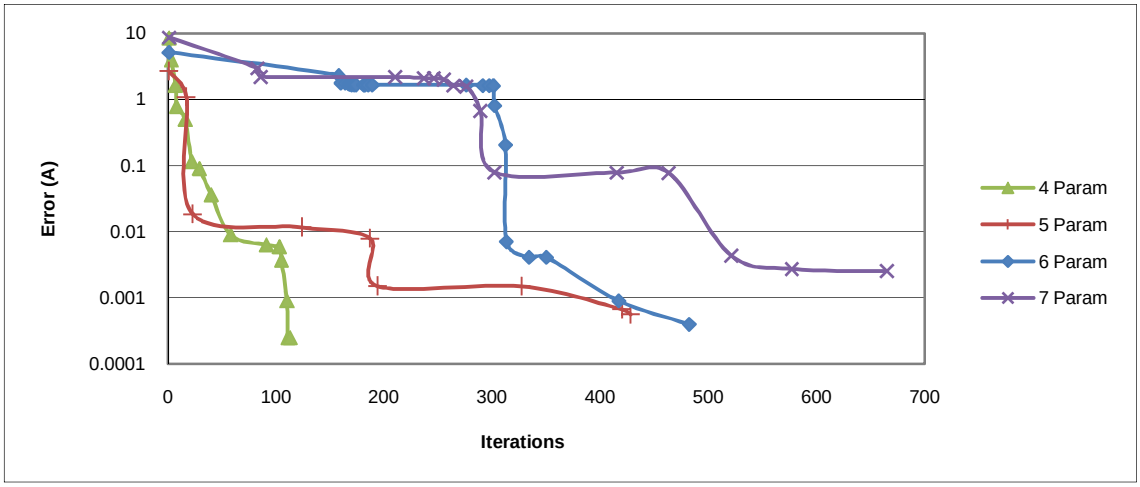

Figure 96 Convergence of differing variable number searches using a short circuit perturbation (83); log scale

Figure 96 shows a similar graph for a short circuit event with the same algorithmic settings and an iteration limit of 1000. It is seen that the final error achieved is not consistent from one search to the next and the error achieved in several is significantly better. This shows that as the number of dimensions increases, the search space is larger, so searching to find the same criteria for convergence becomes more difficult. This results in differing error values. It is likely that if the algorithms were allowed to continue, they would eventually reach a similar end value of error. To consider this further, the line switch and line fault and clearance perturbation results are seen in figure 90.

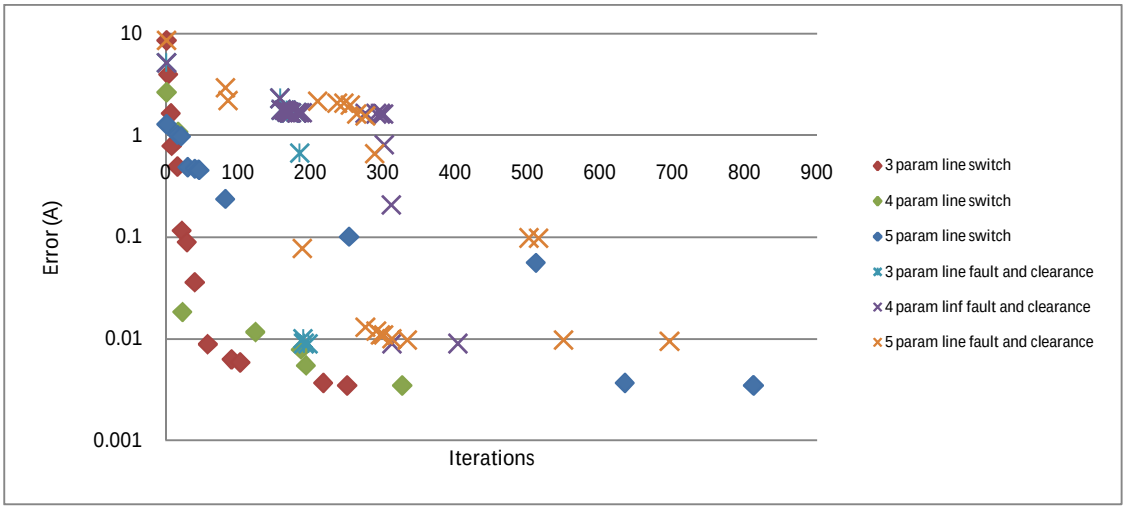

Figure 97 Convergence of differing variable number searches using differing perturbations; log scale

As can be seen above, the computational cost is proportional to the number of parameters identified which is consistent with what has already been seen. What is noticeable is the difference in minima that the two perturbations develop. Much like the load drop perturbation, the number of parameters has little effect on the overall minima, but the

relative level of minima that both achieve is different from one another. This suggests this subtle difference in model performance carries on from one perturbation to the next (as discussed in previous chapters). The relative difference in ultimate minima value becomes quite problematic from a practical point of view as it is difficult to know which perturbation type is the input to the optimisation method through observation alone. Thus, setting a convergence value that is realistic for all perturbations is difficult as it will fluctuate from one to the next. The fact that the ultimate error of the line fault then clearance perturbation is higher than that of the line switch perturbation would support the argument that the secondary perturbation has a negative effect of the ultimate convergence error when compared against a synthetic data source such as DigSilent.

Parameter	Machine	4 Param	5 Param	6 Param	7 Param	8 Param	9 Param	10 Param	11 Param	12 Param
Rs Armature resistance (Ω)	0.0048	0.0039	0.0033	0.0056	0.0041	0.0020	0.0054	0.0031	0.0021	0.0067
X_d d-axis reactance (Ω)	1.79	1.78	1.79	1.76	1.82	1.72	1.84	1.84	1.71	1.76
X_q q-axis reactance (Ω)	1.66	1.64	1.59	1.66	1.61	1.71	1.65	1.59	1.58	1.63
X'_d transient d-axis reactance (Ω)	0.355	0.250	0.301	0.322	0.411	0.367	0.400	0.388	0.423	0.369
X''_d sub-transient d-axis reactance (Ω)	0.275		0.203	0.223	0.314	0.276	0.332	0.285	0.320	0.268
T'_{do} Open circuit transient time constant (s)	7.9			8.2	7.6	7.1	7.4	7.5	7.5	7.3
T''_{do} Open circuit sub transient time constant (s)	0.032				0.031	0.025	0.062	0.034	0.053	0.077
H Inertia Constant (pu)	7.9					6.4	8.3	7.4	6.6	7.4
K_f Exciter feedback constant (pu)	0.03						0.023	0.032	0.049	0.062
K_E exciter gain (pu)	1							0.91	0.94	1.08
T_E exciter saturation time constant (s)	0.8								0.84	0.83
$K_{turbine}$ (pu)	1									0.96

Table 2 Results of identification tests using the load drop perturbation of identifiable parameters

The results seen in Table 2 show a reasonable adherence of parameter value to the machine value (used in the synthetic datasets). There appears to be larger deviation in parameter value as the number of parameters is increased. This would suggest that as the number of parameters to be identified is increased, the compound minima that these parameters produce are larger. Because of this increase in minima area the range of values that the particle can possess whilst still having the same error value is increased. This increase in minima size is only small however, so it would be fair to say that the parameter identification was successful using the variables that were classified as suitable for optimisation.

Parameter	Machine	1 Param	2 Param	3 Param
T''_{qo} Open circuit sub transient time constant (s)	0.055	0.088	0.113	0.120
X_{ls} Leakage Reactance (pu)	0.215		0.282	0.351
T_4 turbine time constant (s)	0.35			0.43

Table 3 Results of identification tests using the load drop perturbation of possibly identifiable parameters

Moving on to the parameters that were classified as being possible to optimise, the results become fairly mixed from the point of view of optimisation. It is seen from Table 3 that the identification follows the same base pattern as seen before, the actual parameter values identified at the point of convergence occupy a far wider range.

Parameter	Machine	1 Param	2 Param	3 Param	4 Param
X''_q sub transient reactance (pu)	0.275	0.286	0.302	0.271	0.243
K_{A1} voltage regulator gain	400		360	432	420
T_{A1} voltage regulator time constant (s)	0.02			0.015	0.032
T_{f1} voltage regulator feedback time constant (s)	1				0.98

Table 4 Results of identification tests using the load drop perturbation of perturbation dependent parameters

The results of the perturbation dependent parameters seen in Table 4 are far more favourable than that of the parameters seen above in Table 3. When using a perturbation that has been seen to produce the appropriate influence distribution characteristics for identification, the algorithm produces results consistent with that of parameters which are in the 'identifiable' category.

Having observed the results that the parameter identification produces, it is necessary to observe how the PSO algorithm behaves as it is running in order to be able to improve its performance. Taking a typical data set, in this case from a four dimension parameter identification, the chart below is developed. Figure 98 shows the percentage difference of each parameter being identified from its true value (as used in DigSilent) for the iteration it is recorded in. The height of the bars themselves is the phase current output error that that particular iteration achieved.

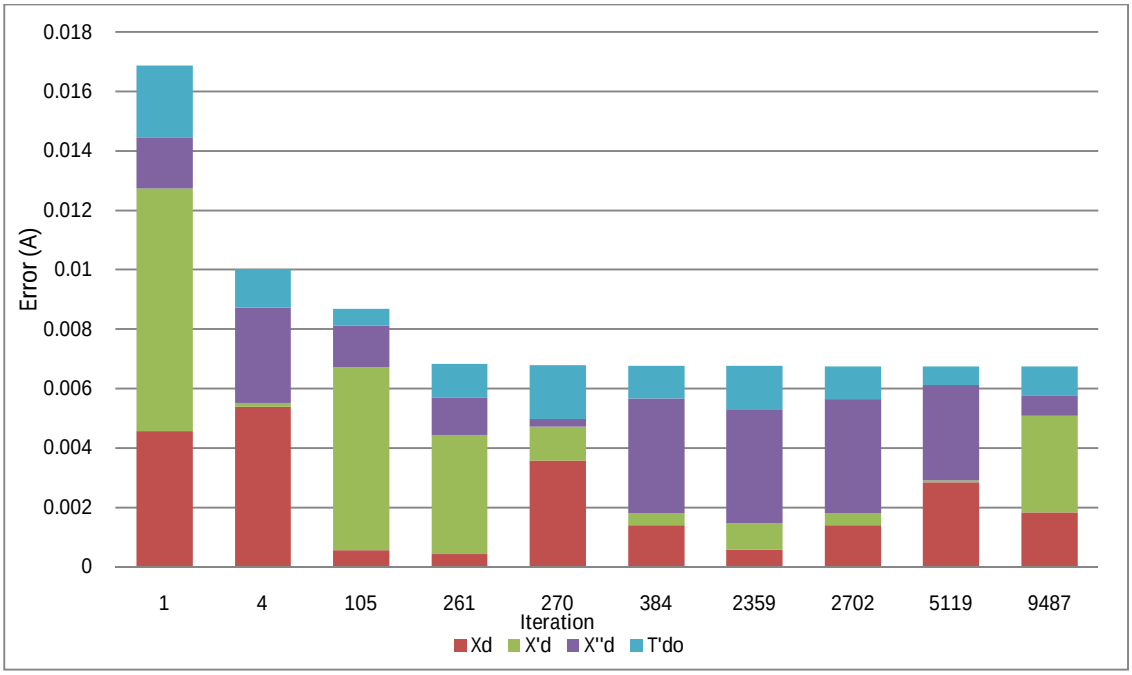

Figure 98 The difference in parameter value from real parameter per iteration with respect overall error achieved per iteration for a 10% load drop; linear scale

It is seen in Figure 98 above that there is no real set pattern when considering the deviation of each parameter from its true parameter value. This can create larger percentage errors in certain parameters for extended periods. Ultimately the search algorithm will proceed to find an appropriate value through differing areas of search space. By that point the error is small enough to satisfy the convergence criteria. It is seen that in some cases the percentage difference between the true value and the estimated value looks very large. This is open to interpretation as parameters of a very low value will obviously register a large percentage change when the actual difference between the identified result and the real result is very small. A good example of this would be armature resistance which at a real value of 0.0048 could create a large percentage difference if the value deviated by even 0.01.

To confirm that this lack of pattern is not perturbation or variable number specific, Figure 99 below exhibits a similar result for a different perturbation. The only significant difference is that the first iteration error is higher. This higher initial error forces the PSO to display a more characteristic convergence curve that would be expected with wider search limits. This has been seen in related published work on this subject (83). The more obvious convergence curve is simply due to a wider search space from initialisation onwards.

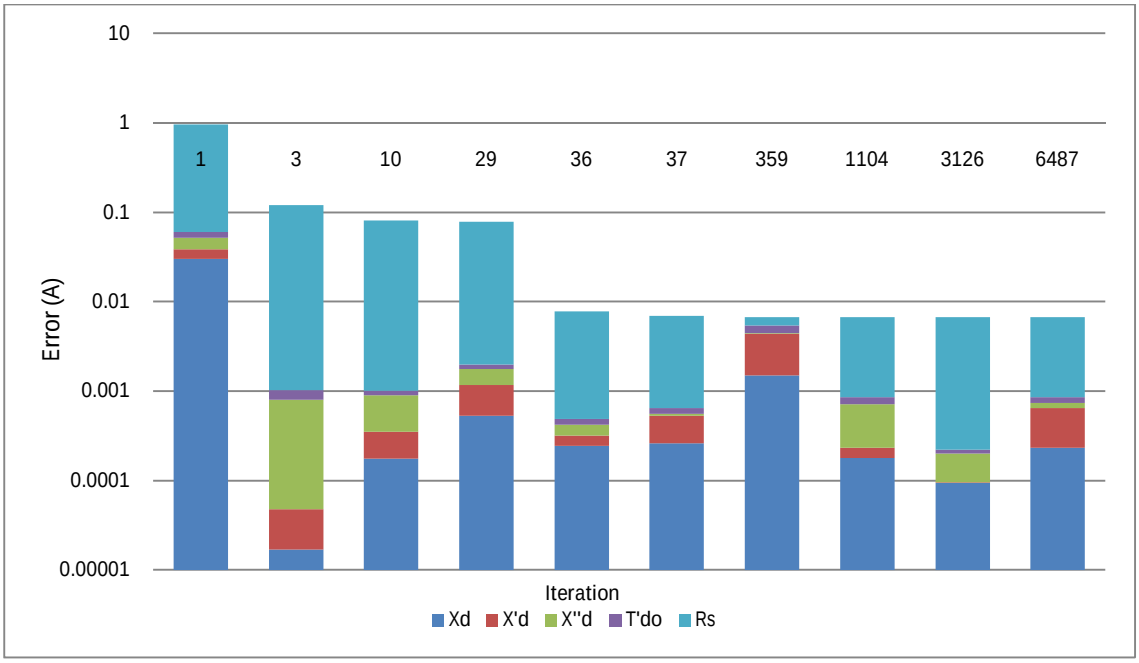

Figure 99 The difference in parameter value from real parameter per iteration with respect overall error achieved per iteration for a line switch perturbation; log scale

As mentioned previously, Figure 98 and Figure 99 are distinctly different in regard to the initial error and thus characteristically the second chart has a more obvious incremental improvement. This is due to the initial boundary conditions that define the search space over a wider area. This can create a higher initial error. Although this was done to demonstrate the PSO classical convergence characteristic, it also highlights how important initial conditions are to achieve a swift convergence. When a high value is registered, it means that the parameter values are quite far away from the true value or location. As soon as this happens the first registered G_{best} and P_{best} values are defined. These values define the location of search as seen in equations 48 and 49. Because of this poor initial set of values, the search will take significantly longer than is necessary.

Because of the way that G_{best} and P_{best} define how the search is conducted, there is a fluctuation in the parameter value during the search as seen in Figure 99. Looking further at this fluctuation of parameter value allows a unique understanding of where the swarm is searching and if the swarm is converging in an appropriate manner. Observing the convergence pattern for several parameters also allows the algorithm constants to be altered to optimise its search. Figure 98 and Figure 99 show the random fluctuation of the parameter values which is attributed to the movement of the particle swarm as it searches. This movement in itself is quite insightful. Figure 100 below shows the movement the swarm informant exhibits during a search. Because it is difficult to graphically illustrate a 6 dimension

search space, 3 parameters are selected to observe the swarms movement around their specific search space.

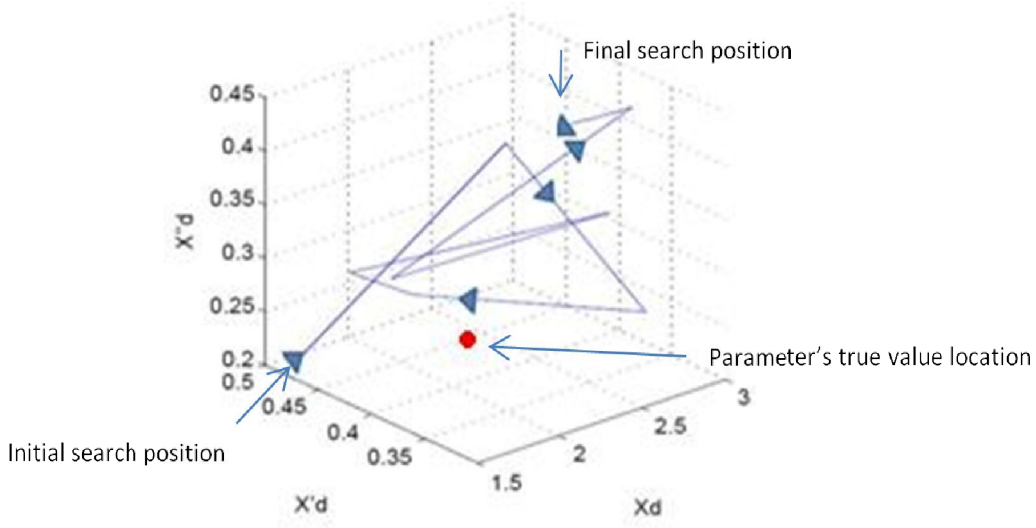

Figure 100 Search path for 3 parameters in a search using a load drop perturbation

During the search depicted in Figure 100, it is seen that the search encompasses a wide area of reasonable parameter values. A significant issue observed is that the distance between one improvement and the next is very large. The larger distance is somewhat surprising as it would be expected to see small incremental improvements, particularly as the swarm starts to converge. This suggests that, from an algorithmic point of view, the velocity of the particles is too high; this means they are overshooting an advantageous search area to consider another area of the search space.

In considering the effect of search velocity, the relative inertia of the particles also comes into question in this regard. Up to this point the inertia of the particles have been set to zero, meaning the particles have no momentum ($\omega = 0$ in equation 47). In regard to the early stages of a search, this is useful as it allows a quicker search of a larger area. When nearing a convergence, this lack of momentum does prove counterproductive as the inherent randomness found in the PSO, coupled with the lack of momentum makes the particles volatile and prone to rapid directional change (86). This volatility can mean that once an improvement is made, the particles can change direction, rapidly looking at a different area. This, when considered with the high particle velocity means that it becomes difficult for the swarm to find gradual improvement in an area when approaching a global minima. For this reason, when considering terminal data, the particles require inertia to make an improvement in this area.

Another aspect seen in Figure 100 is that the particles pass near the real parameter value individually but they do not find combined minima for all dimensions at the same time. This infers that each parameter has a reduced influence on the phase current output error as the parameter number increases. This is logical and is linked to that as the parameter number to be identified is increased, the range in the minima value is also increased, as has already been seen.

As seen in the results: The larger the parameter number, the larger the minima area is. As the parameter number grows the relative influence that each parameter can exert on the output phase current is depleted. Increasing the parameter number also introduces different parameter influence behaviours affecting the phase current output error in different ways. Some of these are more clearly defined than others (as seen in the previous chapter). For this reason, the larger minima area and the different influence characteristics create a search space that has many local minima. This means that although the optimisation is still possible with larger parameter numbers, the length of time it requires to optimise is proportional to the number of parameters to be identified. The larger number of parameters will also dilute the minima to occupy a larger area. This in turn means that if the optimisation is successful, the range of values that can be developed is larger with every parameter added. This means that the accuracy of the parameter identification can be reduced when identifying significant quantities of parameters at the same time.

The reduced accuracy of result and high computational cost leads to the idea that although high parameter number identification is possible, it might be tempting to reduce the parameter number and run several algorithms identifying smaller groups of parameters to reduce the computational cost. This is not feasible however as the identification would then be invalid since the substitute values that would have to be used for some parameters would also affect the phase current outputs.

10.1.1 Summary

The results of the parameter identification using particle swarm optimisation and synthetic data have delivered some significant base points that will be taken forward into later chapters. In following on from the parameter influence chapter it becomes clear that, for the perturbations used, the larger the parameter number to be identified, the larger the possible range of values that can be derived with the same error value. This shows that in increasing the parameter number, the minima point that signifies a convergence, is increased in area, thus increasing the range of possible values that can be occupied while still being classified as

at the global minima. For this reason it seems logical, wherever possible in performing parameter identification to maintain a low number of parameters that require identification. It is also seen that, as the number of parameters to be identified increases, the level of influence that each parameter is able to exert on the phase current output error is diminished. This results in it being more computationally intensive to identify parameters to a high level of accuracy.

This section of the chapter has also shown which particular parameters are feasible as parameters to be identified. It has also shown which parameters are more dependent on perturbations that the power plant will encounter.

Overall the most significant point in this section has to be that parameter identification using particle swarm optimisation for varying forms of perturbations is possible and practical. When dealing with unknown parameter values there is inherently going to be limits as to what can be derived and the range of values that parameters can occupy. This range appears defined by the influence characteristics that each parameter possesses, and which parameters are being identified communally at any given time.

10 .2 Parameter Identification of not Usually Identified Variables

Up to this point an equal weighting has been placed on parameter identification of all parameters without any further consideration as to whether they are parameters that have been previously identified using classical invasive techniques or not. In itself the non invasive nature of using perturbations to identify parameters is original. Consideration is given to parameters which are not commonly identified. Further analysis is performed on these parameters to understand whether this method provides a way of identifying them by non invasive means.

Taking the table of parameters that are seen to be identifiable or have some degree of parameter influence provides a list of parameters that may be identified.

High likelihood of identification (High influence)	Possible identification (Lower influence)	Dependent on perturbation (Variable influence)
X_d, X'_d, X''_d, T'_{do}, T''_{do} X_q, R_s, H, K_F, K_E, T_E, $K_{Turbine}$	T''_{qo}, X_{LS}, T_4	X''_q, K_{A1}, T_{A1}, T_{F1}

Table 5 Parameters of influence that may be identifiable

The parameters are then separated into two sections, 'usually identified' and 'difficult to identify'. This shows which parameters this method of identification allows access to that standard invasive testing does not.

Classically identifiable	Not usually identified
X_d, X'_d, X''_d, T'_{do}, T''_{do}, X_q, R_s, H	X''_q, K_{A1}, T_{A1}, T_{F1}, T''_{qo}, X_{LS}, T_4, K_F, K_R, T_E, $K_{Turbine}$

Table 6 Separation of commonly identified parameters and parameters difficult to identify

In many respects the distribution of classically identifiable and not usually identified parameters is of little surprise. The classical machine manufacturer tests, like the open and short circuit tests are seen to provide a significant proportion of the classically identified parameters. The parameters in the not usually identified section are likewise, pretty indicative of the methods originality. This is because excitation system and turbine parameters are not usually identified through standard invasive testing and are generally given by manufacturers using their own specific tests.

Machine parameters of interest that are not usually identified by classical means are leakage reactance and sub transient quadrature axis reactance. As already discussed, leakage reactance is a compound of several variables that develop a unique distribution as seen in Figure 80. Its very nature has meant that historically, it has not been identified with much success because of this. The non invasive testing presented in this work has shown that leakage reactance produces results that could be optimised and thus identified provided particular attention was given to setting appropriate boundary conditions. Sub transient quadrature reactance is equally uncommon in identification. Methods like a three phase short circuit to ground or more original methodologies (89) have been employed previously, but are less commonly used. For this reason, the fact that it is a parameter that is identifiable using this approach is highly advantageous.

10.3 Improving PSO Performance

10.3.1 Use of a Constricted PSO Algorithm

In Chapter 8 it was stated that a constricted PSO algorithm would produce better results than that of a standard PSO algorithm. This was justified (83), but the inclusion of the results were necessary to understand the algorithm behaviour further.

When considering the PSO for this particular application, several things appear significant in its ability to converge in an appropriate number of iterations. Firstly, an aspect quite prominent

is that of search space. It is necessary to be realistic in identifying the search area that is required for multidimensional problems such as this. Setting pragmatic limits to parameters such as X_d or R_s where, in reality all synchronous machines of this type possess very similar value range, means that the search can be far more accurately targeted which reduces the space that particles can search without finding an optimum solution.

A comparison of the ability to identify parameters using a constricted PSO algorithm against that of a non constricted algorithm is seen in Figure 101. This comparison is based on a short circuit transient. Settings can be found in (84).

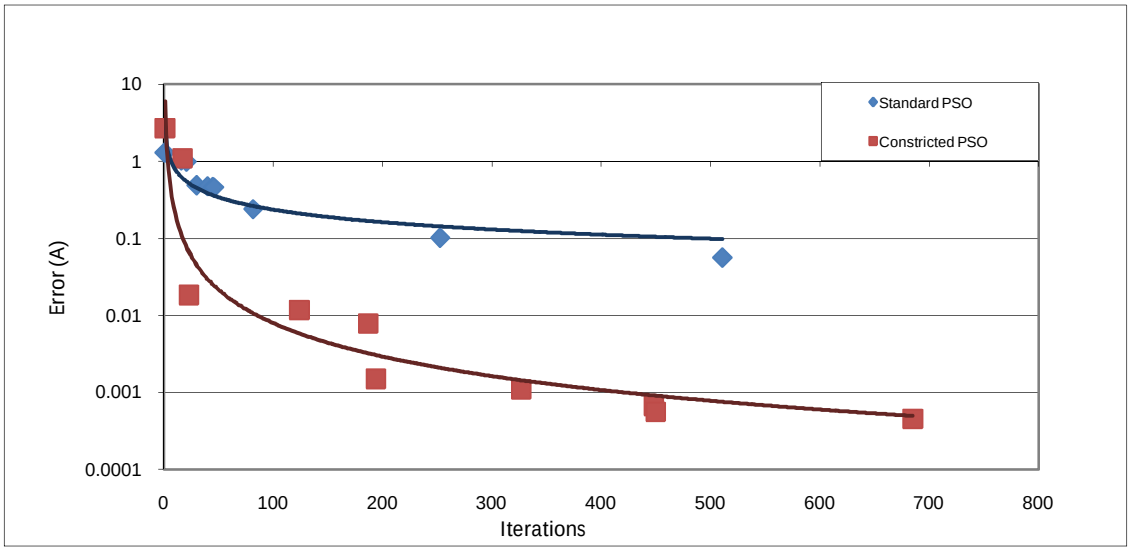

Figure 101 Comparison of standard PSO against constricted PSO (83); log scale

By using a constriction factor in conjunction with a refined search area, setting correct weighting values and acceleration coefficients, the particles travel at an appropriate speed to converge on a lower error. In reaching this lower error search space, the constriction factor slows the velocities of the searching particles further. This means that the area is more accurately searched.

Applying a constriction factor produces favourable results in the initial stages of convergence in that, as the search area is large, it forces the algorithm to search a wide area of search space quickly. When reaching the later stages of the convergence, this becomes counterproductive. It is seen that the most appropriate course of action may be to reduce the constriction factors significance proportionally with relative error to provide the best balance between search area and algorithm convergence.

10.3.2 Boundary Conditions

PSO has the ability to define the search space which the particles occupy. As discussed in the implementation chapter, this confinement has differing forms which could have a significant effect on the optimisation and identification of parameters in the model. For this reason, differing methods of confinement were considered and evaluated, with the best solution being used in the optimal PSO algorithm. The forms of boundary conditions evaluated were:

- Interval Confinement
- Imperative and Indicative Confinement
- Granular Confinement
- Confinement by Dichotomy

Confinement is necessary in optimisation. The fact that there are limits or the value of these is not in question. The question is as to how the PSO algorithm reacts when a particle reaches these limits or breaks its conditions of confinement. From this an optimal method of confinement can be found for this project.

Quantifying which form of confinement is the best is challenging in that, the different forms of confinement can be tested for function, but whether they improve the efficiency of conversion can only be seen in the final result. For this reason, a four parameter identification algorithm was used as a basis for testing, with the same perturbation used throughout the simulations (a load drop of 10%). The differing confinement methods were applied to the algorithm and the simulation ran ten times per confinement method to develop a result.

Because of the inherent problems in applying imperative and indicative confinement, it had to be discounted as the indicative aspect of the confinement could not be applied in this scenario. Because of this, the confinement essentially became interval confinement, which is already tested.

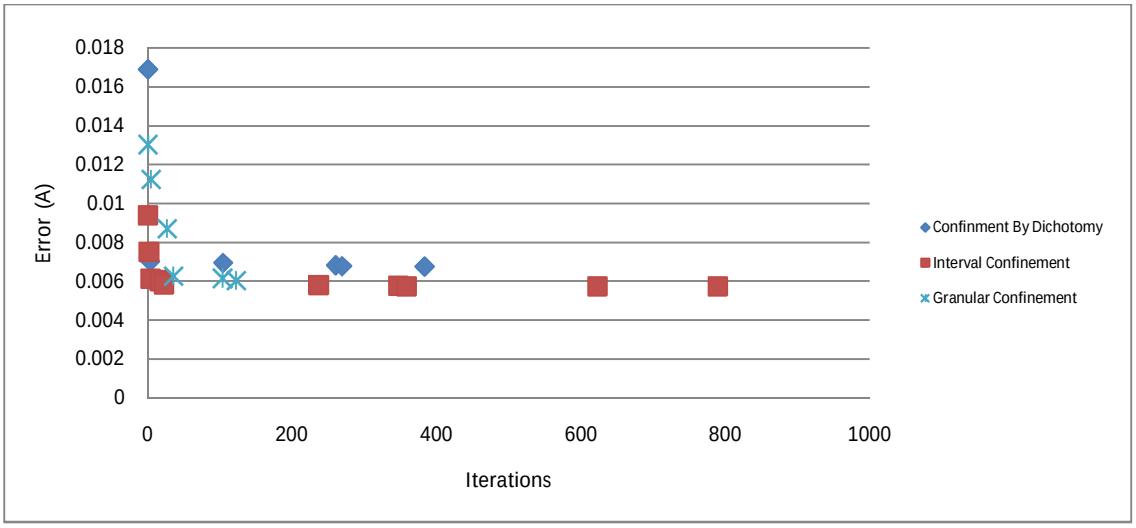

Figure 102 Analysis of differing forms of confinement; linear scale

Figure 102 is a typical set of results for the varying forms of confinement[21]. The results of the differing forms of confinement are fairly similar. The relative error that all the forms of confinement reach is similar, in a similar time frame. It is seen that the confinement by dichotomy nearly reaches the level of error that the interval confinement achieves, but then struggles to reach the same final value. Granular confinement is quite similar in result to interval confinement, ultimately reaching around the same final error.

Interval confinement produces results very similar to the other forms of confinement. It is marginally better than the other two, in that it reaches a low near minimum value faster than the other confinement methods and is seen to continue to improve further with more iterations. The confinement method is tuned to explore the boundary region as exhaustively as possible. This is done by setting the confinement so that when a particle 'steps' out of bounds, the particle is returned to a region just prior to the border region. The velocity of the particle is retained in order to maintain the integrity of the search.

It seems the relative difference in moving from one form of confinement to another has a nearly negligible effect on the final result in practical terms for this application. Overall the most traditional form of boundary conditions, interval confinement would appear to be slightly better for this application than the other methods investigated. The difference in efficiency and the relative simplicity in application of interval confinement suggest that, moving forward, it provides the most appropriate method of confinement in PSO for this application.

[21] The equations defining the varying forms of confinement are found in chapter 8.

10.3.3 Initialisation Particle Distribution

The implementation highlighted two forms of differing initial distribution that could be tested. These are compared against the conventional method of distribution which is characterised per dimension by the equations below where R_{and} is the random number generator in Matlab that will produce a value between zero and one.

$$X_d(i) = X_{min} + \{(X_{max} - X_{min})\} * R_{and} \quad (62)$$

$$V_d(i) = X_{min} + \{(X_{max} - X_{min})\} * R_{and} \quad (63)$$

This form of distribution is seen to introduce the particles at random throughout the search space to achieve a thorough search.

$$V(i)_{dimension} \leftarrow C_1 V_d + k(0, C_{max})(P_{best} - X_d) + k(0, C_{max})(G_{best} - X_d) \quad (64)$$

$$X_d(i) \leftarrow X_d + V_d \quad (65)$$

In a rectangular distribution, the particles are distributed in a cubic format which occupies the search area considered for the algorithm in order to reduce issues regarding the distributions along axes (as considered in the implementation). The distribution is slightly reduced in size to be within the search boundaries and is defined by equations 52 and 53 above. The ellipsoidal distribution is implemented in a similar fashion to that of the rectangular distribution in order to compare the two forms. As described by equations 54 and 55 below where $S_{phere}(0, \rho)_d$ is a function that gives a random point in the sphere of dimension ρ.

$$V(i)_{dimension} \leftarrow C_1 v V_d + C_{max}\left|S_{phere}(0, \rho)_d\right|(P_{best} - X_d) + C_{max}\left|S_{phere}(0, \rho)_d\right|(G_{best} - X_d) \quad (66)$$

$$X_d(i) \leftarrow X_d + V_d \quad (67)$$

Much like the boundary conditions review, a four parameter identification algorithm was used as a basis for testing, with the same perturbation used throughout. The differing distributions were applied to the algorithm and the simulation ran ten times per confinement method to develop an average result.

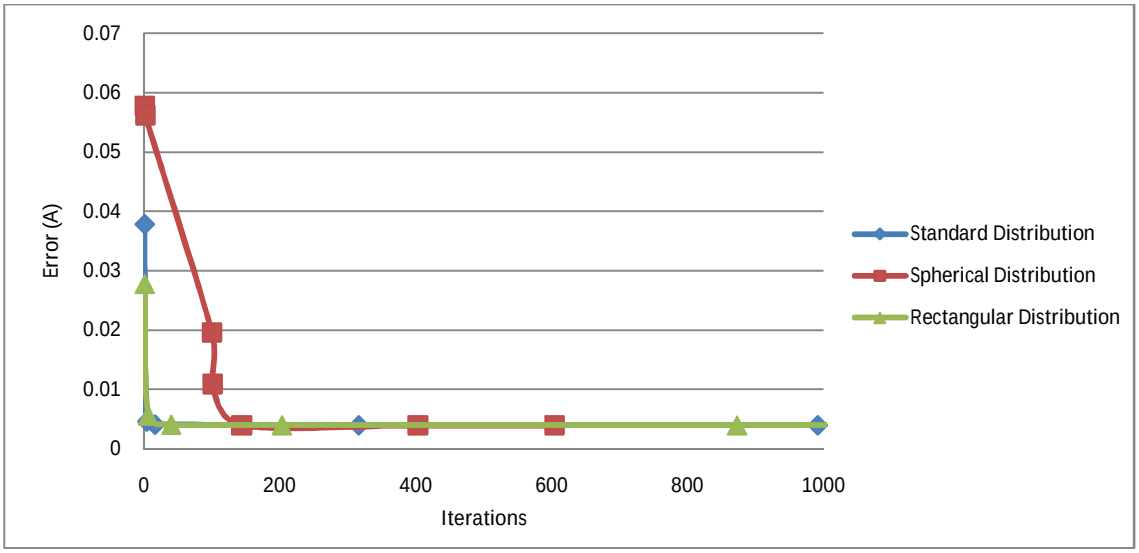

Figure 103 Analysis of differing distribution types; linear scale

When looking at the typical results seen above, all three forms tested achieve a similar final error level and perform reasonably for this particular search. It should be noted that in practice, only the first few iterations are particularly relevant in understanding the differing distribution types. After this point the search will have moved the particles to different search spaces and so its relevance becomes reduced.

Looking more closely at the search results, it is seen that the ellipsoidal distribution performs worse than that of the standard distribution and that of the rectangular distribution. The reason for this is likely due to the form of distribution itself and its ability to cover cornered areas of the search space. In the search algorithm, one of the parameters considered is that of armature resistance, which in reality possesses an inherently low value. Because of this low value and the search space that is defined by the boundary conditions, the spherical distribution may not cover the optimal armature resistance location sufficiently. This would appear to have a negative effect on the overall error that can be achieved with a given initialisation distribution.

Considering the rectangular distribution and the standard distribution, it is seen that both have similar initialisation characteristics. The rectangular distribution seems to cover the search area better than the spherical distribution, thus allowing an initially lower value and because of the swarm distribution overall, it is more capable of improving faster than that of the spherical form.

The standard distribution is seen to produce equally favourable results as the rectangular distribution. This may be due to the randomness injected into the distribution allowing an

unstructured, but thorough search. The implementation of this method also seems to function favourably in the iterations following the initialisation.

Overall it is seen that of the forms of distribution evaluated, the rectangular and the standard distribution function in the most efficient manner for this application. From an evaluation point of view, both sets perform admirably, the only real difference being the increased complexity and thus computational cost that the rectangular distribution would incur (although this would be very small). For this reason it seems that the most appropriate distribution would seem the standard distribution, which continues to be implemented.

10.3.4 Summary

Based on the results presented in this section, several conclusions can be made. Firstly it is clear that, based on the results attained from the comparison of the constricted PSO against the classical PSO, the constricted PSO results in a more efficient conversion on an optimal result. Because of this, going forward the constricted PSO is considered a better solution in this regard.

As part of the optimisation, varying forms of confinement were tested to identify the most practical type to use as part of the PSO algorithm. The results showed that there wasn't a significant advantage in any of the confinement methods over each other. Ultimately interval confinement was chosen as it was marginally better for the current work.

The results of the analysis of the distribution characteristics echoed that of the confinement analysis in that, all methods considered were suitable to be used. Of the three tested, the rectangular and standard distributions achieved the best results, thus were equally favoured. Only the small difference in computational cost resulted in selection of a standard distribution.

11. Parameter Identification Using Recorded Terminal Data

The primary purpose of the results presented in Chapters 9 and 10 was to establish the influence of each parameter in order to understand which variables have characteristic behaviour that would make them susceptible to optimisation and thus parameter identification. Once this was established, the parameters that were 'optimisable' were then used with a PSO algorithm in order to identify synchronous machine, excitation system and turbine parameters of a synthetic test system. In doing this, the methodology was evaluated and modified to allow for the most efficient form of optimisation going forward.

The final aspect of the investigation is the parameter identification of real system parameters using recorded transient data from the national grid of the UK. The machine data used in conjunction with the recorded data set is from a 178MVA steam turbine generator unit that is used in a combined cycle gas power station. The manufacturer's machine and excitation system parameters are found in appendix 4.

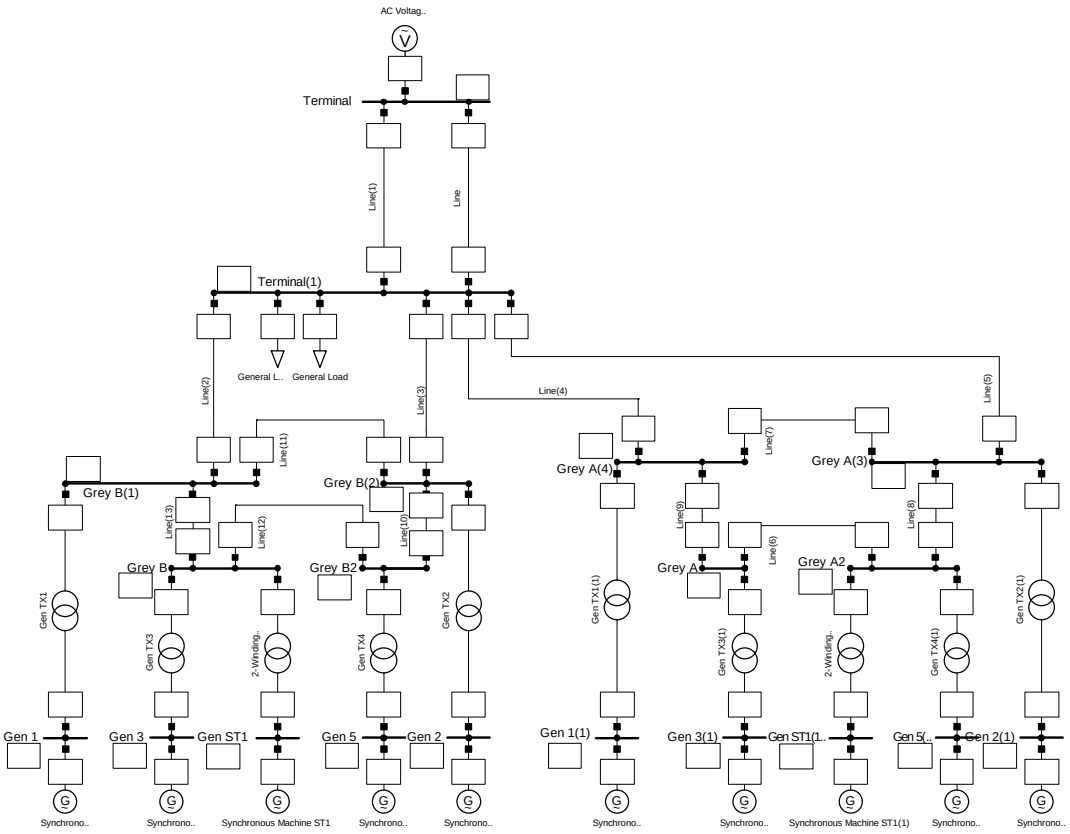

Figure 104 Combined cycle power station layout

Figure 104 shows the basic layout of the combined cycle power station from an electrical perspective. As can be seen, there are ten large generators, two of which are steam turbines working with four gas turbines each, in order to develop sufficient steam to power the turbine.

Further analysis is required before progressing to parameter identification. These include; the use of recorded transient terminal datasets, the machine type and the form of perturbation utilised.

This chapter considers:

- The type of recorded transient and the relative implications of using it.
- How the transient may affect the influence of the parameters to be identified on the phase current output.
- The generator / excitation system themselves and how they affect the optimisation process.
- The parameter identification of the steam turbine generator using recorded terminal data.
- Analysis of the parameter identification results.

11.1 The Recorded Dataset

Several datasets were obtained from the power station data recorders, with only one being suitable for parameter identification. The main challenge in obtaining an appropriate transient for parameter identification is that, for the power plant recorders to deem a transient worth recording for review, the transient has to be onerous in nature. Because the fault is sufficiently onerous to be recorded, the protection surrounding the generator invariably is activated. If the protection is activated, the representation of the power plant used in this work becomes invalid as there is an external input controlling the generator behaviour that the model is not aware of. Paradoxically, it is difficult to obtain a less onerous network disturbance because the data recorders do not deem them onerous enough to be considered, and are ignored as there is no further analysis required by the engineers at the site.

The transient dataset utilised for this work is that of a phase to phase fault on the external network. In Figure 105 it is seen that initially the generator is running in steady state. At 0.08 seconds a phase to phase fault occurs at a point in the network. The phases faulted together are phase A and Phase C. This is seen by both phases displaying the same phase voltage waveform. Phase B is in anti phase at double their amplitude in order to satisfy Kirchhoff's law

at the star point of the machine. Figure 106 shows the phase currents for A and B are seen to be effectively in anti phase of one another. Phase C has a steadily increasing current level.

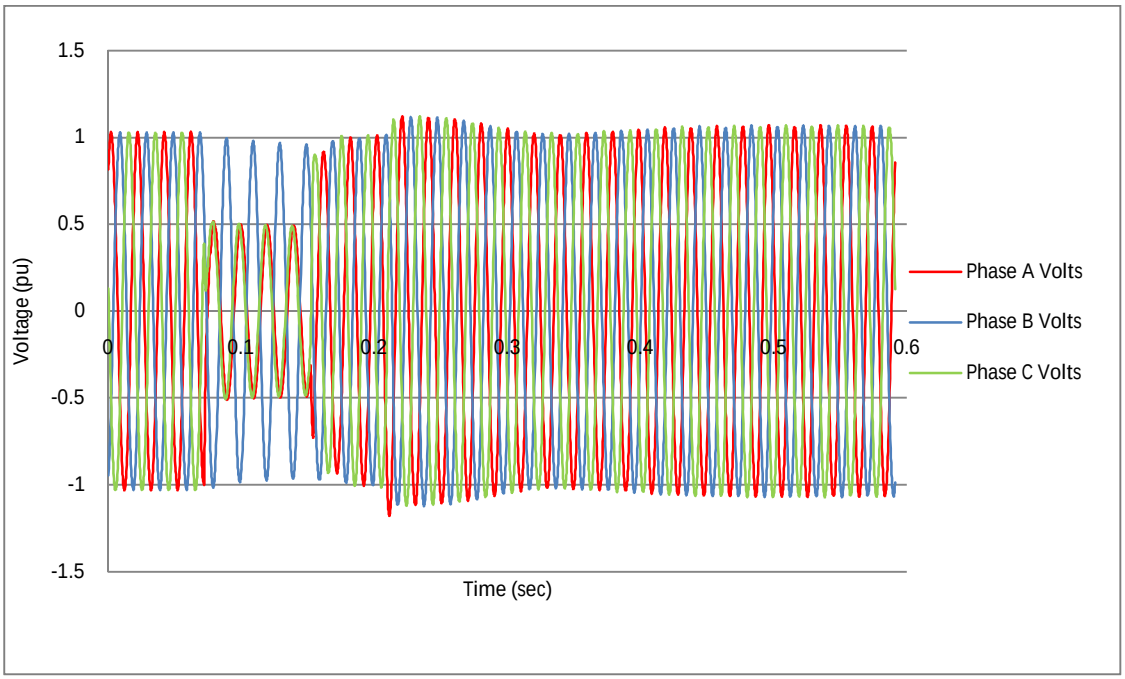

Figure 105 Voltage waveform from phase to phase fault from 'under voltage relay' on Generator 11 (steam turbine)

At 0.16 seconds the line protection trips the line and clears the fault. This is signified by a period of returning stability in the phase voltage and phase current waveforms. Unfortunately the protection at the generator end registers the fault, specifically the under voltage relay. This protection trips off the generator at around 0.21 seconds. The open circuit characteristic on the generator is signified by it remaining at roughly steady state phase voltage. The current waveform shows the trip, causing no current to flow as seen in Figure 106. There is a noticed gradual decrement to 0 in the phase current from the point of tripping till around 0.7 seconds. This current is residual current in the current transformer creating a small dc offset.

Figure 106 displays the phase current waveform of the perturbation. As is mentioned in the explanation of the transient and in the figure itself, the under voltage relay is activated, this trips off the generator, forcing it to operate in an open circuit state until reconnection. This aspect of the transient cannot be used for parameter identification as the protection has affected the machine response in a way that makes it impossible to perform such actions. This is because the model does not account for protection, therefore the model responds to the open circuit voltage condition like it would in standard operating conditions as discussed in chapter 7 which makes the output during this period unsuitable. The transient leading up to this point however, is valid. For this reason, provided the simulation is ended at the point of

the protection being activated, there is no fundamental reason why the recorded perturbation cannot be used.

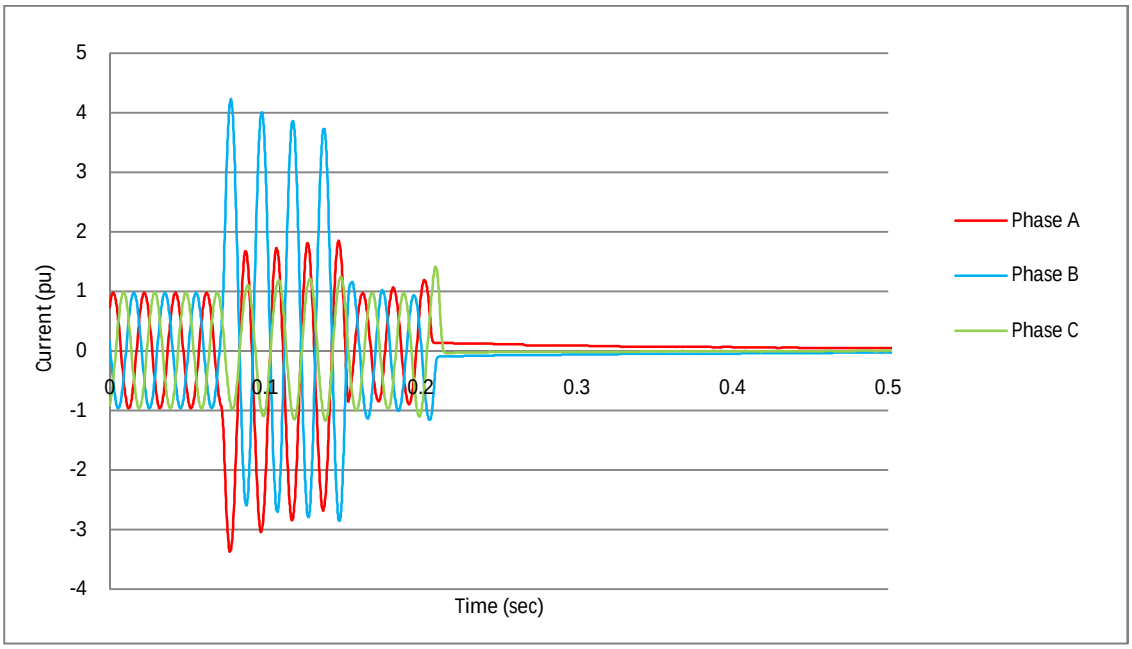

Figure 106 Current waveform from phase to phase fault from 'under voltage relay' on Generator 11 (steam turbine)

Figure 107 shows the recorded phase current dataset of the generator against that of the simulated machine phase current output. As can be seen, there are obvious differences in the effective magnitudes reached during the stages of the recorded fault during the recorded transient, this is particularly evident in phase B between 0.075 seconds and 0.14 seconds.

During the fault period of the transient, phase B of the recorded data set is seen to not reach the magnitude of the generator model "Simulated Phase B" in regard to fault current contribution. There are several possible reasons for this. Firstly the values of reactance given by the manufacturer were the saturated values; this would explain the higher fault current in the simulated phase currents. Conventionally power station generators operate in a mildly saturated mode in order to maximise the efficiency of the machine and minimise the amount of steel required in order to build a generator of that power level. If under the conditions seen in the fault, the machine was not operating as far up the saturation curve as is conventionally expected from that machine type, then the transient and sub transient unsaturated impedance of the machine would be higher than that of the saturated value. This would result in the fault current contribution being lower. To confirm that this is the case would require further information that is not available.

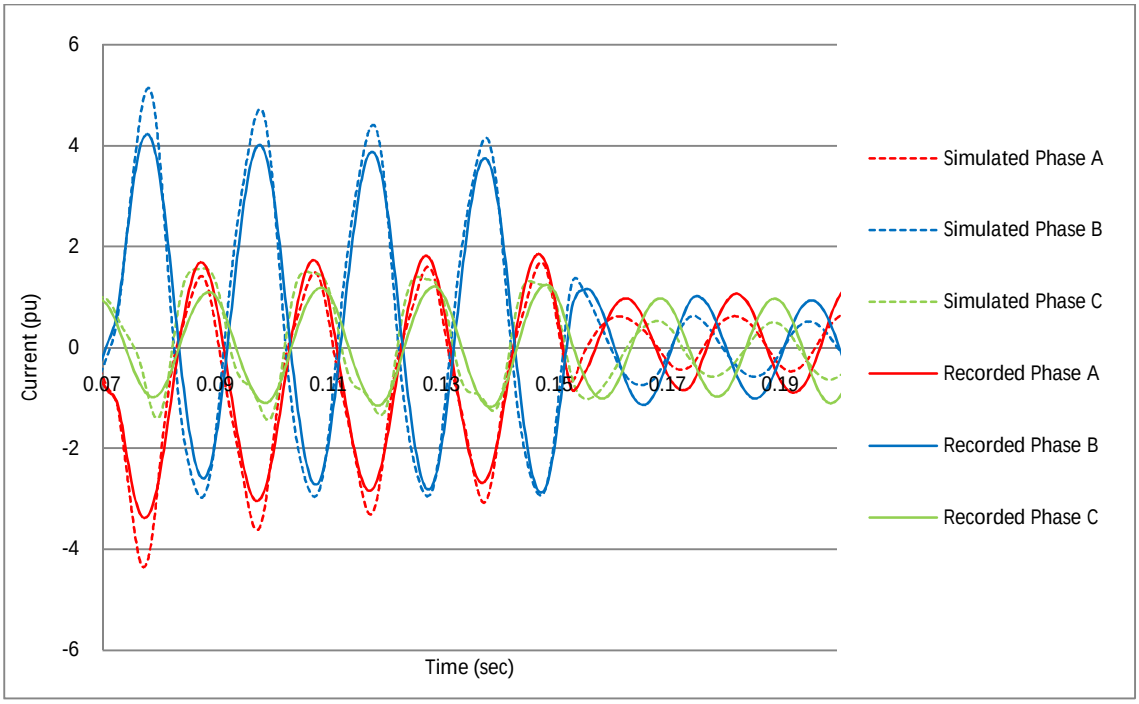

Figure 107 Comparison of recorded phase currents to that of simulated phase currents

Perhaps the most likely reason for the discrepancy is that the manufacturer's declared values are not particularly accurate. As seen in (54), commissioned machine parameters can have a significant tolerance between the declared value of the machine parameter and the real machine value. This, coupled with the lack of information with regard to the machines operating region, means the likelihood that there is some discrepancy in parameter value is only enhanced.

The implications of having manufacturer parameter values with a wide tolerance of accuracy for the machine are significant from a validation perspective. From an optimisation point of view the PSO algorithm will attempt to match the recorded phase current waveforms to that of the phase current output waveform of the identification machine model. If the model does not produce results bearing an adequate resemblance to the recorded waveforms, the algorithm will iteratively improve the parameter values in the generator model until they do match the recorded dataset. The interesting aspect of this is that if the manufacturer values are incorrect, and the optimisation is successful, the values of the parameters identified and that of the manufacturer declared values will not match. This means that the method may be identifying the correct parameter values, particularly for the transient and sub transient reactance. On the other hand, from a validation perspective it is difficult to confirm that the results that have been developed are correct, even if they are more accurate than the manufacturer data.

Considering another aspect, as can be seen in Figure 107, the recorded phase current waveforms and that of the model's output current waveforms are in phase with each other. This would suggest that there is limited deviation in rotor speed between synchronous speed and the speed of the turbine during recording. For the synchronous machine and the excitation system, this fairly short time period means that rotor speed change is neglected as it has limited effect on the parameter identification process for such a small time period.

In considering this short time period and the relative effects it has on parameters that influence the behaviour of the machine over a longer time scale, the turbine is a particular area of interest. This is because the short time period may affect the ability of the turbine parameters to influence the phase current waveform sufficiently for the optimisation to occur to a satisfactory level. The main reason this in this case is because the relative inertia of the turbine and the rotor of the synchronous machine possesses is significant enough to produce little change in such a short time period.

Another aspect related to this is that the dataset and generator type in this research is a steam turbine generator forming part of a combine cycle gas turbine power station. As mentioned in Chapter 3, in combined cycle power stations the waste energy from the surrounding gas turbines is used to create steam. This steam drives the steam turbine generator. This would have implications with regard to network transients that are recorded over a longer period of time. This is because, if like in this case, the protection for the machine was tripped off for the surrounding gas turbines, there would be an effect on the supply of steam which would affect the steam turbines dynamic response. This is less of a concern in this case, as the dynamic response for such turbine interaction is of the order of a minute (11), but it would be applicable for longer transients. It would also have implications with regard to the turbine model and would require a thermo dynamic model type that accounts for more than one turbine. This is beyond the scope of this investigation.

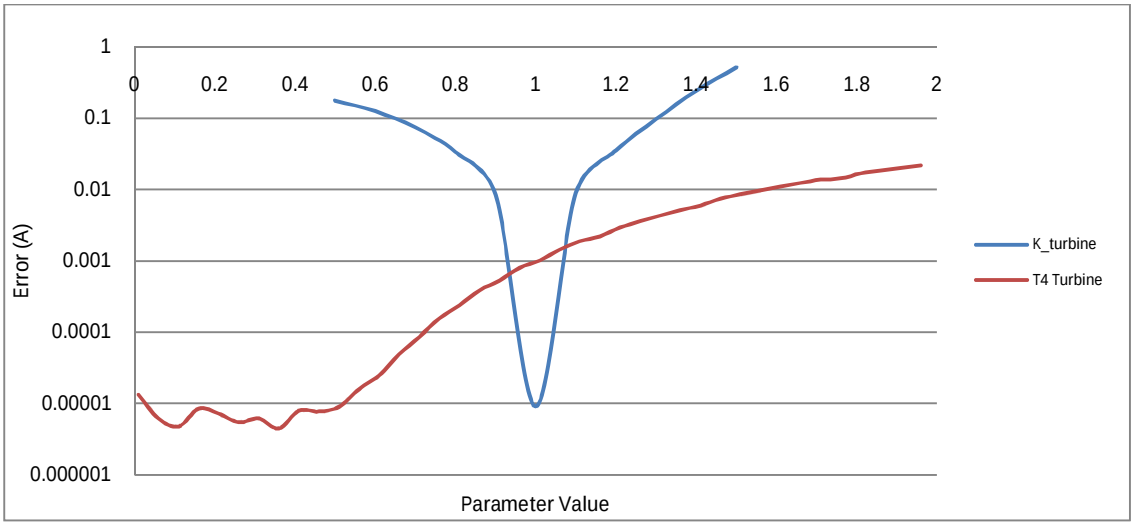

Figure 108 Influence characteristics of turbine parameters; log scale

In order to understand whether the datasets relatively short time period has an impact on the ability of the turbine parameters to be identified, it is necessary to reassess the influence of the turbine parameters on the output phase current. Figure 108 shows the influence characteristics of the turbine time constant T_4 and turbine gain $K_{turbine}$ for the recorded transient used. In many respects the results presented are very similar to that seen in chapter 9. This is quite positive as it shows that the results of using synthetic datasets were the same as would be expected from real transient data which provides a degree of self validation. The results also indicate that the turbine has similar influence characteristics over a shorter time period. This means that the turbine gain term should be capable of optimisation and thus parameter identification is still likely.

T_4 has a somewhat different influence to that seen in the synthetic datasets previously. It is seen that, much like before, there is a good gradient of descent on the high side of the parameter value. Between 0 and 0.5 however, there is a highly non linear behavioural characteristic with several minima observed. This has implications as to whether the parameter can be accurately identified. The parameter was classified as 'possibly' identifiable as the elongated minima produced a high likelihood of a larger variable value range. The results from this would suggest that even this classification is probably too optimistic as the nonlinear surface of the minima could produce convergences at three differing local minima in this value range. This is clearly not satisfactory when considering the accurate parameter identification of the turbine. To mitigate the possibility of this, the interval confinement of this parameter has a lower boundary value that will minimise the possible locations of local minima.

Looking further at Figure 107, it is interesting to observe the difference in response between the recorded phase currents and the model phase currents during the period of fault clearance and return to steady state (between 0.15 and 0.2 seconds). The particular area of interest is the relative magnitudes that both sets of phase current and voltage waveforms achieve during this period. In Figure 105, during this period, the real generator is seen to recover to near steady state voltage in a very short period. This translates to the recovery of phase current in a very similar way in Figure 106 and Figure 107, respectively. When considering the parameter identification model phase current waveforms in Figure 107, it is seen that the phase current magnitude is recovering, but at a far slower rate than that of the real system. It is likely that the phase current of the model would have reached steady state values in a fairly short period of time, but the tripping of under voltage relay makes this difficult to confirm.

The behavioural difference in this period highlights the fundamental difference an excitation system can make to a recovering system provided the parameters are appropriately set. The excitation system in the model has a generic set of values (57) that are designed to respond in a reasonable way to a transient, hence the phase current recovery is constant but not particularly fast. The excitation system characteristics the real system adopts are specifically tuned to the network in which they operate. This is seen specifically when the voltage and current recover in a single cycle.

11.2 Parameter Identification Using the Recorded Transient

Having considered the varying relevant aspects of the transient datasets and their implications with regard to the synchronous machine and the excitation system specifically, it is necessary to consider the parameter identification of the steam turbine generator using the recorded terminal dataset.

Based on the results from the previous chapter, the PSO algorithm adopted is in a constricted form. As part of the algorithm, the optimisation strategy utilises interval confinement and has a random initial distribution. As alluded to in the previous chapter, it would appear that as the parameter number is increased, the range of values that the parameter can occupy whilst still maintaining the same minima value is also increased. Because of this, parameters will be identified in the same order as in the previous chapter. To give a point of comparison, a second set of parameter identifications is presented with three parameters identified at a time in order to compare the relative accuracy of the parameter identification process as the variable number is increased.

As seen previously there are parameters that are identifiable but only if the perturbation type allows it to do so. For this reason it is necessary to evaluate X''_q, K_{A1}, T_{A1} and T_{F1} to ascertain whether the perturbation considered is suitable for parameter identification.

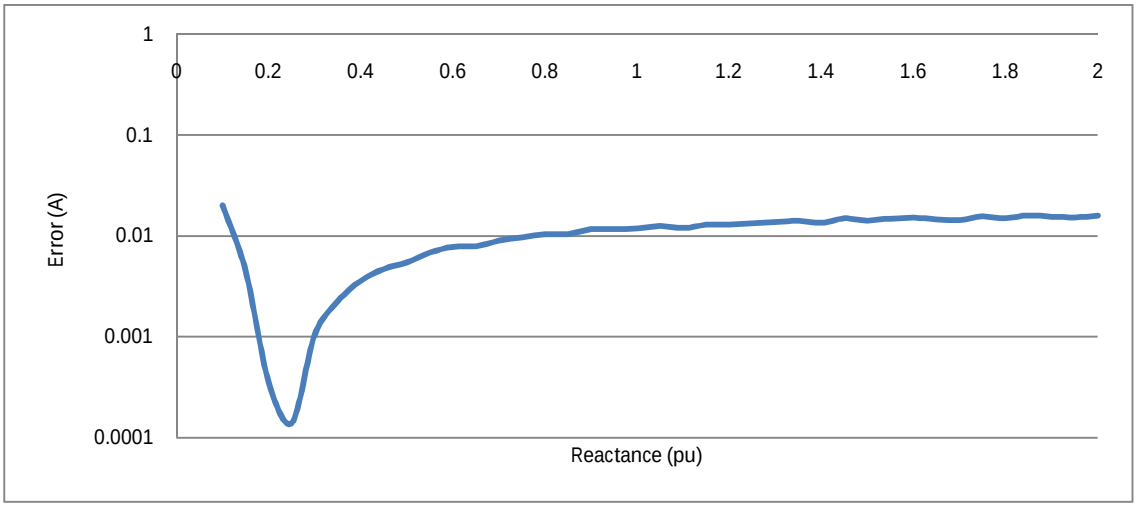

Figure 109 Influence of X''q on recorded transient dataset; log scale

As can be seen from Figure 109, sub transient quadrature axis reactance displays characteristics that are likely to be identifiable. The minima that is displayed is sharp and the gradient of descent to this minima is appropriate for identification. The only aspect that could be considered troublesome is that the effective error for parameter values of above 0.8 is relatively low. This suggests that although the parameter is capable of being identified, its strength of influence on the transient is relatively low which may have an impact on the parameter identification. From a practical point of view, this is unlikely to be problematic as the boundaries set by the interval confinement will constrain the search area to realistic values of sub transient reactance. For this reason the upper limit that the search area will consider is of the order of 0.5 per unit reactance.

Moving to the performance of the excitation system parameters that were considered parameter dependent, the relative influence of K_{A1} is seen in Figure 110.

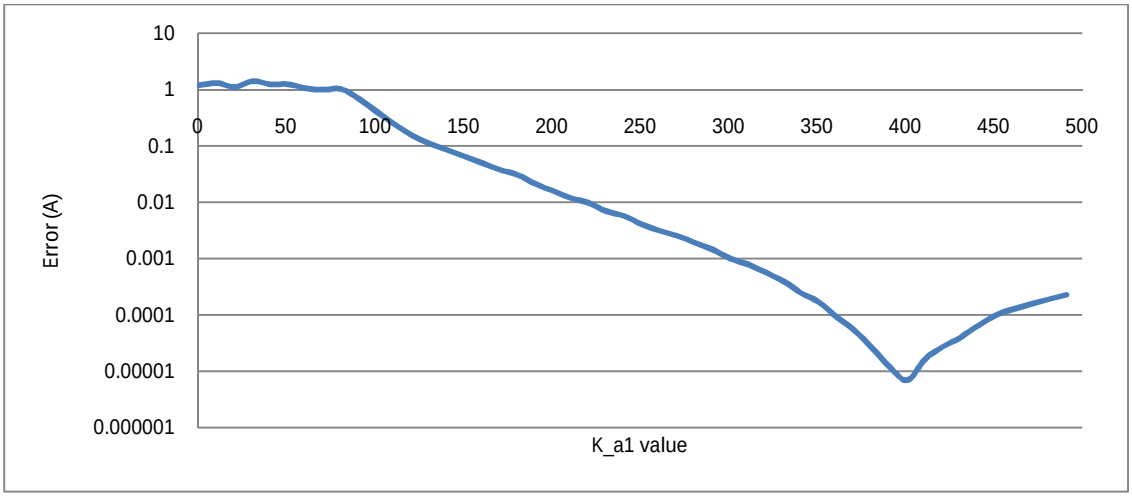

Figure 110 Influence of KA1 on recorded transient dataset; log scale

The influence characteristics of excitation system gain K_{A1} is seen to display broadly positive optimisation characteristics. The clearly defined minima and gradient of descent would suggest that the parameter would be suitable for identification for this specific dataset. Because the excitation system characteristics are unknown due to the use of a tuned excitation system with a differing generic model type, it is important that the search boundaries set for the defined search space are wider than those of the synchronous machine parameters would be. This is because the synchronous machine parameters are defined by physical constraints that define its behaviour whereas although the excitation system does have the same physical constraints, they are only known by the manufacturer. Even when setting a wider search area, the characteristics displayed in Figure 110 suggest that the optimisation of K_{A1} would still be possible.

Moving on to T_{A1}, the time constant that is associated with K_{A1}; it can be seen in Figure 111 that the performance characteristics are similar to that of sub transient quadrature reactance. The sharp minima and good gradient of descent to the minima would suggest that optimisation of the parameter is likely. The overall strength of influence of the parameter however, would have to be considered less than K_{A1}, whose gradient to the minima begins at a higher error value and thus has a higher influence.

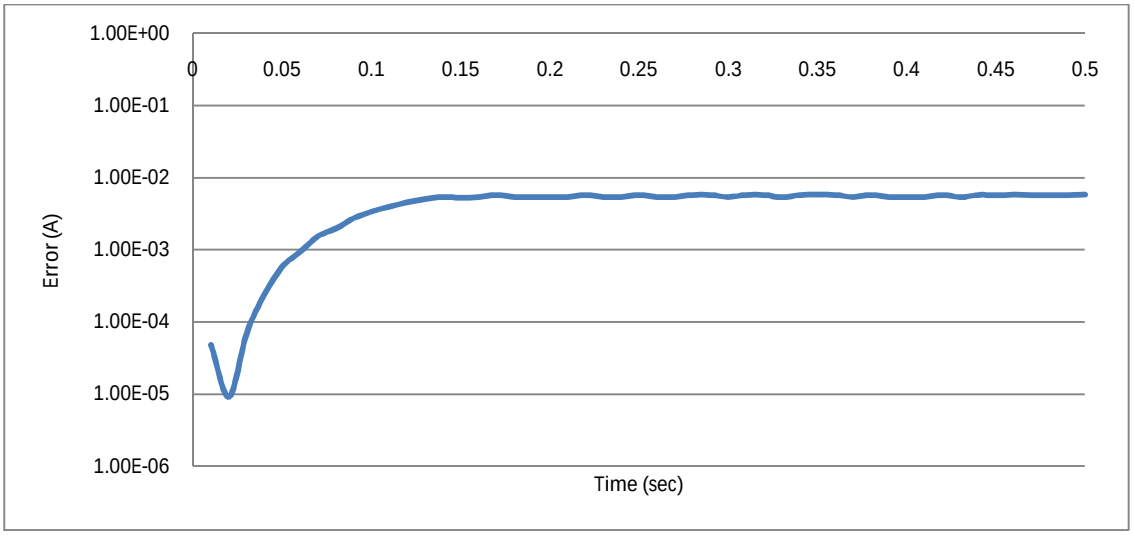

Figure 111 Influence of TA1 on recorded transient dataset; log scale

Figure 112 shows T_{F1}, the final parameter that was seen to be perturbation dependent in the chapter 9. As is seen by the distribution, much like the parameter previously seen, the influence the parameter has on the phase current output error would appear to be sufficient to allow for optimisation.

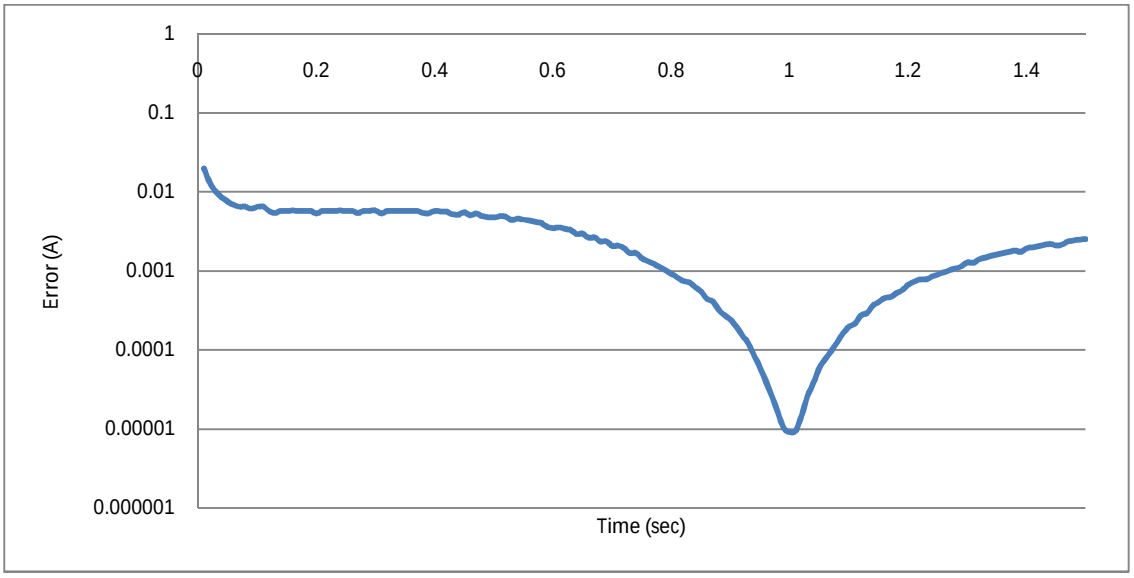

Figure 112 Influence of TF1 on recorded transient dataset; log scale

Having considered the parameters that displayed perturbation dependent characteristics, it can be seen that these parameters have sufficient influence to suggest parameter identification should be possible. This may be in part due to the onerous nature of the phase to phase fault which means that there will be a significant deviation in error as the parameter value changes. This is quite advantageous in that more parameters become identifiable.

The influence characteristic that the recorded transient produces gives the list of parameters seen in Table 7. This list of variables is considered suitable for parameter identification.

Higher likelihood of identification (Suitable influence)	Possible identification (Irregular influence)
X_d, X'_d, X''_d, T'_{do}, T''_{do}, X_q, R_s, H, K_F, K_R, T_E, $K_{Turbine}$, X''_q, K_{A1}, T_{A1}, T_{F1}, T_4	T''_{qo}, X_{LS},

Table 7 Identifiable parameters

Having established the parameters which can be considered identifiable from the perturbation type, the parameter identification is performed as previously discussed. The results are seen below in Table 8 below. The results seen in the 'Ident Results' column are from the parameter identification of three parameters at a time in order to give a result for comparison.

Parameter	Name Plate Data	Ident Results (3 Param)	4 Param	5 Param	6 Param	7 Param	8 Param	9 Param	10 Param	11 Param	12 Param
Rs Armature resistance (pu)	0.0048	0.0033	0.0076	0.0023	0.002	0.004	0.0033	0.0021	0.0013	0.0025	0.003
X_d d-axis reactance (pu)	1.68	1.67	1.64	1.67	1.67	1.7644	1.64	1.63	1.66	1.7522	1.73
T'_{do} Open circuit transient time constant (s)	0.83	0.85	0.81	0.85	0.8048	0.8009	0.7496	0.8677	0.7424	0.7613	0.848
X'_d transient d-axis reactance (pu)	0.301	0.325	0.304	0.27	0.286	0.335	0.3405	0.33	0.2605	0.2767	0.2694
X''_d sub-transient d-axis reactance (pu)	0.238	0.247		0.258	0.2632	0.253	0.256	0.2133	0.2047	0.2068	0.2638
X_q q-axis reactance (pu)	1.65	1.586			1.7414	1.6481	1.546	1.577	1.72	1.6431	1.64
T''_{do} Open circuit sub transient time constant (s)	0.035	0.0471				0.0589	0.0574	0.0116	0.0164	0.0227	0.0103
H Inertia Constant (pu)	3.74	4.19					4.19	3.97	4.19	4.01	3.6771
X''_q sub-transient q-axis reactance (pu)	0.228	0.229						0.2249	0.219	0.258	0.2061
T''_{qo} Open circuit sub transient time constant (s)	0.035	0.0202							0.0202	0.0387	0.0533
$K_{turbine}$ (pu)	unknown	0.8582								0.8695	0.8584
T4 turbine time constant (s)	unknown	0.6732									0.6581

Table 8 Parameter identification from recorded terminal data results

As can be seen from Table 8 and Figure 113 the parameter identification was successful with a surprisingly consistent parameter value deviation for each variable as the number of parameters to be identified was increased. This is somewhat surprising as, in the work using synthetic data the parameter value deviation is seen to increase as the parameter number is increased. The reason for this is the onerous nature of the fault creating a high degree of influence in the parameters identified. This could also instigate a more sharply defined

minima throughout the parameters identified which would minimise the impact of the phenomena. Another possible aspect that could have lessened the impact to a certain degree is the more appropriately set interval confinement boundaries. The more refined boundaries means that the search space is smaller than previously seen thus the relative deviation that was common in the previous chapter is less obvious. This aspect could be noted as a method of mitigating the increased value range when dealing with less onerous perturbations that do not define parameter influence as emphatically.

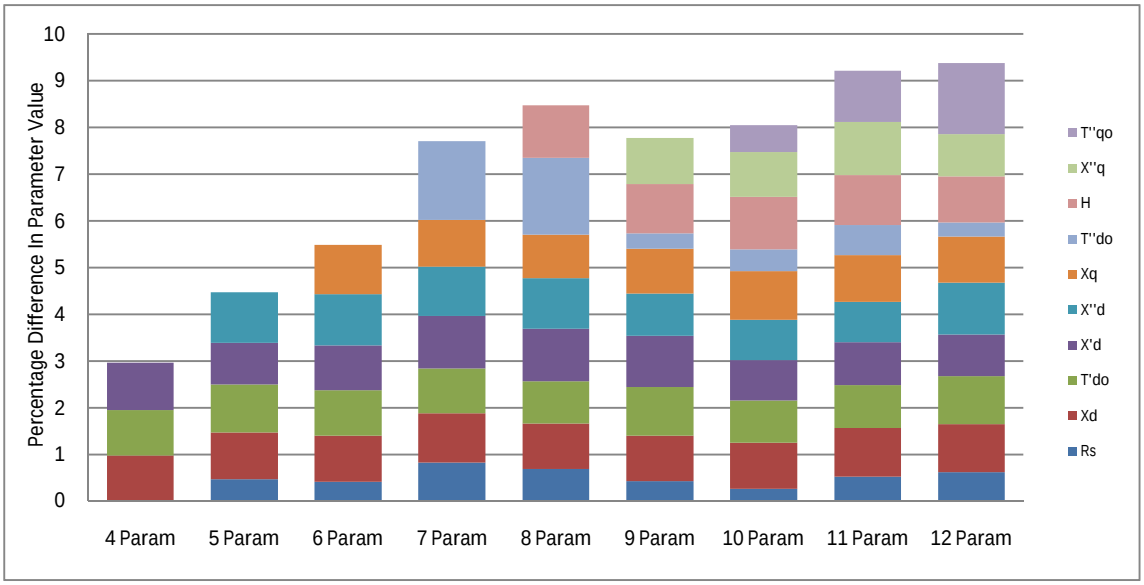

Figure 113 Percentage difference of the parameter identification against manufacturer data; linear scale

Though not seen in Figure 113 above, the phase current output error that defines the algorithms convergence was relatively high for the datasets seen above. This is largely due to the recorded data being used having a phase to phase fault followed by the fault clearance. During the fault itself the machine parameters identified reached a good resemblance to the manufacturer parameter values. During the fault clearance however, there was a significant deviation between the result achieved by the phase current output of the parameter identification model and the recorded dataset. This deviation is due to the fact that the parameters identified were machine parameters and not excitation system parameters. During the fault clearance section of the recorded transient dataset, the excitation system defines the recovery characteristics of the machine in this case and thus the output phase current. The excitation system of the recorded dataset is tuned to the network in which it operates, whereas the excitation system that is used in the identification process is generic and has typical operational values.

The relative impact that this added error has had on the search cannot be fully defined. It is seen that the values identified for sub transient and transient direct axis reactance are not too dissimilar to that of the manufacturer stated values. This isn't surprising since the fault current recorded during the phase to phase fault is quite significant and creates a high degree of influence. Although the result is successful, the relative improvement in parameter value that the PSO algorithm is capable of, could have been hindered by the error from the excitation system discrepancy seen in the fault recovery part of the transient.

In order to establish the excitation system parameter values, a further parameter identification step was carried out on the full recorded transient dataset. The results of which are seen below.

Parameter	Original Value	4 Param	5 Param	6 Param
K_f	0.03	0.048	0.06	0.0343
K_E	1	0.57	1.72	1.4714
T_E	0.8	1.2627	0.59	1.1421
K_{A1}	400	416.27	424.2	384
T_{F1}	1		1.0975	0.8937
T_{A1}	0.02			0.0032

Table 9 Parameter identification of excitation system parameters

The results of the parameter identification of the excitation system are problematic to interpret as the results of the four parameters identification cannot be compared against either the original values, or the values of the five and six parameters identification. This is because the parameter in the excitation system model transfer function will be optimised to reach an excitation system performance that is similar to the performance of the real excitation system during the recorded transient. As the parameter number is changed, the transfer function also changes. This affects the ability of the excitation system to change the phase current output. This alteration in the transfer function changes the ability of the algorithm to optimise the characteristics of the excitation system. This change manifests itself in a different set of excitation system values for that dataset and every dataset where another parameter is added.

The relative success of the parameter identification of the excitation system parameters creates the ability to tune excitation systems from recorded transient data in a non invasive way. This in itself is a novel aspect of the work.

Another aspect worth noting is that of the discrepancy in error created by machine parameters during the fault. This error is much less in magnitude than the error that is created by having incorrect excitation system values, but still could have a similar effect in reducing the ability of the PSO to identify parameter values efficiently.

11.3 Perturbation Specific Identification

The results of the parameter identification using the entire transient have produced some interesting and positive results. The most challenging aspect of the identification is that there is an inherent error created by the unknown excitation system parameters and the unknown machine parameters. In this regard the level of error can be reduced by modifying the period of time that the identification uses as its point of reference.

By only considering the phase to phase fault in the dataset and not the recovery stage (Figure 114) the parameter identification is able to remove the inherent error that is created in the fault recovery period by the difference in excitation system parameters. The fault period used for the identification is quite short, however, it is sufficient to identify machine parameters in the sub transient, transient and steady state regions.

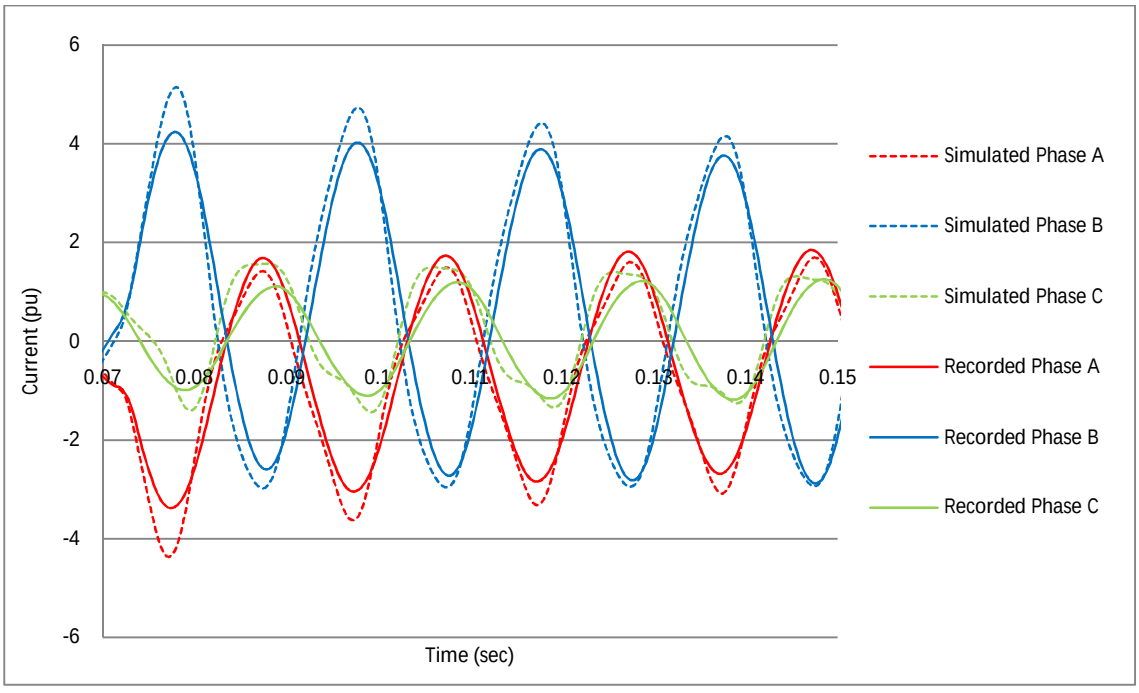

Figure 114 Comparison between synthetic phase current dataset and recorded phase current dataset for phase to phase fault period

Parameter	Name Plate Data	Ident Results (3 Param)	4 Param	5 Param	6 Param	7 Param	8 Param	9 Param	10 Param	11 Param	12 Param
Rs Armature resistance (pu)	0.0048	0.0032	0.03	0.0067	0.0018	0.00035	0.0003	0.0038	0.0027	0.0009	0.0017
X_d d-axis reactance (pu)	1.68	1.675	1.66	1.61	1.79	1.61	1.64	1.648	1.61	1.61	1.72
T'_{do} Open circuit transient time constant (s)	0.83	0.85	0.801	0.76	0.711	0.79	0.8299	0.07264	0.7932	0.896	0.73
X'_d transient d-axis reactance (pu)	0.301	0.316	0.29	0.33	0.2769	0.2629	0.2729	0.29	0.3387	0.34	0.32
X''_d sub-transient d-axis reactance (pu)	0.238	0.246		0.269	0.255	0.2801	0.25	0.2096	0.2512	0.2517	0.254
X_q q-axis reactance (pu)	1.65	1.589			1.66	1.7	1.72	1.78	1.7025	1.78	1.57
T''_{do} Open circuit sub transient time constant (s)	0.0035	0.0472				0.012	0.032	0.038	0.044	0.0454	0.0422
H Inertia Constant (pu)	3.74	4.19					4.18	3.07	3.15	3.52	3.17
X''_q sub-transient q-axis reactance (pu)	0.228	0.228						0.2235	0.2504	0.2522	0.2706
T''_{qo} Open circuit sub transient time constant (s)	0.035	0.0203							0.0168	0.0423	0.0306
$K_{turbine}$ (pu)	unknown	0.8583								0.968	1.09
T4 turbine time constant (s)	unknown	0.6734									0.6573

Table 10 Parameter identification from recorded phase to phase fault results

The results seen in Table 10 and Figure 115 show the similar consistent deviation from manufacturer declared values previously seen when using the full transient. This could ultimately be because of the two reasons previously discussed. The first is that, because the excitation system parameters in the identification model are not optimised against the real system, they may have an impact on the phase current output during the fault which causes the discrepancy in identified values.

The other possible reason for the discrepancy in machine values is that some of the declared values are not very accurate. As already mentioned, this inaccuracy could be due to commissioning or that the percentage tolerance in these values is rather large. Either way, this results in inaccurate values being used as the operation values for the generator. Ultimately the question becomes which set of results better matches the transient data, the manufacturers or the identified? In this regard the identified results are better.

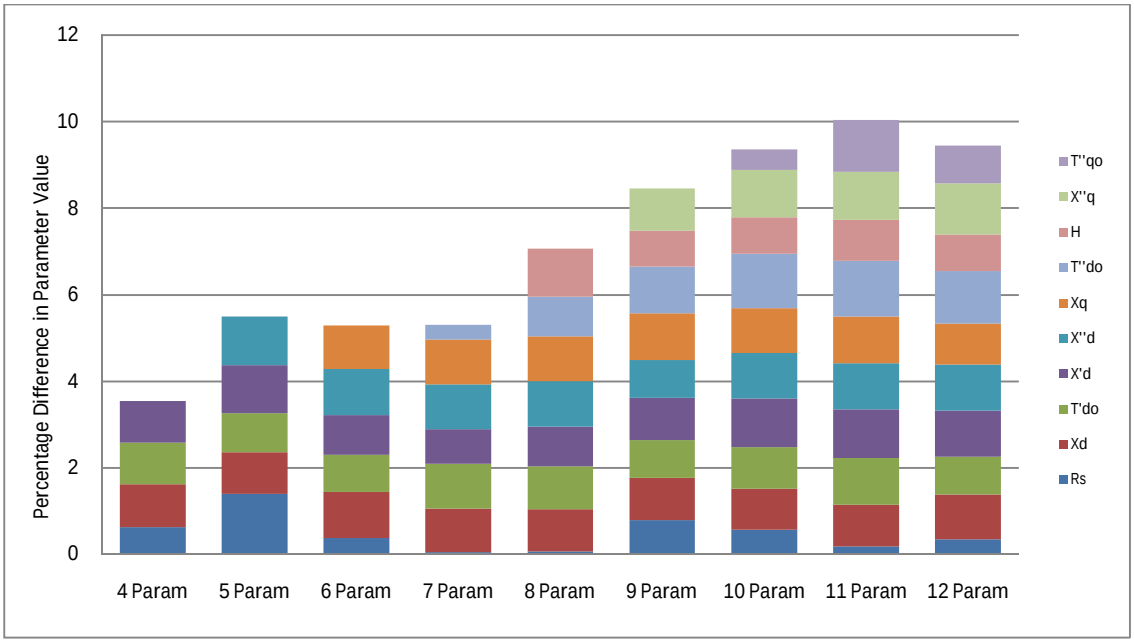

Figure 115 Percentage difference between of identified parameter value and declared manufacturer value for phase to phase fault; linear scale

Parameter	Original Value	4 Param	5 Param	6 Param
K_f	0.03	0.095	0.095	0.059
K_E	1	0.6112	0.4092	0.28
T_E	0.8	0.56	0.68	1.24
K_{A1}	400	383	407.2	453
T_{F1}	1		1.214	1.0654
T_{A1}	0.02			0.0029

Table 11 Parameter identification of the excitation system from recorded phase to phase fault results

Of the two possible reasons it seems logical to examine the exciter parameter values that would be derived if using just the phase to phase fault part of the recorded transient as seen above in Table 11. This gives insight into the influence the excitation system has during the fault. Having similar values as derived previously would have suggested that there is significant excitation influence and that the influence was consistent through the fault and the recovery. The results observed however are not similar. This would suggest that the excitation system has a marginal effect on the phase current output during the fault period.

There is little similarity in the two excitation system result sets when comparing the values of the parameter identification using the entire transient and the results of the parameter identification using the phase to phase fault seen in Table 11. The impact that the excitation system values have on the phase current output during the fault has been seen to be small. This suggests that the impact the excitation system has on the overall transient is of a lesser magnitude on the fault current and has more impact on the current waveform during

recovery. Based on this it would also be reasonable to say that if the exciter has no or little influence on the phase current output waveforms during the fault period and that the generator characteristics define the fault response of the generator.

11.4 Multistage Parameter Identification

Identification of all the required parameters of the turbogenerator using the original technique is difficult because of the large number of parameters (18 in this case) to be identified simultaneously. This would require a significantly high computational cost and would also affect the accuracy of the results by increasing the possible range of values parameters could occupy.

However, having established that the excitation system performance dominates the fault recovery period and that the synchronous generator dominates the phase current output during the phase to phase fault, a multistage identification method is then possible in which the identification process is separated into two distinct parts.

In the first part, the identification process only considers the phase to phase fault identifying machine and turbine parameters only. Once the first stage of identification has been performed, a set of machine/turbine parameter values are developed. The parameter values are averaged over several runs to give valid and repeatable results. These identified parameters are then used in the power plant model for the second stage of the identification process.

The newly developed parameter results are input into the power plant model in order to characterise the performance of the machine under fault more accurately. The recorded transient dataset is then expanded to consider both the fault and the recovery time periods. In the second stage of identification, the only set of parameters identified are the excitation system parameter values[22].

In splitting the identification the computational cost is significantly reduced, but more importantly, the base error that has been seen to be problematic, no longer exists because the machine and the excitation system dominance of their respective parts of the transient are largely isolated.

The results from the first section of the identification are essentially the same as the results seen in the original method using the phase to phase fault part of the transient. For that

[22] A listing of the PSO algorithm used is found in Appendix 5

reason it is not necessary to display the results for the incremental increase in parameter number. The results of this are summed and averaged to produce a set of parameter values seen in Table 12. The averaging of these results is reasonable due to the consistent discrepancy in parameter value that the variables are seen to display in Figure 115. For further information in respect to repeatability, several averaged results are included to indicate divergence in average value

Parameter	Value 1	Value 2	Value 3
Rs Armature resistance (pu)	0.0054	0.0047	0.0051
X_d d-axis reactance (pu)	1.655	1.610	1.713
T'_{do} Open circuit transient time constant (s)	0.709	0.711	0.712
X'_d transient d-axis reactance (pu)	0.302	0.300	0.035
X''_d sub-transient d-axis reactance (pu)	0.253	0.301	0.267
X_q q-axis reactance (pu)	1.702	1.680	1.712
T''_{do} Open circuit sub transient time constant (s)	0.099	0.112	0.098
H Inertia Constant (pu)	3.418	3.42	3.391
X''_q sub-transient q-axis reactance (pu)	0.249	0.252	0.255
T''_{qo} Open circuit sub transient time constant (s)	0.030	0.027	0.033
$K_{turbine}$ (pu)	1.029	1.032	1.027
T4 turbine time constant (s)	0.657	0.660	0.648

Table 12 Multistage identification machine and turbine parameter values

The derived parameter values of specific interest in the set seen in Table 12 are the transient and sub transient direct axis reactances. It can be seen that compared to the declared values (seen in Table 8), the identified values are slightly higher. This could have a specific bearing on the fault current contribution from the generator model, in that the higher impedance value may reduce the fault current to a value closer to the recorded value. This would reduce the discrepancy seen in Figure 107.

Another parameter that is observed to have interesting results is the constant of inertia, H. The derived value is seen to be marginally lower than the declared value. This difference could be reflective of gas turbine operation of the plant at the time, as if there was a lower number of turbines operational, the steam density would be reduced. This would reduce the steams momentum into the turbine which may reduce inertia of the turbine system.

The phase current waveforms that these identified parameter values create are seen in Figure 116. It is seen that the difference between the peak value of recorded and calculated fault currents is marginally reduced, when compared with the waveforms shown in Figure 107.

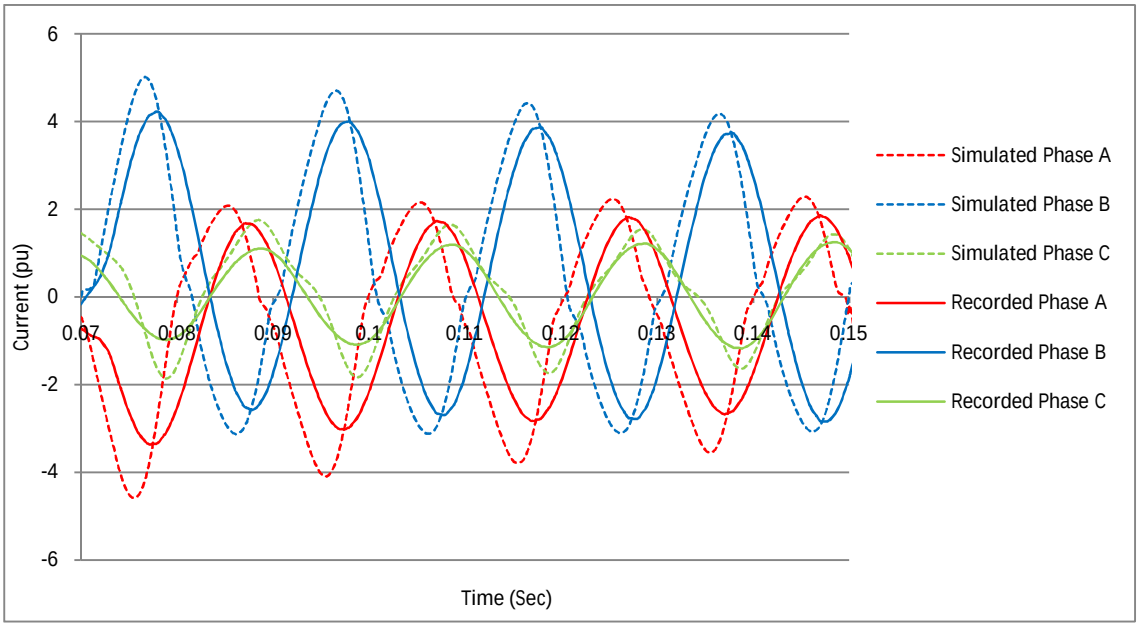

Figure 116 Current waveforms calculated from identified parameter values in comparison to recorded data

Having identified a set of parameter values that provide a low error value, the identification process is then focussed on the identification of excitation system model parameters. Table 13 shows results of the parameter identification process when the time period of the parameter identification is extended to include the phase to phase fault and the fault recovery.

Parameter	Original Value	4 Param	5 Param	6 Param
K_F	0.03	0.062	0.0731	0.0438
K_E	1	1.36	0.4248	1.11
T_E	0.8	0.71	0.7345	0.5762
K_{A1}	400	373.3	390.9	457.07
T_{F1}	1		0.8255	0.776
T_{A1}	0.02			0.0021

Table 13 Multistage parameter identification excitation system values

In order to ascertain the level of adherence of the newly developed parameter values during the fault recovery to that of the recorded terminal data, the synthetic response is compared against the recorded transient during the fault recovery period (Figure 117).

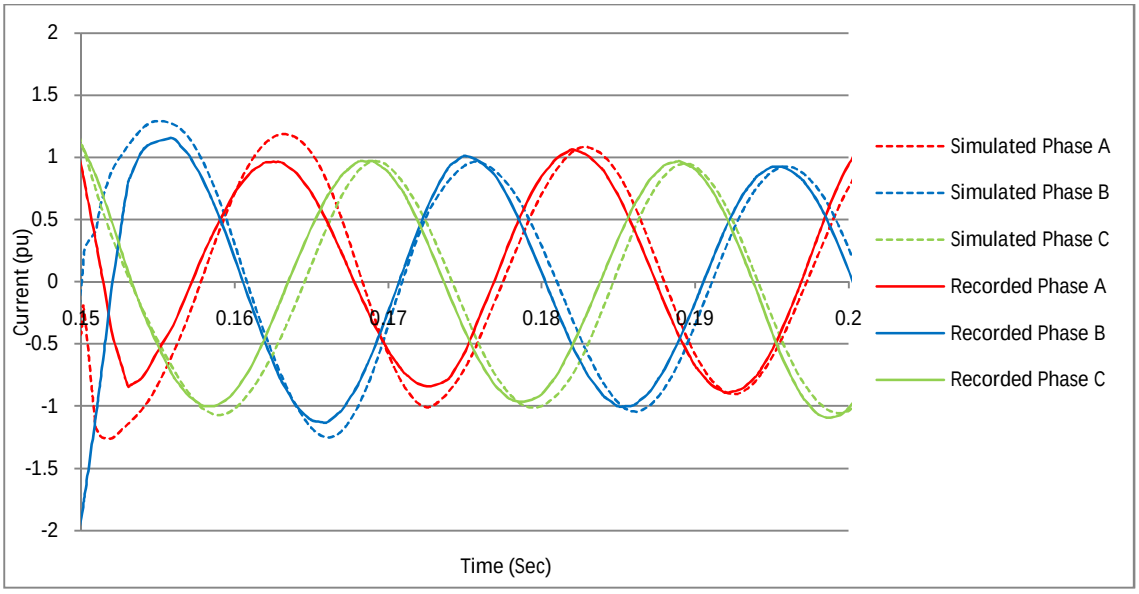

Figure 117 Multistage parameter waveform results against the recorded dataset of the fault recovery

Figure 117 shows good agreement between the synthetically created phase current waveform developed by the model and that of the recorded phase current waveform. This would suggest that the excitation system values the parameter identification method produced were valid for the fault recovery period of the recorded transient.

In combining the results of both stages of the parameter identification process the results seen in Figure 118 show that although the excitation system performance during fault recovery has been significantly improved (reducing the overall error from 0.021A to 0.007A) the revised excitation system characteristics have marginally altered the machine behaviour during the phase to phase fault period.

Considering the complete set of parameters developed using the multistage method in comparison to that of the other, more conventional method, it can be seen that in some respects the results are very similar. The machine parameters bear a fairly high similarity to those of the identified parameters seen in Table 8. This suggests that any difference in phase current output that is generated by the excitation system characteristic discrepancy only marginally affects the identification of the parameters in the conventional method. In considering the excitation system parameters developed by the multistage identification, it can be seen that the results are far more effective in driving the phase current output during recovery in a form similar to that of the tuned excitation system found on the real generator. This suggests that the result of the parameter identification of the excitation system values is more effective when considering machine parameter values that are more appropriate to the recorded transient data.

The multistage method is advantageous in many ways. Provided an appropriate transient event is used, the level of computational effort required to identify a large number of parameters is significantly reduced to that which would be required in order to achieve the same end by conventional means. The only significant issue with the method is that it is likely to be very transient dependent, in that, the method depends on:

1. Finding an appropriate multiple stage transient that displays characteristics that can be separated.
2. That the machine and exciter have minimal impact on the separate transient events.

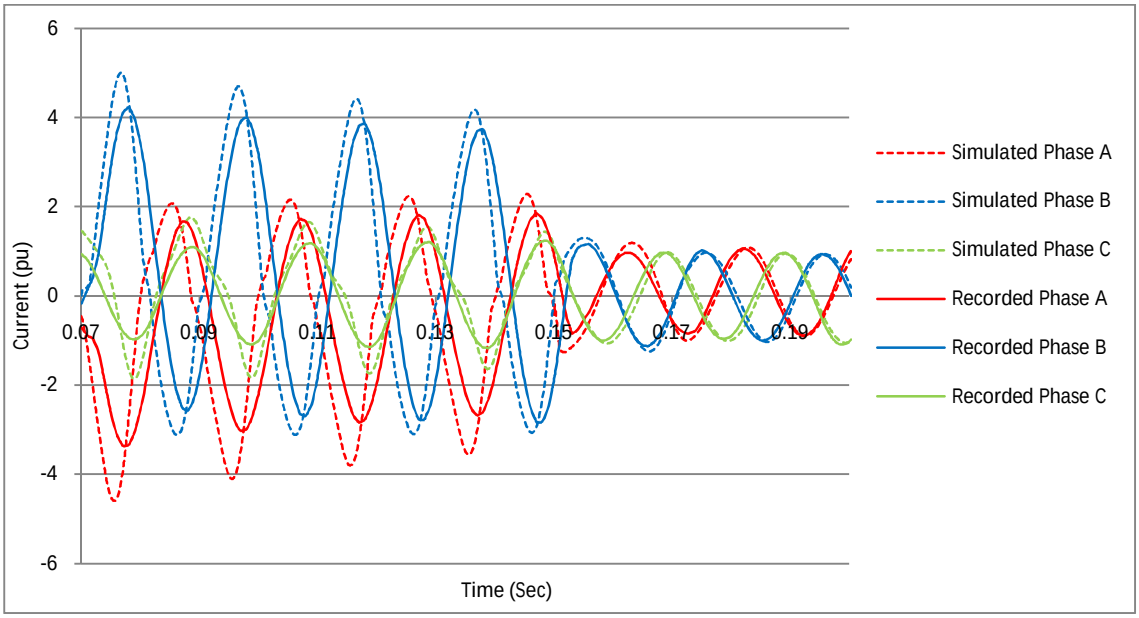

Figure 118 Multistage parameter waveform results against the recorded dataset of completer transient

Overall, the value of the multistage method has to be recognised as being as applicable as conventional parameter identification. The methodology is advantageous provided the correct circumstances present themselves, though if an appropriate transient is not available the multistage method becomes less useful.

11.5 Summary

The identification of parameters using recorded terminal data has allowed the use of some original methods and presented some unique results. The final identification methodology utilised was that of a multistage identification process. The multistage process allowed for the identification of a far larger number of parameters in a format that was more computationally efficient than the other forms available. It was seen that the results produced were very favourable when comparing the phase current waveforms of the identified parameters to that of the recorded transient. The only aspect that is of concern regarding this method is that, in

picking a transient for such a parameter identification method, care must be taken to use a transient that has minimal cross over in equipment influence in the transient stages. This crossover in parameter influence can undermine the results produced from the identification.

The results derived from all the forms of parameter identification seen in this chapter have been positive, all bearing a reasonable resemblance to what would be expected to be appropriate parameter values. In most cases, the machine parameter results derived have produced results that are comparable to that of the declared parameter value dataset. Particularly successful aspects of the work were the results gained from the parameter identification of excitation system parameters in the multistage identification. The results provided from this suggest that non invasive excitation system tuning could be possible provided the transient is appropriate.

12 Conclusions and Further Work

The question posed at the start of this work was whether it was possible to non invasively identify power plant parameters using recorded terminal data from a network. By building a complex generator model that encompasses excitation control and a turbine model, a method of comparing modelled phase current outputs was developed. Using a particle swarm optimisation algorithm it has been shown, first with synthetic datasets, then with real recorded network data, that parameter identification is possible for specific power plant parameters, some of which are not commonly identifiable with invasive techniques.

This thesis has proven that this method of identification is possible and in doing so provides a significant addition to learning. This is because the work identifies exciter, synchronous machine and turbine governor parameters at the same time. Much work has been done individually identifying their characteristics but never together, thus this is step forward in this area of research. Additionally the development of a multi stage identification process is equally original and has not been utilised in any form of parameter identification of this type.

The work that this thesis discusses has been utilised in real world applications, specifically the characterisation of gas turbines in dynamic power system studies.

12.1 Background

The accurate modelling of power station characteristics is highly challenging due to the nonlinear nature of the components involved in power generation. Conventional parameter identification is performed by manufacturers and carried out during commissioning of equipment. This form of identification is invasive in nature and can require onerous events to define parameters. An example of this is a three phase short circuit.

The work in this thesis investigates non invasive identification of power station parameters. Such methods would produce benefits like:

- No need for disconnection of equipment during identification, which would be costly.
- More accurate power system modelling which would facilitate better transient studies of power networks.
- The development of generic excitation models that could be used to accurately describe their transient response in the network.
- Less need to perform onerous testing on equipment, which could reduce power plant product lifetime.

In this work the turbine or prime mover associated with the power station is critical to driving the synchronous generator. The forms considered for this work were steam turbine and gas turbine prime movers. Either form assumes a speed of revolution between 1500 rpm and 3600rpm. The synchronous generator type considered in this work is of a two or four pole turbo generator topology. The voltage of the synchronous generator field winding is controlled during transient and steady state by the excitation system. The excitation system can take several forms depending on how the power plant is implemented. These varying forms are fundamentally different in topology and design.

12.2 Steam Turbines

A steam turbine system has many stages to efficiently generate sufficient steam for power generation. A furnace heats water to create steam. Additional heat and pressure is added in order to increase its enthalpy. This is limited by the power plant physical limitations. This high pressure steam is used to drive the steam turbine. Steam turbines take differing forms, the more likely types in heavy duty generation are single casing, tandem compound or cross compound. These define the shaft design that is coupled to the generator's rotor. The rate at which the steam drives the turbine is defined by the governor. The governor defines the dynamic behaviour of the turbine generator.

Significant work has been done in modelling of steam turbines. The most notable and useful is that of the IEEE working group on prime movers, who developed models for steam turbine and governors that are flexible depending on the station topology.

12.3 Gas Turbines

Gas turbines are the other main form of generation source this work considers. The gas turbine is considered to work in one of two basic formats: in open cycle, where the gas turbine operates alone, or combined cycle, where the waste energy from the gas turbine feeds a heat recovery steam generator in order to increase efficiency. Gas turbines can take several forms, mostly defined the shaft configuration which is designed based on the combustion required and the pressure necessary for it. Gas turbines have a more sophisticated control topology than simple steam turbines but essentially, the result is the same, with the governor defining the turbine rotor speed.

Modelling of gas turbines has been considered by other authors in detail with highly sophisticated models. Parameter estimation has been performed on such turbine types but has used far more detailed input data to define characteristics than would be available for this

work. Ultimately the models available are highly detailed but it is not realistic to use such model types for non invasive identification of this variety.

12.4 Synchronous Generators

Synchronous machine modelling has been a topic of research for many decades, the most appropriate form for this work is that developed in the dq reference frame. The level of data that is available for parameter identification renders the possibility of modelling accurately in saturation unlikely. Invasive techniques such as a three phase short circuit are instigated by the manufacturer in order to ascertain generator operating characteristics. Some less invasive techniques have been observed (54) but the consideration has been solely with regard to the synchronous machine.

12.5 Excitation Systems

Excitation control systems for synchronous generators take one of three core forms: DC excitation, AC pilot excitation or ST static excitation. From a modelling point of view, the AC and the DC excitation systems possess similar operating characteristics and speeds of response. The static excitation system, which does not utilise an additional electrical machine to feed the rotor directly, is faster in some respects. The IEEE standard models (57) provide an industrially accepted set of excitation system types, with the AC5A and the DC1A being considered particularly good at modelling a multitude of differing forms of excitation system types.

12.6 Search Algorithms

Of the varying forms of search algorithms commonly used, each has differing behavioural traits that make some more suitable than others for parameter identification of this type. Gradient descent has an inability to escape from local minima which undermines its usefulness. Steady State Evolution, Differential Evolution and Generational Evolutionary algorithms, although efficient when considering more basic functions, would become computationally inefficient given the application. Bacterial Chemotaxis, although advantageous in some respects, could not be appropriately applied because repellents are unknown for the application. Ant colony optimisation requires a high computational effort in searching, and then requires additional repetition to confirm an optimal solution. Of the methods considered, PSO is the most appropriate for this form of identification.

Particle swarm optimisation balances the computational cost of the optimisation with a comprehensive search that can escape local minima as necessary.

12.7 Implementation of the Parameter Identification Process

A classical machine model was implemented using the AC5A excitation system. Given the fundamental dichotomy in developing sophisticated steam and gas turbine models, a realistic model was developed that allows for appropriate characterisation of the prime mover for both gas and steam turbine alike. The model includes a speed governor to define rotor dynamic response. The complete model was validated against the synthetic response of a unit with the same operational specification simulated in DigSilent power system software. A PSO algorithm was implemented with further investigation into confinement methods, distribution and constriction to be performed.

12.8 Results and Discussion: Parameter Influence

Assessing parameter's influence on the objective function allowed for an understanding as to which parameters had the capacity to be identified. The direct axis parameters were more influential than the quadrature equivalent in many respects. Transient quadrature reactance exerts no influence on the model and thus cannot be identified. Some parameters like leakage reactance were seen to exert characteristics that made them challenging for optimisation and thus identification. Governor characteristics were seen to not exert sufficient influence for a successful identification for the transients utilised.

Ultimately a group of parameters were derived that exerted sufficient influence on phase current output error (the objective function) to be considered suitable for parameter identification. A group of parameters were derived that exerted some influence on the objective function (possible identification). A group of parameters that exerted sufficient influence if the transient was appropriate (perturbation dependent) were also identified. This showed that the form of transient used for the identification has an impact on the ability of the method to identify certain parameters.

12.9 Results and Discussion: Parameter Identification Using PSO

Having identified the parameters that are susceptible to optimisation, the identification was performed, developing values for differing quantities of parameters. As the variable number was increased, the computational cost of reaching a suitable convergence is also increased. Using different perturbation types is seen to alter the magnitude of objective function minima that is achievable in the identification. It is seen that as the number of parameters to be identified is increased, the global minima value range is also increased suggesting a trade off in parameter number against accuracy of result.

The results attained from the parameter identification using synthetic data are seen to be very positive against the synthetic parameter values. The results from the identification of the excitation system parameters were particularly positive as they are not a commonly identifiable set of parameters.

Testing of the algorithm shows that the use of a constricted PSO algorithm is better for this application than the standard unconstrained version. Interval confinement and a random initial distribution were seen to the most practical approach for this application.

12.10 Results and Discussion: Parameter Identification Using Recorded Terminal Data

The transient used in the parameter identification is from a combine cycle gas turbine plant, recorded from the terminals of a 178MVA steam turbine generator. The transient itself (a phase to phase fault followed by fault clearance) meant that the influence of the perturbation dependent parameters was sufficient for them to be considered identifiable. The transient also allowed for more than one identification methodology to be used other than the conventional method. Conventional identification showed that identification of larger parameter numbers was possible with the recorded transient dataset. This was because the onerous nature of the transient reduced the range of values the global minima could occupy.

A multistage identification was also performed. This allowed all identifiable parameters to be identified and maintained the accuracy of the identified values by reducing the risk of increased minima value range. The results were comparable with the manufacturers declared values. In some cases the identified parameters created a better resemblance to the recorded waveform than a simulated waveform created by the declared values. This suggests the tolerance of the manufacturer declared results may be considerable.

The results derived by the secondary transient show that identification of excitation system parameters is also possible from such recorded transient datasets.

12.11 Further Work and Recommendations

The culmination of this work has been the successful parameter identification of power station generator parameters using recorded transient network data. Whilst there is some discrepancy in identified parameter values, testing has verified the methods performance and validity.

The work described in this thesis is an addition to the area of parameter identification. Recommendations for further work are of the form:

- Identification of saturated parameters during recorded transients.

Identification of saturated machine parameters has been a topic of interest for synchronous machine designers for many years. It would be interesting to observe if using this form of method and more elaborate datasets could deliver appropriate saturation characteristics for large generators

- The tuning of excitation systems from recorded transient data sets.

Excitation tuning is performed in order to provide an optimal machine response for a generator in a network. It would be insightful to understand if a modification of this method could be adopted to optimise tuning settings without the need of human interaction.

- Understanding the limitations of parameter influence under small signal perturbations.

It has been seen in this work that different perturbations have fluctuating influence on parameter characteristics. It would be insightful to investigate this further in order to establish a more precise understanding of the impact of small signal perturbations on the magnitude of parameter influence.

- The implications of multi-machine interaction to parameter identification of synchronous machines.

Invariably large power stations have many turbine generators connected to a common busbar arrangement. It would be interesting to understand the impact the surrounding generators have on the parameter identification of a single generator during a transient event.

- The identification of more elaborate turbine models using recorded data in the dynamic time domain.

This work has considered a pragmatic turbine model in order to perform power system studies. It would be insightful to understand if parameter identification of a more detailed specific turbine could be performed give the input types that have been adopted in this work.

13. Bibliography

1. *British Electricity International, Modern Power Station Practice, 3d ed.* Oxford, UK : Pergamon Press, 1991.

2. Kiameh, P. *Power Generation Handbook: Selection, Application, Operation, Maintenance.* s.l. : McGraw Hill, 2002.

3. *Dynamic Modelling of Power Plant Turbines for Controller Design.* Ray, A. April 1980, Appl. Math. Modelling, Vol. 4, pp. 109-112.

4. *The Flexibility of the Supercritical Boiler as a Partner in Power System Design and Operation.* F. Läubli, F.H. Fenton. NY : s.n., 1971. IEEE Winter power meeting. pp. pp1725-1733.

5. *Boiler Models for Dynamic Performance Studies.* Mello, F.P. 1, Feb 1991, IEEE Trans on Power Systems, Vol. 6, pp. 66-74.

6. *Modelling and State Estimation of Power Plant Steam Turbines.* K.L. Lo, P.L. Zeng, E. Marchand, A. Pinkerton. 2, march 1990, IEE Proceedings, Vol. 137, pp. 80-94.

7. *A Nonlinear Steam Turbine model for Simulation and State Monitoring.* A. Chaibakhsh, A. Ghaffari. Malaysia : s.n., 2008. Proceedings of IASTED international Conf (Asia PES 2008). pp. 347-352.

8. *Dynamic Models for Steam and Hydro Turbines in Power System Studies.* Report, IEEE Committee. 6, 1973, IEEE Trans in Power Apparatus and Systems, Vol. 92, pp. pp1904-1915.

9. *Dynamic models for Fossil Fuelled Steam Units in Power System Studies.* Performance, Working Group on Prime Mover and Energy Supply Models for System Dynamic. 2, May 1991, IEEE Trans on Power Systems, Vol. 6, pp. 753-761.

10. Kundur, Prabha. *Power System Stability and Control.* s.l. : McGraw-Hill, 1994.

11. *Modelling of Gas Turbines and Steam Turbines in Combined Cycle Power Plants.* Taskforce 25, advisory group 2 of study committee 38 (C4.02.25). Paris : s.n., April 2003, Conférence Internationale des Grand Réseaux Électriques a Haute Tension (CIGRE).

12. *Dynamic Models for Combined Cycle Plants in Power System Studies Vol. 9, No. 3 1994, pp1698-1708.* Studies, Working Group on Prime mover and energy Supply Models for System Dynamic Performance. 3, 1994, IEEE Trans on Power Systems, Vol. 9, pp. 1698-1708.

13. *Experimental Verification of a Digital Computer Simulation Method for Predicting Gas Turbine dynamic Behaviours.* A. J. Fawke, H. I. H. Savanamuttoo, M. Holmes. 27, 1972, Proceedings of the Institution of Mechanical Engineers, Vol. 186, pp. 323-329.

14. *Modeling, Numerical Optimisation and Irreversibility Reduction of a Triple Pressure Reheat Combined Cycle.* Bassily, A. M. 2007, Proceeding of Energy, Vol. 32, pp. 778-794.

15. *Dynamic Simulation of Gas turbine Unit.* Hung, W. W. 4, July 1991, IEE Proceedings, Vol. 138, pp. 342-350.

16. *A Governor/Turbine Model for a Twin Shaft Combustion Turbine.* L. N. Hannett, G. Jee, F. Fardanesh. 1, Feb 1995, IEEE Transactions on Power Systems, Vol. 10, pp. 133-140.

17. *Combustion Turbine Dynamic Model Validation from Tests.* L. N. Hannett, A. Khan. 1, Feb 1993, IEEE Trans on Power Systems, Vol. 8, pp. 152-158.

18. *Modelling Combined Cycle Power Plant for Simulation of Frequency Excursions.* K. Kunitomi, A. Kurita, Y. Tada, S. Ihara, W. Price, L. M. Richardson, G. Smith. 2, May 2003, IEEE Trans on Power Systems, Vol. 18, pp. 724-729.

19. *Experiences in Modelling the Performance of Generating Plant for Frequency Response Studies on the British National Grid.* R. Pearmine, Y. H. Song, A. Chebbo. 2007, Electric Power Systems Research, Vol. 77, pp. 1575-1584.

20. *The dependence of Gas Turbine Power Output on System Frequency and Ambient Conditions.* Poubeik, P. Paris : s.n., 2002. International Conference on Large High Voltage Electric Systems, Conférence Internationale des Grand Réseaux Électriques a Haute Tension (CIGRE). pp. 38 - 101.

21. *Experience with Testing and Modelling of Gas Turbines.* M. Nagpal, A. Moshref, G. K. Morison, P. Kundur. 2001. IEEE Power Engineering Society Winter Meeting. Vol. 2, pp. 652-656.

22. *Dynamic Modelling of a Combined Cycle Plant for Power System Stability Studies.* Q. Zhang, P. L. So. IEEE Power Engineering Society Winter Meeting 2000. Vol. 2, pp. 1538-1543.

23. *The Salient Pole Synchronous Machine.* Blondel, A. 1904, Trans Int'l Elec Congress, p. 634.

24. *Two Reaction Theory of Synchronous Machines Part 1.* Park, R.H. 1929, AIEE Trans, p. 716.

25. *Two Reaction Theory of Synchronous Machines Part II.* Park, R. H. 1933, AIEE transactions, Vol. 52, p. 352.

26. *A New Model of Saturated Synchronous Machines for Power System Transient Stability Simulations.* J. Tamura, I. Takeda. 2, 1995 , IEEE Transactions on Energy Conversion, Vol. 10, pp. 218-224.

27. IEEE Guide For Synchronous Generator Modelling Practices and Applications in Power System Stability Analyses. *IEEE Std 1110 – 2002.*

28. Kimbark, Edward. *Power System Stability:Synchronous machines.* s.l. : Dover Publications, 1956. p. 40.

29. A. E. Fitzgerald, C. Kingsley Jr, S. D. Umans. *Electric Machinery - 6th edition.* s.l. : McGraw Hill. series in Electrical Engineering Power and Energy.

30. *Experimental Study of Saturation and Cross-Magnetizing Phenomenon in Saturated Synchronous Machines.* A.M. El-Serafi, A. S. Abdallah, M. K. El-Sherbiny, E. H. Badawy. 4, 1988, IEEE Transactions on Energy Conversion, Vol. 3, pp. 815-823.

31. *A Phase Domain Synchronous Generator Model Including Saturation Effects.* J. R. Marti, K. W. Louie. 1, 1997, IEEE Transactions on Power Systems, Vol. 12, pp. 222-229.

32. *Direct and Quadrature Axis Equivalent Circuits for Solid Rotor Turbine Generators.* W. B. Jackson, R. L. Winchester. 7, 1969, IEEE Transactions on Power Apparatus and Systems, Vols. PAS-88, pp. 1121-1136.

33. *On Turbine-Generator Rotor Equivalent Circuits.* Kirtley, J. L. 1, 1994, IEEE Transactions on Power Systems, Vol. 9, pp. 262-271.

34. *Validation of Turbo Generator Stability Models by Comparisons with Power System Tests.* P. L. Dandeno, P. Kundur, A. T. Poray, M. E. Coultes. 4, 1981, IEEE Transactions on Power Apparatus and Systems, Vols. PAS-100, pp. 1637-1645.

35. *Causes of Discrepancies on Calculation of Rotor Quantities and Exact Equivalent Diagrams of the Synchronous Machine.* Canay, I.M. 7, July 1969, IEEE Trans on Power Apparatus and Systems, Vols. PAS-88, pp. 1114-1120.

36. *Modelling of Solid Rotor Turbo Generators Part 1: Theory and Techniques.* S. D. Umans, J. A. Mallick, G. L. Wilson. 1, 1978, IEEE Transactions on Power Apparatus and Systems, Vols. PAS-97, pp. 269-277.

37. *An analysis of the Results from the Computation of Transients in Synchronous Generators using Frequency Domain Methods.* A. G. Jack, T. J. Bedford. 2, 1988, IEEE Transactions on Energy Conversion, Vol. 3, pp. 375-383.

38. *Recent Trends and Progress in Synchronous Machine Modelling in the Electric Utility Industry.* P. L. Dandeno, P. Kundur, R. P. Schultz. 7, 1974, Proceedings of the IEEE, Vol. 62, pp. 941-950.

39. *Static Exciter Stabilising Signals on Large Generators – Mechanical Problems.* W. Watson, M. E. Coultes. 1973, IEEE Transactions on Power Apparatus and Systems, Vols. PAS-92, pp. 204-211.

40. *Dynamic Models of Turbine Generators Derived from Solid Rotor Equivalent Circuits.* R. P. Schultz, W. D. Jones, D. N. Ewart. 926-933, IEEE Transactions on Power Apparatus and Systems, Vols. PAS-92, pp. 926-933.

41. *Effects of Synchronous Machine Modelling in Large Scale System Studies.* P. L. Dandeno, R. L. Hauth, R. P. Schultz. 1973, IEEE Transactions on Power Apparatus and Systems, Vols. PAS-92, pp. 574-582.

42. *Online Estimation of Synchronous Generator Parameters using PRBS Perturbations.* H.J. Vermeulen, J.M. Strauss, V. Shkoana,. 3, Aug 2002, IEEE Trans on Power Systems, Vol. 17, pp. 694-700.

43. *Identification of Armature, field and Saturated Parameters of a Large Steam Turbine Generato.* A.B. Karayaka, A. Keyhani, B.L. Agrawal, D.A. Selin, G.T. Heydt. 2, June 2000, IEEE Trans on Energy Conversion, Vol. 15, pp. 181-187.

44. *Neural Network Synchronous Machine Modelling.* M. Chow, R.J. Thomas. 1989, IEEE International Symposium on Circuits and Systems, Vol. 1, pp. 495-498.

45. *Nonlinear systems parameter estimation using neural networks: Application to synchronous machines.* T.A.-Ali, G. Kenné and F.L.-Lagarrigue. 4, August 2007, Mathematical and computer modelling of Dynamical Systems, Vol. 13, pp. 365-382.

46. *"Neural Network Based Modelling of Round Rotor Synchronous Generator Rotor Body Parameters from Operating Data.* S. Pillutla, A. Keyhan. 3, Vol.14 No.3 : s.n., Sept 1999, IEEE Trans on Energy Conversion, Vol. 14, pp. 321-327.

47. *Neural Network Based Saturation Model for Round Rotor Synchronous Generator.* S. Pillutla, A. Keyhan. 4, Dec 1999, IEEE Trans on Energy Conversion, Vol. 14, pp. 1019-1025.

48. *Neural Network Based Modelling of a Large Steam Turbine-Generator Rotor Body Parameters From On-Line Disturbance Data.* A.B. Karayaka, A. Keyhani, G.T. Heydt, B.L. Agrawal, D.A. Selin. 4, March 2001, IEEE Trans on Energy Conversion, Vol. 16, pp. 305-311.

49. *Synchronous Generator Model Identification and Parameter Estimation From Operating Data.* A.B. Karayaka, A. Keyhani, G.T. Heydt, B.L. Agrawal. D.A. Selin. 1, March 2003, IEEE Trans on Energy Conversion, Vol. 18, pp. 121-126.

50. *Iteratively Re-weighted Least Squares for Maximum Likelihood Identification of Synchronous Machine Parameters from On-line Tests.* R. Wamkeue, I. Kamwa, X.D. –Do, A. Keyhan. 2, June 1999, IEEE Trans on Energy Conversion, Vol. 14, pp. 159-166.

51. *On-line Synchronous Machine Parameter Estimation from Small Disturbance Operating Data.* H. Tsai, A. Keyhani, J. Demko, R.G. Farmer. 1, March 1995, IEEE Trans on Energy Conversion, Vol. 10, pp. 25-36.

52. *Maximum likelihood estimation of generator stability constants using SSFR test data.* A. Keyhani, S. Hao, R.P. Schulz. 1, IEEE Trans on Energy Conversion, Vol. 6, pp. 140-154.

53. *Saturation functions for synchronous generator from finite elements.* S.H. Minnich, R.P Schulz, D.H. Baker, R.G. Farmer, D.K. Sharma, J.H. Fish. 4, Dec 1987, IEEE Trans on Energy Conversion, Vols. EC-2, pp. 680-692.

54. *A Dynamic On-Line Parameter Identification and Full-Scale System Experimental Verification for Large Synchronous Machines.* Z. Zhoa, F. Zheng, J. Gao, L. Xu. 3, Sept 1995, IEEE Trans on Energy Conversion, Vol. 10, pp. 392-398.

55. *Permanent Magnet Synchronous Motor Parameter identification using Particle Swarm Optimization.* L. Liu, W. Liu, D.A. Carte. 2, 2008, Int'l Journal on Computational Intelligence Research, Vol. 4, pp. 211-218.

56. *A particle swarm digital identification of synchronous machine parameters from short circuit tests.* K. M. El-Naggar, A. K. Al-Othman, J.S. Al-Sumait. August 2006, Proc IASTED Int'l Conf on artificial intelligence and soft computing.

57. IEEE. *IEEE Recommended Practice for Excitation System Models for Power System Stability Studies.* s.l. : IEEE, 2006. 421.5.

58. Kiameh, P. *Power Generation Handbook: Selection, Applications, Operation, and Maintenance.* s.l. : McGraw Hill, 2002.

59. *Identification of Brushless Excitation System Model Parameters at Different Conditions via Field Tests.* M. Rasouli, M. KarrarI. Sevilla : s.n., 2002. 14th PSCC.

60. *A High Initial Response Brushless Excitation System.* T. L. Dillman, J. W. Skooglund, F. W. Keay, W. H. South and C. Raczkwowsk. 1971, IEEE Transactions on Power Apparatus and Systems, Vols. PAS-90, pp. 2089-2094.

61. *Experience with ALTERREX Excitation for Large Turbine Generators.* J. S. Bishop, D. H. Miller and A. C. Shartrand. 1974. IEEE/ASME Power Conference.

62. *Generator and Power System Performance with the GENERREX Excitation System.* P. H. Beagles, K. Carlson, M. L. Crenshaw and M. Temoshok. 1976, IEEE Transactions on Power Apparatus and Systems, Vols. PAS-95, pp. 489-493.

63. Ong, Chee-Mun. *Dynamic Simulation of Electrical Machinery Using Matlab/Simulink.* s.l. : Prentice Hall, 1998.

64. *Concepts of Synchronous Machine Stability as Affected by Excitation Control.* C.Concordia, F. P. Demello and. 1969, IEEE Transactions on Power Apparatus and Systems, Vols. PAS-88, pp. 316-329.

65. *Genetic Algorithm-Based Parameter Identification of a Hysteretic Brushless Exciter Model2006 pp 148-154.* D. C. Aliprantis, S. D. Sudhoff, B. T. Kuhn. 1, 2006, IEEE Transactions on Energy Conversion, Vol. 21, pp. 148-154.

66. *Identification of Excitation System Models Based on On-line Digital Measurements.* J. Wang, H. Chang, Y. Chen, C. Chang, C. Huang. 3, 1995, IEEE Transactions on Power Systems, Vol. 10, pp. 1286-1293.

67. *Nonlinear Parameter Estimation of Excitation Systems.* R. Bhaskar, M. L. Crow, E. Ludwig, K. T. Erickson and K. S. Shah. 4, 2000, IEEE Transactions on Power Systems, Vol. 15, pp. 1225-1231.

68. Goldberg, D. E. *Genetic Algorithms in search optimization and machine learning.* Reading, MA : Addison-Wesley, 1989.

69. Holland, J. H. *Adaption in natural and artificial systems.* Ann Arbor, MI : University of Michigan Press, 1975.

70. *Differential evolution-a simple evolution strategy for fast optimization.* K. V. Price, R. Storn. 4, 1997, Dr Dobbs Journal, Vol. 22, pp. 18-24.

71. *Particle swarm optimization.* Eberhart, J. Kennedy and R. 1995. Proc IEEE Int'l conference on neural networks. Vol. 4, pp. 1942-1948.

72. J. Kennedy, R. Eberhart, Y. Shi. *Swarm Intelligence.* San Francisco : Kauffman Publishers, 2001.

73. *Ant colony algorithms for system swarms.* V. S. Hernandez, A. Weitzenfeld. 2006. IEEE LAR's 06. pp. 74-79.

74. *Model-based search for combinational optimisation:A critical survey.* M.Zlochin, M. Birattari, N. Meuleau, M. Dorigo. 2004, Annals of Opreations Research, Vol. 131, pp. 373-395.

75. *Optimization based on bacterial chemotaxis.* S. D. Miller, J. Marchetto, S. Airagni, P. Kournoutsakos. 1, Feb 2002, IEEE Trans on evolutionary computation, Vol. 6, pp. 16-29.

76. *An improved particle swarm optimization based on bacterial chemotaxis.* B. Niu, Z. Yunlong, H. Xiaoxian, Z. Xiangping. 2006. WCICA 2006. Vol. 1, pp. 3193-3197.

77. *Optimization by simulated annealing.* S. Kirkpatrick, C. D. Gelatt, M. P. Vechi. 1983, Science, Vol. 220, pp. 671-680.

78. *An electromagnetism-like mechanism for global optimization.* S. Birbil, S. C. Fang. 3, 2003, Journal of Global Optimization, Vol. 25, pp. 263-282.

79. *A new algorithm for stochastic optimization.* Andradottir, S. 1990. simulation conference. pp. 364-366.

80. *A Connectionist machine for machine climbing.* Ackley, D. H. Boston : Kluwer Academic Publishers, 1987.

81. *Identification of induction motor using a genetic algorithm and quazi-Newton algorithm.* H. Razik, C. Defranoux, A Rezzoug. 2000. Power electronics congress, CIEP 2000, VII IEEE international. pp. 65-70.

82. *No free lunch theorems for optimization.* D. H. Wolpert, W.G. Macready. 1997, IEEE Trans on evolutionary computation, Vol. 1, pp. 67-82.

83. *Sychronous Machine Parameter Identification using Particle Swarm Optimization.* G. Hutchison, B. Zahawi, D. Giaouris, K. Harmer, B. Stedall. Brighton : IEEE, 2010. IET International Conference on Power Electronics, Machines and Drives.

84. *Parameter Estimation of Synchronous Machines using Particle Swarm Optimisation.* G. Hutchison, B. Zahawi, D. Giaouris, K. Harmer, B. Stedall. Singapore : IEEE, 2010. IEEE International Conference on Probablistic Methods Applied to Power Systems.

85. *IEEE 421.5.* Report, IEEE Comittee. 2007, IEEE Recommended Practice for Excitation System Models for Power System Stability Studies.

86. Clerc, Maurice. *Particle Swarm Optimization.* London : ISTE Ltd, 2006.

87. *Effect of Rounding errors on Variable Metric Method.* Rosenbrock, H.H. 1, s.l. : Plenum Press, 1960, The Computer Journal, Vol. 3, pp. 175-184.

88. *A particle swarm optimization approach to nonlinear resource allocation problem.* J.Wang, P. Yin and. 2006, Applied Mathematics and Computation, Vol. 183, pp. 232-242.

89. *Determination of Synchronous machine Constants by Test.* Wright, S. Dec 1931, Trans of A.I.E.E, pp. 1331-1351.

90. *On-Line Synchronous Machine Parameter Estimation from Small Signal Disturbance Operating Data.* H. Tsai, A. Keyhani, J. Demko, R. G. Farmer. 1, March 1995, IEEE Trans on Energy Conversion, Vol. 10, pp. 25-36.

91. *A Study of Frequency Response of Turbo generators with Special Reference to Nanticoke GS.* T. J. Bedford, A. G. Jack. 3, 1987, IEEE Trans on Energy Conversion, Vol. 2, pp. 496-505.

92. *Effect of Oscillatory Torque on the Movement of Generator Rotors.* Shackshaft, G. 10, 1970, Proceedings of the IEE, Vol. 117, pp. 1969-1979.

93. Spall, J.C. *introduction to stochastic search and optimization.* s.l. : Wiley, 2003.

94. *Particle Swarm Optimization.* Shi, Y. Feb 2004, electronic data systems, IEEE Neural networks society.

95. *Equation of state calculations by fast computing machines.* N. Metropolis, A. Rosenbluth, M. Rosenbluth, A. Teller, E. Teller. 1953, Journal of chemical physics, Vol. 21, pp. 1087-1092.

96. *Mosquito Attack Optimization.* S. K. Bandyopadhyay, D. Bhattacharyya, P. Das. August 2006, Ubiquity, Vol. 7.

97. *A comparative study of stochastic optimization methods in motor design.* T.Tusar, P. Korosec, G. Papa, B. Filipic, J. Silc. 2007, Appl Intel, Vol. 27, pp. 101-111.

Appendix 1

Parameter Identification Techniques

An Unsaturated Value of Synchronous Reactance

By considering the open circuit characteristics and short circuit characteristics of the synchronous machine as previously seen, it is possible to derive an unsaturated value of synchronous reactance.

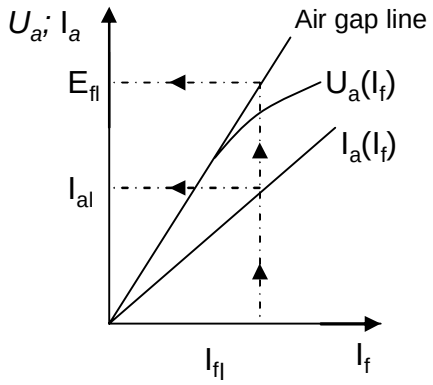

Figure 119 open and short circuit characteristics of a synchronous machine

For the excitation current I_{fl}, the short circuit armature current takes the value I_{al}. The excitation voltage corresponding to I_{fl} and E_{fl} is taken from the air gap line. U_a is terminal voltage. I_f and I_a are field current and stator current respectively. E_{fl} is the voltage behind unsaturated synchronous reactance. I_{fl} is the base field current required to achieve 1pu terminal voltage. Since the saturated value of synchronous reactance is determined, then ignoring armature resistance, synchronous reactance is characterised as:

$$X_s = \frac{E_{fl}}{I_{al}} \tag{68}$$

This can be seen to be the quotient of open circuit terminal voltage and short circuit armature current at a convenient value of I_f.

Identification through a Three Phase Symmetrical Short on the Armature

A three phase short circuit test is a frequently used technique used to evaluate parameters. The stator windings of an unloaded synchronous machine, running at synchronous speed are shorted simultaneously. Readings are taken from the stator and field winding's to find

reactance's and time constants of the machine. It is assumed that prior to the short, the synchronous generator is running at synchronous speed with no load. After the short circuit it is assumed to be running at synchronous speed. Ordinarily due to the short and the machines unloaded nature, it would be expected that the only currents flowing would be that of the field, this however is not the case. Because of the short circuit, the stator currents flow to maintain the flux linkage quantities that were found previous to the short. Based on the short circuit waveforms the graph is extrapolated.

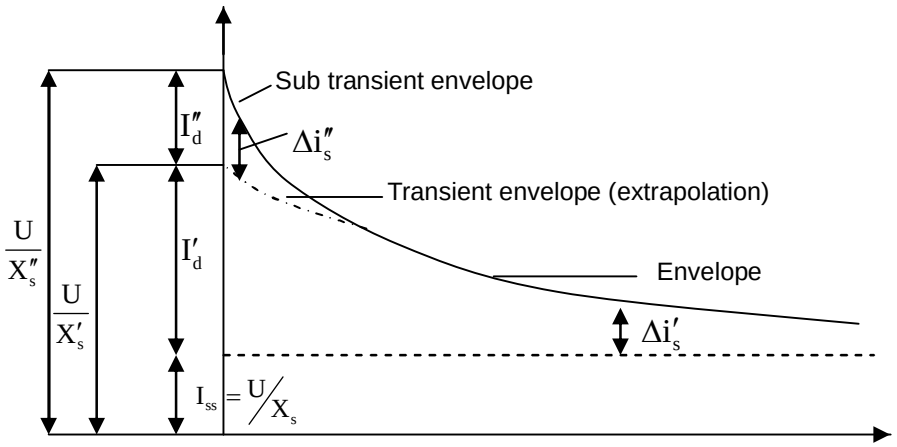

Figure 120 envelope of short circuit current

Based on what is seen above i_s is considered:

$$i_s = I_{ss} + \Delta i'_s + \Delta i''_s = I_{ss} + I'_d e^{-t/T'_d} + I''_d e^{-t/T''_d} \quad (69)$$

$$= I_{ss} + (U/X'_d - U/X_s)e^{-t/T'_d} + (U/X''_d - U/X'_d)e^{-t/T''_d} \quad (70)$$

Where T'_d is the d axis transient time constant and T''_d is the d axis sub transient time constant.

Appendix 2

Supporting Equations

Power Derivation

$$P_{in} = V_a I_a + V_b I_b + V_c I_c + V_f I_f + V_g I_g \tag{71}$$

when stator phase quantities transformed to dq and $\omega_r = \frac{d\theta_r}{dt}$

$$P_{in} = \frac{3}{2}(V_q I_q + V_d I_d + 3V_0 I_0 + V_f I_f + V_g I_g) \tag{72}$$

$$P_{in} = \frac{3}{2}\left\{r_s\left(I_q^2 + I_d^2\right) + I_q \frac{d\lambda_q}{dt} + I_d \frac{d\lambda_d}{dt} + \omega_r(\lambda_d I_q - \lambda_q I_d)\right\} + 3I_0^2 R_0 + 3I_0 \frac{d\lambda_0}{dt} + 3I_f^2 R_f + 3I_f \frac{d\lambda_f}{dt} + 3I_g^2 R_g + 3I_g \frac{d\lambda_g}{dt} \tag{73}$$

Ignoring ohmic losses and rate of change of magnetic energy

$$P_e = \frac{3}{2}\omega_r(\lambda_d I_q - \lambda_q I_d) \tag{74}$$

Torque Expression

Electromagnetic torque is torque developed by machine across the air gap from power

dq Voltage Conversion

The winding equations that we have developed can now be developed into a synchronous machine model that uses voltages as an input and current as an output. the main input of the method is phase voltage. the phase voltages are transformed into the dq reference frame attached to the rotor.

$$v_q = \frac{2}{3}\left\{v_a \cos\theta_r(t) + v_b \cos(\theta_r(t) - \frac{2}{3}\pi) + v_s \cos(\theta_r(t) - \frac{4}{3}\pi)\right\} \tag{75}$$

$$v_d = \frac{2}{3}\left\{v_a \sin\theta_r(t) + v_b \sin(\theta_r(t) - \frac{2}{3}\pi) + v_s \sin(\theta_r(t) - \frac{4}{3}\pi)\right\} \tag{76}$$

$$v_0 = \frac{1}{3}(v_a + v_b + v_c) \tag{77}$$

Then by expressing the voltage equations as integrals of flux linkage, the above stator dq voltages, with other inputs can be used can then be used to solve the flux linkage in the windings

$$\psi_{mq} = X_{MQ}\left(\frac{\psi_q}{X_{ls}} + \frac{\psi'_{kq}}{X'_{lkq}}\right) \tag{78}$$

$$\psi_{md} = X_{MD}\left(\frac{\psi_d}{X_{ls}} + \frac{\psi'_{kd}}{X'_{lkd}} + \frac{\psi'_f}{X'_{lf}}\right) \tag{79}$$

where:

$$\frac{1}{X_{MQ}} = \frac{1}{X_{mq}} + \frac{1}{X'_{lkq}} + \frac{1}{X_{ls}} \tag{80}$$

$$\frac{1}{X_{MD}} = \frac{1}{X_{md}} + \frac{1}{X'_{lkd}} + \frac{1}{X'_{lf}} + \frac{1}{X_{ls}} \tag{81}$$

having the flux linkage values of the windings and those of mutual flux linkages along the d and q axes, the currents are derived as:

$$i_q = \frac{\psi_q - \psi_{mq}}{X_{ls}} \tag{82}$$

$$i_d = \frac{\psi_d - \psi_{md}}{X_{ls}} \tag{83}$$

$$i'_{kd} = \frac{\psi'_{kd} - \psi_{md}}{X'_{lkd}} \tag{84}$$

$$i'_{kq} = \frac{\psi'_{kq} - \psi_{mq}}{X'_{lkq}} \tag{85}$$

$$i'_f = \frac{\psi'_f - \psi_{md}}{X'_{lf}} \tag{86}$$

the stator currents are then transferred using the rotor to stationary dq0 equations, then the dq0 to phase current transformations.

Equations of motion for the Rotor Assembly

Given the motoring convention, the net accelerating torque , $T_{em}+T_{mech}-T_{damp}$, is in the direction of the rotors rotation. Here T_{em}, the torque developed by the machine is positive is positive when motoring and negative when generating. T_{mech} is externally applied mechanical torque supplied by the turbine in the direction of rotation. T_{damp} is the frictional torque acting against rotor rotation.

Equating net acceleration to inertial torque:

$$T_{em} + T_{mech} - T_{damp} = J\frac{d\omega_{rm}(t)}{dt} = \frac{2J}{p}\frac{d\omega_r}{dt} \quad (87)$$

The rotor angle δ is defined as the angle of the q_r axes of the rotor with respect to the q_e axis of the rotating reference frame

$$\delta(t) = \theta_r(t) - \theta_e(t) \quad (88)$$

$$\int_0^t \frac{(\omega_r(t) - \omega_e)}{dt} + \theta_r(0) - \theta_e(0) \quad (89)$$

given a constant ω_e

$$\frac{d(\omega_r(t) - \omega_e)}{dt} = \frac{d\omega_r(t)}{dt} \quad (90)$$

from replacing the equations above and replacing terms we then get

$$\omega_r(t) - \omega_e = \frac{2J}{p}\int_0^t (T_{em} + T_{mech} - T_{damp})\ dt \quad (91)$$

Where ω_r is linked to θ_r and ω_{re} is linked to θ_e are the respective angles of the q_r axis and the q_e axis of the rotor and the synchronously rotating reference frame measured with respect to the stationary axis of the A phase location.

δ is equal to the power angle defined as that between the q_r axis and the terminal voltage phasor. If the phasor of v_a is aligned with the q_e axis synchronously rotating reference frame;

$$v_a = V_m \sin(\omega_e t + \theta_e(0)) \quad (92)$$

where $\theta_e(0)$ =0

If $\theta_e(0)$ is not zero, as with a sinusoidal excitation of :

$$v_a = V_m \sin(\omega_e t) = V_m \cos\left(\omega_e t - \frac{\pi}{2}\right) \quad (93)$$

where $\theta_e(0) = \frac{-\pi}{2}$, the no load steady state value of δ will be $\frac{-\pi}{2}$ instead of zero. In this case, the a phase voltage will still be aligned with the q_r axis of the rotor at no load but both will be lagging $\frac{\pi}{2}$ behind the q_e axis of the synchronously rotating reference frame.

If there is a discontinuity with the initial values of $\theta_e(0)$ for bus voltage, $\theta_r(0)$ for the variable frequency oscillator and $\delta(0)$ then the model will not settle properly causing a distorted flux

linkage through the model and making the model output not consistent with what would be expected from a real machine. It is therefore important that these values be consistent when initialising the model or re-initialising after a fault is created, i.e. on closing after a fault.

Derivation Example

$$\psi_q = X_{ls} i_q + \omega_b L_{mq}(i_q + i'_{kq}) \tag{94}$$

$$\psi_q = \omega_b \int \left[V_q - \omega_r \frac{\psi_d}{\omega_b} + \frac{R_s}{X_{ls}} \left(\psi_{mq} - \left\{ X_{ls} i_q + \omega_b L_{mq}(i_q + i'_{kq}) \right\} \right) \right] \tag{95}$$

$$\psi_q = \omega_b \int \left[V_q - \omega_r \frac{\psi_d}{\omega_b} + \frac{R_s}{X_{ls}} \left(- X_{ls} i_q \right) \right] dt \tag{96}$$

Thus all terms are considered voltages and with the rotor speed term we can equate to (Weber turns/sec)

$$\psi_q = \omega_b \int \left[V_q - \omega_r \frac{\psi_d}{\omega_b} - R_s i_q \right] dt \tag{97}$$

Supporting Machine Equations

$$X'_{lf} = X_{md} * \frac{X'_d - X_{ls}}{X_{md} - (x'_d - X_{ls})} \tag{98}$$

$$X'_{lkd} = * X'_{lf} * \frac{X''_d - X_{ls}}{X'_{lf} * X_{md} - (X''_d - X_{ls}) * (X_{md} + X'_{lf})} \tag{99}$$

$$X'_{lkq} = X_{mq} * \frac{X''_q - X_{ls}}{X_{mq} - (X''_q - X_{ls})} \tag{100}$$

$$R'_f = \frac{X'_{lf} + X_{md}}{\omega_{base} * T'_{do}} \tag{101}$$

$$R'_{kd} = \frac{X'_{lkd} + X'_d - X_{ls}}{\omega_{base} * T''_{do}} \tag{102}$$

$$R'_{kq} = \frac{X'_{lkq} + X_{mq}}{\omega_{base} * T''_{qo}} \tag{103}$$

Computing dq steady-state variables of machine

$$E_{q0} = |E_q| \tag{104}$$

$$I = I_t * (cos\,\theta - sin\theta * j) \tag{105}$$

$$E_{f0} = E_{q0} + (X_d - X_q) * I_{d0} \tag{106}$$

$$I_{f0} = \frac{E_{f0}}{X_{md}} \tag{107}$$

$$\psi_{ad0} = X_{md} * (-I_{d0} + I_{f0}) \tag{108}$$

$$\psi_{aq0} = X_{mq} * (-I_{q0}) \tag{109}$$

$$\psi_{q0} = X_{ls} * (-I_{q0}) + \psi_{aq0} \tag{110}$$

$$\psi_{d0} = X_{ls} * (-I_{do}) + \psi_{ad0} \tag{111}$$

$$\psi_{f0} = X'_{lf} * I_{f0} + \psi_{ad0} \tag{112}$$

$$\psi_{kq0} = \psi_{aq0} \tag{113}$$

$$\psi_{kd0} = \psi_{ad0} \tag{114}$$

$$V_{t0} = V_t * (cos\,\theta - sin\theta * j) \tag{115}$$

$$E'_{q0} = V_{qo} + X'_d * I_{do} + R_s * I_{qo} \tag{116}$$

$$E'_{d0} = V_{do} + X'_q * I_{qo} + R_s * I_{do} \tag{117}$$

Appendix 3

Synthetic Parameter Values and Traces

Machine Values

Parameter	Value
F_{rated}	50
Poles	4
Pf_{rated}	0.9
V_{rated}	18e3
P_{rated}	828315e3
Rs	0.0048
Xd	1.790
Xq	1.660
X_{ls}	0.215
X_d	0.355
X'_q	0.570
X''_d	0.275
X''_q	0.275
T'_{do}	7.9
T'_{qo}	0.410
T''_{do}	0.032
T''_{qo}	0.055
H	7.9
D_{omega}	0

AC5A Exciter Values

Parameter	Value
V_ref	1.03
K_a1	400
T_a1	0.02
K_f1	0.03
T_f1	1
T_f2	0
T_f3	0
SeEfd1	0.86
T_e	0.8
V_rmax	4.1
V_rmin	-4.1
K_e	1

Governor Constants

Parameter	Value
T1	0.25
T2	0
T3	0.1
K	0.95
Pup	10
Pdown	-10
Pmax	1.1
Pmin	0

network data.txt

Length of Lines		200.0000	km
Grid:Grid	Syst.Stage:Grid	Annex:	/ 2
Type CCT	Line Type	1	/1
Rated Voltage		500.0000	kV
Rated Current		2.0000	kA
Nominal Frequency		50.0000	Hz
Cable / OHL	Overhead Line		
System Type	AC		
Phases		3	
No. of Neutrals		0	
Parameters per Length 1,2-Sequence			
Resistance R'		0.0500	Ohm/km
Reactance X'		0.2500	Ohm/km
Parameters per Length Zero Sequence			
Resistance R0'		0.2000	Ohm/km
Reactance X0'		1.0000	Ohm/km
Parameters per Length 1,2-Sequence			
Capacitance C'		0.0150	uF/km
Ins. Factor		0.0000	
Parameters per Length Zero Sequence			
Capacitance C0'		0.0100	uF/km
Ins. Factor		0.0000	
Max. End Temperature		80.0000	degC
Rated Short-Time (1s) Current (Conductor)		0.0000	kA
Frequency Dependency of Pos.-Sequence Capacitance			
Capacitance C'		0.0150	uF/km
C1'(f)			
Frequency Dependency of Zero-Sequence Capacitance			
Capacitance C0'		0.0100	uF/km
C0'(f)			
Frequency Dependencies of Pos.-Sequence Impedance			
Resistance R'		0.0500	Ohm/km
R1'(f)			
Inductance L'		0.7958	mH/km
L1'(f)			
Frequency Dependencies of Zero-Sequence Impedance			
Resistance R0'		0.2000	Ohm/km
R0'(f)			
Inductance L0'		3.1831	mH/km
L0'(f)			
Stochastic model			

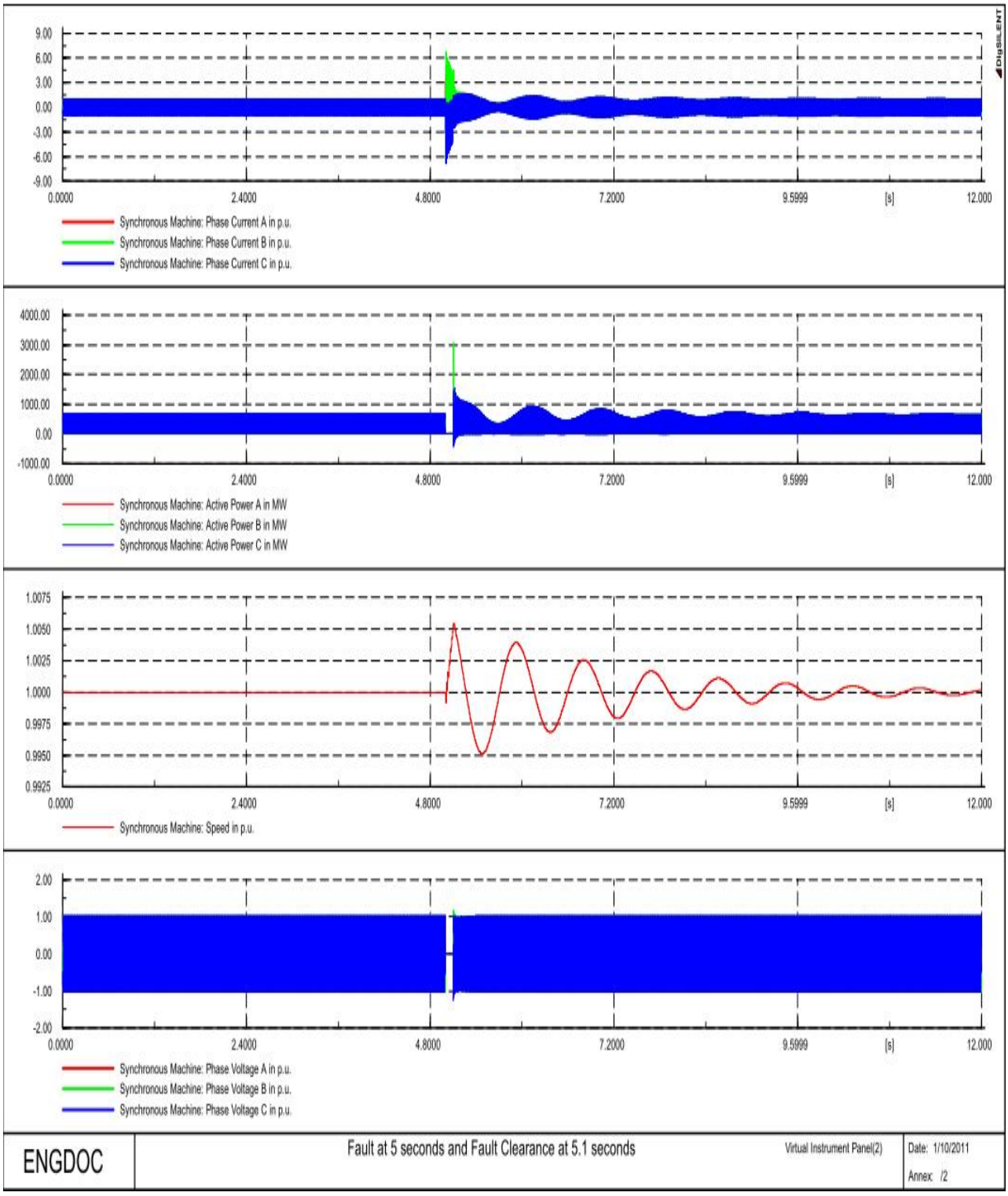
9.00
6.00
3.00
0.00
-3.00
-6.00
-9.00
0.0000
2.4000
4.8000
7.2000
9.5999
[s]
12.000
Synchronous Machine: Phase Current A in p.u.
Synchronous Machine: Phase Current B in p.u.
Synchronous Machine: Phase Current C in p.u.
4000.00
3000.00
2000.00
1000.00
0.00
-1000.00
Synchronous Machine: Active Power A in MW
Synchronous Machine: Active Power B in MW
Synchronous Machine: Active Power C in MW
1.0075
1.0050
1.0025
1.0000
0.9975
0.9950
0.9925
Synchronous Machine: Speed in p.u.
2.00
1.00
0.00
-1.00
-2.00
Synchronous Machine: Phase Voltage A in p.u.
Synchronous Machine: Phase Voltage B in p.u.
Synchronous Machine: Phase Voltage C in p.u.
ENGDOC
Fault at 5 seconds and Fault Clearance at 5.1 seconds
Virtual Instrument Panel(2)
Date: 1/10/2011
Annex: /2

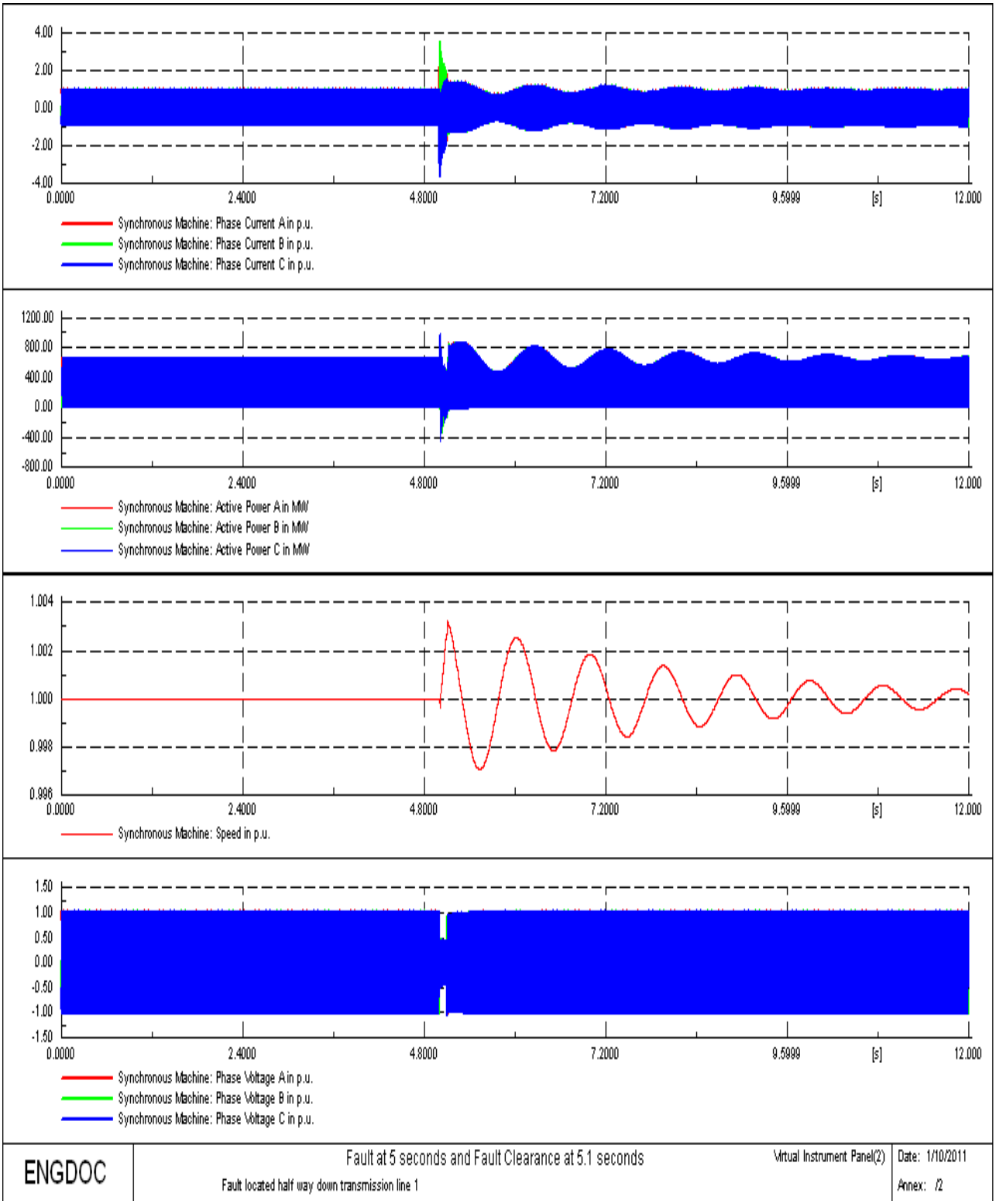
4.00
2.00
0.00
-2.00
-4.00
0.0000
2.4000
4.8000
7.2000
9.5999
[s]
12.000
Synchronous Machine: Phase Current A in p.u.
Synchronous Machine: Phase Current B in p.u.
Synchronous Machine: Phase Current C in p.u.
1200.00
800.00
400.00
0.00
-400.00
-800.00
Synchronous Machine: Active Power A in MW
Synchronous Machine: Active Power B in MW
Synchronous Machine: Active Power C in MW
1.004
1.002
1.000
0.998
0.996
Synchronous Machine: Speed in p.u.
1.50
1.00
0.50
0.00
-0.50
-1.00
-1.50
Synchronous Machine: Phase Voltage A in p.u.
Synchronous Machine: Phase Voltage B in p.u.
Synchronous Machine: Phase Voltage C in p.u.
ENGDOC
Fault at 5 seconds and Fault Clearance at 5.1 seconds
Fault located half way down transmission line 1
Virtual Instrument Panel(2)
Date: 1/10/2011
Annex: /2

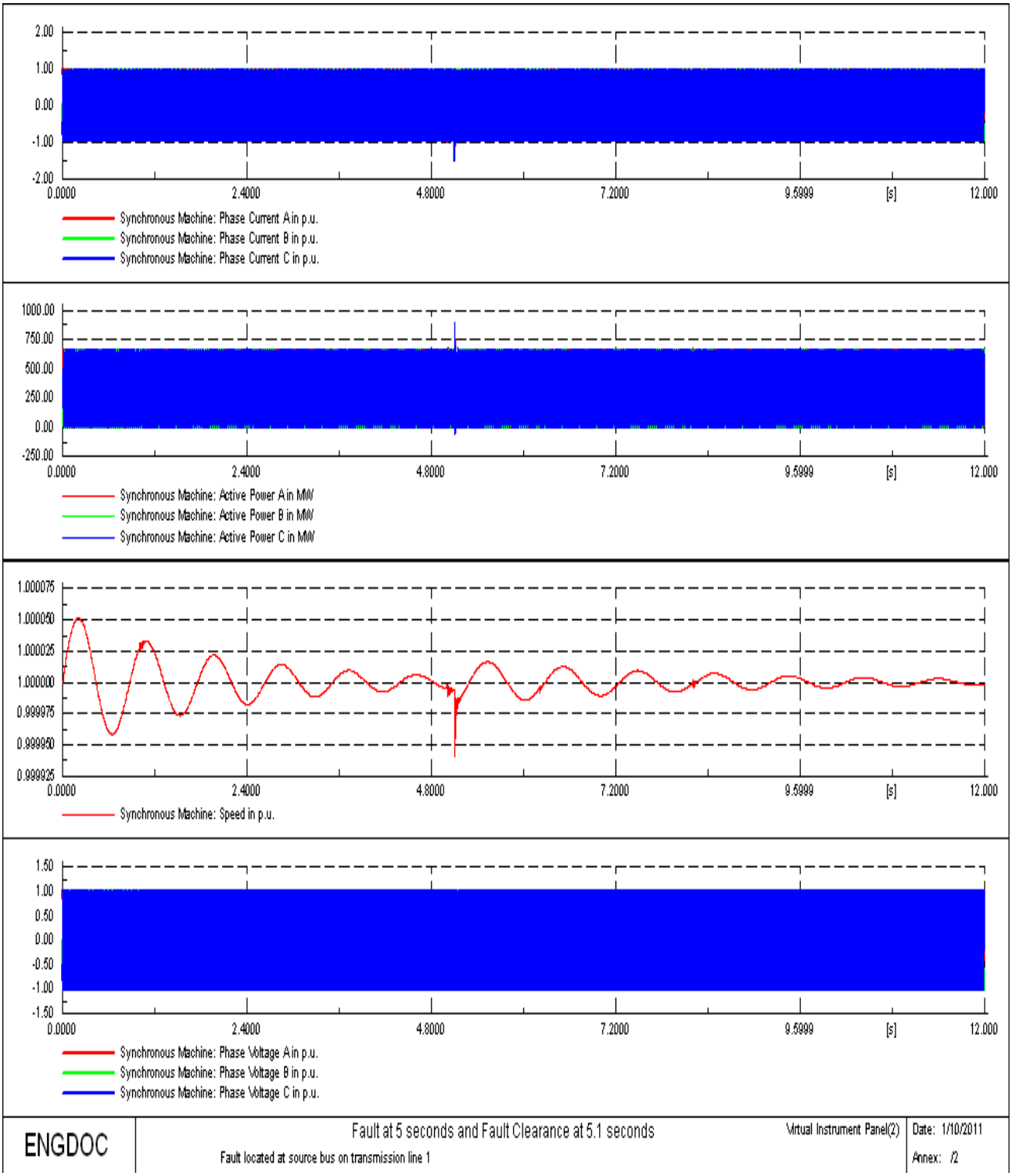
2.00
1.00
0.00
-1.00
-2.00
0.0000
2.4000
4.8000
7.2000
9.5999
[s]
12.000
Synchronous Machine: Phase Current A in p.u.
Synchronous Machine: Phase Current B in p.u.
Synchronous Machine: Phase Current C in p.u.
1000.00
750.00
500.00
250.00
0.00
-250.00
Synchronous Machine: Active Power A in MW
Synchronous Machine: Active Power B in MW
Synchronous Machine: Active Power C in MW
1.000075
1.000050
1.000025
1.000000
0.999975
0.999950
0.999925
Synchronous Machine: Speed in p.u.
1.50
1.00
0.50
0.00
-0.50
-1.00
-1.50
Synchronous Machine: Phase Voltage A in p.u.
Synchronous Machine: Phase Voltage B in p.u.
Synchronous Machine: Phase Voltage C in p.u.
ENGDOC
Fault at 5 seconds and Fault Clearance at 5.1 seconds
Fault located at source bus on transmission line 1
Virtual Instrument Panel(2)
Date: 1/10/2011
Annex: /2

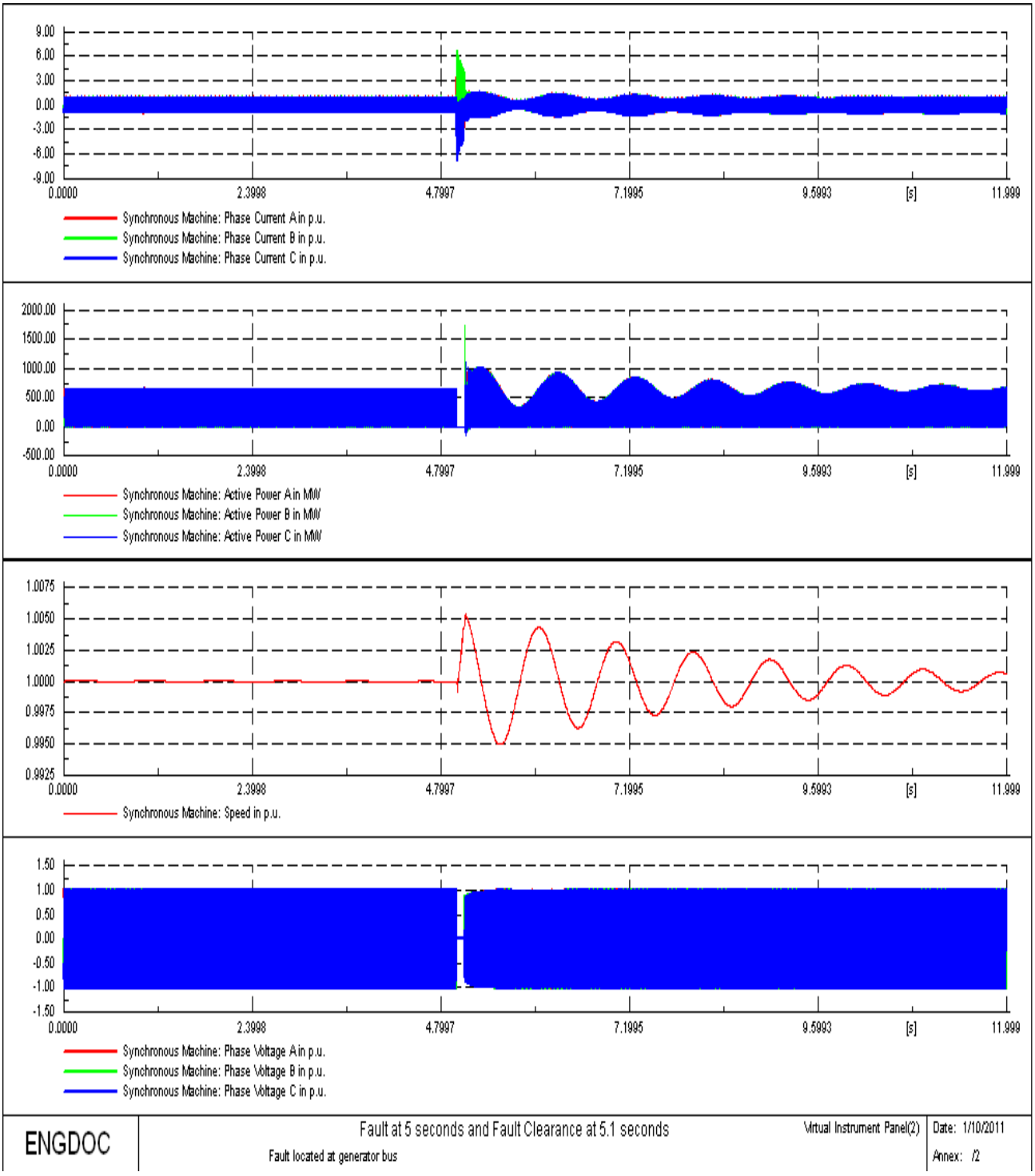
9.00
6.00
3.00
0.00
-3.00
-6.00
-9.00
0.0000
2.3998
4.7997
7.1995
9.5993
[s]
11.999
Synchronous Machine: Phase Current A in p.u.
Synchronous Machine: Phase Current B in p.u.
Synchronous Machine: Phase Current C in p.u.
2000.00
1500.00
1000.00
500.00
0.00
-500.00
Synchronous Machine: Active Power A in MW
Synchronous Machine: Active Power B in MW
Synchronous Machine: Active Power C in MW
1.0075
1.0050
1.0025
1.0000
0.9975
0.9950
0.9925
Synchronous Machine: Speed in p.u.
1.50
1.00
0.50
0.00
-0.50
-1.00
-1.50
Synchronous Machine: Phase Voltage A in p.u.
Synchronous Machine: Phase Voltage B in p.u.
Synchronous Machine: Phase Voltage C in p.u.
ENGDOC
Fault at 5 seconds and Fault Clearance at 5.1 seconds
Fault located at generator bus
Virtual Instrument Panel(2)
Date: 1/10/2011
Annex: /2

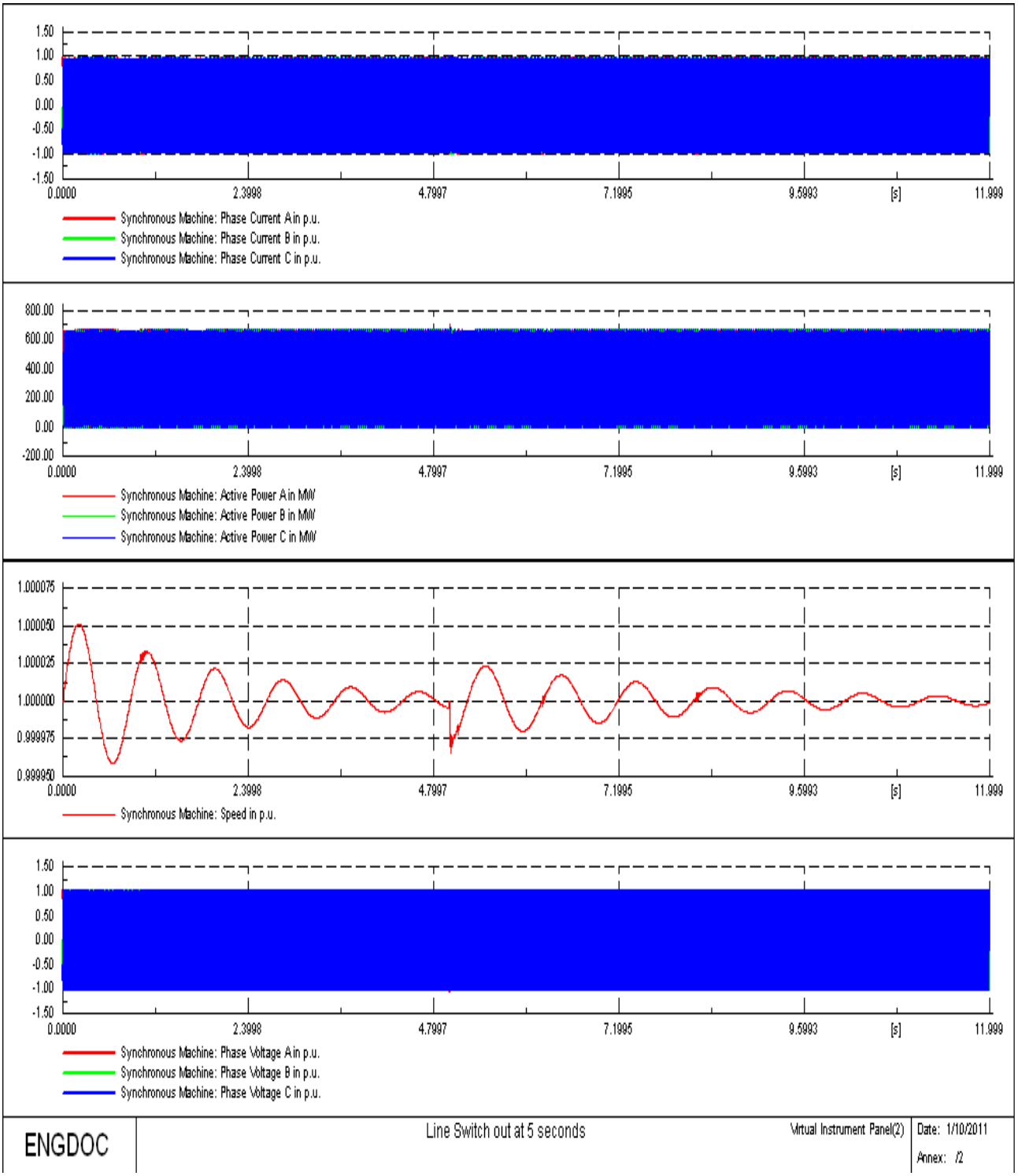
1.50
1.00
0.50
0.00
-0.50
-1.00
-1.50
0.0000
2.3998
4.7997
7.1995
9.5993
[s]
11.999
Synchronous Machine: Phase Current A in p.u.
Synchronous Machine: Phase Current B in p.u.
Synchronous Machine: Phase Current C in p.u.
800.00
600.00
400.00
200.00
0.00
-200.00
Synchronous Machine: Active Power A in MW
Synchronous Machine: Active Power B in MW
Synchronous Machine: Active Power C in MW
1.000075
1.000050
1.000025
1.000000
0.999975
0.999950
Synchronous Machine: Speed in p.u.
Synchronous Machine: Phase Voltage A in p.u.
Synchronous Machine: Phase Voltage B in p.u.
Synchronous Machine: Phase Voltage C in p.u.
ENGDOC
Line Switch out at 5 seconds
Virtual Instrument Panel(2)
Date: 1/10/2011
Annex: /2

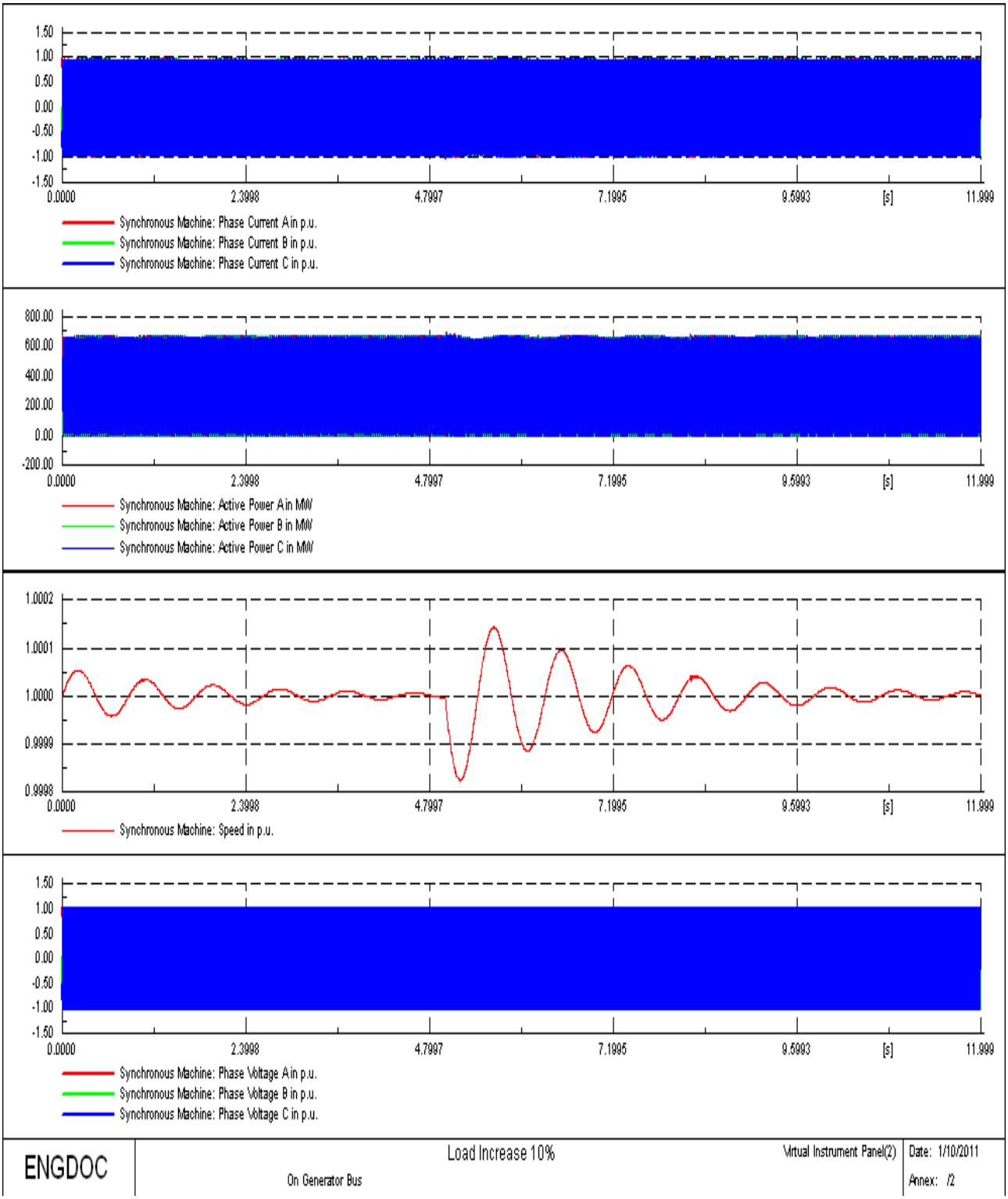
1.50
1.00
0.50
0.00
-0.50
-1.00
-1.50
0.0000
2.3998
4.7997
7.1995
9.5993
[s]
11.999
Synchronous Machine: Phase Current A in p.u.
Synchronous Machine: Phase Current B in p.u.
Synchronous Machine: Phase Current C in p.u.
800.00
600.00
400.00
200.00
0.00
-200.00
Synchronous Machine: Active Power A in MW
Synchronous Machine: Active Power B in MW
Synchronous Machine: Active Power C in MW
1.0002
1.0001
1.0000
0.9999
0.9998
Synchronous Machine: Speed in p.u.
Synchronous Machine: Phase Voltage A in p.u.
Synchronous Machine: Phase Voltage B in p.u.
Synchronous Machine: Phase Voltage C in p.u.
ENGDOC
Load Increase 10%
On Generator Bus
Virtual Instrument Panel(2)
Date: 1/10/2011
Annex: /2

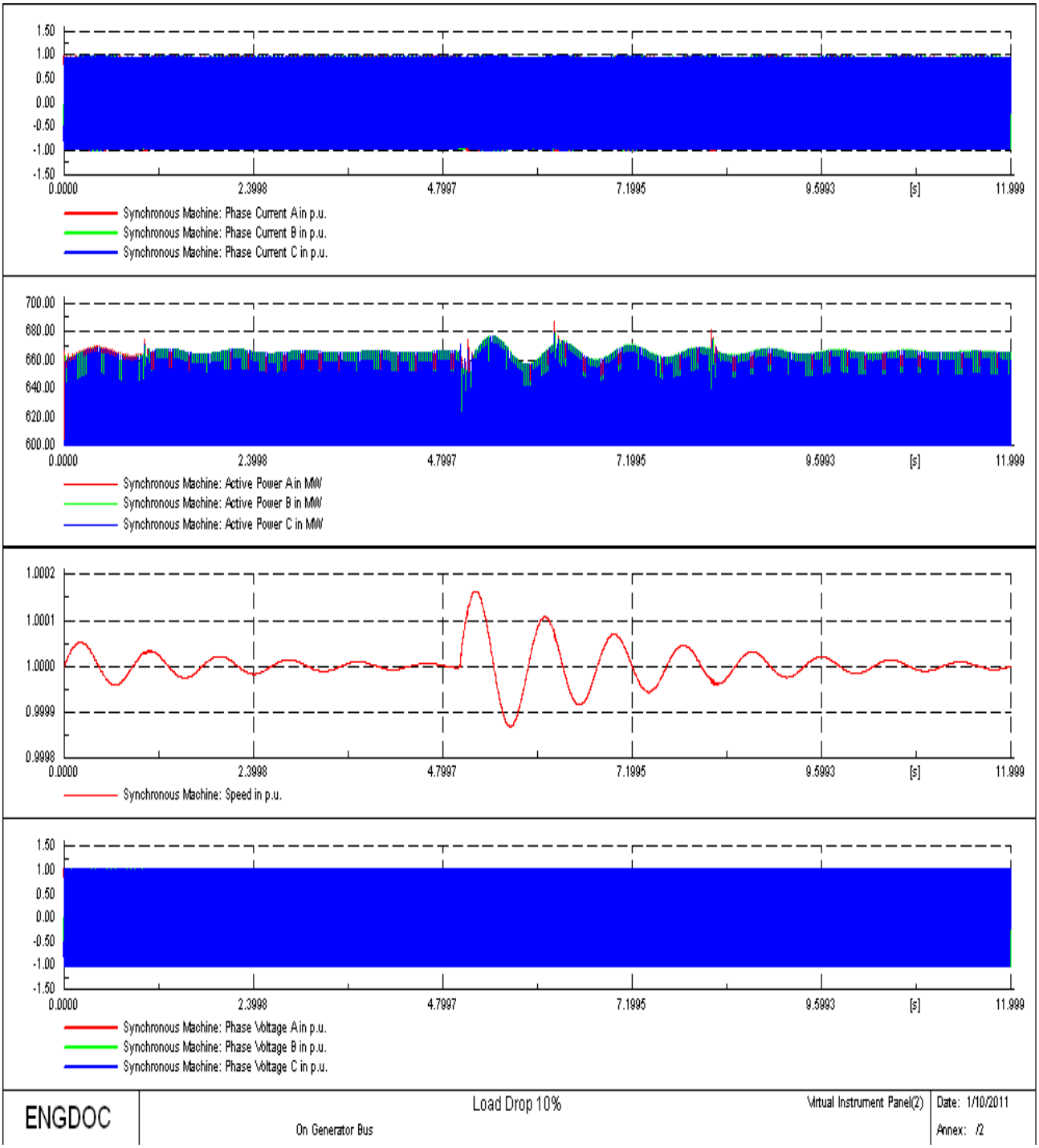
1.50
1.00
0.50
0.00
-0.50
-1.00
-1.50
0.0000
2.3998
4.7997
7.1995
9.5993
[s]
11.999
Synchronous Machine: Phase Current A in p.u.
Synchronous Machine: Phase Current B in p.u.
Synchronous Machine: Phase Current C in p.u.
700.00
680.00
660.00
640.00
620.00
600.00
Synchronous Machine: Active Power A in MW
Synchronous Machine: Active Power B in MW
Synchronous Machine: Active Power C in MW
1.0002
1.0001
1.0000
0.9999
0.9998
Synchronous Machine: Speed in p.u.
Synchronous Machine: Phase Voltage A in p.u.
Synchronous Machine: Phase Voltage B in p.u.
Synchronous Machine: Phase Voltage C in p.u.
ENGDOC
Load Drop 10%
On Generator Bus
Virtual Instrument Panel(2)
Date: 1/10/2011
Annex: /2

Appendix 4

Power Station Parameter Values

Machine Values

Parameter	Value
F_{rated}	50
Poles	2
Pf_{rated}	0.9
V_{rated}	18e3
P_{rated}	304e6;
Rs	0.0048
Xd	1.68
Xq	1.650
X_{ls}	0.169
X_d	0.301
X'_q	0.301
X''_d	0.23
X''_q	0.228
T'_{do}	0.83
T'_{qo}	0.83
T''_{do}	0.035
T''_{qo}	0.035
H	3.74
D_{omega}	0

AC2Exciter Values

Parameter	Value
V_R	0.19
R_F	0.0098
R_B	0.3
V_S	205
T_E	0.04
K_E	1
S_{Efd75}	0.06
S_{Efd100}	0.31
K_D	1.18
V_{rmax}	42
V_{rmin}	0
E_{fd}	155
I_{FD}	782
V_{LR}	289
T_A	0.47
T_B	0.01
T_C	0
T_F	0.31
K_A	1216
K_B	10
K_H	0.29
K_F	0.036

Appendix 5

PSO Algorithm

```
%                           to Ackley but with a 3rd dimension added for complexity
%
%                     Graeme Hutchison, Department of Electrical, Electronic and Computer
%                                 Engineering, University of Newcastle Upon Tyne


%%
% Declaration of Some initial conditions and variables
Particles = 15;
inform = 4;                                          %Number of informants
W_interia = 0.3;                                    %Inertia constant in PSO
C_1 = 2.05;                                          %Constant of PSO Algorithm
C_2 = 2.05;                                          %Constant of PSO Algorithm
Constr = 0.742;                                      %Constriction factor

X_minxd = 1.6;                                          %identification of search space min
X_minxpd = 0.25;                                          %identification of search space min
X_mintpdo = 0.7;                                          %identification of search space min
X_maxrs = 0.007;                                       %identification of search space max for rs
X_minrs = 0.003;                                       %identification of search space max for rs
X_maxxd = 1.8;                                         %identification of search space max
X_maxtpdo = 0.9;                                         %identification of search space max
X_maxxpd = 0.35;
X_minxppd = 0.2;                                          %identification of search space min
X_maxxppd = 0.3;                                        %identification of search space max
X_minxq = 1.5;                                          %identification of search space min
X_maxxq = 1.8;                                         %identification of search space max
X_mintppdo = 0.01;                                            %identification of search space min
X_maxtppdo = 0.06;                                        %identification of search space max
X_minH = 3;                                           %identification of search space min
X_maxH = 4.2;                                         %identification of search space max
X_minxppq = 0.2;                                          %identification of search space min
X_maxxppq = 0.3;                                        %identification of search space max
X_mintppqo = 0.01;                                            %identification of search space min
X_maxtppqo = 0.06;                                        %identification of search space max


X_max = 5;                                           %identification of search space max
X_min = 0;
Exec = 0;                                            %an incremental block
Error = 0.0000001;                                      %size of error in convergenc
Eval_max = 10000;                                     %maximu/m number of iterations
Counter = 0;                                         %an incremental block
BestF = 20;
DATAOUT = zeros(50000,12);
E = 0;


%% initialise Locations and Velocities

        for i=1:Particles                                           % from 1 to the number of particles
            X1(i) = X_minxd + (X_maxxd - X_minxd)*rand;             % Initalise variable location/value
            X2(i) = X_minxpd + (X_maxxpd - X_minxpd)*rand;          % Initalise variable location/value
            X3(i) = X_minxppd + (X_maxxppd - X_minxppd)*rand;       % Initalise variable location/value
            X4(i) = X_mintpdo + (X_maxtpdo - X_mintpdo)*rand;       % Initalise variable location/value
            X5(i) = X_min + (X_maxrs - X_minrs)*rand;                 % Initalise variable location/value
            X6(i) = X_minxq + (X_maxxq - X_minxq)*rand;             % Initalise variable location/value
            X7(i) = X_mintppdo + (X_maxtppdo - X_mintppdo)*rand;       % Initalise variable location/value
            X8(i) = X_minH + (X_maxH - X_minH)*rand;       % Initalise variable location/value
            X9(i) = X_minxppq + (X_maxxppq - X_minxppq)*rand;       % Initalise variable location/value
            X10(i) = X_mintppqo + (X_maxtppqo - X_mintppqo)*rand;       % Initalise variable location/value

            V1(i) = X_min + (X_max - X_min)*rand;           % Initalise variable velocity
            V2(i) = X_min + (X_max - X_min)*rand;           % Initalise variable velocity
            V3(i) = X_min + (X_max - X_min)*rand;           % Initalise variable velocity
            V4(i) = X_min + (X_max - X_min)*rand;           % Initalise variable velocity
            V5(i) = X_min + (X_max - X_min)*rand;           % Initalise variable velocity
            V6(i) = X_min + (X_max - X_min)*rand;           % Initalise variable velocity
            V7(i) = X_min + (X_max - X_min)*rand;           % Initalise variable velocity
            V8(i) = X_min + (X_max - X_min)*rand;           % Initalise variable velocity
            V9(i) = X_min + (X_max - X_min)*rand;           % Initalise variable velocity
            V10(i) = X_min + (X_max - X_min)*rand;           % Initalise variable velocity

            P1(i) = X1(i);                                  %assigns the best position to P1
            P2(i) = X2(i);                                  %assigns the best position to P2
            P3(i) = X3(i);                                  %assigns the best position to P3
            P4(i) = X4(i);                                  %assigns the best position to P3
```

```
            P5(i) = X5(i);                                  %assigns the best position to P3
            P6(i) = X6(i);                                  %assigns the best position to P3
            P7(i) = X7(i);                                  %assigns the best position to P3
            P8(i) = X8(i);                                  %assigns the best position to P3
            P9(i) = X9(i);                                  %assigns the best position to P3
            P10(i) = X10(i);                                  %assigns the best position to P1

            G1(1)=200;                                    %assigns p best to gbest
            G2(1)=200;                                    %assigns p best to gbest
            G3(1)=200;                                    %assigns p best to gbest
            G4(1)=200;                                    %assigns p best to gbest
            G5(1)=200;                                    %assigns p best to gbest
            G6(1)=200;                                    %assigns p best to gbest
            G7(1)=200;                                    %assigns p best to gbest
            G8(1)=200;                                    %assigns p best to gbest
            G9(1)=200;                                    %assigns p best to gbest
            G10(1)=200;                                    %assigns p best to gbest
        end



        Counter = Counter + 1;                          %increment


%% Setting of main loop

            while ((Counter < Eval_max) & (abs(BestF) > Error))


%% Calculate New Velocities and Positions
                    for i = 1 : Particles
                        Informants = ceil(Particles * rand (inform,1)); %Informants are equal to the number
of particles*random*(one of 4 rows, 1 column
                       A = Informants(1);                              % declare informants
                       B = Informants(2);                              % declare informants
                       C = Informants(3);                              % declare informants
                       D = Informants(4);                              % declare informants
                    end
                        xd = X1(A) ;
                        xpd = X2(A) ;
                        xppd = X3(A) ;
                        Tpdo = X4(A) ;
                        rs = X5(A) ;
                        xq = X6(A) ;
                        Tppdo = X7(A) ;
                        H = X8(A) ;
                        xppq = X9(A) ;
                        Tppqo = X10(A) ;

                        run ('Hailmary10');
                       sim ('Teesidemdl');

%% Calculation of Average of error coming from machine model
                    sumof = 0;                                          % Develops Average Error of the the
model Error output
                    Colm_lnth = size(Error_out);
                    for j=1:Colm_lnth
                        sumof = sumof + Error_out(j);
                    end
                    Avg_err = sumof / Colm_lnth(1,1);                   %Model Error Average Output
                    Result1 = Avg_err;

                        xd = X1(B) ;
                        xpd = X2(B) ;
                        xppd = X3(B) ;
                        Tpdo = X4(B) ;
                        rs = X5(B) ;
                        xq = X6(B) ;
                        Tppdo = X7(B) ;
                        H = X8(B) ;
                        xppq = X9(B) ;
                        Tppqo = X10(B) ;

                        run ('Hailmary10');
                       sim ('Teesidemdl');

%% Calculation of Average of error coming from machine model for 2nd
%% informant
                    sumof = 0;                                          % Develops Average Error of the the
model Error output
                    Colm_lnth = size(Error_out);
                    for j=1:Colm_lnth
                        sumof = sumof + Error_out(j);
                    end
```

```
                    Avg_err = sumof / Colm_lnth(1,1);                %Model Error Average Output
                    Result2 = Avg_err;

                        xd = X1(C) ;
                        xpd = X2(C) ;
                        xppd = X3(C) ;
                        Tpdo = X4(C) ;
                        rs = X5(C) ;
                        xq = X6(C) ;
                        Tppdo = X7(C) ;
                        H = X8(C) ;
                        xppq = X9(C) ;
                        Tppqo = X10(C) ;


                        run ('Hailmary10');
                       sim ('Teesidemdl');
%% Calculation of Average of error coming from machine model for 3rd
%% informant
                    sumof = 0;                                       % Develops Average Error of the the
model Error output
                    Colm_lnth = size(Error_out);
                    for j=1:Colm_lnth
                        sumof = sumof + Error_out(j);
                    end
                    Avg_err = sumof / Colm_lnth(1,1);                %Model Error Average Output
                    Result3 = Avg_err;

                        xd = X1(D) ;
                        xpd = X2(D) ;
                        xppd = X3(D) ;
                        Tpdo = X4(D) ;
                        rs = X5(D) ;
                        xq = X6(D) ;
                        Tppdo = X7(D) ;
                        H = X8(D) ;
                        xppq = X9(D) ;
                        Tppqo = X10(D) ;


                        run ('Hailmary10');
                       sim ('Teesidemdl');

%% Calculation of Average of error coming from machine model for 4th
%% informant
                    sumof = 0;                                       % Develops Average Error of the the
model Error output
                    Colm_lnth = size(Error_out);
                    for j=1:Colm_lnth
                        sumof = sumof + Error_out(j);
                    end
                    Avg_err = sumof / Colm_lnth(1,1);                %Model Error Average Output
                    Result4 = Avg_err;




%%
                        if ((Result1<Result2)&(Result1<Result3)&(Result1<Result4))
                        Z=A;
                        Tot_result = Result1;

                        elseif ((Result2<Result1)&(Result2<Result3)&(Result2<Result4))
                        Z=B;
                        Tot_result = Result2;

                        elseif ((Result3<Result2)&(Result3<Result1)&(Result3<Result4))
                        Z=C;
                        Tot_result = Result3;

                        elseif ((Result4<Result2)&(Result4<Result3)&(Result4<Result1))
                        Z=D;
                        Tot_result = Result4;
                        end


                        P1(i)=X1(Z);                                  %assigns p best
                        P2(i)=X2(Z);                                  %assigns p best
                        P3(i)=X3(Z);
                        P4(i)=X4(Z);
                        P5(i)=X5(Z);
                        P6(i)=X6(Z);
                        P7(i)=X7(Z);
```

```
                    P8(i)=X8(Z);
                    P9(i)=X9(Z);
                    P10(i)=X10(Z);

                    if  (Tot_result < BestF)
                        E=E+1;
                        BestF = Tot_result
                        Counter
                        G1(1)=P1(Z);                                    %assigns p best to gbest
                        G2(1)=P2(Z);                                    %assigns p best to gbest
                        G3(1)=P3(Z);                                    %assigns p best to gbest
                        G4(1)=P4(Z);                                    %assigns p best to gbest
                        G5(1)=P5(Z);                                    %assigns p best to gbest
                        G6(1)=P6(Z);                                    %assigns p best to gbest
                        G7(1)=P7(Z);                                    %assigns p best to gbest
                        G8(1)=P8(Z);                                    %assigns p best to gbest
                        G9(1)=P9(Z);                                    %assigns p best to gbest
                        G10(1)=P10(Z);

                        DATAOUT(E,1) = Counter;
                        DATAOUT(E,2)= BestF;
                        DATAOUT(E,3)= G1(1);
                        DATAOUT(E,4)= G2(1);
                        DATAOUT(E,5)= G3(1);
                        DATAOUT(E,6)= G4(1);
                        DATAOUT(E,7)= G5(1);
                        DATAOUT(E,8)= G6(1);
                        DATAOUT(E,9)= G7(1);
                        DATAOUT(E,10)= G8(1);
                        DATAOUT(E,11)= G9(1);
                        DATAOUT(E,12)= G10(1);
                    end



                for i = 1 : Particles
                    V1(i)= Constr*(W_interia*V1(i)+C_1*rand*(P1(i)-X1(i))+C_2*rand*(G1(1)-X1(i)));
%PSO algo for velocity update
                    X1(i)=X1(i)+ V1(i);                                 %Update of position
                    V2(i)= Constr*(W_interia*V2(i)+C_1*rand*(P2(i)-X2(i))+C_2*rand*(G2(1)-X2(i)));
%PSO algo for velocity update
                    X2(i)=X2(i)+ V2(i);                                 %Update of position
                    V3(i)= Constr*(W_interia*V3(i)+C_1*rand*(P3(i)-X3(i))+C_2*rand*(G3(1)-X3(i)));
%PSO algo for velocity update
                    X3(i)=X3(i)+ V3(i);                                 %Update of position
                    V4(i)= Constr*(W_interia*V4(i)+C_1*rand*(P4(i)-X4(i))+C_2*rand*(G4(1)-X4(i)));
%PSO algo for velocity update
                    X4(i)=X4(i)+ V4(i);                                 %Update of position
                    V5(i)= Constr*(W_interia*V5(i)+C_1*rand*(P5(i)-X5(i))+C_2*rand*(G5(1)-X5(i)));
%PSO algo for velocity update
                    X5(i)=X5(i)+ V5(i);                                 %Update of position
                    V6(i)= Constr*(W_interia*V6(i)+C_1*rand*(P6(i)-X6(i))+C_2*rand*(G6(1)-X6(i)));
%PSO algo for velocity update
                    X6(i)=X6(i)+ V6(i);                                 %Update of position
                    V7(i)= Constr*(W_interia*V7(i)+C_1*rand*(P7(i)-X7(i))+C_2*rand*(G7(1)-X7(i)));
%PSO algo for velocity update
                    X7(i)=X7(i)+ V7(i);                                 %Update of position
                    V8(i)= Constr*(W_interia*V8(i)+C_1*rand*(P8(i)-X8(i))+C_2*rand*(G8(1)-X8(i)));
%PSO algo for velocity update
                    X8(i)=X8(i)+ V8(i);                                 %Update of position
                    V9(i)= Constr*(W_interia*V9(i)+C_1*rand*(P9(i)-X9(i))+C_2*rand*(G9(1)-X9(i)));
%PSO algo for velocity update
                    X9(i)=X9(i)+ V9(i);                                 %Update of position
                    V10(i)= Constr*(W_interia*V10(i)+C_1*rand*(P10(i)-X10(i))+C_2*rand*(G10(1)-
X10(i)));  %PSO algo for velocity update
                    X10(i)=X10(i)+ V10(i);                                %Update of position

                    if  X1(i)< X_minxd
                        X1(i) = (X_minxd);
                        V1(i) = 0.01;
                    end
                    if  X1(i) > X_maxxd
                        X1(i) = (X_maxxd);
                        V1(i) = 0.01;
                    end
                    if  X2(i)< X_minxpd
                        X2(i) = (X_minxpd);
                        V2(i) = 0.1;
                    end
                    if  X2(i) > X_maxxpd
                        X2(i) = (X_maxxpd);
                        V2(i) = 0.01;
                    end
                    if  X3(i)< X_minxppd
                        X3(i) = (X_minxppd);
                        V3(i) = 0.01;
```

```
                    end
                    if  X3(i) > X_maxxppd
                        X3(i) = (X_maxxppd);
                        V3(i) = 0.01;
                    end
                    if  X4(i)< X_mintpdo
                        X4(i) = (X_mintpdo);
                        V4(i) = 0.01;
                    end
                    if  X4(i) > X_maxtpdo
                        X4(i) = (X_maxtpdo);
                        V4(i) = 0.01;
                    end
                    if  X5(i)< X_minrs
                        X5(i) = (X_minrs);
                        V5(i) = 0.001;
                    end
                    if  X5(i) > X_maxrs
                        X5(i) = (X_maxrs);
                        V5(i) = 0.001;
                    end                                                 % Assign the informants
to each particle
                    if  X6(i)< X_minxq
                        X6(i) = (X_minxq);
                        V6(i) = 0.001;
                    end
                    if  X6(i) > X_maxxq
                        X6(i) = (X_maxxq);
                        V6(i) = 0.001;
                    end
                    if  X7(i)< X_mintppdo
                        X7(i) = (X_mintppdo);
                        V7(i) = 0.01;
                    end
                    if  X7(i) > X_maxtppdo
                        X7(i) = (X_maxtppdo);
                        V7(i) = 0.01;
                    end
                    if  X8(i)< X_minH
                        X8(i) = (X_minH);
                        V8(i) = 0.1;
                    end
                    if  X8(i) > X_maxH
                        X8(i) = (X_maxH);
                        V8(i) = 0.1;
                    end
                    if  X9(i)< X_minxppq
                        X9(i) = (X_minxppq);
                        V9(i) = 0.01;
                    end
                    if  X9(i) > X_maxxppq
                        X9(i) = (X_maxxppq);
                        V9(i) = 0.01;
                    end
                    if  X10(i)< X_mintppqo
                        X10(i) = (X_mintppqo);
                        V10(i) = 0.01;
                    end
                    if  X10(i) > X_maxtppqo
                        X10(i) = (X_maxtppqo);
                        V10(i) = 0.01;

                    end
                Counter = Counter + 1;

                end
            end
```

SYNCHRONOUS MACHINE PARAMETER IDENTIFICATION USING PARTICLE SWARM OPTIMIZATION

G.I. Hutchison, B. Zahawi, K. Harmer, B. Stedall and D. Giaouris

G. I. Hutchison is with Newcastle University, UK; Email: g.i.hutchison@ncl.ac.uk
B. Zahawi & D. Giaouris are with Newcastle University, UK
K. Harmer & B. Stedall are with Parsons Brinkerhoff, UK

Keywords; Parameter Identification; Particle Swarm Optimization; PSO; Synchronous Machines

Abstract

Synchronous machines are the most widely used machines in power generation. Identifying their parameters in a non invasive way is very challenging due to the inherent nonlinearity of machine performance. This paper proposes a synchronous machine parameter identification method using particle swarm optimization (PSO) with a constriction factor. The PSO allows a synchronous machine model output to be used as the objective function to give a new, more efficient method of parameter identification. This paper highlights the effectiveness of the proposed method for the identification of synchronous machine model parameters, using both simulation and manufacturers measured experimental data. The paper will also consider the effectiveness of the method as the number of parameters to be identified is increased.

1 Introduction

Parameter identification in synchronous machines has been a field of research for several decades. Due to the inherent need to characterize the transient performance of such machines, it becomes necessary to identify characteristics such as the d and q axis sub transient, transient and steady state reactances. Conventionally the tests performed to identify such parameters are invasive in nature. Tests like the standstill resistance test [1] produce an accurate characterization of the armature and field windings but needless to say require the machine to be at a standstill. Synchronous machines, specifically generators are in service for a large proportion of their product lifetime. It would be beneficial if a method could ultimately be developed that would allow for parameters to be identified with the machine still being in service. Whilst this paper does not go that far, it highlights a technique that could be developed to achieve such a target.

This use of a stochastic search algorithm, particle swarm optimization, to identify the parameters of a classical synchronous machine model [2] using short circuit test data is described in this paper. Results are compared against manufacturer's experimentally measured reference data. PSO has been used in previous studies for the identification of synchronous machine parameters. The algorithm was used in conjunction with a small permanent magnet synchronous machine tested under laboratory conditions [3]. El-Neggar *et al* [4] characterized the response of the synchronous machines d-axis in the sub transient region as a single nonlinear equation describing the short circuit currents envelope which was then used as an objective function to be minimized. The PSO algorithm employed in this study uses an additional term, known as a constriction factor, to allow for a more efficient convergence in the optimization whilst reducing the likelihood of particle explosion in the particle swarm [5]. This paper sets out to demonstrate that the modified PSO algorithm can be effective in identifying the parameters of a synchronous machine model using short circuit test data from a 14MW, 6.6kV synchronous generator. Additionally, the paper considers the ability of the algorithm to identify differing numbers of parameters and whether this has an effect on the convergence characteristics of the process. The method is evaluated against manufacturer data.

2 Synchronous Machine Model

Equations (1)-(8) below form a classical model of the synchronous machine [6].

$$\psi_q = \omega_b \int \left[V_q - \omega_r \frac{\psi_d}{\omega_b} + \frac{R_s}{X_{ls}} \left(\psi_{mq} - \psi_q \right) \right] dt \tag{1}$$

$$\psi_d = \omega_b \int \left[V_d + \omega_r \frac{\psi_q}{\omega_b} + \frac{R_s}{X_{ls}} \left(\psi_{md} - \psi_d \right) \right] dt \tag{2}$$

$$\psi_0 = \omega_b \int \left[V_0 - \frac{R_s}{X_{ls}} \psi_0 \right] dt \tag{3}$$

$$\psi'_{kq} = \frac{\omega_b R'_{kq}}{X'_{lkq}} \int \left[\left(\psi_{mq} - \psi'_{kq} \right) \right] dt \tag{4}$$

$$\psi'_{kd} = \frac{\omega_b R'_{kd}}{X'_{lkd}} \int \left[\left(\psi_{md} - \psi'_{kd} \right) \right] dt \tag{5}$$

$$\psi'_f = \frac{\omega_b R'_f}{X_{md}} \int \left[E_f + \frac{X_{md}}{X'_{lf}} \left(\psi_{md} - \psi'_f \right) \right] dt \tag{6}$$

The mechanical function of the machine is based on the equations below.

$$T_e = \frac{P_e}{\omega_r} = \frac{3}{2} \frac{1}{\omega_b} \left(\psi_d i_q - \psi_q i_d \right) \tag{7}$$

$$T_{mech} + T_e - T_{damp} = J\frac{d\omega_r(t)}{dt} \quad (8)$$

The model includes d and q axes damper windings on the rotor. These represent the ammortiseur windings and damping effects of the solid iron portions of the rotor poles. This is advantageous given the machine type is a high speed generator [7]. Because the rotor is not usually laminated, the damper winding currents flow in the rotor body as well as the slot wedges giving an infinite number of current paths. To characterize this would be difficult therefore the d and q classical winding structure was chosen to provide a robust characterization of the rotor. Other second and third order models could be considered if specifically required [6 & 8].

Saturation effects are not explicitly considered in the model; however these can be added by adjusting reactances along the d and q axes with 'saturation factors' or by introducing a compensation component to field excitation.

3 Particle Swarm Optimisation

PSO is a stochastic search algorithm that uses cooperation between its search populations to reach an optimum solution. Since its inception [9], PSO has been used with many differing optimization strategies. Using "Socio cognition human agents" [4] and evolutionary operations to mimic the behavior of groups of animals in social activities where multi lateral group communication is needed. This for example could be a flock of birds evading a predator or a swarm of bees looking for pollen.

In PSO the individual animals are characterized as particles, all with certain velocities and positions in the search space. The group of particles is classed as a swarm. The swarm generally begins with a randomly initialized population, each particle flying through the search space and remembering its optimal position thus far. The particles communicate and based on the best positions found, dynamically adjust the search position and relative velocity of the swarm. Because of this, the swarm will fly towards better possible results [4, 9 & 10].

The PSO algorithm initializes with a set of randomly generated variable velocities and location values. As the PSO operates, an error is developed at the output of the model. The error is used to define how far away from an appropriate result the current particles are. Informants are randomly assigned with the best overall result defining which informant influences the search area for the next iterative cycle. Based on this new search information, new values for the location and the velocities are developed. These new values are then used, to develop a new error which propagates as is already stated. The equations that define the PSO's behavior are:

$$v_i^{(k+1)} = K(w_i\, v_i^{k} + c_1 rand_1 \times (pbest_i - x_i^{k}) + c_2 rand_2 \times (gbest - x_i^{k})) \quad (9)$$

$$x_i^{(k+1)} = x_i^{k} + v_i^{(k+1)} \quad (10)$$

where c_1 and c_2 are positive constants classed as acceleration coefficients, w is the inertia weighting factor and $rand_1$, $rand_2$ are two functions that generate the inherent randomness in the PSO. x_i represents the position of the i^{th} particle, $pbest_i$ is the best previous position of x_i and gbest is the best previous position among the members of the population chosen at random as informants. v_i is the velocity of particle x_i. This combination of equations calculates a new velocity that drives the particles towards pbest and gbest. K is the constriction factor of the search. Every particle's current position is then evolved according to (10), which produces a new position in the solution space.

When a particle discovers a better position to that of its previous best, the coordinates are stored as $pbest_i$. The difference between this best and the particles current position is iteratively added to the velocity of the particle. This causes an search trajectory where the particle will tend to oscillate around its target area. The result, if good enough is added to the best result that any of the group or swarm has reached. This causes the particles to consider two distinct areas as prime locations of search. The weighting of equation (9) defines which result is considered with a higher priority and so defines the search velocity of the individual particles whilst maintaining the inherent randomness of search that is found in PSO.

One other aspect presented that is not common to other examples of PSO for parameter identification purposes is that of the constriction factor K in (9). This factor limits the search space per iteration [11]. The constriction factor is a constant and the value used is calculated from the chosen values of c_1 and c_2:

$$K = \frac{2}{|2 - \sigma - \sqrt{\sigma^2 - 4\sigma}|} \quad (11)$$

where $\sigma = c_1 + c_2$ and $\sigma > 4$.

4 Implementation of the PSO algorithm

The model is based on a state space methodology with the state variable being the flux linkages. As previously stated, the dq synchronous machine model used in this study adopts a classical structure [2]. Voltages are used as an input variable with the rotor equations characterizing the mechanical function of the machine. The model current outputs are used to develop the error function that is used in the particle swarm algorithm.

The synchronous machine model is classified as the estimator model. This estimator model begins the stochastic search process with initial values. A short circuit is created at the terminals of the three phases of the synchronous machine. The short circuit provides a significant disturbance that will allow a clear indication of the machines transient characteristics. This is advantageous in an optimization process as it allows clearer differences to be identified between the measured short circuit reference data and the model results. To maintain a valid simulation with respect to reference data, the mechanical

inertia of the machine is set to be infinite so that the machine will maintain a constant velocity during the short circuit. The field excitation voltage is fixed during the test. Fig.1 depicts how the PSO is used in conjunction with the synchronous machine model to identify the required parameters. The model output is compared against manufacturer test data to develop an error. This error is then used with the PSO optimization algorithm to develop new values for the estimator model. The process iteratively cycles until the error is within set tolerances.

The disturbing effects of a short circuit are calculated using the machine model. The short circuit currents outputs are then used to calculate the error function using equation (12)

$$Error=[\int[i_a-\bar{i}_a]dt+\int[i_b-\bar{i}_b]dt+\int[i_c-\bar{i}_c]dt \quad (12)$$

where i_{abc} are the phase current outputs of the real machine reference data with $\bar{i}_{abc}$ being the phase current outputs of the estimator model.

Using the error function, the current value of p_{best} is identified. This value is then compared against g_{best}. If p_{best} gives a lower value of error than the current g_{best} then p_{best} replaces the old g_{best}. If not, then the two values are used in the PSO equations seen above to calculate the new search velocity. The process continues with successive iterations until the error function is within a preset tolerance value. The model parameters at this point match the real machine parameter values as closely as the convergence criteria set by the chosen tolerance value allows. Compared with previous published material on the use of PSO algorithms for parameter identification [3] this method allows for a more sophisticated model to be developed that could include excitation and turbines controller models.

Each iteration four informants are selected at random from the swarm. The machine model is run four times [12] to generate four errors values. These errors are compared to identify p_{best} for that iteration.

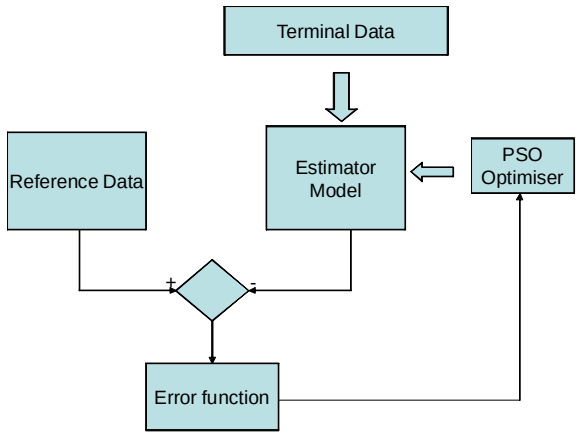

Figure 1 Optimization Structure

Search boundaries are defined so that when a particle is seen to step outside of the search space, the particle is moved to a location inside the boundary. The velocity of that particular particle is reset to a predefined value for the next iteration. Although search boundaries would appear almost fundamental to many search algorithms and an aspect that is less important to the search this is not the case. It is important to not set boundaries too 'tight' as although this limits the area that the PSO has to cover, it can inhibit the PSO's function in that it reduces the trajectoral possibilities the PSO can use without stepping outside of the defined boundaries.

Search boundaries are fundamentally different to the previously mentioned constriction factor. The search boundaries provide a 'hard' boundary that the particles cannot pass. This is unlike the constriction factor which acts as a guide to the particles to constrain the area of the search. The constriction factor does not remove the inherent randomness of the search process but alters the velocity of the particles. This allows a more careful search of a smaller area when the objective function value has been reduced to near convergence but also allows for a higher particle velocity in the primary stages of a search to instigate a faster convergence and error reduction.

5 Results

The results from a short circuit test of a 14MW, 6.6kV, 4-pole salient rotor synchronous generator are shown in Fig. 2. The three phase short circuit currents were chosen as optimization parameters as they allow for a significant change in output of the machine. The short circuit data and the output of the machine model were used to develop the output error.

	Machine	4 Param	5 Param	6 Param	7 Param
Rs Armature resistance (Ω)	0.00388	0.0039	0.0045	0.0042	0.0040
Xd D-axis reactance (Ω)	2.38	2.54	2.14	2.48	2.86
Xq Q-axis reactance (Ω)	1.186	1.266	1.141	1.477	1.3357
Xls armature leakage Reactance (Ω)	0.089	0.095	0.087	0.071	0.100
X'd transient D-axis reactance (Ω)	0.272		0.371	0.190	0.5096
X"d sub-transient D-axis reactance (Ω)	0.180			0.180	0.6004
X"q sub-transient Q-axis reactance (Ω)	0.238				0.4011

Table 1 Machine Specifications against Estimated Values

The PSO was set to optimize between 4 and 7 parameters including X_d and $X_{'d}$ using a swarm of 20 particles and 4 informants per iteration. Acceleration coefficients c_1 and c_2

were both set to 2.05 giving a constriction factor of 0.729. An iteration limit of 1000 iterations was set. The results of the optimization are compared against machine manufacturer data in Table 1.

Figure 4 shows the error function plotted against the number of iterations for several PSO algorithms, identifying between four to seven parameters. The convergence criterion was set to a value of the objective function error of 0.0001. It could be argued that this criterion is 'tighter' than is necessary for the purposes of parameter identification. A low value of error was chosen to observe the convergence behavior of the PSO when arriving at very low error values.

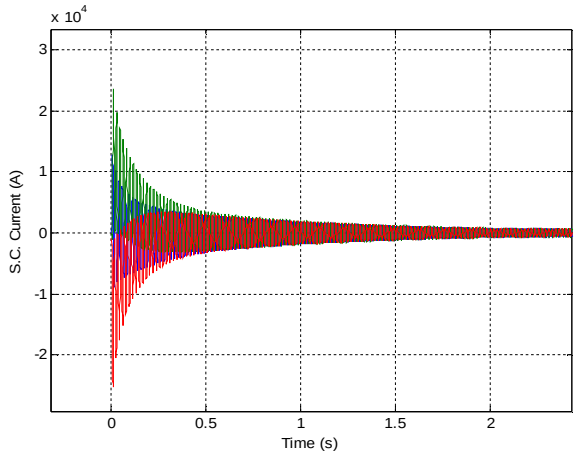

Figure 2 Synchronous machine short circuit currents

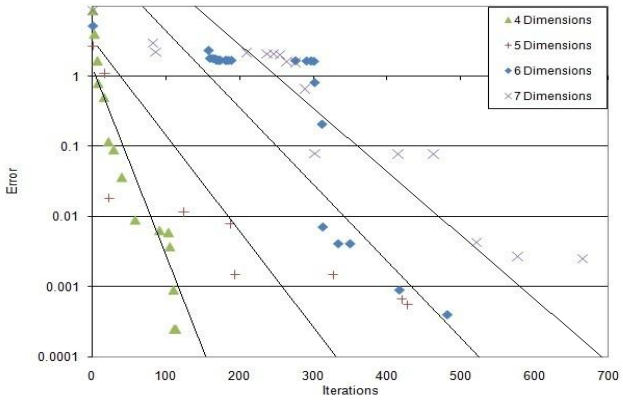

Figure 3 Error function for differing dimensional PSO searches

When considering the PSO for this particular application, several factors need to be taken into account when assessing its ability to converge in an appropriate number of iterations. For example, it is necessary to be realistic in identifying the required search area for multidimensional problems. Setting realistic limits to parameters such as X_d or R_s means that the search can be far more accurately targeted. Further to this, it becomes obvious that as the search dimensional number increases so does the search area that has to be covered. In order to evaluate the ability of the method to search for differing numbers of parameters fairly, the search boundaries are kept constant throughout the tests.

Using a constriction factor in conjunction with a refined search area, setting correct weighting values and acceleration coefficients, the particles are able to travel at an appropriate speed to converge on a lower error. It becomes self evident from the relative increase of iteration number against convergence (Fig. 3) that the increased number of parameters makes it harder for the PSO to reach a minima although the actual final result of the parameter identification is not specifically affected.

6 Conclusions

Using manufacturers short-circuit test data for a 14MW, 6.6kV synchronous generator; this paper has highlighted the benefits of parameter identification using a particle swarm optimization. The results suggest that this method is valid for parameter identification of large synchronous generators. The performance of the PSO as the number of parameters is increased has shown that although convergence time is adversely effected the overall result of the parameter identification is not.

7 References

[1] M. G. Say, Alternating Current Machines, John Wiley & Sons, 1984

[2] P. L. Dandeno, P. Kundur, A. T. Poray, M. E. Coultes, "Validation of Turbo Generator Stability Models by Comparisons with Power System Tests", IEEE Transactions on Power Apparatus and Systems, Vol.PAS-100, No.4 pp 1637-1645, 1981

[3] L. Liu, W. Liu and D.A. Cartes, "Permanent Magnet Synchronous Motor Parameter identification using Particle Swarm Optimization", Int'l Journal on Computational Intelligence Research, Vol.4, No.2 2008, pp211-218

[4] K. M. El-Naggar, A. K. Al-Othman, J.S. Al-Sumait, "A particle swarm digital identification of synchronous machine parameters from short circuit tests", Proc IASTED Int'l Conf on artificial intelligence and soft computing, August 2006

[5] M. Clerc and J. Kennedy "The Particle Swarm-Explosion, Stability and Convergence in a Multidimensional Complex Space" IEEE Trans on Evolutionary Computation, Vol.6, No.1, Feb 2002 pp58-73

[6] IEEE Std 1110 – 2002, "IEEE Guide For Synchronous Generator Modeling Practices and Applications in Power System Stability Analyses"

[7] J. Tamura, I. Takeda, "A New Model of Saturated Synchronous Machines for Power System Transient Stability Simulations", IEEE Transactions on Energy Conversion, Vol.10 No.2 1995 pp 218-224

[8] J. L. Kirtley, "On Turbine-Generator Rotor Equivalent Circuits", IEEE Transactions on Power Systems, Vol.9 No.1 1994 pp 262-271

[9] J. Kennedy and R. Eberhart, "Particle swarm optimization", Proc IEEE Int'l Conf on neural networks, vol 4 1995, pp1942-1948,

[10] Y. Shi, "Particle Swarm Optimization", feature article, electronic data systems, IEEE Neural networks society, Feb 2004

[11] P. Yin and J.Wang, "A particle swarm optimization approach to nonlinear resource allocation problem", Applied Mathematics and Computation 183, 2006, pp 232-242

[12] M. Clerc, "Particle Swarm Optimisation", Wiley Blackwell, Feb 2006

Parameter Estimation of Synchronous Machines Using Particle Swarm Optimization

Graeme Hutchison, Bashar Zahawi, Damian Giaouris
Newcastle University
United Kingdom
g.i.hutchison@ncl.ac.uk

Keith Harmer, Bruce Stedall
Parsons Brinckerhoff
Newcastle
United Kingdom

Abstract— **Synchronous machines are the most widely used electrical machine in power generation. Identifying the parameters of these machines in a non invasive way is very challenging due to the inherent nonlinearity of machine performance. This paper proposes a synchronous machine parameter identification method using particle swarm optimization (PSO) with a constriction factor. PSO is an intelligent computational method based on a stochastic search that has been shown to be a versatile and efficient tool for complicated engineering problems. A modified version of PSO allows a synchronous machine model output to be used as the objective function, thus allowing a new, more efficient method of parameter identification. This paper highlights the effectiveness of the proposed method for the identification of synchronous machine model parameters, using both simulation and manufacturers measured experimental data.**

Keywords-component; Parameter Identification; Particle Swarm Optimization ; PSO; Synchronous Machines

I. INTRODUCTION

Parameter estimation, particularly in synchronous machines, has been a topic of much research for several decades. The most accurate method of establishing armature and field parameters is through a standstill resistance test [1] which comes with the inherent disadvantages related to the fact that the test has to be performed at standstill. The more common method for defining machine parameters is therefore to perform the customary short circuit and open circuit tests and then to use the results to calculate the various machine parameters. The major drawback with this method, however, is its invasive nature in regard to testing which isn't practical when considering network connected generators. Identification has been attempted with varying degrees of success using differing algorithms to produce detailed pictures of the armature d-axis and the rotor field windings. Algorithms like gradient decent, evolutionary strategies and generational evolution have all been utilized in searching for appropriate and more efficient methods of parameter identification. Gradient decent [2], a local search algorithm which iteratively improves on a singular solution is fast; however has an inability to escape local minima for certain optimization problems thus never reaches a global solution. Likewise, evolutionary strategies [3] use a Gaussian mutation that allows for the consideration of differing paths unlike gradient decent, but ultimately one singular result is developed per iteration limiting the choice of avenues for future iterations. Generation evolutionary algorithms [4] are similar in result, which is defined by the biological imperative of improvement on a generational level. Again, although the algorithm allows for the investigation of differing avenues and theoretically can escape local minima, these methods require significant computational resources and may be unsuitable for this type of application. It is seen that all methods possess advantages, like speed of convergence or efficiency. However they also possess disadvantages like failure to converge at optimal solutions or can have an inability to exit local solutions in search of a global solution. Ultimately a definitive solution method that solves accurately and efficiently non linear problems has not been reached.

In this paper we utilize a different approach for machine parameter identification based on a stochastic search algorithm, namely particle swarm optimization. This method utilizes the classical synchronous machine equations of its forebears [5] under short circuit conditions compared against manufacturers experimentally measured reference data. PSO has been used previously for synchronous machine parameter identification [6]. In the previous case, a small permanent magnet synchronous machine was tested in laboratory conditions with a differing form of PSO algorithm. The PSO algorithm used in this investigation uses an additional constriction factor that allows for a more efficient convergence in the optimization and parameter identification strategy to identify the characteristics of a large synchronous generator. The validity of the technique is evaluated and the relative efficiency of the algorithm is considered.

II. SYNCHRONOUS MACHINE MODEL

The Equations shown below form a classical model of the synchronous machine [7].

$$\psi_q = \omega_b \int \left[V_q - \omega_r \frac{\psi_d}{\omega_b} + \frac{R_s}{X_{ls}} \left(\psi_{mq} - \psi_q \right) \right] dt \quad (1)$$

$$\psi_d = \omega_b \int \left[V_d + \omega_r \frac{\psi_q}{\omega_b} + \frac{R_s}{X_{ls}} \left(\psi_{md} - \psi_d \right) \right] dt \quad (2)$$

$$\psi_0 = \omega_b \int \left[V_0 - \frac{R_s}{X_{ls}} \psi_0 \right] dt \quad (3)$$

$$\psi'_{kq} = \frac{\omega_b R'_{kq}}{X'_{lkq}} \int [(\psi_{mq} - \psi'_{kq})] dt \quad (4)$$

$$\psi'_{kd} = \frac{\omega_b R'_{kd}}{X'_{lkd}} \int [(\psi_{md} - \psi'_{kd})] dt \quad (5)$$

$$\psi'_{f} = \frac{\omega_b R'_{f}}{X_{md}} \int \left[E_f + \frac{X_{md}}{X'_{lf}} (\psi_{md} - \psi'_{f}) \right] dt \quad (6)$$

The mechanical function of the machine is based on the equations below.

$$T_e = \frac{P_e}{\omega_r} = \frac{3}{2} \frac{1}{\omega_b} (\psi_d i_q - \psi_q i_d) \quad (7)$$

$$T_{mech} + T_e - T_{damp} = J \frac{d\omega_r(t)}{dt} \quad (8)$$

III. Particle Swarm Optimisation

PSO is a cooperative population based stochastic search optimization algorithm. Since its introduction [8], it has been used to solve a large cross section of optimization tasks. Using "Socio cognition human agents" [9] and evolutionary operations to mimic the behavior of groups of animals in social activities where multi lateral group communication is needed. This for example could be a flock of birds evading a predator or a swarm of bees looking for pollen.

In PSO the individual animals are characterized as particles, all with certain velocities and positions in the search space. The group of particles is classed as a swarm. The swarm generally begins with a randomly initialized population, each particle flying through the search space and remembering its optimal position thus far. The particles communicate and based on the best positions found, dynamically adjust the search position and relative velocity of the swarm. Because of this, the swarm will fly towards better possible results [8-10].

The PSO algorithm initializes with a set of randomly generated variable velocities and location values. As the PSO operates, an error is developed at the output of the model. The error is used to define how far away from an appropriate result the current particles are. Informants are randomly assigned with the best overall result defining which informant influences the search area for the next iterative cycle. Based on this new search information, new values for the location and the velocities are developed. These new values are then used, to develop a new error which propagates as is already stated. The equations that define the PSO's behavior are:

$$v_i^{(k+1)} = K(w_i v_i^k + c_1 rand_1 \times (pbest_i - x_i^k) + c_2 rand_2 \times (gbest - x_i^k)) \quad (9)$$

$$x_i^{(k+1)} = x_i^k + v_i^{(k+1)} \quad (10)$$

where c_1 and c_2 are positive constants classed as acceleration coefficients, w is the inertia weighting factor and $rand_1$, $rand_2$ are two functions that generate the inherent randomness in the PSO. x_i represents the position of the i^{th} particle, $pbest_i$ is the best previous position of x_i and gbest is the best previous position among the members of the population chosen at random as informants. v_i is the velocity of particle x_i. This combination of equations calculates a new velocity that drives the particles towards pbest and gbest. K is the constriction factor of the search. Every particle's current position is then evolved according to (10), which produces a new position in the solution space.

One other aspect presented that is not common to other examples of PSO for parameter identification purposes is that of the constriction factor K in (9). This factor limits the search space per iteration [11]. The constriction factor is a constant and the value used is calculated from the chosen values of c_1 and c_2:

$$K = \frac{2}{|2 - \sigma - \sqrt{\sigma^2 - 4\sigma}|} \quad (11)$$

where $\sigma = c_1 + c_2$ and $\sigma > 4$.

IV. Implementation of the PSO algorithm

As previously stated, the dq synchronous machine model used in this study adopts a fairly classical structure [5]. The model is based on a state space methodology with the state variable being the flux linkages. Due to the nature of the application, voltages are used as an input variable. The rotor equations characterize the mechanical function of the machine. The model current outputs are used to develop the error function that is used in the particle swarm algorithm.

The synchronous machine model forms the basis of the estimator model. This estimator model begins the iterative process with initial values. A short circuit is created at the terminals of the three phases of the synchronous machine. This is done by instantaneously tying the three phases to ground. To maintain a valid simulation with respect to reference data, the mechanical inertia of the machine is set to be infinite inertia so that the machine will maintain a constant velocity during the short circuit. The field excitation voltage is fixed during the test. Fig.1 shows the methodology of how the PSO is used in conjunction with the synchronous machine model to identify the required parameters. The model output is compared against manufacturer test data to develop an error. This is then used with the PSO optimization algorithm to develop new values for the estimator model. The process iteratively cycles until the error is within set tolerances.

The disturbing effects of a short circuit are calculated using the machine Simulink model and the short circuit currents used to calculate the error function using the following equation:

$$Error = [\int [i_a - \bar{i}_a] dt + \int [i_b - \bar{i}_b] dt + \int [i_c - \bar{i}_c] dt \quad (12)$$

where i_{abc} are the phase current outputs of the real machine reference data with $\bar{i}_{abc}$ being the phase current outputs of the estimator model.

Using this error function, the current value of p_{best} is identified and the process continues with successive iterations until the error function is within a preset tolerance value. The model parameters at this point match the real machine parameter values as closely as the convergence criteria set by the chosen tolerance value allow. Compared with previous published material on the use of PSO algorithms for parameter identification [6] this method allows for a more sophisticated

model to be developed that could include excitation and turbines controller models. The operation of the algorithm is described in the flow chart presented in Fig. 2.

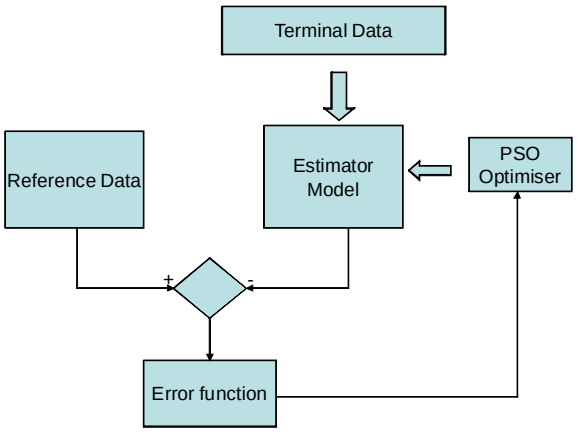

Figure 1 Optimization Structure

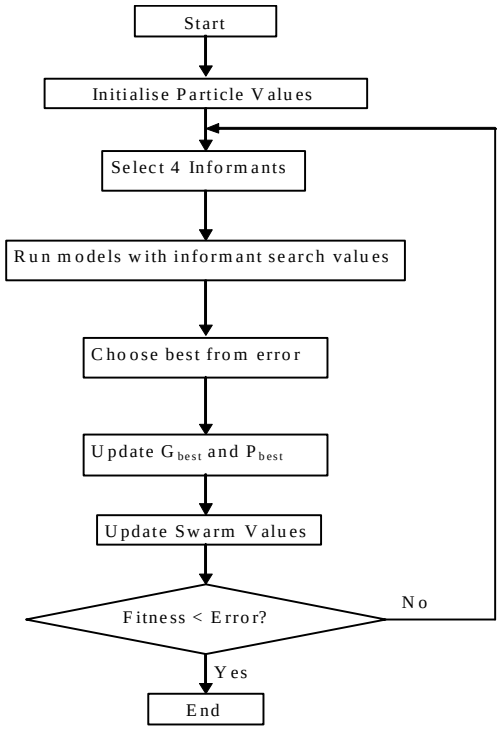

Figure 2 Flow Chart of Algorithm

For each iteration, four informants are selected at random and the machine model is run four times to generate 4 errors values [12]. These errors are compared to identify p_{best} for that iteration. This minimizes computation required and increases efficiency.

Search boundaries are defined so that when a particle is seen to step outside of the search space, the particle is moved to a location near the boundary. The velocity of the particle is reset to a predefined value for the next iteration. Search boundaries are fundamentally different to the previously mentioned constriction factor. The search boundaries provide a 'hard' boundary that the particles cannot pass. This is unlike the constriction factor which acts as a guide to the particles to constrain the area of the search. The constriction factor does not remove the inherent randomness of the search process but alters the velocity of the particles. This allows a more careful search of a smaller area when the objective function value has been reduced to near convergence but also allows for a higher particle velocity in the primary stages of a search to instigate a faster convergence and error reduction.

V. Simulation Results

The results from a short circuit test of an 828MW, 18kV, 4-pole synchronous generator are shown in Fig. 3. The three phase short circuit currents were chosen as optimization parameters as they allow for a significant change in output of the machine. This is advantageous in an optimization process as it allows clearer differences to be identified between the measured short circuit reference data and the model results. The short circuit data and the output of the Simulink machine model are then used to develop the output error.

The PSO was set to optimize 10 variables including X_d and $X_{'d}$ using a swarm of 20 particles and 4 informants per iteration. Acceleration coefficients c_1 and c_2 were both set to 2.05 giving a constriction factor of 0.729. An iteration limit of 1000 iterations was set. The results of the optimization are compared against machine manufacturer data in Table 1.

Table 1 Machine Specifications against Estimated Values

	Machine	**Estimated**
Rs Armature resistance (Ω)	0.0048	0.005
Xd D-axis reactance (Ω)	1.79	1.76
Xq Q-axis reactance (Ω)	1.66	1.68
Xls armature leakage Reactance (Ω)	0.215	0.214
X'd transient D-axis reactance (Ω)	0.355	0.353
X'q transient Q-axis reactance (Ω)	0.57	0.57
X"d sub-transient D-axis reactance (Ω)	0.275	0.273
X"q sub-transient Q-axis reactance (Ω)	0.275	0.275
$T'd_o$ sub-transient D-axis time Const (sec)	7.90	7.91
$T'q_o$ sub-transient Q-axis time Const (sec)	0.410	0.412

Figure 4 shows the error function against the number of iterations. The results are compared against a PSO algorithm searching for the same results but operating without a constriction factor but with acceleration coefficients c_1 and c_2 set at 2 and the inertia weighting set at 0.9 (parameters for c_1, c_2 and w are different to compare best obtained results in both cases). The convergence criterion was set to a value of the objective function error of 0.0001. It could be argued that this

criterion is 'tighter' than is necessarily for the purposes of parameter identification. A low value of E was chosen to observe the convergence behavior of the PSO when arriving at very low error values.

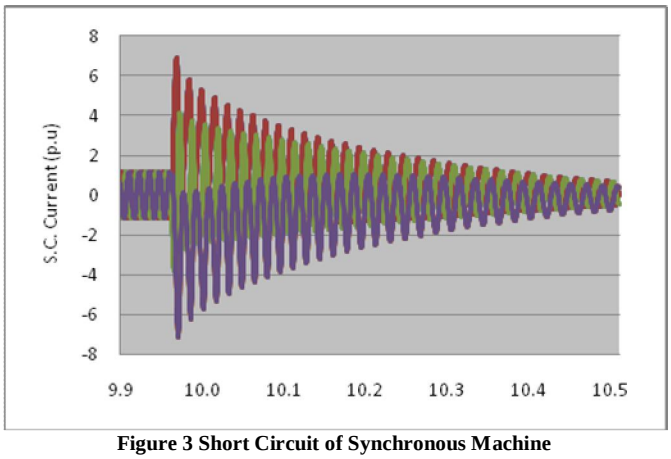

Figure 3 Short Circuit of Synchronous Machine

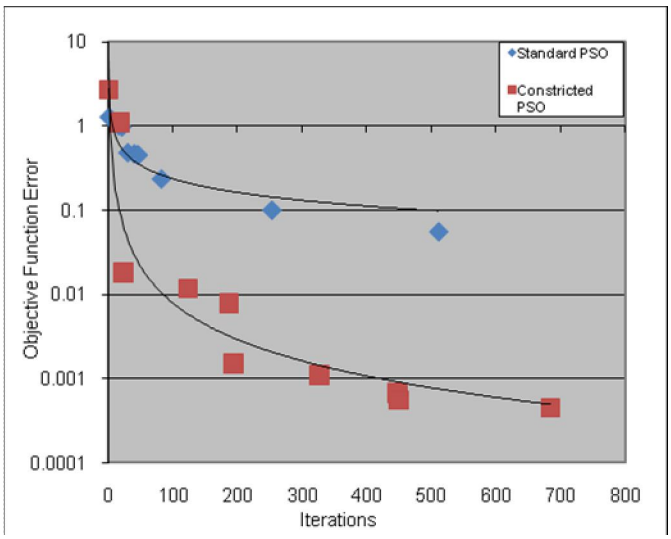

Figure 4 Comparison of error against Iteration for standard PSO against constricted PSO

When considering the PSO for this particular application, several factors need to be taken into consideration when assessing its ability to converge in an appropriate number of iterations. For example, it is necessary to be realistic in identifying the required search area for multidimensional problems. Setting realistic limits to parameters such as X_d or R_s means that the search can be far more accurately targeted.

Using a low constriction factor in conjunction with a refined search area, setting correct weighting values and acceleration coefficients, the particles are able to travel at an appropriate speed to converge on a lower error. At low values of E, the constriction factor slows the velocities of the searching particles. This means that the search area can be more accurately searched, but it increases the number of iterations needed to identify further improvements.

VI. Conclusions

Using manufacturers short-circuit test data for a 828MW, 18kV synchronous generator, this paper has shown that parameter identification using a particle swarm optimization algorithm with a constriction factor produces results that suggest that this method is valid for parameter identification of large synchronous generators. The difference in performance between PSO with a constriction factor in comparison to a conventional PSO algorithm is significant for this application.

VII. References

[1] M. G. Say, Alternating Current Machines, John Wiley & Sons, 1984

[2] R. K. Rasmus and P. Vadstrup, "Parameter identification of induction motors using stochastic optimization algorithms", Applied Soft Computing 4 2004 pp 49-64

[3] D. Flockermann, "Description of electrical machines with non-linear equilavent-circuits", Int'l Conf on Power System Transients 1999, Budapest pp259-264

[4]K. S. Huang, W. Kent, Q. H. Wu, D. R. Turner, "Parameter Identification of An Induction Machine Using Genetic Algorithms", Proc of 1999 IEEE Int'l Symposium on Computer Aided Control System Design, Hawaii pp510-515

[5] P. L. Dandeno, P. Kundur, A. T. Poray, M. E. Coultes, "Validation of Turbo Generator Stability Models by Comparisons with Power System Tests", IEEE Transactions on Power Apparatus and Systems, Vol.PAS-100, No.4 pp 1637-1645, 1981

[6] L. Liu, W. Liu and D.A. Cartes, "Permanent Magnet Synchronous Motor Parameter identification using Particle Swarm Optimization", Int'l Journal on Computational Intelligence Research, Vol.4, No.2 2008, pp211-218

[7] IEEE Std 1110 – 2002, "IEEE Guide For Synchronous Generator Modeling Practices and Applications in Power System Stability Analyses"

[8] J. Kennedy and R. Eberhart, "Particle swarm optimization", Proc IEEE Int'l Conf on neural networks, vol 4 1995, pp1942-1948,

[9] K. M. El-Naggar, A. K. Al-Othman, J.S. Al-Sumait, "A particle swarm digital identification of synchronous machine parameters from short circuit tests", Proc IASTED Int'l Conf on artificial intelligence and soft computing, August 2006

[10] Y. Shi, "Particle Swarm Optimization", feature article, electronic data systems, IEEE Neural networks society, Feb 2004

[11] P. Yin and J.Wang, "A particle swarm optimization approach to nonlinear resource allocation problem", Applied Mathematics and Computation 183, 2006, pp 232-242

[12] M. Clerc, "Particle Swarm Optimisation", Wiley Blackwell, Feb 2006